CRANFIELD UNIVERSITY

NEIL FURMIDGE

PERFORMANCE ENHANCEMENT OF A FLUIDIC OSCILLATOR

SCHOOL OF MECHANICAL ENGINEERING

PhD THESIS

CRANFIELD UNIVERSITY

SCHOOL OF MECHANICAL ENGINEERING

DEPARTMENT OF FLUID ENGINEERING AND INSTRUMENTATION

PhD THESIS

Academic Year 1995-1996

NEIL FURMIDGE

PERFORMANCE ENHANCEMENT OF A FLUIDIC OSCILLATOR

Supervisor: Professor M.L. Sanderson

January 1996

Abstract.

The operational performance criteria of fluidic oscillators are described in relation to the requirements of a domestic water meter. The problems associated with developing a novel water meter using fluidic oscillatory technology are discussed and the performance enhancements required to develop a fluidic oscillator capable of meeting the BS5728 (1979) domestic water meter specifications are presented.

A sensing configuration is described which provides adequate sensitivity over the range required for a water meter with a nominal flowrate of one cubic meter per hour. The nozzle dimensions are investigated to reduce the pressure drop across the fluidic water meter whilst still maintaining the required turndown range and adequate sensitivity at low flowrates.

The development of a novel fluidic oscillator flow conditioning device is described which radically improves the linearity of the fluidic oscillator and helps to reduce susceptibility to upstream disturbances. The device allows debris to pass through the meter without causing blockage and has an acceptable low pressure drop.

Modifications to the fluidic oscillator transducer geometry are investigated which reduce the minimum point of oscillation, thus increasing the turndown range of the water meter. Also geometry modifications are developed which improve the strength of the jet oscillation at low flowrates and thereby significantly increase the strength of signal.

The effects of geometry modification on meter linearity and meterfactor response are investigated and a transducer design with enhanced range performance and improved linearity is described. Transducer designs are presented which are capable of meeting the BS5728 (1979) specification for both Class C and Class D Q_N1.0 domestic water meters.

Acknowledgements.

The Author would like to thank his supervisor Professor M.L. Sanderson for his continual assistance and guidance throughout the project and during the production of this thesis.

The author would also like to express his gratitude to Severn Trent Water and to Fusion Meters for funding the research under the Severn Trent Water Research Fellowship Scheme. The author would like to acknowledge the aid of Fusion Meters for supplying the fluidic oscillator transducer mouldings and for their assistance and technical input into the project.

Thanks are due to all the members of the Department of Fluid Engineering and Instrumentation for their help, in particular to Dr. Alex Guilbert and Duncan MacLeod for assistance in their respective areas of expertise.

The author would also like to thank Alison for her support and help during the preparation of this thesis.

Contents.

Figures.

Chapter 1

Introduction and Literature Review.

1.1 Introduction.

This thesis is concerned with the linearity and range performance enhancements developed and carried out on a fluidic oscillator to produce a fluidic water meter which is capable of meeting the BS5728 (1979) domestic water metering specifications. The fluidic oscillator must produce an output which is practical for use as a domestic water flowmeter and be an advancement upon the rotating piston mechanical water meter used at present for the metering of domestic supplies.

This chapter details the requirements of the BSI domestic water metering specifications and examines alternative metering technologies to the rotating piston mechanical meter. The need for a water meter with no moving parts is described detailing the problems associated with mechanical metering of domestic supplies. The operating principles of fluidic oscillators are described and the specific performance criteria concerning the operation of a fluidic oscillator for practical use as a domestic water flowmeter are considered. A literature review of fluidic oscillator flowmeters is given including examples of existing fluidic devices. The contents of subsequent chapters are summarised at the end of this chapter.

1.2 Domestic Water Meter Performance Specifications.

The British Standard BS5728 (1979) specifies requirements for meters for the measurement of cold potable water. Part 1 deals with the terminology, technical characteristics, metrological characteristics and pressure loss of single meters.

Tables 1.1 and 1.2 show the performance specifications required for Class C and Class D domestic water meters respectively.

Nominal flowrate $Q_n(m^3h^{-1})$	Meter size(mm)	Q_{min} (m^3h^{-1})	Q_t (m^3h^{-1})	Q_{max} (m^3h^{-1})
0.75	15	7.5×10^{-3}	1.125×10^{-2}	1.5
1.0	15	1.0×10^{-2}	1.500×10^{-2}	2.0
1.5	15	1.5×10^{-2}	2.250×10^{-2}	3.0
2.5	22	2.5×10^{-2}	3.750×10^{-2}	5.0

Table 1.1 Performance Specifications of Class C Meters.

Nominal flowrate $Q_n(m^3h^{-1})$	Meter size(mm)	Q_{min} (m^3h^{-1})	Q_t (m^3h^{-1})	Q_{max} (m^3h^{-1})
0.75	15	5.625×10^{-3}	8.625×10^{-3}	1.5
1.0	15	7.500×10^{-3}	1.150×10^{-2}	2.0
1.5	15	1.125×10^{-2}	1.725×10^{-2}	3.0
2.5	22	1.875×10^{-2}	2.875×10^{-2}	5.0

Table 1.2 Performance Specifications of Class D Meters.

For a flowmeter of nominal flowrate, Q_N, between the transitional flowrate, Q_t, and the maximum flowrate, Q_{max}, the meter has to be accurate to within ±2%. Between the minimum flowrate, Q_{min}, and Q_t it must be accurate to within ±5%. For a Q_N1.0 meter this results in an accuracy envelope as shown in figure 1.1.

The required turndown range, Q_{max} to Q_{min}, is 200:1 for a Class C meter and 267:1 for a Class D meter.

There is a maximum allowable pressure drop specification which states that the pressure loss across the flowmeter is to be less than 1 bar, 14.7 p.s.i., at the maximum flowrate, Q_{max}.

For Class D meters there is also a startup flow specification, Q_s, which requires that the meter is indicating flow at half Q_{min}. There is no actual accuracy requirement for Q_s and it is intended mainly for mechanical metering technology, as an indication of the seal and bearing quality, and may not be relevant to the operation of a fluidic technology meter.

1.3 Alternative Technologies to Rotating Piston Meter.

An investigation into appropriate technology for the measurement of flow in small diameter pipes carrying cold potable water was carried out by Sanderson and Spendel (1987). They reviewed the technical performance of existing flowmeter technologies and compared them with the requirements of domestic water metering. The existing appropriate flowmeter technologies were classified into 7 major categories; differential pressure devices, positive displacement meters, turbine flow meters, fluidic oscillators, electromagnetic meters, ultrasonic meters and thermal sensors.

Table 1.3 shows the comparison of functional specifications developed by Sanderson and Spendel (1987). They concluded that none of the existing technologies would meet the specification but that a device based on the fluidic oscillator could provide a performance comparable to that of the conventional mechanical domestic water meter at comparable cost.

Measurement Technique	Will It Meet Accuracy Spec?	Power Requirement	Head Loss	No Moving Parts	Non Obstructive	Non Invasive	Velocity Profile Sensitivity	Cost
Orifice/Venturi	N	< 96mW	0.75Δp	Y	N	N	High	Mid
Spring Loaded Aperture	?	?	?	N	N	N	Low	Low
Variable Area	N	?	?	N	N	N	Low	Low
Positive Displacement	Y	0	?	N	N	N	Low	Low
Turbine	N	< 96mW	$0.9Vf^2$	N	N	N	Swirl Sensitive	Mid/High
Swirl Meter	N	< 96mW	10 veloc heads	Y	N	N	Swirl Sensitive	Mid/High
Vortex Shedding	N	< 96 mW	2 veloc heads	Y	N	N	Little Data	Low
Fluidic Oscillator	?	< 96mW	3 veloc heads	Y	N	N	Little Data	Low
Electromagnetic	?	min 480mW	0	Y	Y	N	Low	High
Ultrasonic	N	200-300mW	0	Y	Y	Y	Low	Mid/High
Thermal	N	1.5W	0	Y	Y	N	Little Data	Low/Mid

Table 1.3 Comparison of Major Functional Specifications For Alternative Technologies, Sanderson and Spendal (1987).

1.4 Operating Principles of Fluidic Feedback Water Meter.

The geometry of the fluidic oscillator water meter flow transducer is shown in figure 1.2. The transducer is a feedback type fluidic oscillator which consists of a converging entrance nozzle, a splitter post, two diffuser walls (attachment walls), and two feedback channels.

As fluid enters the meter a jet flow is formed by the converging entrance nozzle. The attachment walls provide two opposing forces on the jet flow through the action of the Coanda effect as described by Kadosch (1967). As a jet flow formed by a nozzle enters a body of relatively stationary fluid some of the stationary fluid will be carried along with the jet. If a diverging wall is placed near the nozzle then the stationary fluid along the surface of the wall will be carried along with the jet flow producing a low pressure region along the wall. The resulting differential pressure between the jet and wall causes the jet to bend towards the wall and flow along it. The feedback meter has two symmetrical diverging walls and the wall to which the jet first becomes attached is determined by random fluctuations in the jet which are amplified by the coanda effect.

The jet flow travels along the attachment wall passing to one side of the splitter post and through the meter outlet. As the flow is biased to one side some of the main flow is entrained within the feedback channel and travels through the channel to the nozzle outlet at an incidence normal to the jet flow. The feedback flow is entrained in the separation bubble between the jet and diffuser wall. As the separation bubble becomes larger the jet moves away from the wall until the jet meets the splitter post where the separation bubble bursts and the jet switches. The jet flow attaches to the opposite diffuser wall and the feedback process is repeated through the opposite feedback channel.

A sustained oscillation is developed, the frequency of which is proportional to flowrate over a wide flow range. The oscillation frequency is proportional to how fast the jet stream travels down the attachment wall and initiates the new switching action. This

implies that the oscillation frequency is inherently linear with the average stream velocity through the nozzle and therefore volumetric flowrate. The fluidic feedback meter has a linearity, accuracy and repeatability comparable with that of the vortex shedding meter but it is capable of operating at much lower Reynolds numbers.

Sensing of the oscillations within the fluidic water meter is carried out using electromagnetic induction as described by Sanderson and Heritage (1989) and Furmidge and Sanderson (1993). Electromagnetic flowmeters incorporating permanent magnetic fields cannot measure flows which have no time varying component, however, the oscillatory nature of the switching flow in a fluidic oscillator employing a constant magnetic field produces an alternating e.m.f. which can be detected using sensing electrodes.

Two permanent, sintered neodymium NdFeB, magnets mounted within the diffuser walls create a magnetic field, orthogonal to the jet flow, which generates an e.m.f. within the liquid itself. The induced voltage is detected using stainless steel electrodes mounted in the top of the flow chamber on each side of the splitter post. Earthing electrodes are mounted upstream and downstream of the sensing arrangement in the form of earthing rings installed between the flow chamber and inlet and outlet flanges. Since the power is generated by the electromagnetic inductive effect the sensor itself requires no power. The only power required by the water meter is for the amplification and processing of the generated signal.

The signal processing for the fluidic flowmeter is implemented using an application specific integrated circuit (ASIC) and a low power microprocessor. The meter is powered by a replaceable 3.6V lithium battery with a no maintenance life expectancy of over 10 years. A block diagram of the meter electronics which carries out the amplification and processing of the signal is shown in figure 1.3.

The oscillatory induced signals detected on the flowmeter electrodes are amplified and conditioned within the head amplifier. The head amplifier produces a square wave pulse

output, at the same frequency as the frequency of oscillation, which is fed into the flowmeter controller. The controller is interfaced with a look-up table in which the meterfactor calibration curve is stored. The controller employs a compensation algorithm which uses the frequency of oscillation, the calibration table and the temperature of the water to produce a linearity corrected and temperature compensated flowrate. The temperature of the water is measured using a thermistor mounted on one of the electrodes. The electrodes are also used by the controller to sense for no-water detection to indicate that the meter has been run dry.

The controller is responsible for managing the specific memory locations in which totalised flow and flow over set time periods are stored. An LCD display provides a visual readout of total flow and the controller is also used to control the receiver and transmitter of a radio link used by the automatic meter reading (AMR) system. The AMR system is capable of using either handheld, vehicle based or telemetry networked data capture methods.

The complete Q_N1.0 fluidic oscillator water meter assembly is shown in figure 1.4.

1.4.1 Other Forms of Fluidic Oscillator.

There are several types of oscillating jet devices including feedback, relaxation, and target fluidic oscillators. Figure 1.5 shows a feedback fluidic oscillator the Osaka gas flowmeter, Medlock (1990), figure 1.6 shows a relaxation fluidic oscillator Shakouchi (1988) and figure 1.7 shows a target meter which was developed for low Reynolds number fluidic flowmetering as described by Honda and Yamasaki (1985).

Feedback oscillators operate on the principle that some of the output flow is returned to the control port through a feedback duct causing the jet to switch sides and the cycle is then repeated on the opposite diffuser wall. Figure 1.8 shows the oscillation cycle for the Osaka gas meter Medlock (1990).

The relaxation type fluidic oscillator has the two control ports connected together by a control loop. The pressure is lower at the control port on the side to which the output flow is attached and the higher pressure at the other port causes a flow in the control loop which results in the output flow switching from one attachment wall to the other.

The target flowmeter developed by Honda and Yamasaki (1985) consists of a target and a pair of edges upstream of the outlet port. The performance of the meter is described as a composite of vortex shedding flowmeter and feedback fluidic flowmeter operating principles. Further analysis of the operation of the target meter was carried out by Boucher and Mazharoglu (1988a).

1.5 Advantages of The Fluidic Oscillator.

The water companies are looking at metering technology more seriously than ever before following the results of the National Metering Trials (1993), which raised as many questions concerning the performance and reliability of mechanical meters as it resolved. The following section discusses the advantages of the fluidic oscillator water meter compared to the existing mechanical meter designs and considers the benefits of using a fluidic oscillator for the measurement of domestic water consumption.

The main advantage of the fluidic oscillator compared to the rotating piston mechanical water meter design is that the fluidic meter has no moving parts. The results of the National Water Metering Trials (1993) indicated how sensitive mechanical meters are to particulate matter. In year 1 tests showed that 15% of meters were found to jam at low flows. The principle cause of mechanical Class D meters jamming, either jamming at low flows or total failure, was particulate matter trapped between the flow seals or bearings.

The flow seals within mechanical meters are manufactured to high tolerances and liable to jam should particulate matter be entrained into the water supply. A study of the

effect of particulate matter on piston type Class D domestic water meters was carried out by Chiwanga (1994). He used several methods to investigate the various aspects of meter stoppage and was able to show that meter stoppage is caused predominantly by a wedging action between the piston and measuring cylinder, the piston and top or bottom surfaces of the measuring chamber or the piston and barrier plate. Figure 1.9 shows the possible jamming mechanisms of particulate matter within a rotating piston mechanical meter.

Continuous operation in water containing particulate matter causes mechanical meters to either stop operating at low flowrates, or decrease the starting flowrate, or rapidly lose accuracy. Chiwanga (1994) recommended that a solution could be provided by stopping particulate matter from entering the meter using a prefilter of the order of 100 microns. However, concern has been expressed over the increased pressure loss due to fine filters and bacterial growth in the deposits on filters.

The sensitivity of the rotating piston mechanical flowmeter design to particulate matter and the problems associated with mechanical metering of domestic supplies highlights the need for a novel low maintenance domestic water meter with no moving parts. Fluidic oscillators are ideally suited to domestic water metering applications because of their large operating range, high level of linearity and, because they have no moving parts, they are very reliable requiring minimal maintenance. The principal cause of mechanical Class D meters jamming, either jamming at low flows or total failure, is particulate matter trapped between the flow seals or bearings. The smallest flow channels within the fluidic oscillator flow meter are at least 2.5mm wide and the meter is capable of allowing debris to flow through the meter without causing jamming or blockage. Figure 1.10 shows a series of flow visualisation experiments showing the passage of 2mm neutrally buoyant polystyrene beads flowing through the fluidic water meter.

The effect of particulate matter and abrasive wear on fluidic oscillator water meters was investigated by Smith (1994). He used an abrasion test rig consisting of a tank, slurry

pump, and an agitator to pump a mixture of 40 litres of water and 2kg of sample grit. The grit was typical of the worst examples found in meter box products returned to Fusion Meters for servicing. A calibrated meter was connected to the rig and the agitated solution was recirculated through the meter continuously for 100 hours. The meter was recalibrated and at the worst point the accuracy was reduced by just 1%. This shows that the meter did not suffer blockage or jamming problems and that the reduction in accuracy due to abrasion is an acceptably low level and within in-service tolerances.

Frost damage is considered to be an installation problem rather than an indication of meter quality or robustness, however, during the meter trials which took place on the Isle of Wight, National Water Metering Trials (1993), 360 meters were replaced as a result of freezing weather conditions during February 1991. In every case the particularly severe weather conditions had caused the water inside the meter to freeze and expand. The body of the meter eventually splits creating large cracks from which water escapes once the meter is thawed.

The flow chamber of the fluidic water meter is made from plastic able to accommodate the expansion of the freezing water through deformation of the flow chamber. A computer model of the flow chamber was used during development to optimise the design of the moulding so that the chamber is both flexible and strong thus able to withstand high internal pressures. This was demonstrated by Smith (1994) who carried out a freeze test on a standard fluidic meter. The meter was filled with water and capped at the flanges, the unit was then held at minus 20°C overnight. After thawing the unit was tested for leaks at pressures of upto 16 bar and then recalibrated. The accuracy of the meter was only altered by a small amount following the freeze test demonstrating that the fluidic water meter is capable of withstanding freezing weather conditions.

There have been reported cases where mechanical meters have registered air passing through the meter following maintenance work to supply pipes and at high points in the

system where air collects. These cases may not be a significant problem, but the media have highlighted the incidents and use them as arguments against metering and to influence public opinion as to whether metering is a fair method of charging for water consumption. The fluidic water meter uses electromagnetic induction within a conducting fluid, ie. water, to generate flow signals. Air is a non-conducting fluid and therefore is not registered by the fluidic oscillator. Any air trapped within the fluidic oscillator is flushed from the flow chamber at high flowrates.

The dimensions of the flow chamber, designed for domestic metering purposes, allow the unit to be within the recommended flange to flange dimensions specified for mechanical meters. The inline fluidic water meter may therefore be installed as a direct replacement for mechanical meters, this is important because many new domestic properties are constructed with a boundary box installation configured to accept mechanical meters. Also initial experiments carried out on a concentric device, Furmidge (1994), indicate that a Class D concentric unit is achievable incorporating standard concentric fittings.

The digital output of the fluidic oscillator is intrinsically suited to automatic meter reading (AMR) systems as opposed to the retro-fitted encoder systems used with existing mechanical meters. The price of the unit must be cost effective for the water companies to consider using the device for universal metering and therefore the meter must be relatively cheap. The fluidic chamber is capable of being injection moulded, as are most of the meter assembly components, making it suitable for cost effective mass production.

These factors show that fluidic metering of domestic water consumption has many benefits and that the fluidic oscillator water meter is an improvement upon the mechanical metering technology used at present.

1.6 Fluidic Oscillator Performance Criteria For Use As Domestic Water Meter.

This section covers how the BSI domestic water metering specifications relate to the performance of fluidic oscillators and details the specific performance criteria concerning the operation of a fluidic oscillator for practical use as a domestic water flowmeter. The areas covered are the pressure drop, linearity, flow range and oscillation frequency of fluidic oscillators and the possible methods employed to detect the oscillation of fluidic oscillator water meters.

The equations used to characterise the performance of fluidic oscillators are well documented including work by Boucher and Mazharoglu (1988b) and Kalsi et al (1988).

1.6.1 Pressure Drop.

The B.S.I. standards for domestic water metering specifications state that the maximum allowable pressure drop at the maximum flowrate is 1bar. The pressure drop of a fluidic meter, Δp, is given by:

$$\Delta p = \frac{1}{2}\rho v^2 E \qquad (1.1)$$

where ρ is the density of the measured fluid, v is the velocity of the jet flow through the nozzle and E is the Euler number. E is constant at high Reynolds numbers and is usually between 0.9 and 1.2 for most fluidic oscillators. The maximum pressure drop is therefore directly proportional to the square of maximum jet velocity, v_{max}, given by:

$$v_{max} = \frac{Q_{max}}{\alpha w^2} \qquad (1.2)$$

where α is the aspect ratio of the fluidic oscillator defined as the ratio of nozzle height, h, to nozzle width, w.

Replacing v_{max} equation (1.1) can be written as:

$$\Delta p_{max} = E_{max} \frac{1}{2} \rho \frac{Q_{max}^2}{\alpha^2 w^4} \quad (1.3)$$

Equation (1.3) shows that the pressure drop of the fluidic oscillator is inversely proportional to the product of the square of the aspect ratio and w^4. This implies significant changes in pressure drop are achievable with only small changes in the nozzle width dimension.

The pressure drop of meter components in addition to the oscillator itself must also be considered when attempting to match the performance of the fluidic oscillator meter to the BSI specification. The fluidic oscillator is not capable of reading reverse flows therefore the device must be fitted with a non-return valve which will have a fixed pressure drop at Q_{max}. Any additional filtering or flow conditioning device within the meter unit will also add to the pressure loss across the flowmeter.

1.6.2 Linearity.

The water meter accuracy specifications defined by the BSI standards result in an accuracy envelope as shown in figure 1.1.

The oscillation frequency of the fluidic oscillator is given by:

$$f = S\frac{v}{w} \quad (1.4)$$

where f is the frequency of oscillation, S is the Strouhal number, v is the velocity of the jet and w is the width of the jet.

If the meter were truly linear then the Strouhal number would not vary with Reynolds number over the flowrange of the meter. This is not the case for the fluidic water meter because the operational range of the meter requires Reynolds numbers which span from fully turbulent jet flow, through a transitional region, and into a fully laminar jet flow. The changing flow patterns during these varying flow conditions and viscous effects result in the Strouhal number changing with Reynolds number, Re, given by:

$$Re = \frac{vw}{\nu} \tag{1.5}$$

where ν is the kinematic viscosity.

Figure 1.11 shows the variation in Strouhal number with Reynolds number for a feedback fluidic oscillator investigated by Boucher and Mazharoglu (1989). Although the Strouhal number is nearly constant at Reynolds numbers of greater than 2000 it is very non-linear at lower Reynolds numbers with percentage variations exceeding those permitted in the flowmeter specifications. Such non-linearities in fluidic meters are caused by the transition from fully turbulent flow conditions to fully laminar at low Reynolds numbers and by the oscillator ceasing to oscillate at low flowrates.

The variation of Strouhal number with Reynolds number and hence linearity of the flowmeter is such that the meter fails to meet the domestic meter accuracy specification shown in figure 1.1. The variation in linearity can be overcome by using a Reynolds number meterfactor calibration stored electronically in memory, however, as Reynolds number varies with viscosity then the viscosity of the water must also be determined by measuring the temperature of the water.

Although the variations in linearity can be overcome with laboratory instrumentation, production fluidic water meters would be limited to relatively simple signal processing power. The complexity of the linearisation and temperature compensation algorithm would be restricted by the limitations of a low power microprocessor based compensation algorithm.

The fluidic oscillator domestic water meter described within this thesis uses a look-up table of discrete frequency bins stored electronically in memory. Each entry within the look-up table contains a 16 bit number. The least significant 11 bits represent the volume flow at 0°C, the next 4 bits represent a temperature correction volume and the most significant bit is the sign of the temperature correction volume.

The number of pulsed edges, or oscillation half cycles, counted within an integration period is used to determine a centre frequency for the oscillations. The number of edges counted and the length of the integration period correspond to a unique address within the look-up table. The stored temperature correction volume is multiplied by the measured temperature of the fluid in °C and then added to the volume flow at 0°C stored within the table. A schematic diagram of the linearity and temperature compensation scheme is shown in figure 1.12.

The volume flow stored within the table is calculated using the oscillation centre frequency and an experimentally derived volume flow per pulse meterfactor at that centre frequency. Before the flow volume is stored it is temperature shifted to a theoretical volume flow at 0°C. The temperature correction volume is derived from the best straight line approximation of a meterfactor against temperature plot for each centre frequency used within the table. The linearity and temperature compensation algorithm is described in more detail in chapter 4.

While this temperature compensation scheme works well for the sections of the meterfactor characteristic with constant slope it is a poor approximation at the sections where the slope of the meterfactor against temperature graph varies most with temperature and can even change sign. The compensation scheme requires that the meterfactor response curve be as linear as possible with variations in meterfactor occurring through smooth transitions rather than rapid step changes. Any variations in meterfactor slope rising positive to negative or vice versa would need to be smooth and separated by linear sections along the curve.

The design of the fluidic oscillator must be optimised to match the meterfactor response of the oscillator to the requirements of a simple compensation algorithm. Methods of improving the linearity of fluidic devices include geometry modifications to the oscillator and flow conditioning of the inlet flow to minimise the effects of changing flow conditions.

1.6.3 Range.

The required turndown range, Q_{max} to Q_{min}, is 200:1 for a Class C meter and 267:1 for a Class D meter. The size of the meter is determined by the pressure drop at Q_{max} and when this is combined with the large range required for domestic meters results in a very demanding minimum flowrate requirement.

At very low Reynolds numbers, for example less than 200, the small fluctuations in the jet flow become too small to be amplified by the Coanda effect. This causes the jet to become stable and the fluidic oscillator ceases to operate. At these low Reynolds numbers the jet flow splits evenly around the splitter post and stabilises.

The minimum flowrate at which the flowmeter is capable of operation is determined by the minimum Reynolds number at which oscillation is maintained before the jet stabilises. With careful design the fluidic oscillator can sustain oscillation at low Reynolds numbers and the range of the device can be significantly extended.

The minimum Reynolds number for oscillation, Re_{min}, based on the jet width, w, the flow velocity, v, through it and the kinematic viscosity, ν, of the fluid remains constant for a given geometry and is given by:

$$Re_{min} = \frac{vw}{\nu} \tag{1.6}$$

As flow velocity is proportional to flowrate then:

$$v = \frac{Q}{wh} \rightarrow Re_{min} = \frac{Q_{min}}{\nu h} \tag{1.7}$$

where Q_{min} is the minimum achievable volumetric flowrate and h is the height of the jet.

The size of the meter is given by the nozzle width dimension, w, determined using the maximum allowable pressure drop. Rearranging equation (1.3) gives the expression for the fluidic oscillator jet width dimension:

$$w = \left(\frac{1}{2}\rho\frac{E_{max}}{\alpha^2}\right)^{1/4} \frac{Q_{max}^{1/2}}{\Delta p_{max}^{1/4}} \tag{1.8}$$

Rewriting equation (1.7) for the minimum flowrate and substituting for w in equation (1.8) gives:

$$Q_{min} = \left(\frac{\rho Q_{max}^2}{2\Delta p_{max}}\right)^{1/4} \nu\ Re_{min}\ \alpha^{1/2}\ E_{max}^{1/4} \tag{1.9}$$

Q_{max} and Δp_{max} are given in the meter specifications and the fluid density and kinematic viscosity are easily determined. The minimum flowrate is therefore set by the lowest value of Re_{min} achievable and the product of $\alpha^{1/2}$ and $E_{max}^{1/4}$.

Reducing Re_{min} is achieved through design modifications and has resulted in alternative types of fluidic oscillator design such as the target meter developed by Honda and Yamasaki (1985).

1.6.4 Oscillation Frequency.

For the fluidic oscillator to be of practical use as a domestic water meter the oscillation frequency for a given flowrate must be high enough so that flow transients may be accurately tracked and relatively short periods of water usage may be metered. The quantity of flow per cycle of oscillation must be low enough to give the meter an acceptable meter resolution. Also if oscillation frequency is to be checked against a meter calibration curve stored in an electronic memory then the maximum oscillation frequency must not be so high that processing speed is either beyond the capabilities of the on board microprocessor or so fast that power consumption of the microprocessor becomes a problem for extended battery life.

The expression for the fluidic oscillator oscillation frequency is given in equation (1.4) which can be written as:

$$S = \frac{f\alpha w^3}{Q} \tag{1.10}$$

Equation 1.10 shows that Strouhal number is directly proportional to the number of cycles per second per volume flow, the meterfactor. The volume flow per pulse is a more useful indication for a volume flow flowmeter and is also termed meterfactor or more correctly K-factor.

A practical maximum acceptable oscillation period would be around 5 seconds at the minimum flowrate, ie. a frequency of 0.2Hz. For a Class D Q_N1.0 meter Q_{min} is 2.0ml pulse^{-1} assuming an oscillation frequency of 0.2Hz at Q_{min} results in a volume flow per pulse of 10ml pulse^{-1}. This would give an oscillation frequency of 55.55Hz at Q_{max}. A rational upper frequency limit would be 100Hz. This would allow for a reasonable processor clock speed and sampling rate. For a Class D Q_N1.0 meter Q_{max} is 555.55ml s^{-1}, assuming an oscillation frequency of 100Hz at Q_{max} results in a volume flow per pulse of 5.55ml pulse^{-1}. This would give an oscillation frequency of 0.36Hz at Q_{min} assuming linearity is maintained.

An ideal volume flow per pulse meterfactor value would be within the range 5.55ml pulse^{-1} to 10.0ml pulse^{-1}. If the meterfactor is lower than 5.5ml pulse^{-1} then the meter is likely to be oscillating at high frequencies at the nominal and higher flowrates resulting in costly power consumption to meet the high speed signal processing and sampling rates required. If the volume flow per pulse is greater than 10ml pulse^{-1} then the oscillation frequency is very low at low flowrates resulting in long time periods and low meter resolution. The meter resolution should be adequate so that flow transients may be accurately tracked and relatively short periods of water usage may be metered.

1.6.5 Oscillation Detection.

The sensing of the oscillation of the fluidic oscillator is a problem in that the sensor itself must be capable of operating over a range which is at least equal to the range required by a fluidic oscillator water meter. Also the power consumption of the sensing mechanism must be such that the system may be powered by an extended life battery required for domestic water meter installations.

Fluidic oscillator designs described by Boucher and Mazharoglu (1988a) and Kalsi et al (1988) use thermal and pressure sensing techniques. Thermal sensors have a limited range of operation usually in the low flow range of fluidic oscillators and are of little use for battery powered devices due to their significant power consumption. Pressure sensors are more suited to the measurement of high flowrates but are limited in range. The sensed pressure is proportional to the square of the velocity and therefore the pressure sensor would be required to operate over a range of over 40000:1 for a fluidic meter with a turndown of 200:1.

For gas metering where the minimum flowrate is unattainable using fluidic techniques a combination arrangement using both pressure sensing and thermal techniques has been identified by Boucher and Mazharoglu (1988a). Detection of high flowrates is possible using pressure sensing techniques and low flowrates using thermal sensing. The thermal

sensing will continue to operate at flowrates below which the fluidic oscillator will cease to operate. A range of overlap where both sensors are operating allows the thermal sensor to be recalibrated periodically to compensate for the effects caused by changes in the heat transfer characteristics between the thermal sensor and the fluid.

Boucher and Mazharoglu (1989) describe a hybrid gas meter consisting of two fluidic oscillators, one small and one large, in series. Low flowrates are measured by the smaller meter until the maximum pressure drop is approached at which time a bypass valve is opened and the flow is measured by the larger meter. Although the entire flow range can be covered by fluidic technology using the hybrid system, the system is complicated using a bypass valve two meters and two sets of sensing arrangements.

A technique for sensing of the oscillations using electromagnetic induction is described by Sanderson and Heritage (1989) and by Furmidge and Sanderson (1993). Electromagnetic flowmeters incorporating permanent magnetic fields cannot measure flows which have no time varying component, however, the oscillatory nature of the switching flow in a fluidic oscillator employing a constant magnetic field produces an alternating e.m.f. which can be detected using sensing electrodes. Since the power is generated by the electromagnetic inductive effect the sensor itself requires no power which is ideal for an extended life battery powered domestic water meter. Also the because output information is essentially frequency sensing rather than signal magnitude it is irrelevant that the magnitude of the induced signal varies with jet velocity provided that sufficient signal strength is available at low flowrates.

The fluidic oscillator enhanced to meet the BSI domestic water meter specifications described in this thesis employs electromagnetic sensing of the oscillations.

1.7 Literature Review of Fluidic Flowmeters.

The literature review of fluidic oscillator flowmeters is divided into four sections giving a historical introduction to fluidic metering, a review of work carried out to increase the range of fluidic oscillators, a review of literature which analyses the performance of fluidic oscillators and a review of investigations into the use of fluidic oscillators for domestic metering applications.

1.7.1 Historical Introduction to Fluidic Metering.

Early experimental investigation to determine the potential of the fluidic oscillator as a flowmeter was carried out by Wilson, Coogan, and Southall (1970). The tests were carried out using a feedback oscillator, shown in figure 1.13, with several test fluids. The oscillations were detected using pressure transducers mounted in the receivers. They were able to show that the oscillation frequency is proportional to flowrate and that the oscillation frequency is independent of density and viscosity for a range of specific gravity as shown in figure 1.14.

The design parameters such as splitter distance, aspect ratio, setback distance, and feedback inlet location were experimentally investigated to determine the correct combination of these parameters required for the jet to oscillate and for the effects on oscillation frequency caused by altering the design parameters. The effects of altering splitter distance, aspect ratio, and setback distance on oscillation frequency are shown in figure 1.15. They were able to show that oscillation frequency is inversely proportional to aspect ratio, for aspect ratios equal to or greater than five.

Relaxation type fluidic oscillators have the two control ports connected together by a control loop. The pressure is lower at the control port on the side to which the output flow is attached and the higher pressure at the other port causes a flow in the control loop which results in the output flow switching from one attachment wall to the other.

Tippetts, Royle, and Ng (1971) carried out experiments on three designs of relaxation oscillator as shown in figure 1.16. The devices were tested with water and air. One of the designs, oscillator '03', has the characteristics required for use as a flowmeter as shown by the frequency flow relationship in figure 1.17. They show that for certain design changes the effects on meter performance can be predicted and that the calibration factor of a basic meter design could easily be altered by adjusting the control loop length, figure 1.17. This has particular significance to fluidic oscillators for domestic metering applications as it provides a mechanism for altering the oscillation frequency at a particular flowrate and therefore the volume flow per cycle.

As early as 1970 a fluid oscillator flowmeter was commercially available as described by Adams (1973). The device is a feedback oscillator using a heat sensor, mounted flush to the wall one of the feed back passages, to detect oscillation as shown in figure 1.18, also a schematic depicting the fluidic flowmeter oscillation cycle is shown in figure 1.19.

Adams (1973) states that the frequency at which oscillations occur depends on how fast the stream travels down the sidewall and initiates the next switching action. The frequency is inherently linear with average stream velocity and, therefore, volume flowrate. Also since the frequency depends only on velocity and not density the meter calibration should be the same for all fluids. Figure 1.20 illustrates both facts by showing the calibration data obtained using fluids of three different densities, however, the minimum flowrate, below which oscillation is not sustained, depends on the kinematic viscosity of the fluid. Figure 1.21 shows the meter linearity for various sizes of the device when tested with water.

1.7.2 Fluidic Flowmeters With Increased Range.

The early fluidic oscillator flowmeters were developed to compete with existing orifice plate and vortex shedding flowmeters and were only required to work over a relatively

small range under fully turbulent flow conditions. For the fluidic oscillator to be of practical use for domestic metering purposes the range of fluidic devices needed to be greatly increased. This section of the review details the literature describing methods investigated to increase the turndown range of fluidic devices.

Honda and Yamasaki (1985) used the complementary relationship between jets and wakes to develop a new type of fluidic oscillator, the target meter. The target flowmeter consists of a target and a pair of edges at the meter outlet port. The performance of the meter is described as a composite of vortex shedding and fluidic feedback operating principals. They used the topological invariant theorem, which states that circulation around a body can be replaced by a vortex, to remove the diffuser walls from a feedback meter whilst maintaining feedback flow. The feedback flow was generated by vortices shed from a bluff target which are recirculated by the edges of the meter outlet port. To maintain oscillation it is necessary to carefully select the dimensions of the target width, nozzle to target distance, flow duct width and the width of the meter outlet port. Figure 1.22 shows the complementary relationship between jets and wakes and figure 1.23 shows the new target meter and the feedback oscillator from which it was derived.

The oscillation of the jet was detected using a hot wire and the linearity of the device tested with varying geometry parameters. Some of the geometry configurations have a linearity comparable to that of the feedback fluidic oscillator, however, one of the devices tested, although non-linear, is stated as having a minimum Reynolds number of 27.

A version of the target meter, similar to that described by Honda and Yamasaki (1985), was developed by Boucher and Mazharoglu (1988a) incorporating adjustable knife edges as shown in figure 1.24. The device was designed to function at small Reynolds numbers which arise when metering oil, respiratory flows, domestic and point of sale metering. The performance characteristics of the device were investigated with varying design parameters including the nozzle to target distance, target to knife edge distance,

knife edge setback from centre line, side wall setback, depth of profile and the width of the target. For low Reynolds number tests the meter was calibrated using a flow rig with oil as the working medium and for high Reynolds numbers an air driven flow rig. Flow visualisations were carried out, by injecting dye at half the nozzle height, which they used to show recirculating vortex flows behind the target. Boucher and Mazharoglu (1988a) noted that the device has two minimum Reynolds numbers, similar to feedback oscillators, one for oscillations starting and the other for oscillations ceasing. Figure 1.25 shows the beginning of oscillations for the device with varying geometry parameters.

They investigated the theory suggested by Honda and Yamasaki (1985) that the new type of fluidic oscillator behaves as a feedback oscillator at high Reynolds numbers and that at low Reynolds numbers oscillation is due to alternate vortices shed from behind the target. During their low Reynolds number flow visualisations Boucher and Mazharoglu (1988a) observed that there was no alternate vortex shedding from the target, however, there were recirculating vortex flows. They surmised that at high Reynolds numbers should the oscillation mechanism be the same as a feedback oscillator, with feedback flow being returned from the knife edges, then removing the knife edges should stop the oscillations altogether. The device was tested without the knife edges and they found that the meter still oscillated but gave a much higher minimum Reynolds number and that the Strouhal number was four times lower. The superior performance produced by the knife edges is because they assist in boundary layer separation which speeds up the deflection of the jet and because they act as flow diverters, causing the pressure between the wall and base of the jet to build up much faster, initiating the switching action. The significant differences in minimum Reynolds number are due to the recirculating flows down stream of the target, introduced by the knife edges, resulting in a greater rate of change of pressures on both sides of the jet. The greater rate of change of pressure above and below the jet increases the likelihood of instability and oscillation.

Honda and Yamasaki (1988) continued the investigation of the oscillation mechanism

of their target meter, described earlier (1985), using experimental flow visualisation and numerically visualised flow fields. The experimental work was carried out using air as the test fluid and a Finite-Difference program, SOLA, was used to solve the two dimensional Navier-Stokes equations for the numerically derived flow fields. They achieved good agreement between experimental and simulated results over a range of flowrates, except at low flowrates where the agreement was only fair.

Yamasaki, Takahashi and Honda (1988) describe a simple target meter which has no control ports or downstream contraction as shown in figure 1.26. The configuration is two dimensional consisting of an inlet nozzle and rectangular target only. The simple design of the oscillator allows easier numerical simulation of the flow fields, which was carried out using the SOLA package as mentioned above. Figure 1.27 shows the oscillation of the jet through numerically generated stream lines. Figure 1.28 shows the variation of Strouhal number against Reynolds number for changes in the dimensions of the target and the distance between nozzle and target. Although the performance of the device is inferior, in terms of uniformity of Strouhal with variation in flow rate, the range of the device is over 40:1.

Simple target fluidic oscillator devices are two dimensional and have constant dimensions in the vertical plane. Yamasaki et al (1991) suggest that it is therefore desirable to have two dimensional jet flow, however, the jet flow tends to become three dimensional because of the drag effects produced by the boundary layers formed along the top and base of the meter. They attempted to generate a two dimensional jet by creating a stationary vortex ring at the outlet of the nozzle. The outlet of the nozzle was machined with a rectangular slot to form a closed vortex ring where the circulation and angular velocity of the vortex is constant around the ring. The concept is that the faster portion of the jet flow gives energy to the vortex ring and is decelerated whilst the vortex ring provides energy to the slower portion of the jet flow, which is accelerated, thus equalizing the velocity profile of the jet flow causing it to become more two dimensional. They carried out experimental tests on two simple target meters, as shown in figure 1.29, with both a single slot and double slot configuration. Figure 1.30 shows

the slot machined into the nozzle exit in which the vortex ring is formed. Computational fluid dynamics techniques were also used to model the effects of vortex rings at the nozzle outlet. Their CFD and experimental results show that the velocity profile becomes flatter with the addition of slots at the nozzle outlet and that improvements in flow range and meter linearity are also achieved.

1.7.3 Fluidic Oscillator Performance Characteristics.

This section of the literature review examines the literature which analyses the performance characteristics of fluidic oscillators and the methods of determining the geometric dimensions required for domestic metering applications.

Beale and Lawler (1974) describe a wall attachment fluidic oscillator which has no target as shown in figure 1.31. They attempted to develop a device with maximum oscillation frequency, accuracy, and linearity, whilst minimising pressure loss and dependence on pipe flow conditions. They tested many experimental models to determine the effect of various geometrical parameters and developed a semi-empirical analysis which characterises most of the parameter effects. Using the analytical model they were able to show that the frequency of oscillation is a function of fluid velocity and geometrical parameters only. To check this result the same meter body was tested in both water and in air. Within the incompressible flow regime the meterfactor was found to be within ±0.5% for both media. Using their analytical model and experimental results they were able to develop a meter with a flow range of 10:1 with a maximum pressure loss of 3 psi.

Wu, Su and Wang (1980) developed a mathematical model for the oscillatory mechanism of the fluidic oscillator and compared their results with experiments carried out on both a relaxation type oscillator and a feedback oscillator as shown in figure 1.32. Using theoretical analysis they were able to show that Strouhal number remains constant for large Reynolds numbers and, therefore, oscillation frequency is

linearly proportional to flowrate for turbulent flow. They carried out an investigation into the effects of geometry changes, concentrating on the splitter distance, loop length, control width, and loop diameter, on the characteristics of the flow meter. Their results are shown in figure 1.33. They also state that for a fixed nozzle area it is possible to improve both sensitivity and linear range by varying the aspect ratio.

Boucher and Mazharoglu (1988b) developed fluidic flowmeter scaling equations after analysing the performance characteristics of several fluidic meters. They highlighted the importance of aspect ratio and showed that the linearity characteristic of the meter depends upon the variation of Strouhal number with Reynolds number. The fluidic scaling equations they developed were based around non-dimensional formula for determining the geometric nozzle dimensions from the maximum allowable pressure loss at the maximum required flowrate. Using the equations they were able to show that the minimum flowrate achievable and the meterfactor, flow per pulse, depend on Euler number, Strouhal number and minimum Reynolds number for any device. They carried out experimental work to determine optimum geometry values. Figure 1.34 shows minimum Reynolds number against aspect ratio and figure 1.35 shows Strouhal number against Reynolds number for different aspect ratios. For the target meter tested they derived an optimum aspect ratio of 6 which would produce a typical flow per pulse meterfactor of around 50.

Kalsi et al (1988) reviewed the considerations which have influenced the development of a feedback type fluid oscillator designed by Thorn EMI Flow Measurement. They developed equations similar to those described by Boucher and Mazharoglu (1988b) based around the pressure drop at maximum flow and the minimum flowrate at which the meter will continue to work and were able to show that the range of a meter of a given class, ie. meters possessing similar geometry, is proportional to its physical size only. Experimental work carried out on the Thorn EMI Flow Measurement Meter U100, shown in figure 1.36, produced performance plots of minimum flowrate achievable against aspect ratio, figure 1.37, and linearity expressed in dimensionless terms as shown in figure 1.38. The optimum aspect ratio was found to be 3.9 and the working

range was linear to within 0.24% of the maximum flowrate. They also carried out investigation into the effect of obstructions to the flow upstream of the meter and the fluidic meter was seen to be comparatively unaffected by quite severe disturbances upstream.

Glynn and Kalsi (1987) used computational fluid dynamics to optimise the design of the Thorn EMI Flow Measurement U100 meter described above. The aim of the work was to predict the changes in meter performance, produced by modifications to the transducer geometry, in a faster timescale than by using conventional experimental techniques. They used PHOENICS software to mathematically model two dimensional laminar flow through the fluidic oscillator and set the inlet velocity at 5m s^{-1}, which is equivalent to a Reynolds number of 800 through the nozzle. The predictions are illustrated by plots of velocity vectors at successive times during the cycle and by time histories of velocity and pressure oscillations at specific locations within the device. The model predicted strong oscillation, in a regular cyclic pattern, at a frequency within 25% of the actual experimentally derived oscillation frequency.

1.7.4 Fluidic Oscillator Domestic Metering Applications.

This section of the literature review examines the investigations carried out into the use of fluidic oscillators for domestic metering applications.

An investigation into the application of the fluidic oscillator flowmeter as a replacement for the membrane gas meter and the problems associated with achieving the domestic gas metering specifications was carried out by Kawano et al (1985). They describe the development of fluidic oscillators with a wider range than conventional types, figure 1.39, and methods of increasing the flow range whilst remaining within the maximum pressure loss of the domestic gas metering specification.

Experiments were carried out using trial meters to determine the effects of nozzle height

and aspect ratio on the operational flow range of the meter. They discovered that as nozzle height was increased the upper flow limit increased greatly whilst the lower flower rate limit increased to a lesser extent therefore increasing the range of the device. Experiments performed on trial meters gave a maximum range with an aspect ratio of about 20.

The prototype flowmeter, figure 1.40a, was revised to reduce the pressure drop of the device by shaping the nozzle like a venturi. To reduce the minimum flowrate and increase the flow range the gate of the wall face was throttled to allow suction to occur from the negative pressure zone. Also the outlet of the meter was narrowed to increase feedback flow. The stages of transducer modification are shown in figure 1.40. The feedback loops were lengthened and the corner sections curved to improve the signal to noise ratio of the thermistors, mounted in the feedback loops, by reducing turbulence in the feedback flow. The configuration of the final revised meter is shown in figure 1.41.

The fluidic oscillator is considered for use as a domestic gas meter by Boucher and Mazharoglu (1989). They show that their present fluidic device would not meet the gas metering specifications and investigated the effect of critical geometry changes. They developed a design with improved performance but the fluidic oscillator was still unable to measure the range of flowrates required by the specifications.

To measure flowrates below the meters minimum point of oscillation they suggest using another flow sensor, a thermistor for example, whose calibration may be compared to the fluidic oscillator, at flowrates when both devices are operating simultaneously, and updated. They also propose using two fluidic devices in series, a large meter followed by a smaller meter. The smaller meter is used to measure low flowrates until the maximum pressure drop is approached where a valve is opened and the smaller device is bypassed with the flow being measured by the larger meter only. They show that using a hybrid or two meter device the flow range required by the gas metering specifications is achievable.

The linearity of their device is out of specification but they suggest that provided the Reynolds number of a flow is known, using temperature measurements to provide the viscosity, then a calibration stored in electronic memory may be used to compensate for a non-linear meterfactor. They state that because further improvements in fluidic oscillator performance are likely then they are likely to have considerable potential for domestic gas metering applications.

1.8 Discussion of Existing Fluidic Oscillator Meters For Domestic Water Metering.

Existing fluidic oscillator designs fail to meet the requirements of the domestic water metering specifications because of the large operational flowrange required. The development of the target meters described by Honda and Yamasaki (1985), Kawano et al (1985) and Boucher and Mazharoglu (1988a) etc. do give significant reductions in the minimum point of oscillation but the oscillation frequency is also reduced by a factor of around 4 to 5 times. Boucher (1995) states that the oscillation frequency of his target device is four times slower than his feedback oscillator. This results in a high volume flow per pulse, giving a low meter resolution, and long time periods for a single oscillation cycle at low flowrates. The low resolution creates problems for the tracking of flow transients and low flow measurement making the present design of fluidic target meters unacceptable for use as a domestic water metering device.

Due to the low oscillation frequency of target meters work has been carried out to extend the range of the more practical feedback fluidic oscillators. The fluidic oscillator transducer described within this thesis is a feedback device. A recently published paper by Boucher (1995) describes a feedback oscillator with an extended range as shown in figure 1.42. Table 1.4 shows Boucher's results which imply that his target meter will make the Q_N1.0 Class D start up flow specification and that his extended range feedback meter will meet the Class D Q_{min} specification at 20°C.

Meter Type	E_{max}	$Re_{min}\alpha^{½}$	Q (lh^{-1})
Target	1.09	120	2.8
Feedback	1.19	275	6.1
Q_{min}- spec			7.5
Q_s - spec			3.75

Table 1.4 Values of Q_{min} for Different Types of Meter, Boucher (1995), and Q_{min} Required By Specifications.

The information in the table is quoted for a maximum pressure drop of 1 bar at a maximum flowrate of $1.0m^3 h^{-1}$. The maximum flowrate for a $Q_N1.0$ meter is $2.0m^3 h^{-1}$, this would result in a significantly smaller range than the table implies. It is not clear which figure Boucher used in his equations as the figure given may be a typing error. If a value of $2.0m^3 h^{-1}$ was used then it is apparent that Boucher has developed a feedback fluidic oscillator that will reach the $Q_N1.0$ Class D Q_{min} specification at 20°C and at temperatures above 12°C.

Given that the device has no non-return valve or any form of flow conditioning arrangement it is likely that the minimum point of oscillation for the present device would be increased after these units are fitted to the flowmeter. This is because it would be necessary to increase the scale of the device, reducing the minimum flowrate, to compensate for the additional pressure losses. A non-return valve is required because unless the meter is capable of reading reverse flows, which a fluidic oscillator is not, then the water meter must be fitted with a non-return mechanism to prevent customers from being charged for the same water twice.

The linearity of the extended range feedback meter is shown in figure 1.43. The percentage errors of the calibration curve are far from within the specification shown in figure 1.1. Boucher (1995) does not describe any methods of improving the linearity of the device such as altering the velocity profile of the inlet flow or attempting to reduce the effects of transition from fully laminar to fully turbulent flow conditions within the jet flow.

Boucher states that if a calibration for the meter is stored electronically in memory and the temperature of the water is known then the exact flowrate can be determined. The accuracy is then limited only by repeatability of performance against the stored calibration and the accuracy to which temperature and frequency can be measured. The latter is a complex problem involving considerations of frequency jitter, signal noise, sensor characteristics, sampling times and computational algorithms. He states that although these are readily soluble with laboratory instrumentation under steady flow conditions, the topic warrants separate investigation in order to specify achievable accuracy under field conditions.

The calibration of the extended range feedback meter is too complex to be used within a simple linearity and temperature compensation algorithm of the type used by the fluidic oscillator water meter described within this thesis.

The methods of signal detection employed by the fluidic oscillators described by Boucher employ thermal and/or pressure sensing of the oscillations. These methods are not practical for use within a domestic water meter because they do not cover the entire flow range and, thermal sensors in particular, have a high power consumption for an extended life battery powered device.

1.9 Work Required.

This section details the performance enhancements required to the Cranfield fluidic oscillator flowmeter to develop a fluidic water meter which is capable of meeting the BSI domestic water metering specifications.

Early fluidic oscillator transducers, based on the now enhanced design shown in figure 1.2, were for the Q_N1.0 Class C domestic water. These early meter designs did not have sufficient signal strength to allow electronic signal detection at low flowrates below the transitional flowrate, Q_t, and they had a very non-linear meterfactor response which was too complex to be used within an electronically stored lookup table. The range of the device was insufficient for the Class C minimum flowrate specification because the strength of oscillation was weak at the minimum flowrates and oscillation at low temperatures was very weak due to viscous damping effects. Also at the maximum flowrate, Q_{max}, the pressure drop across the meters was above 20 p.s.i. and out of specification.

The geometry of the prototype fluidic oscillator design required improvement to reduce the pressure drop across the device. The area of the fluidic oscillator most critical to pressure drop is the dimensions of the inlet nozzle geometry. The dimensions of the inlet nozzle are also critical to the velocity of jet flow, and therefore signal strength, and the minimum point of oscillation.

The signal strength of the fluidic oscillator needed to be increased at the low flowrates, below Q_t, so that electronic detection of the oscillation signal is possible throughout the flowrange of the device. Work was required to determine the most suitable magnetic material, optimum locations for the magnetic field and sensors and the optimum geometry of the magnet configuration.

The linearity of the fluidic oscillator required significant improvement so that the meterfactor response curve is not too complex for a relatively simple linearity and

temperature compensation algorithm. The compensation algorithm must be relatively simple because it is for a mass produced low power production meter. Also the frequency response of the meter must be such that the meter has adequate resolution throughout the range.

The range of the oscillator required to be increased to enable the detection of Class D minimum flowrate requirement with a reasonable margin of safety for low temperature measurement. Also the strength of oscillation jet switching at low flowrates needed to be improved to boost the signal strength and increase the margin of safety for the Class C minimum flowrate specification.

1.10 Outline of Thesis.

In this chapter the BSI domestic water metering specifications have been given and the need for a novel meter with no moving parts for domestic water metering purposes has been described. The principles of operation for the fluidic oscillator water have been described and the advantages of fluidic flow measurement over existing mechanical metering technologies detailed. The specific performance criteria of fluidic oscillators for use as a domestic water meter have been considered. A literature review of fluidic oscillators is given and existing fluidic oscillators developed for domestic metering discussed. The work required to enhance the design of the Cranfield fluidic oscillator for use as a production domestic water meter is described.

Chapter 2 describes the Cranfield Class D fluidic oscillator flow rig and calibration procedures.

In chapter 3 the work carried out to improve the signal strength of the Cranfield fluidic oscillator at low flowrates is described and the improvements made to the nozzle geometry to reduce the pressure drop across the device at the maximum flowrate.

Chapter 4 details the development of flow conditioning devices which improve the linearity of the fluidic oscillator. The changes in meterfactor response and the flow conditioning mechanisms are discussed along with the linearity requirements for the simple compensation algorithm used by the production meter.

Investigations into methods of reducing the minimum point of oscillation for the fluidic oscillator are detailed in Chapter 5. The successful methods developed are highlighted presenting the reductions in flowrate achieved and the effects on oscillation strength at the minimum flowrate speciation.

The effects on the meter linearity caused by the modifications carried out to reduce the minimum point of oscillation are described in Chapter 6. The possible combinations of low flow performance modifications are examined for their combined effects on meter linearity. A compromise between linearity and low flow performance is discussed considering the probable advancement in linearity compensation methods.

Finally chapter 7 discusses the results of the work presented in this thesis and proposes possible future developments of the fluidic oscillator water meter.

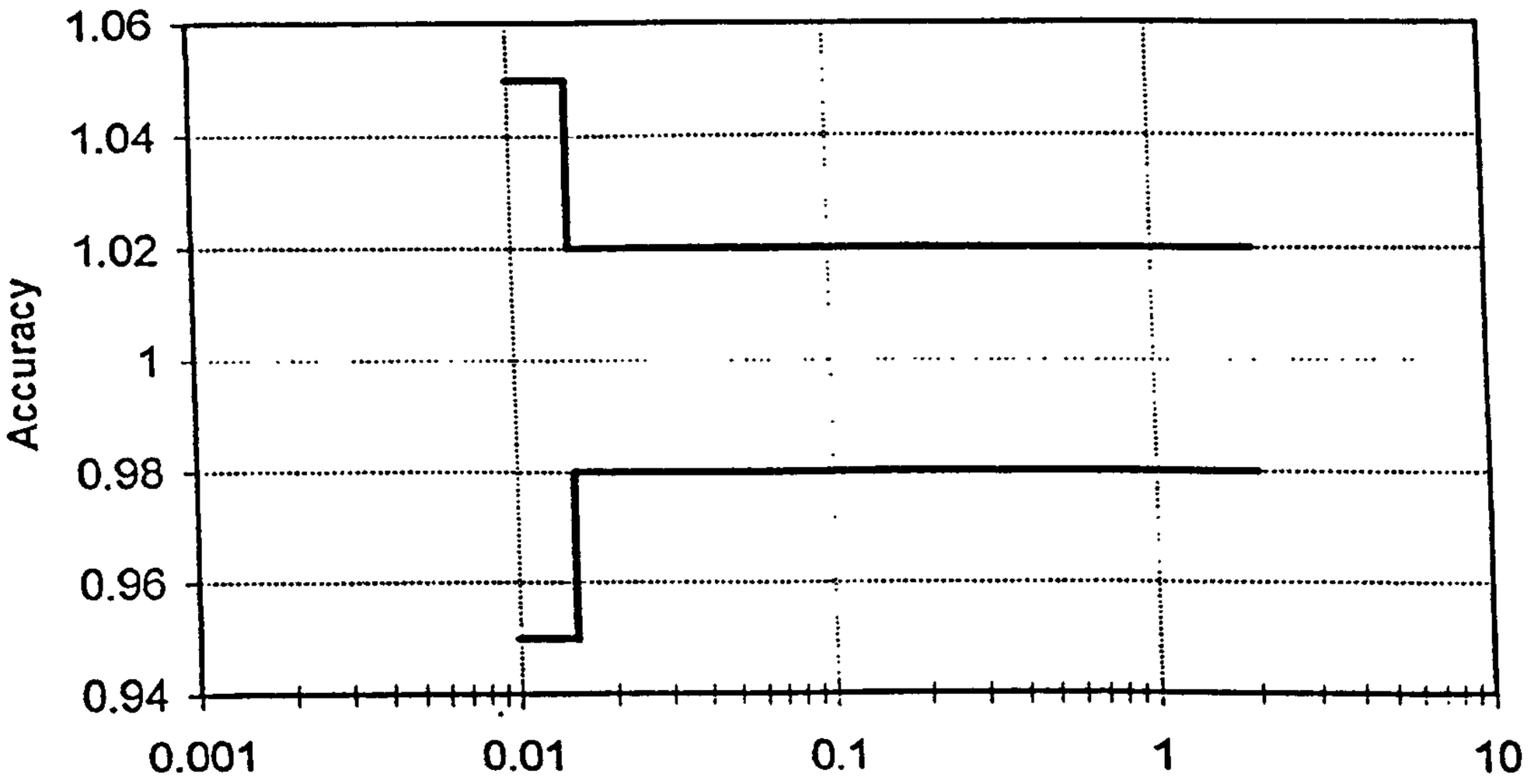

Figure 1.1: Metrological Accuracy Specifications Q_N1.0 Water Meter.

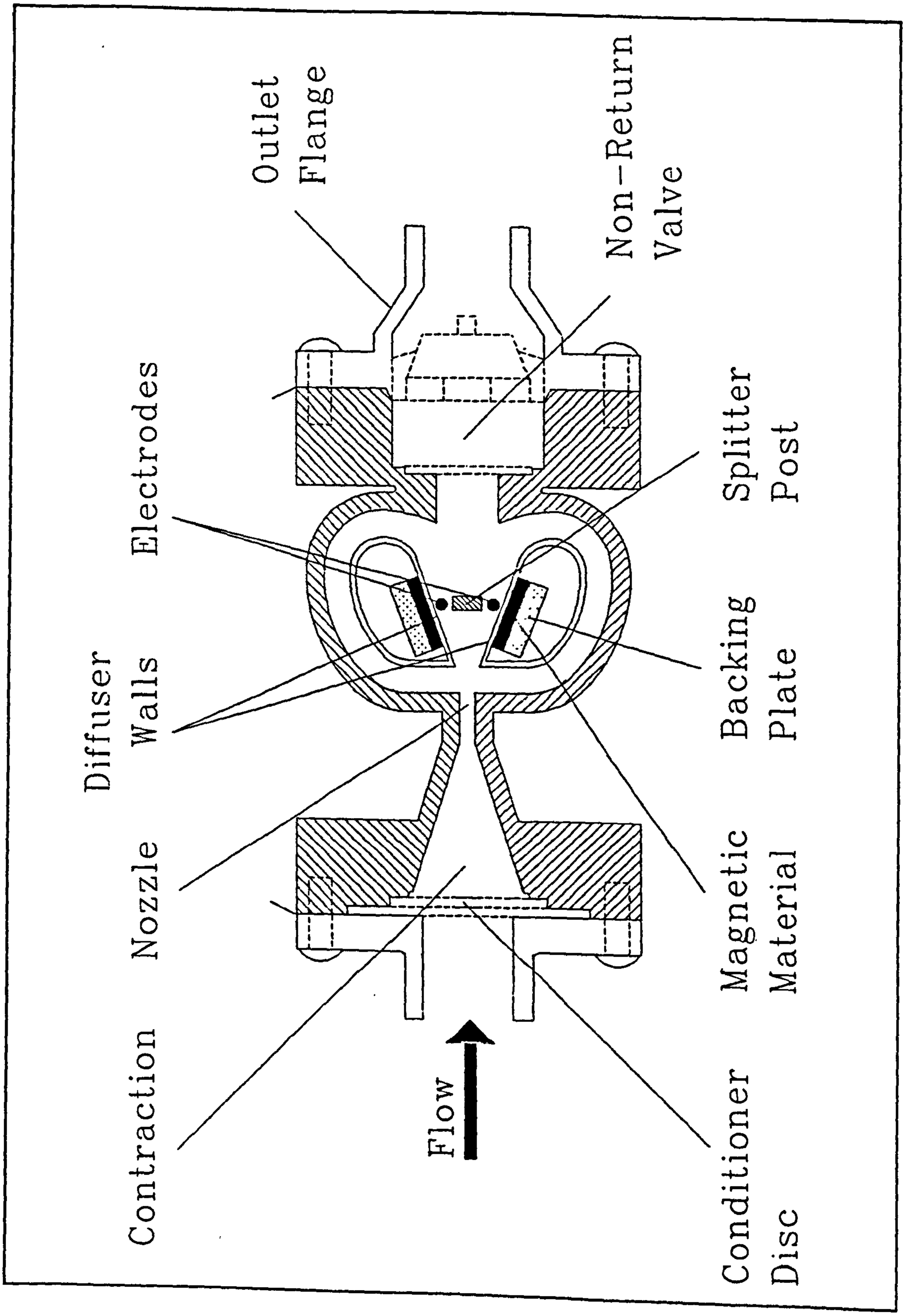

Figure 1.2: Geometry of Fluidic Oscillator Water Meter Transducer.

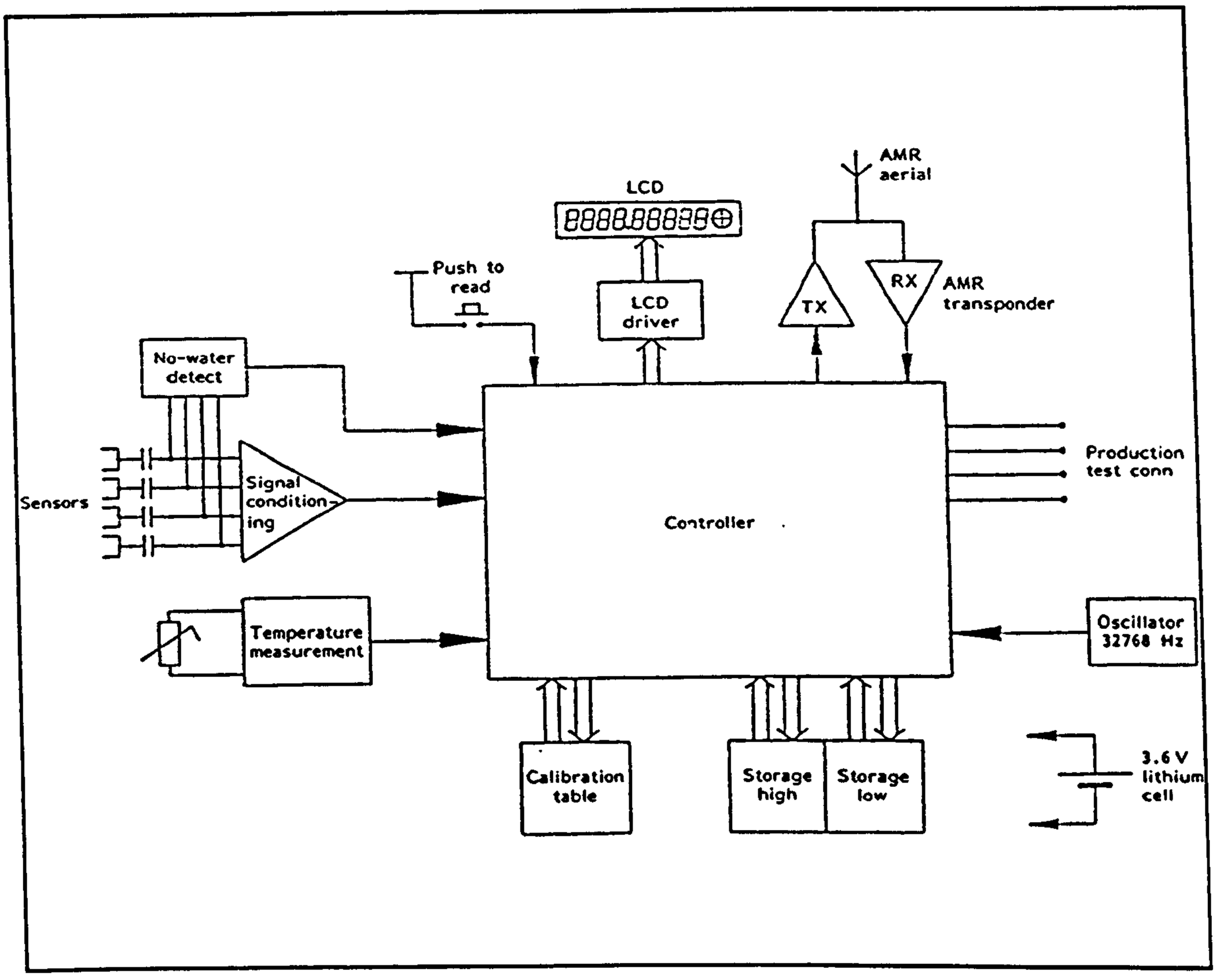

Figure 1.3: Schematic of Fluidic Water Meter Signal Processing.

Figure 1.4: Fluidic Oscillator Q_N1.0 Domestic Water Meter.

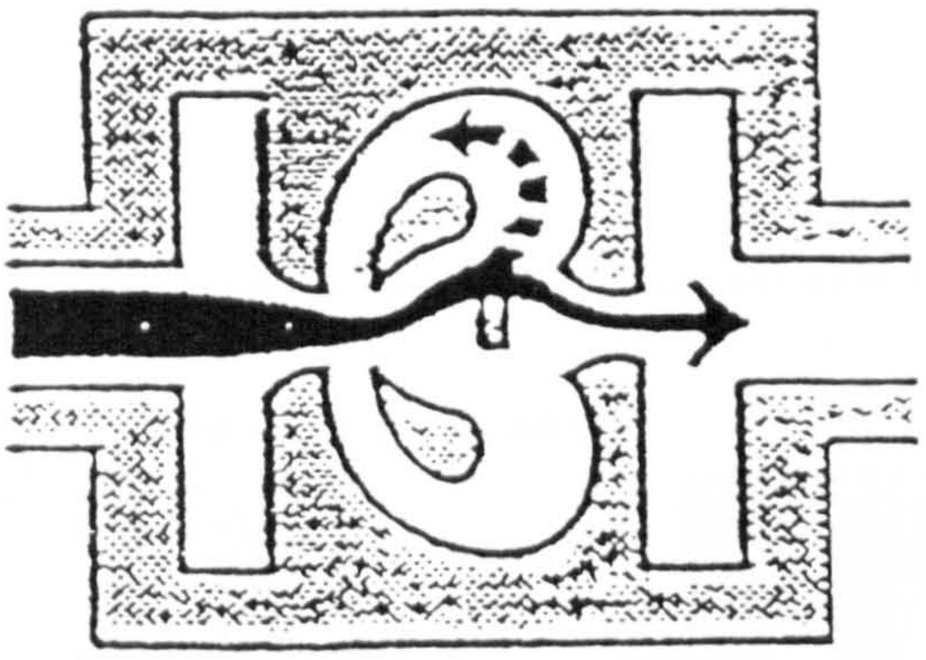

Figure 1.5: Osaka Gas Feedback Oscillator.

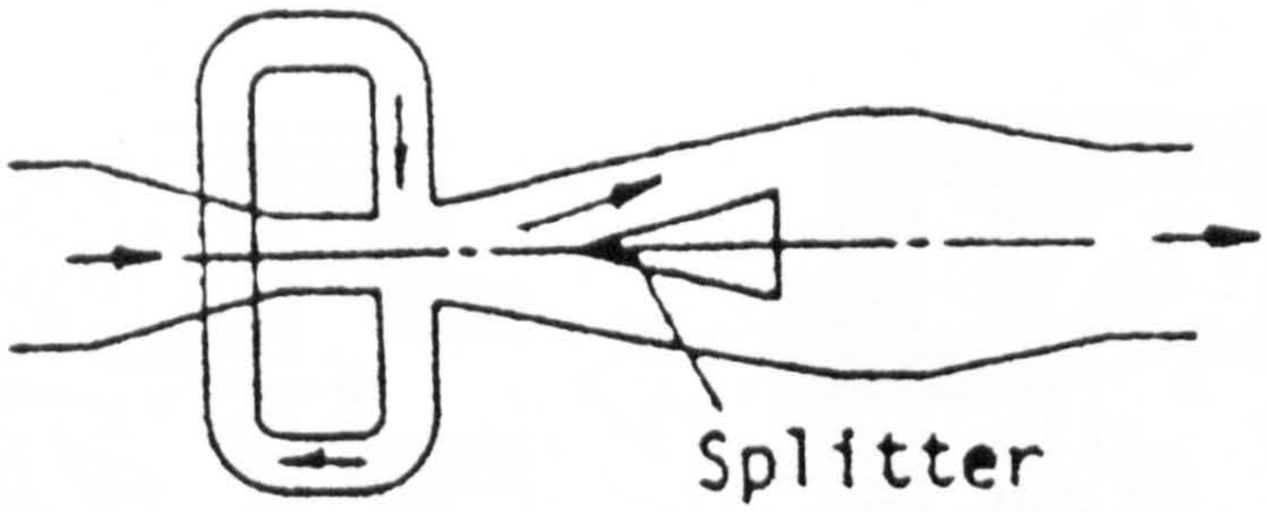

Figure 1.6: Relaxation Oscillator As Investigated By Shakouchi (1988).

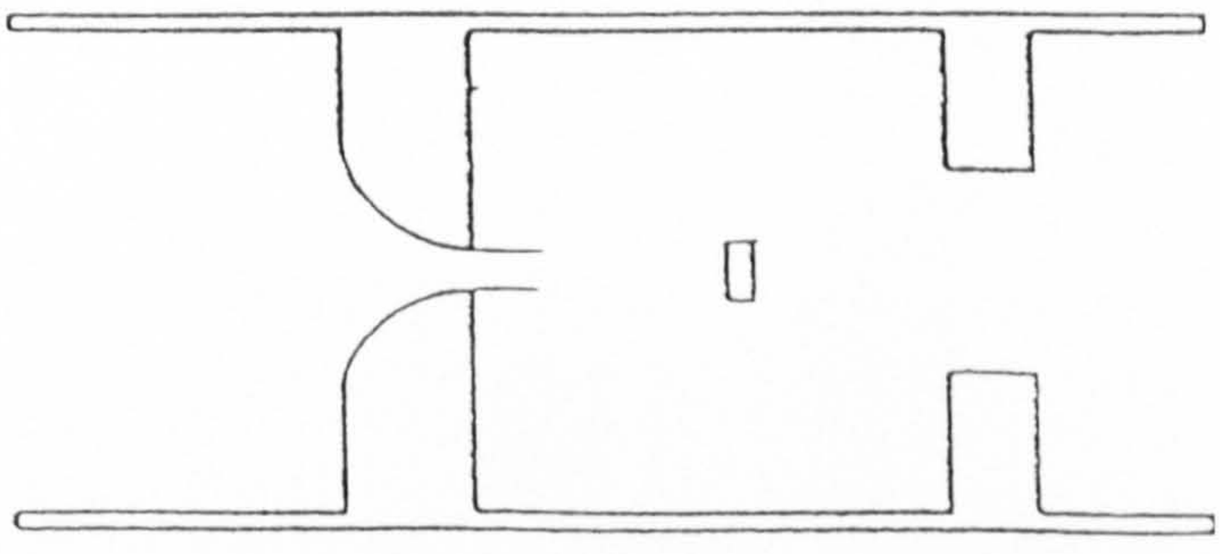

Figure 1.7: Fluidic Target Meter As Investigated By Honda and Yamasaki (1985).

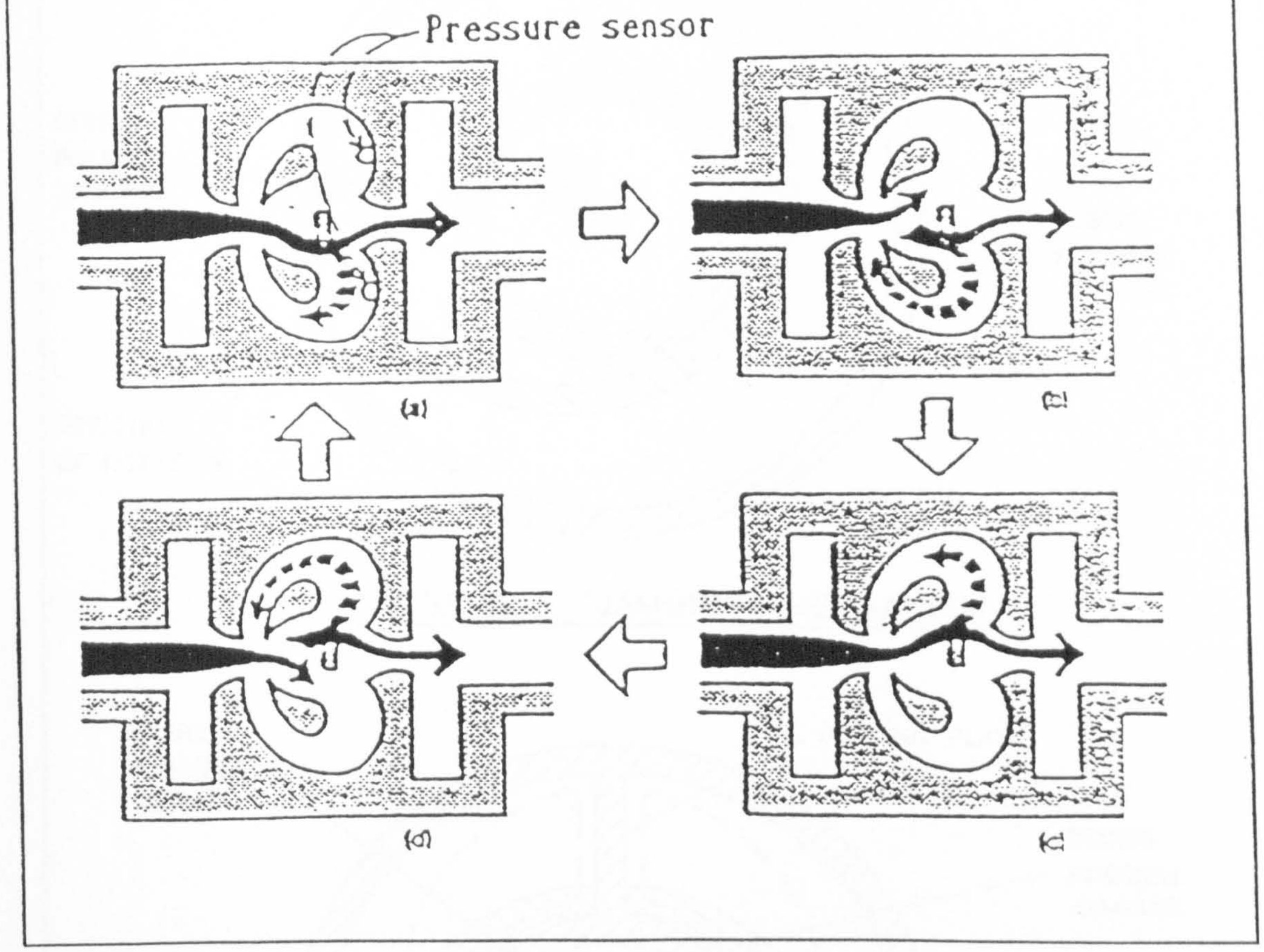

Figure 1.8: Fluidic Oscillation Cycle For Osaka Gas Meter.

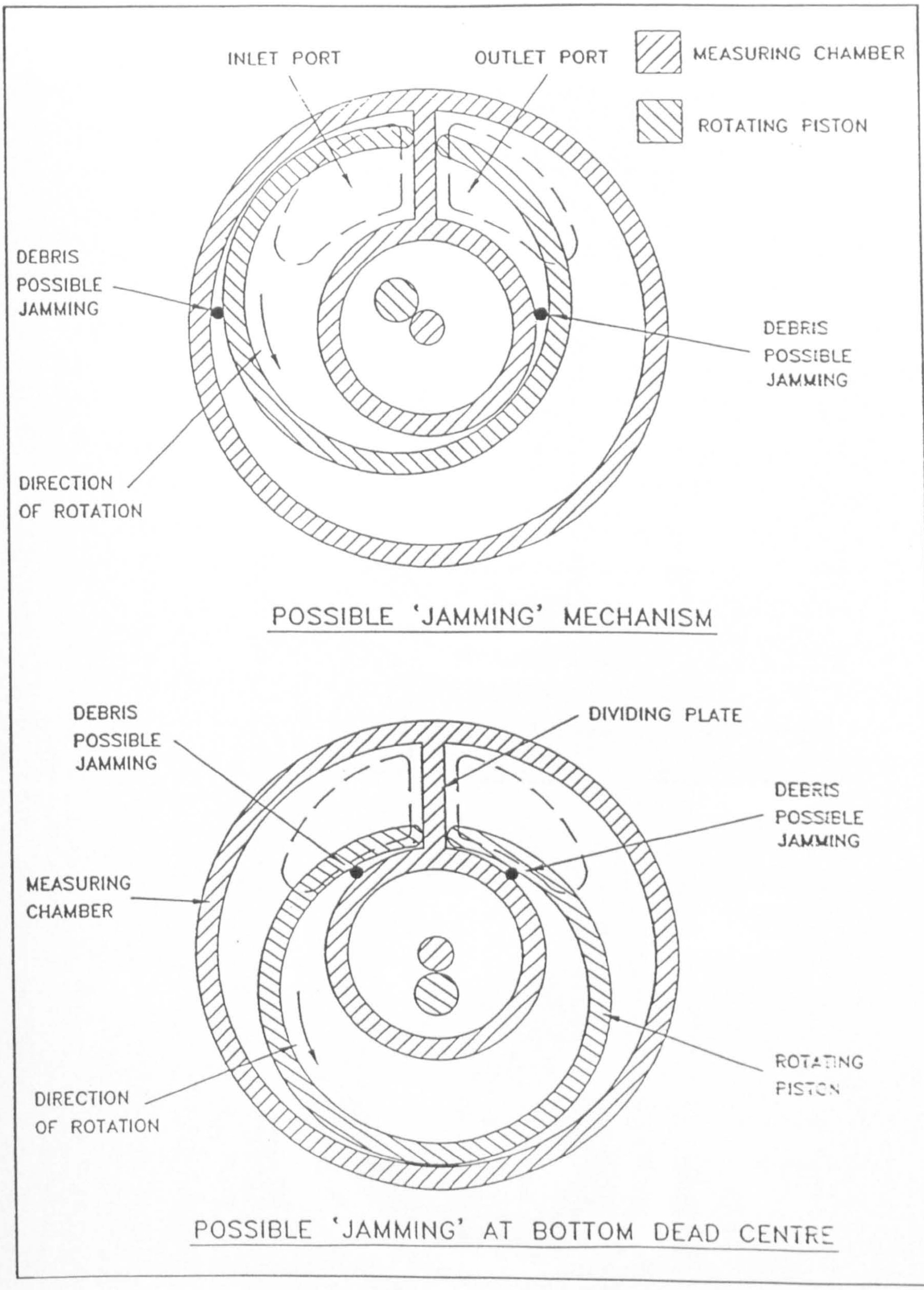

Figure 1.9: Jamming Mechanisms of Particulate Matter Within Mechanical Water Meters, Chiwanga (1994).

Figure 1.10: Particulate Matter Passing Through Fluidic Oscillator.

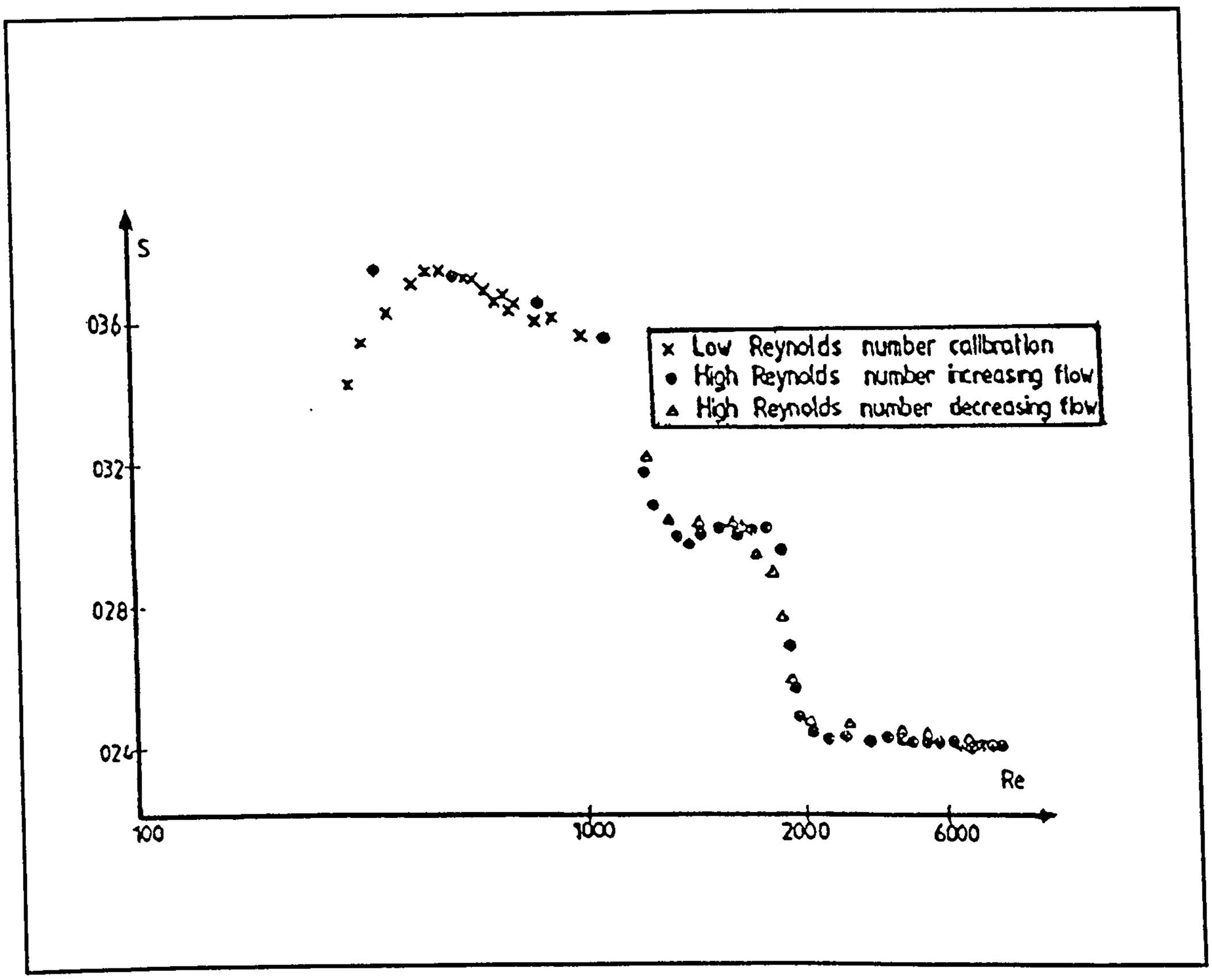

Figure 1.11: Variation of Strouhal Number With Reynolds Number For Feedback Oscillator, Boucher (1989).

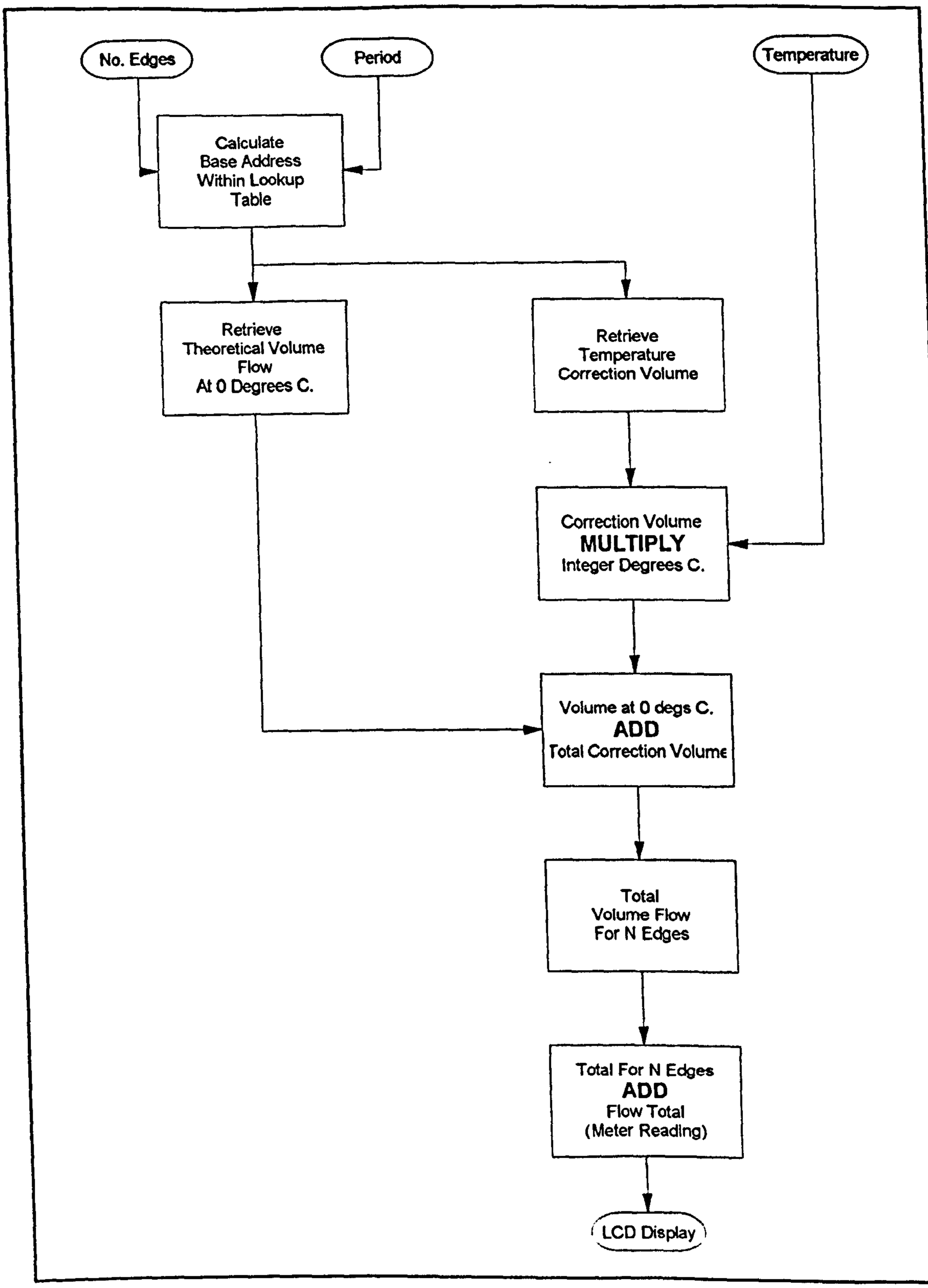

Figure 1.12: Block Diagram Depicting Operation of Temperature Compensation Scheme.

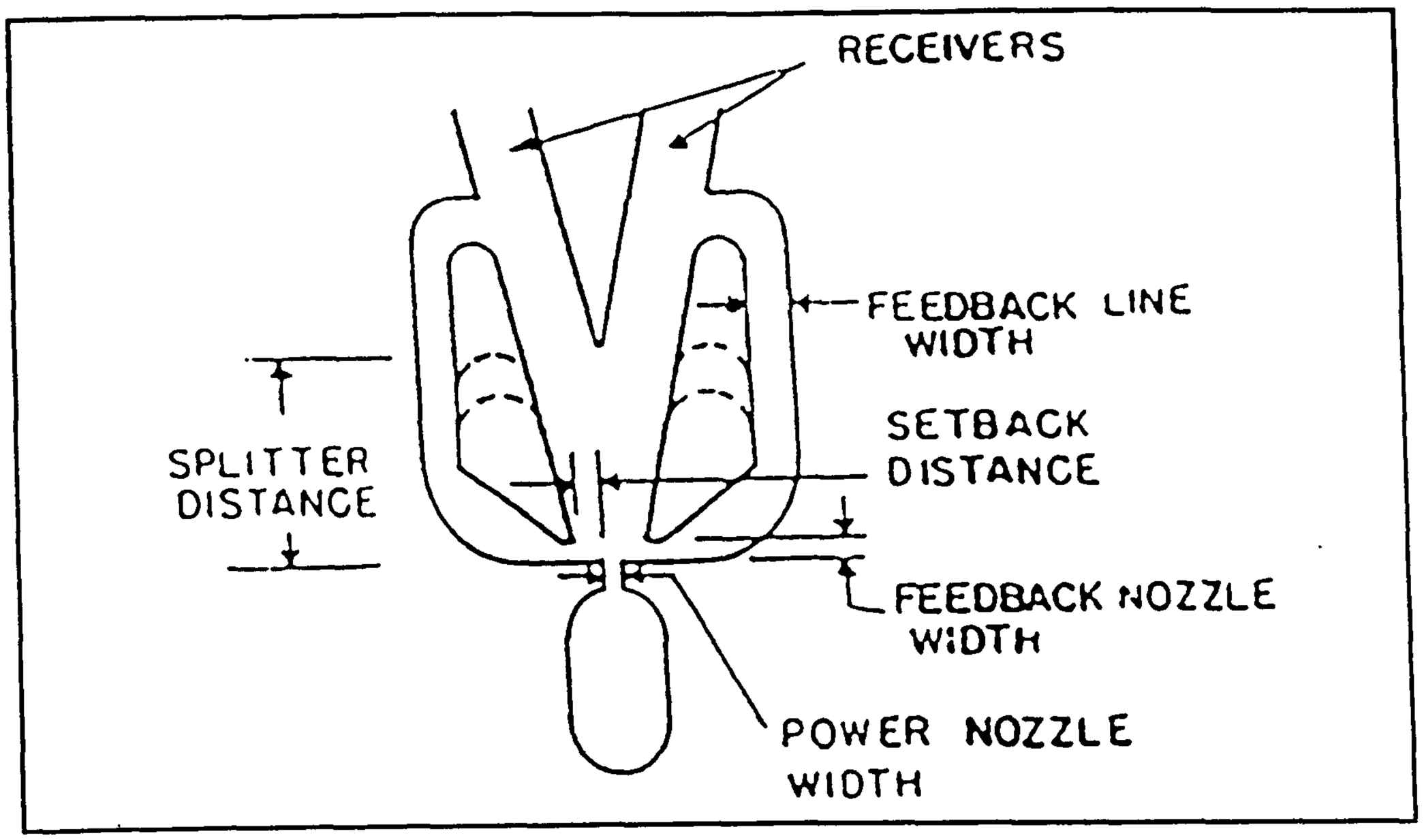

Figure 1.13: Feedback Fluidic Oscillator Investigated By Wilson et al (1970).

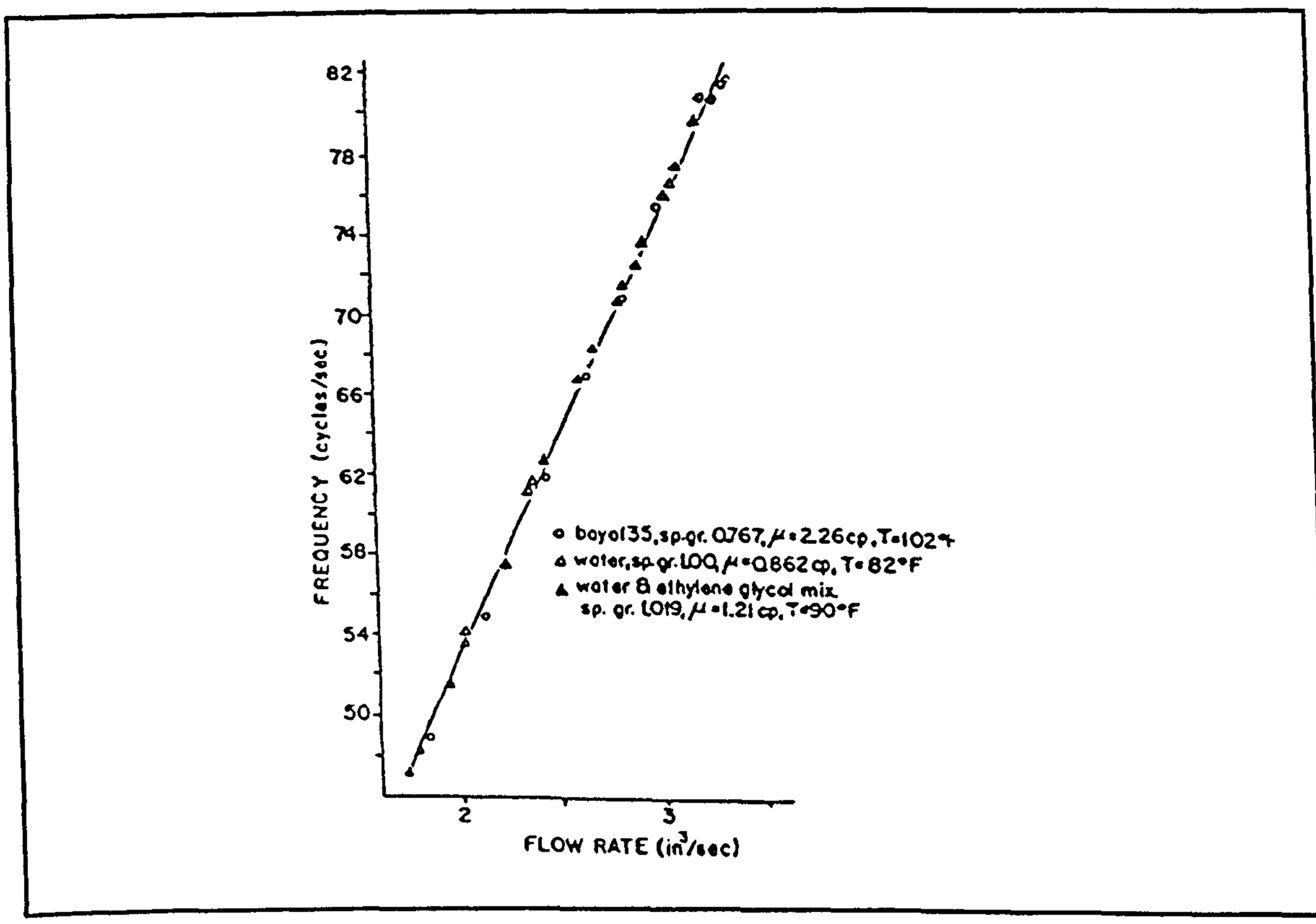

Figure 1.14: Frequency Against Flowrate For Several Test Fluids, Wilson et al (1970).

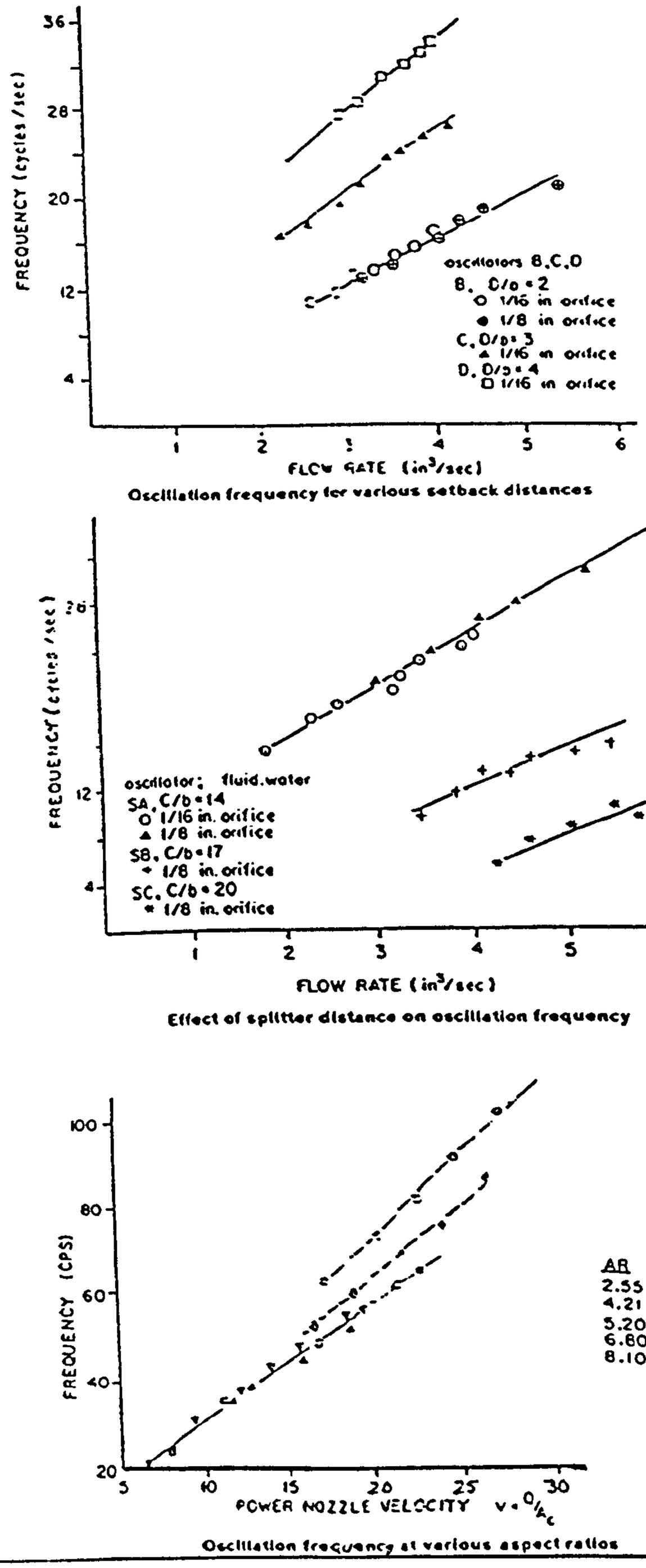

Figure 1.15: Effect On Oscillation Frequency Caused By Altering Design Parameters, Wilson et al (1970).

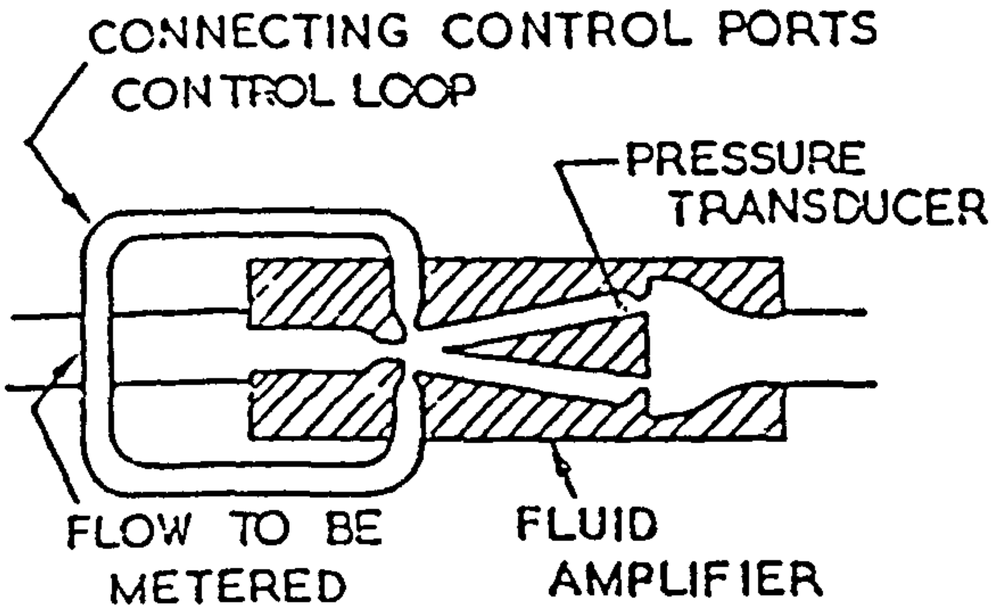

a. FLUIDIC FLOWMETER

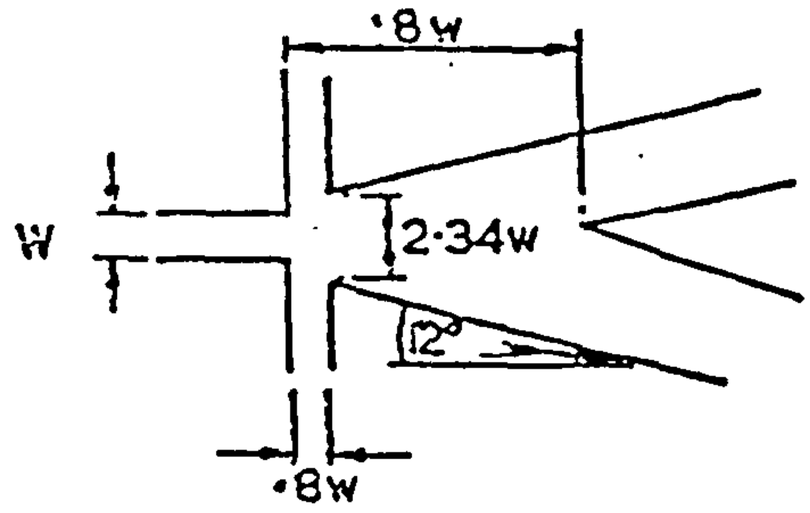

DEPTH = aw

b AMPLIFIER DESIGN

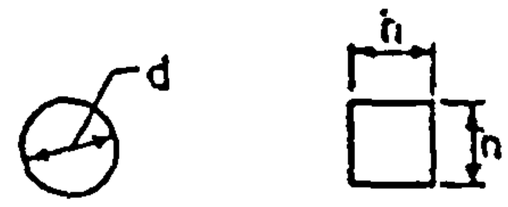

CONTROL LOOP
CROSS-SECTIONS

OSCILLATOR	O1	O2	O3
Wmm	3·28	1·6	6·35
a	4	6	1
dmm	9·5	——	25·4
hmm	——	9·5	——

c. DATA RELATING TO O1, O2, & O3.

Figure 1.16: Relaxation Oscillator Designs Investigated By Tippetts et al (1971).

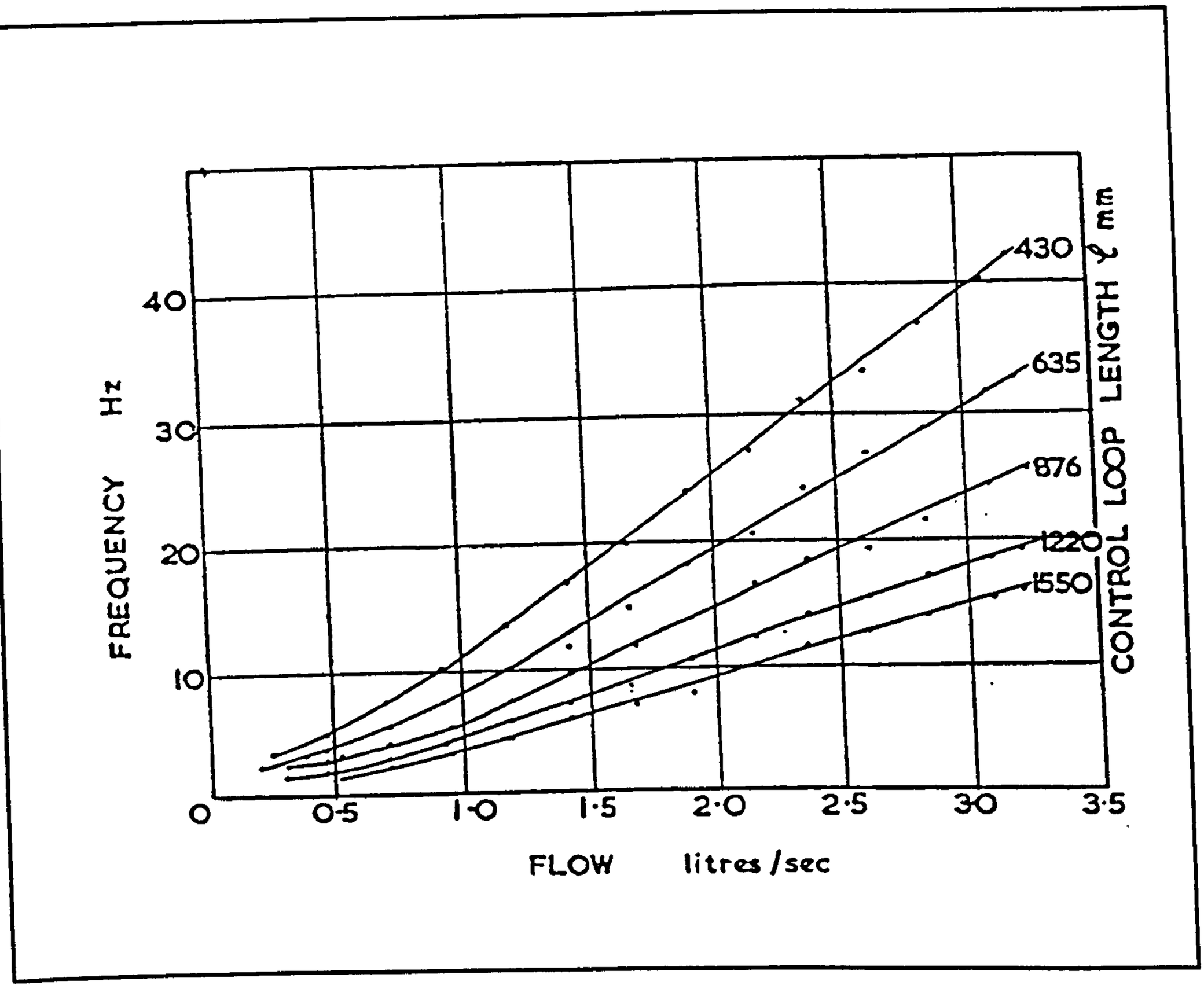

Figure 1.17: Effect On Oscillation Frequency Caused By Altering Control Loop Length, Tippetts et al (1970).

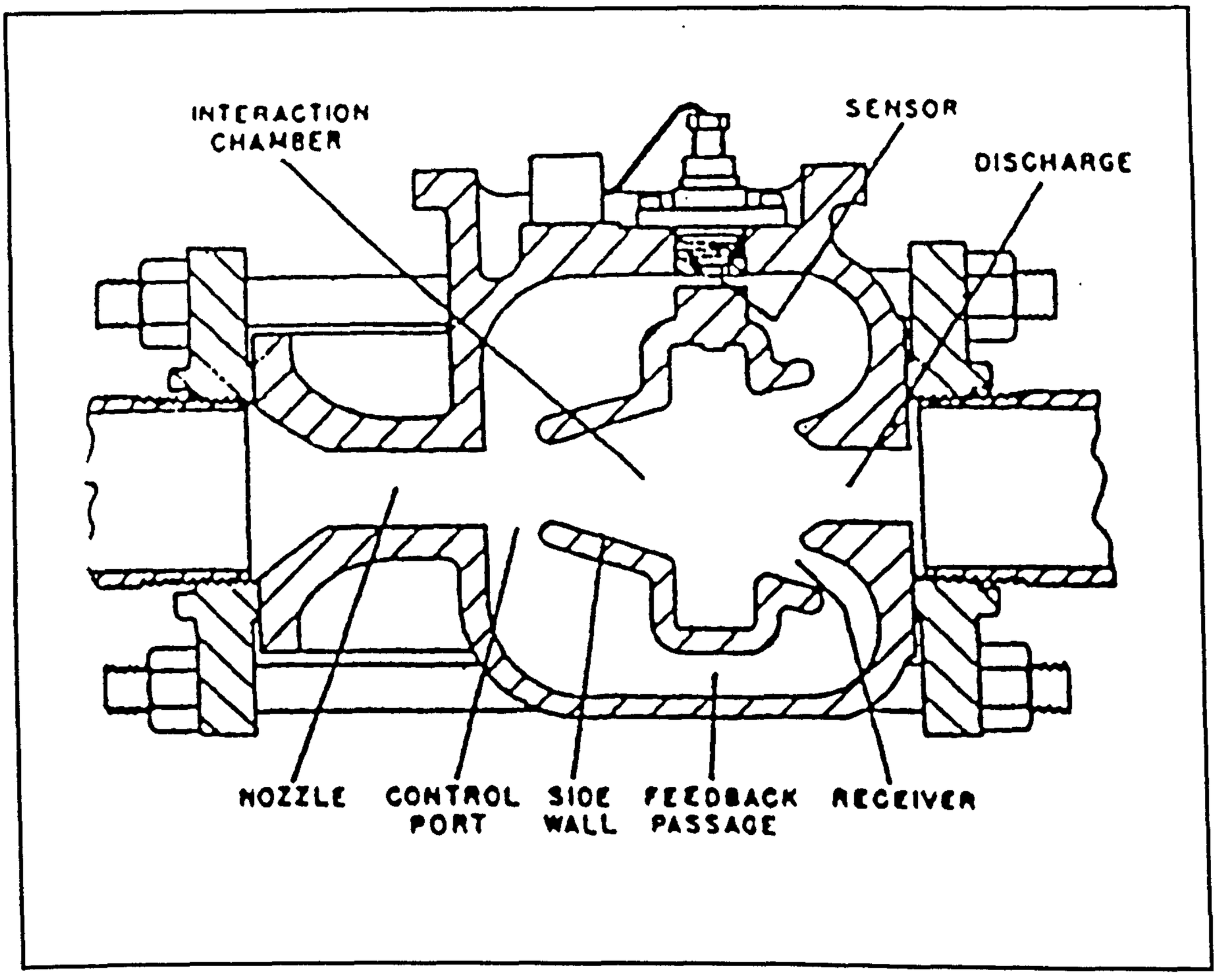

Figure 1.18: Commercial Feedback Fluidic Oscillator, Adams (1973).

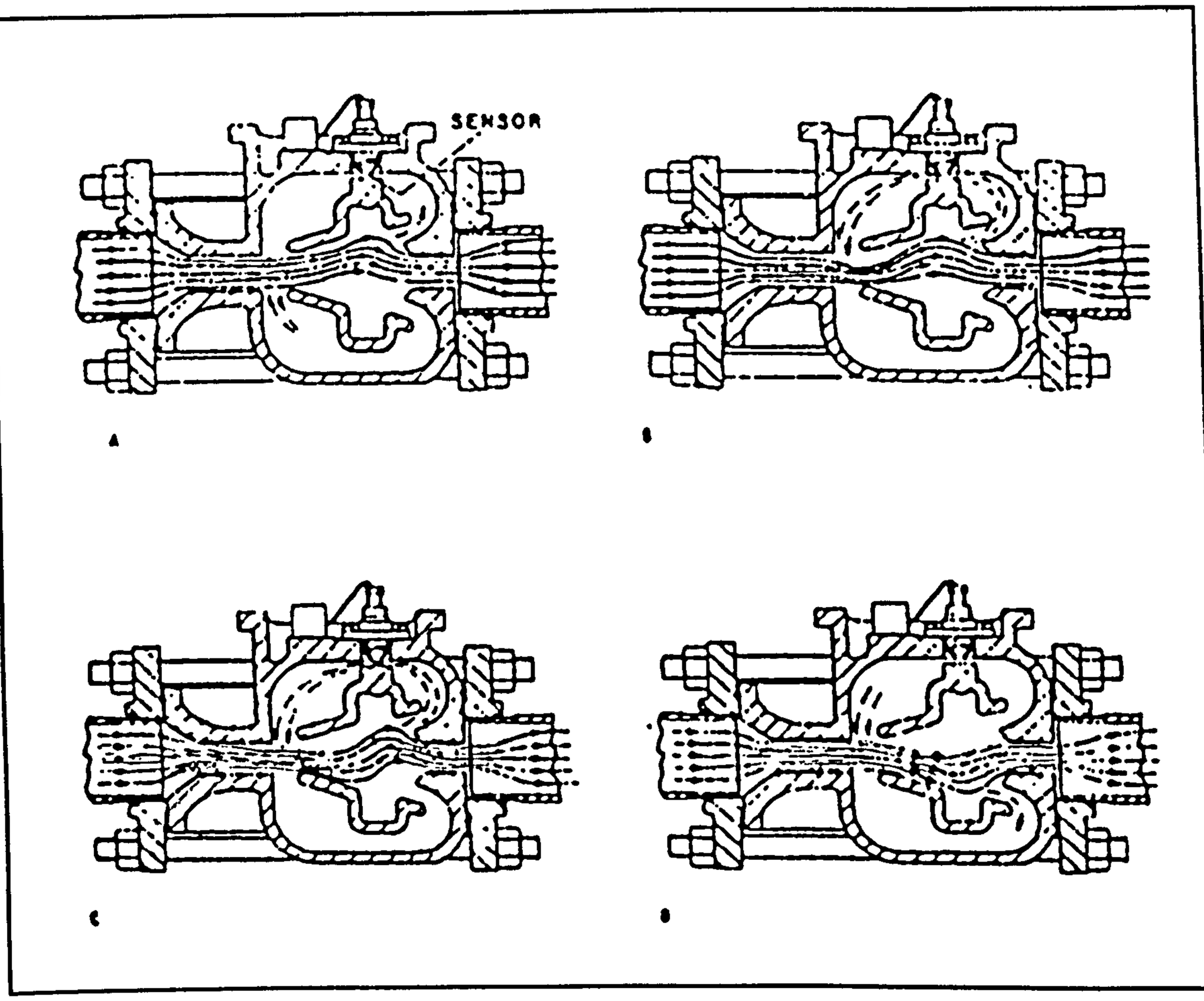

Figure 1.19: Oscillation Cycle For Feedback Fluidic Oscillator, Adams (1973).

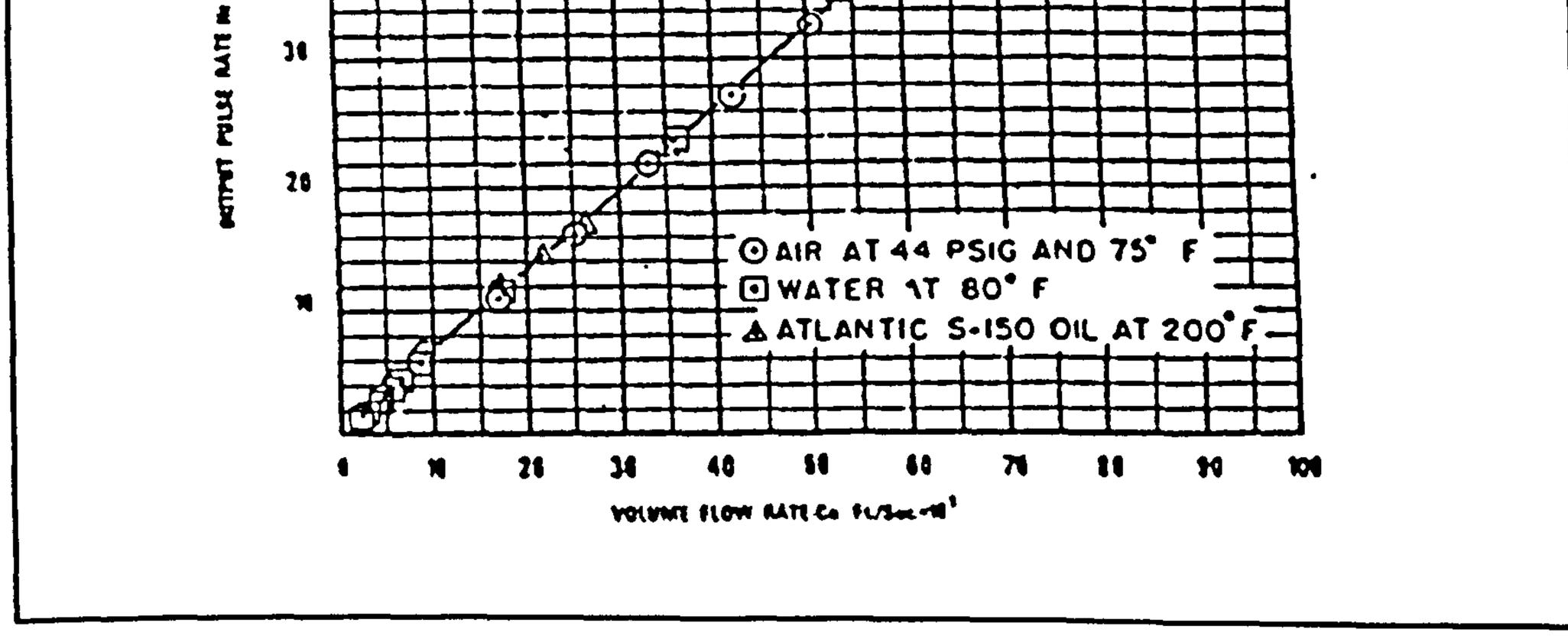

Figure 1.20: Frequency Against Flowrate Using Fluids of Different Densities, Adams (1973).

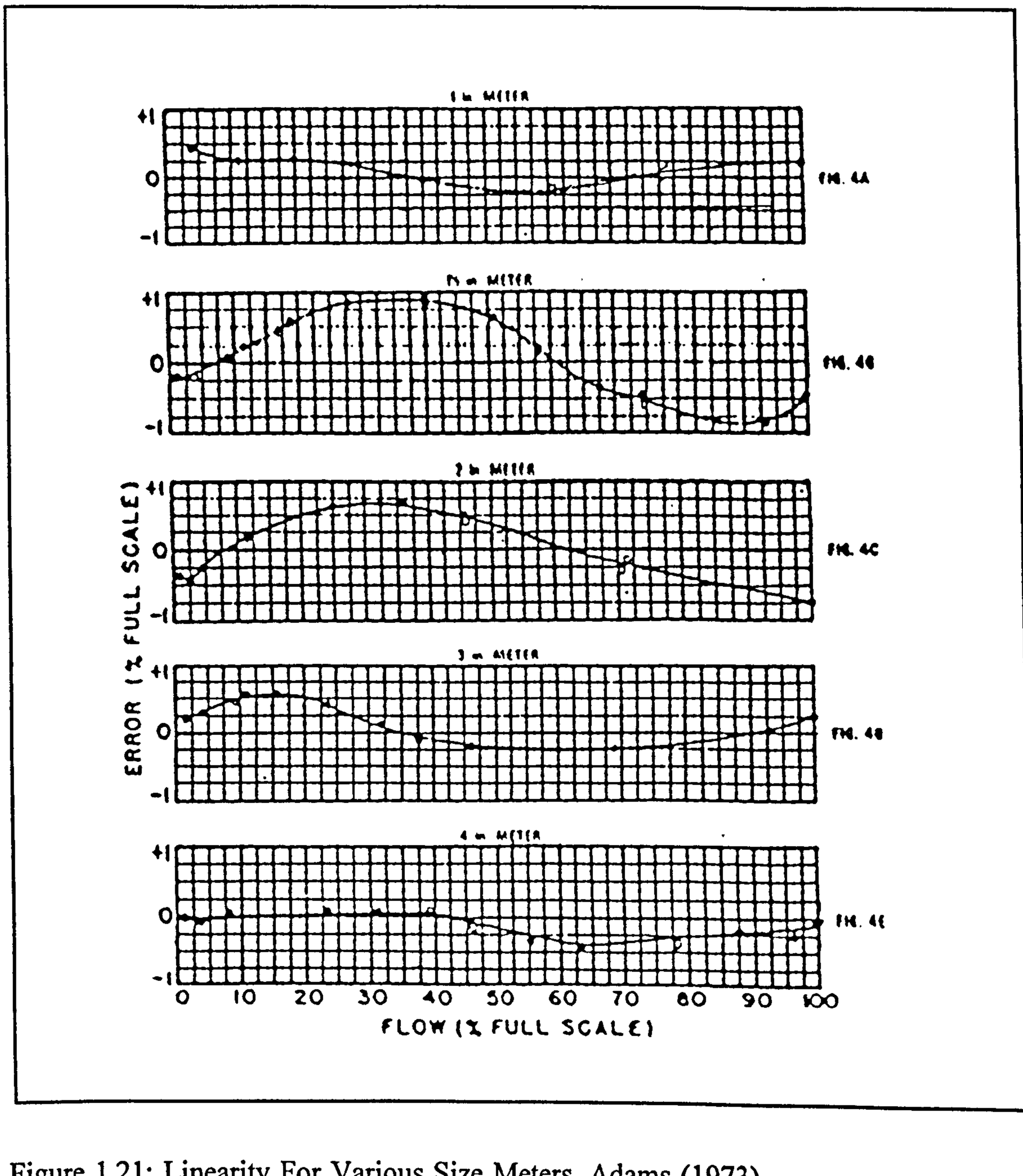

Figure 1.21: Linearity For Various Size Meters, Adams (1973).

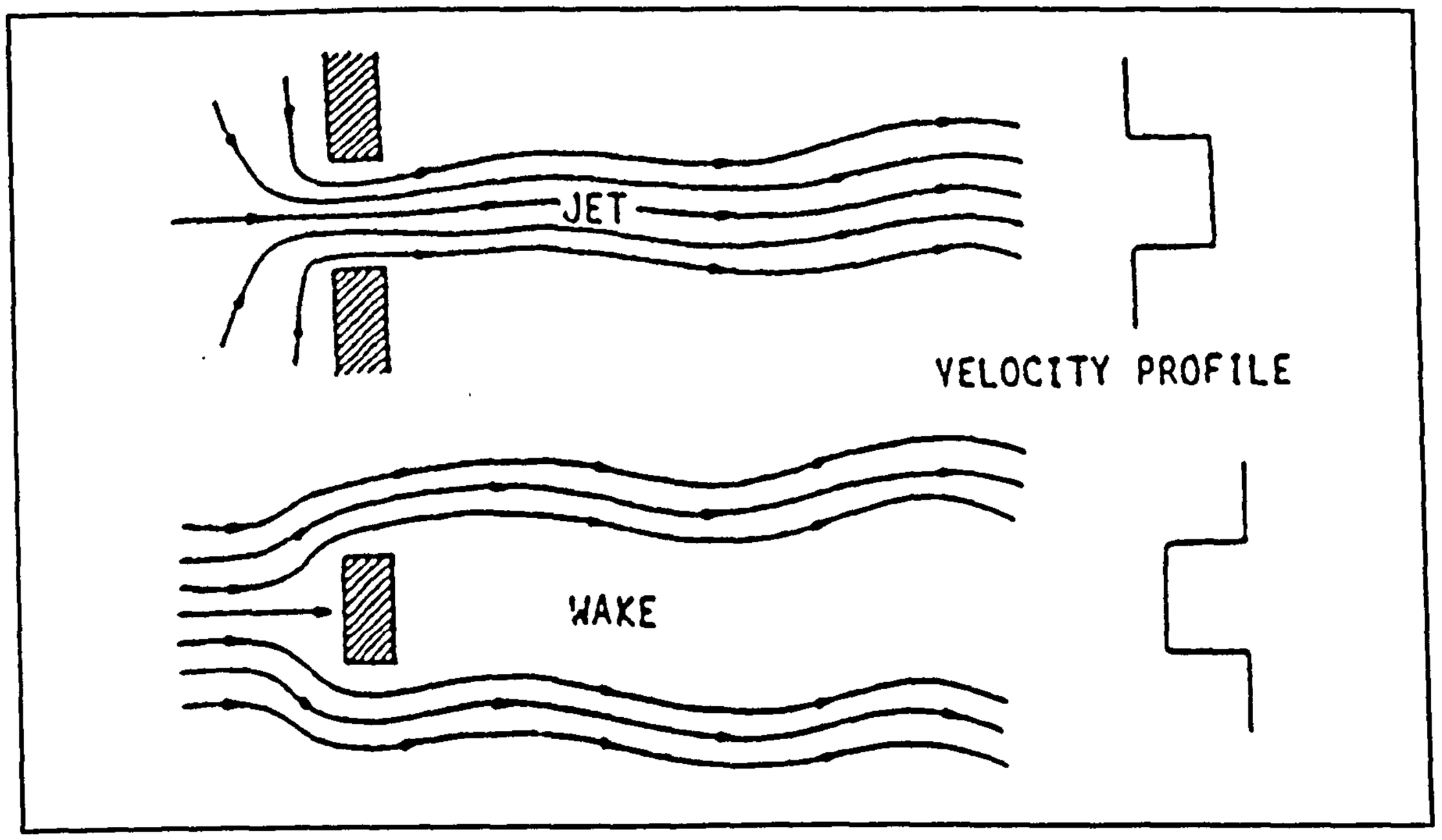

Figure 1.22: Complementary Relationship Between Jets and Wakes,
Honda and Yamasaki (1985).

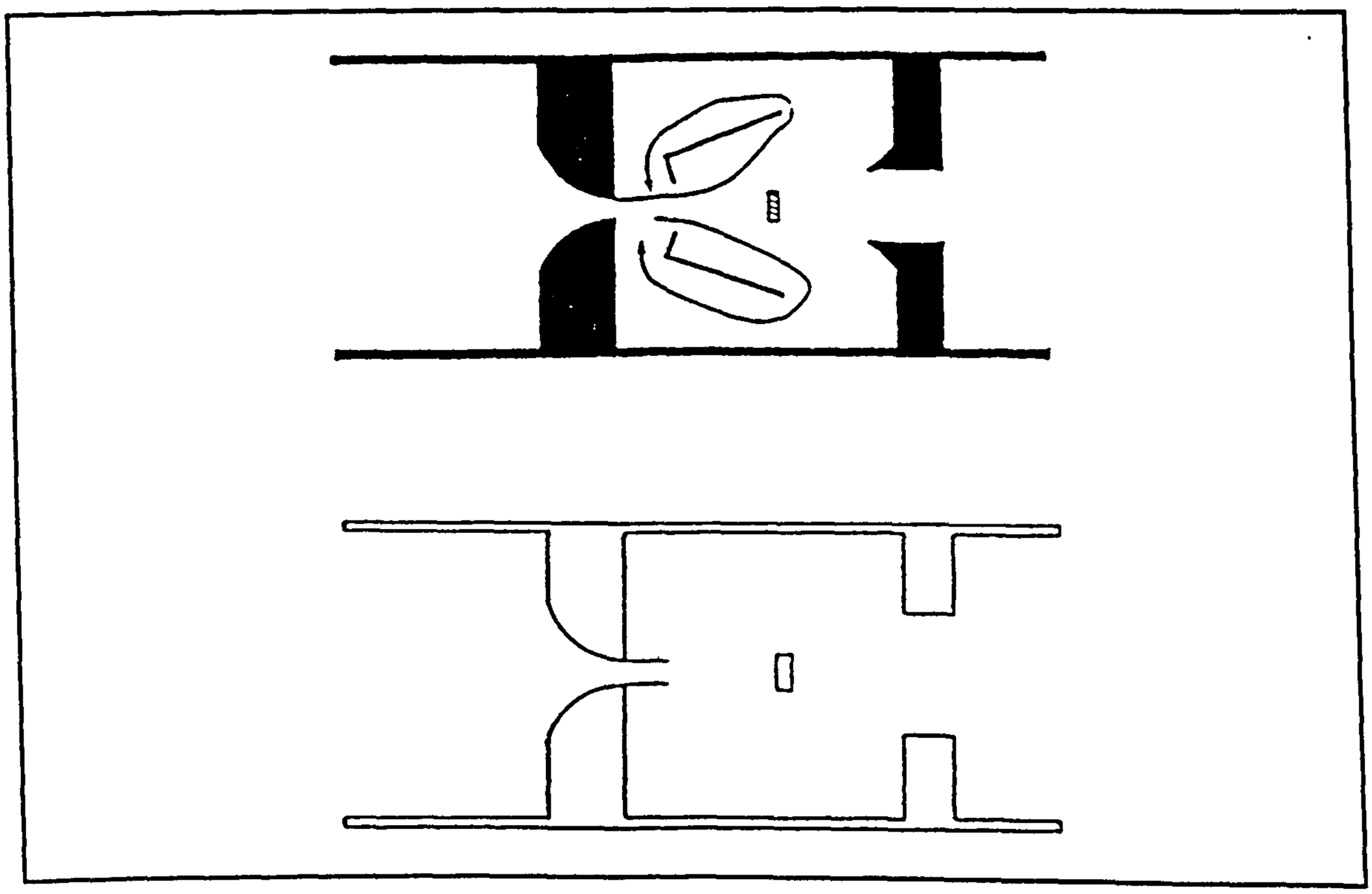

Figure 1.23: Fluidic Target Meter and Feedback Oscillator From Which It Was Derived,
Honda and Yamasaki (1985).

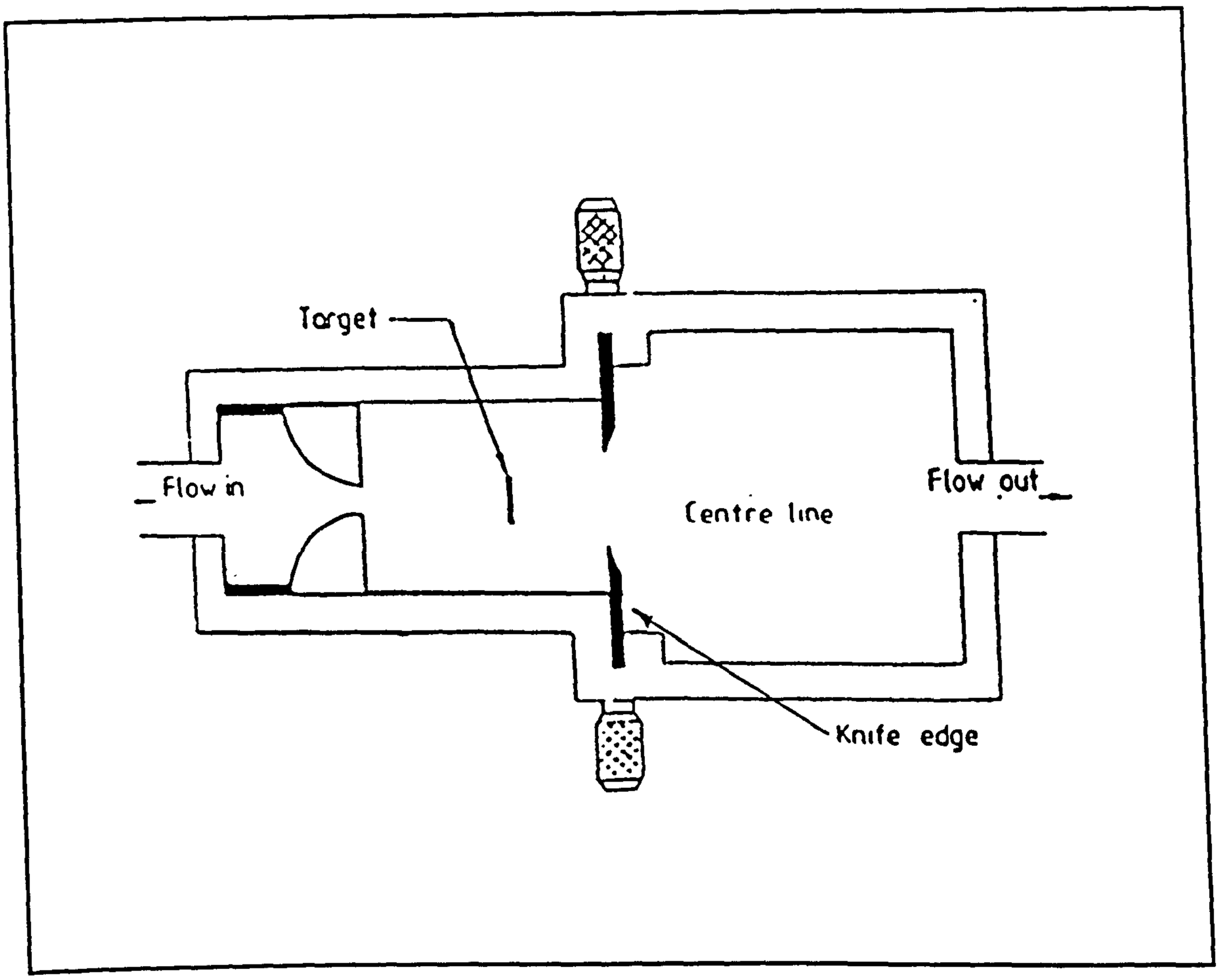

Figure 1.24: Fluidic Target Meter Developed By Boucher and Mazharoglu (1988).

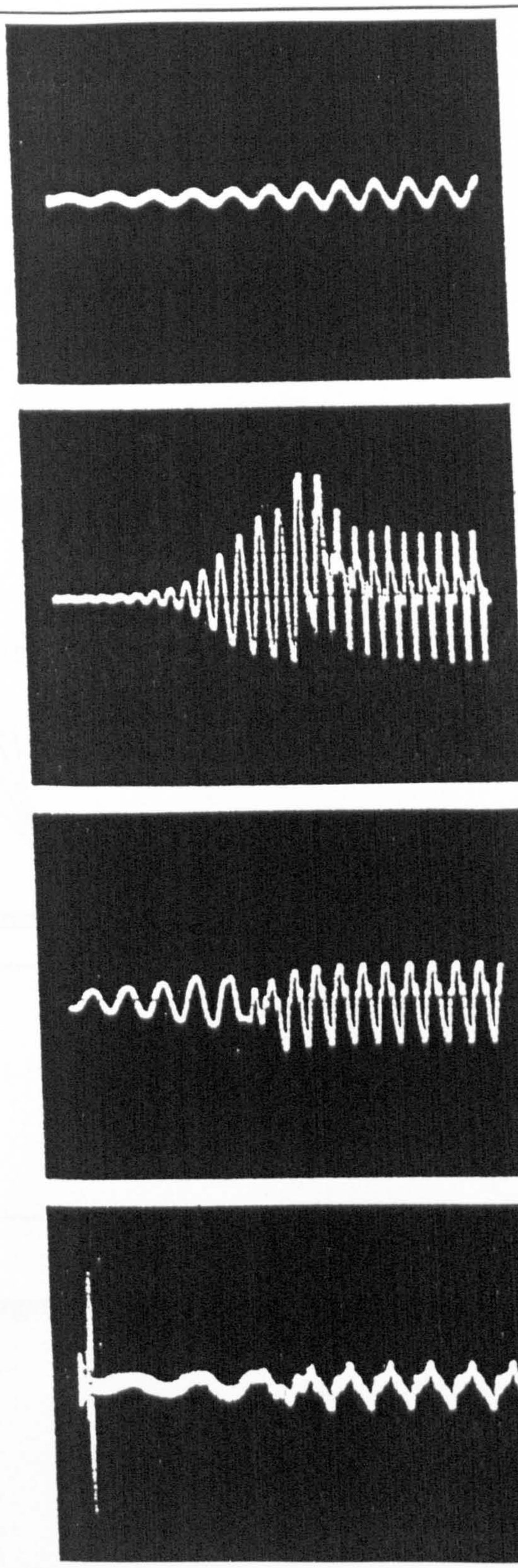

Figure 1.25: Beginning of Oscillations For Target Meter With Varying Design Parameters, Boucher and Mazharoglu (1988).

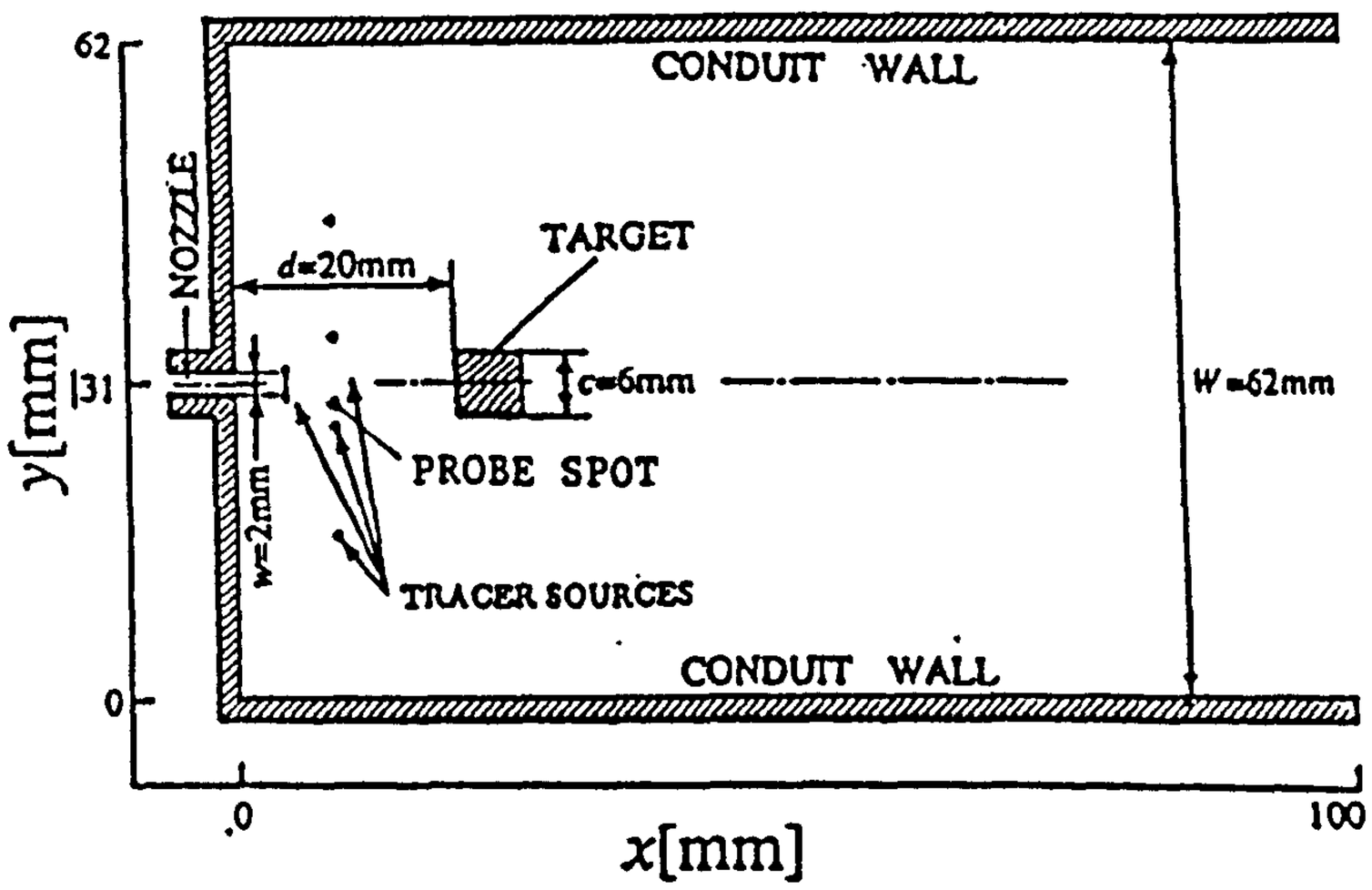

Figure 1.26: Simple Target Meter, Yamasaki et al (1988).

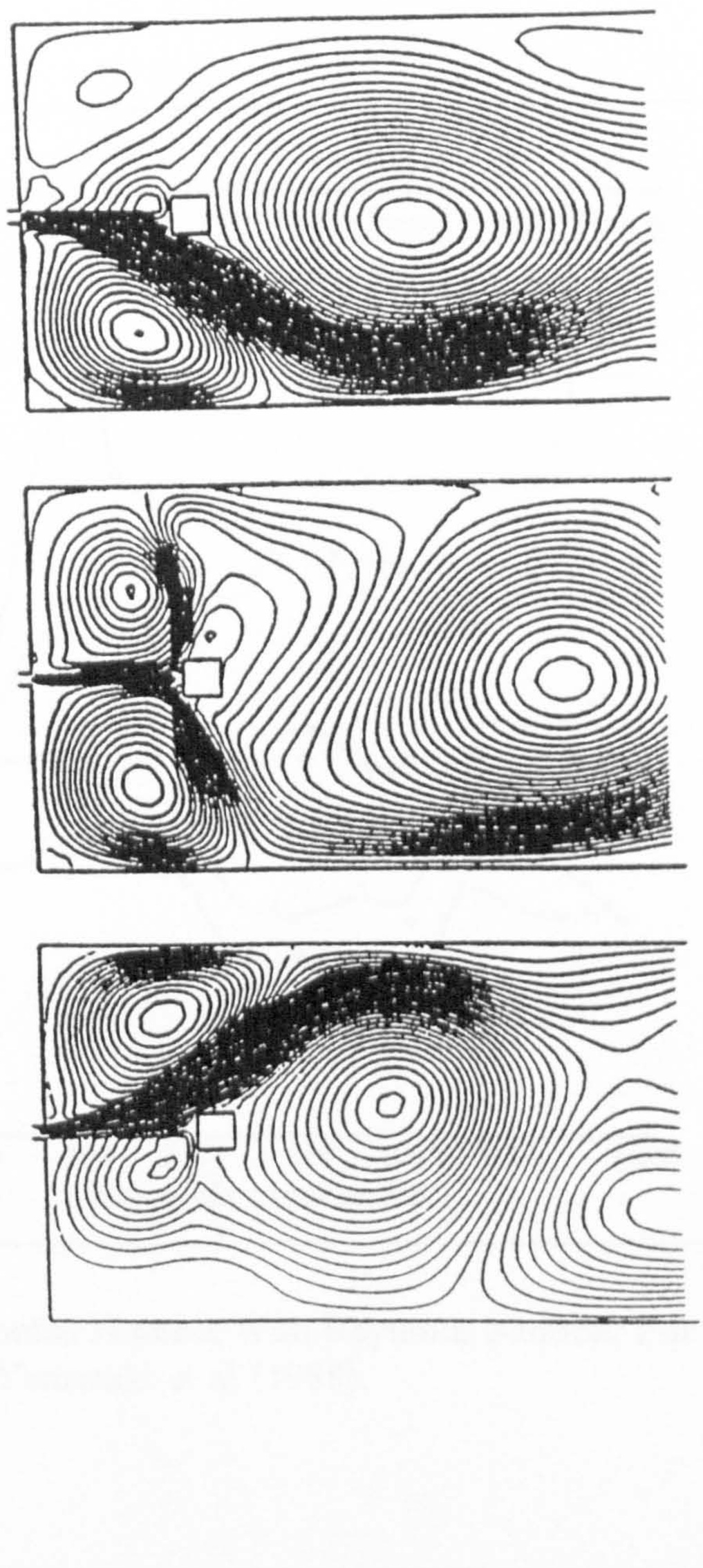

Figure 1.27: Numerically Generated Stream Lines Showing Oscillation of Jet For Simple Target Meter, Yamasaki et al (1988).

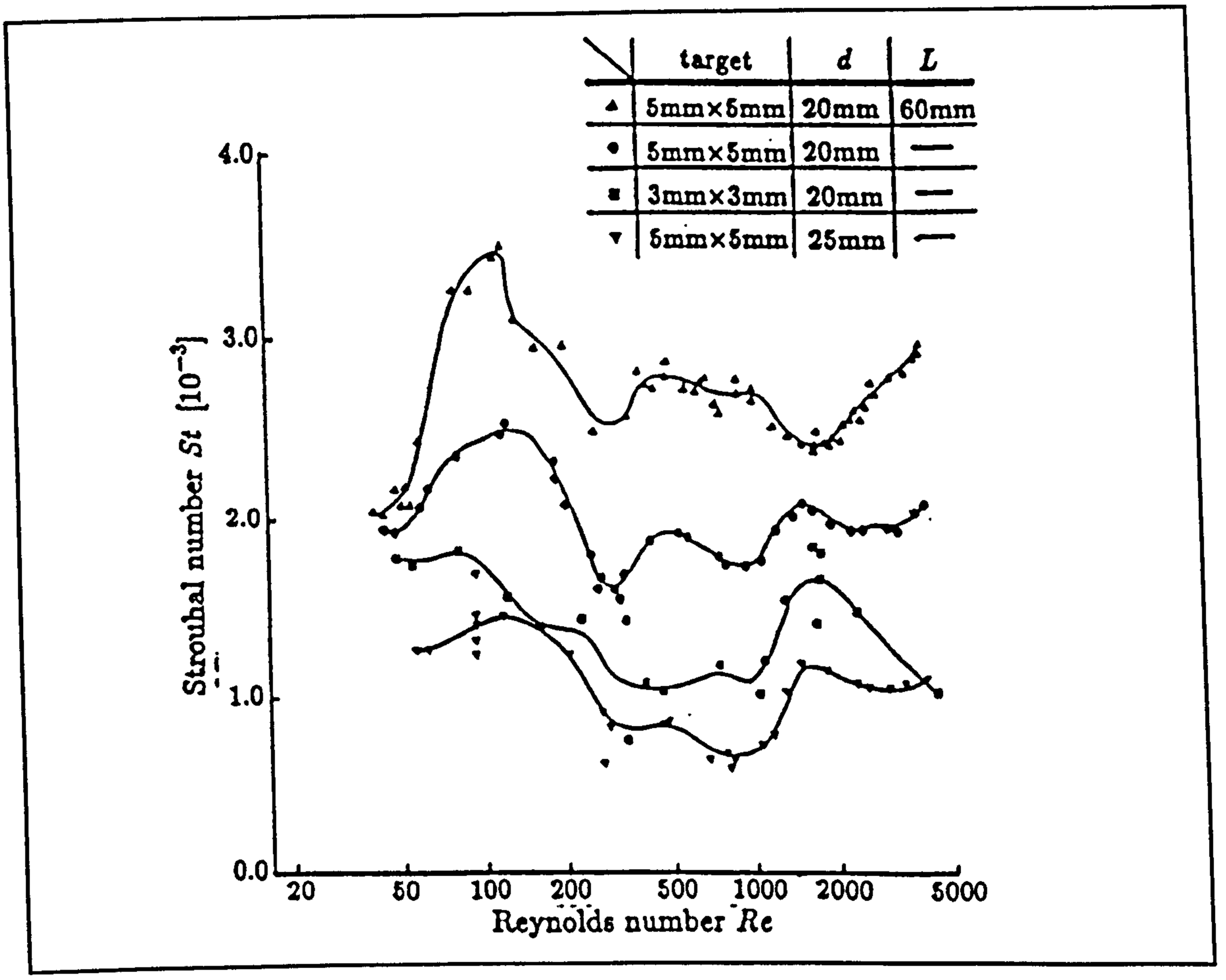

Figure 1.28: Variation of Strouhal Number With Reynolds Number For Various Design Parameters, Yamasaki et al (1988).

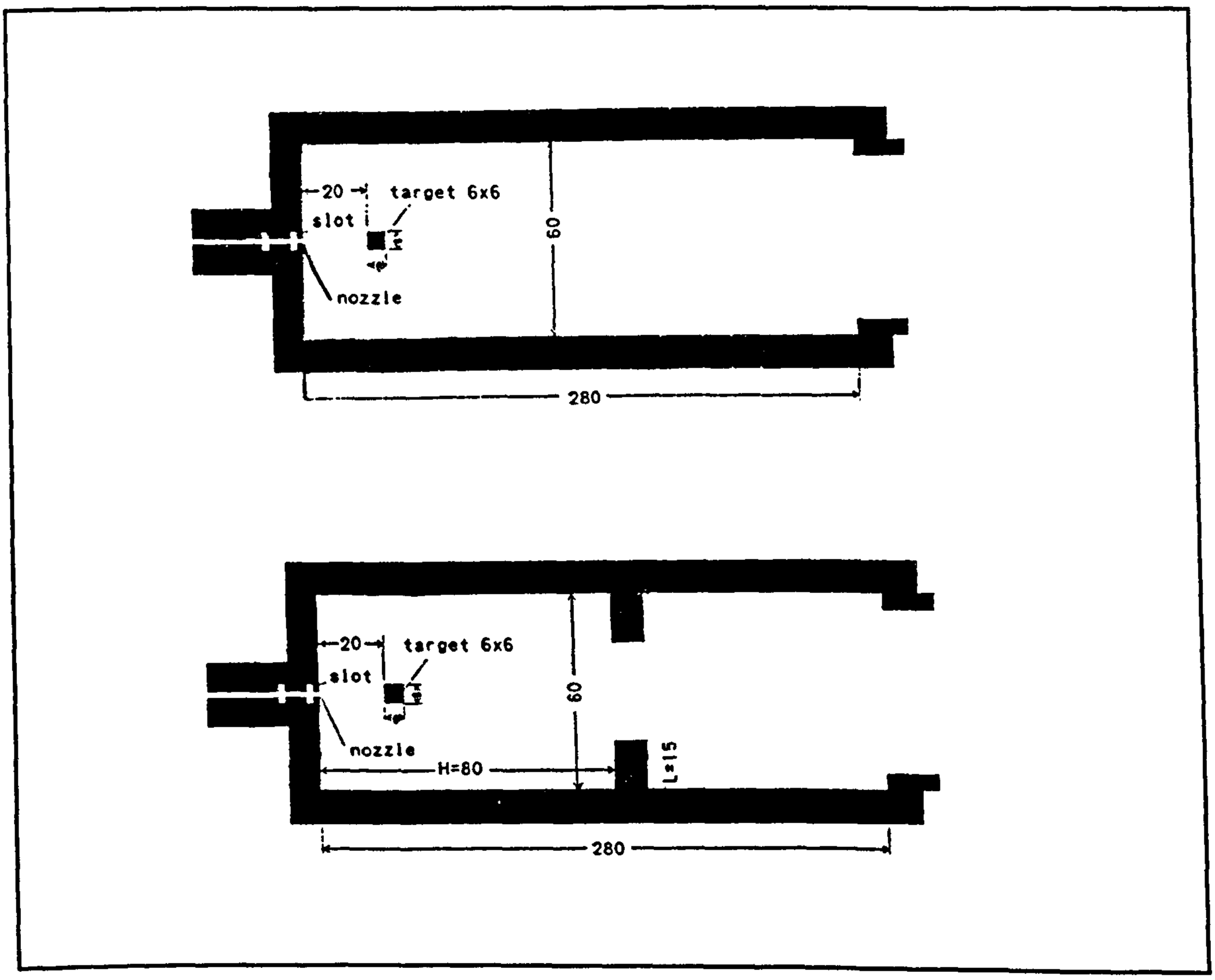

Figure 1.29: Two Simple Target Meters Investigated For Effect of Vortex Ring, Yamasaki et al (1991).

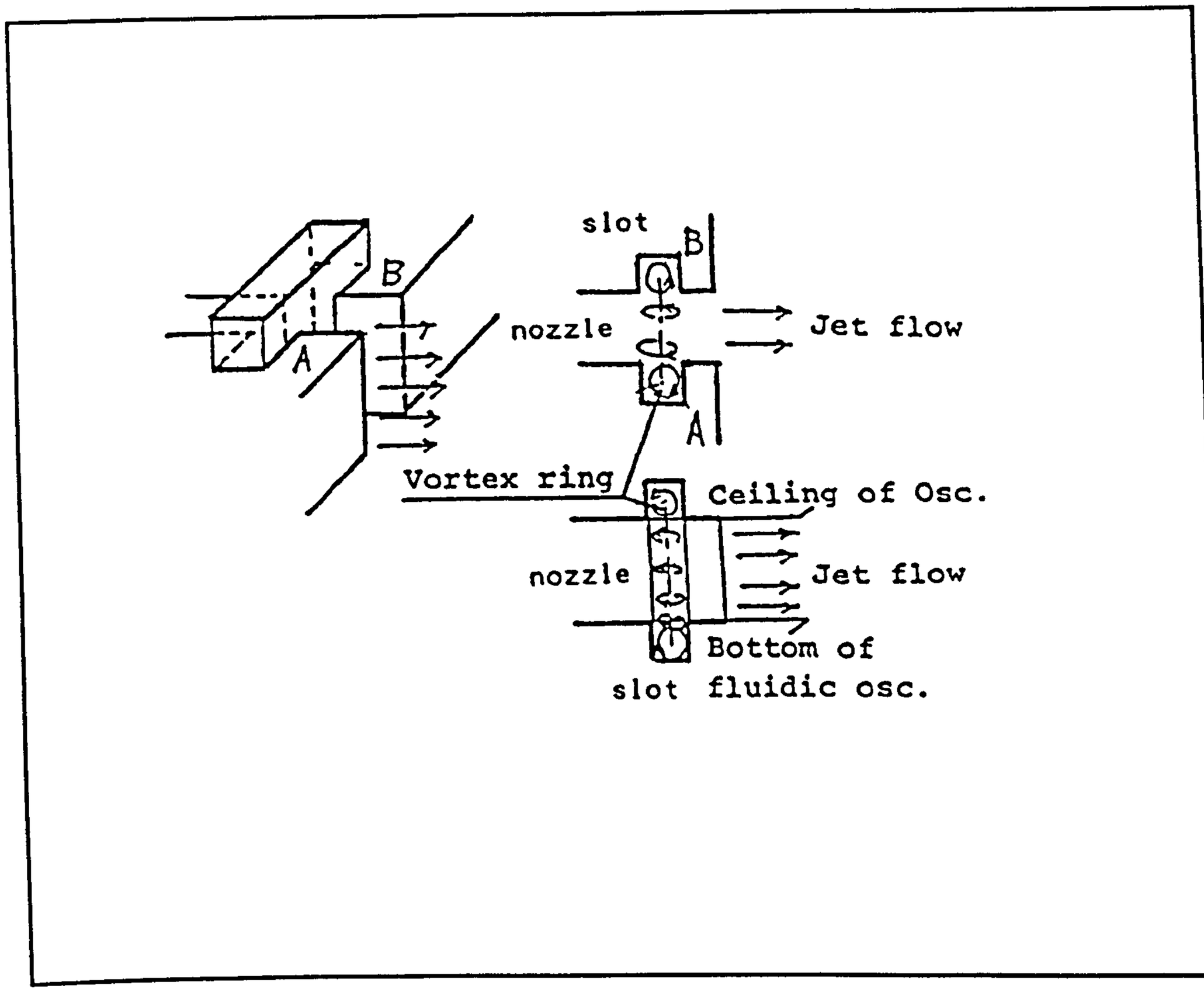

Figure 1.30: Slot Machined Into Nozzle Exit In Which Vortex Ring Is Formed, Yamasaki et al (1991).

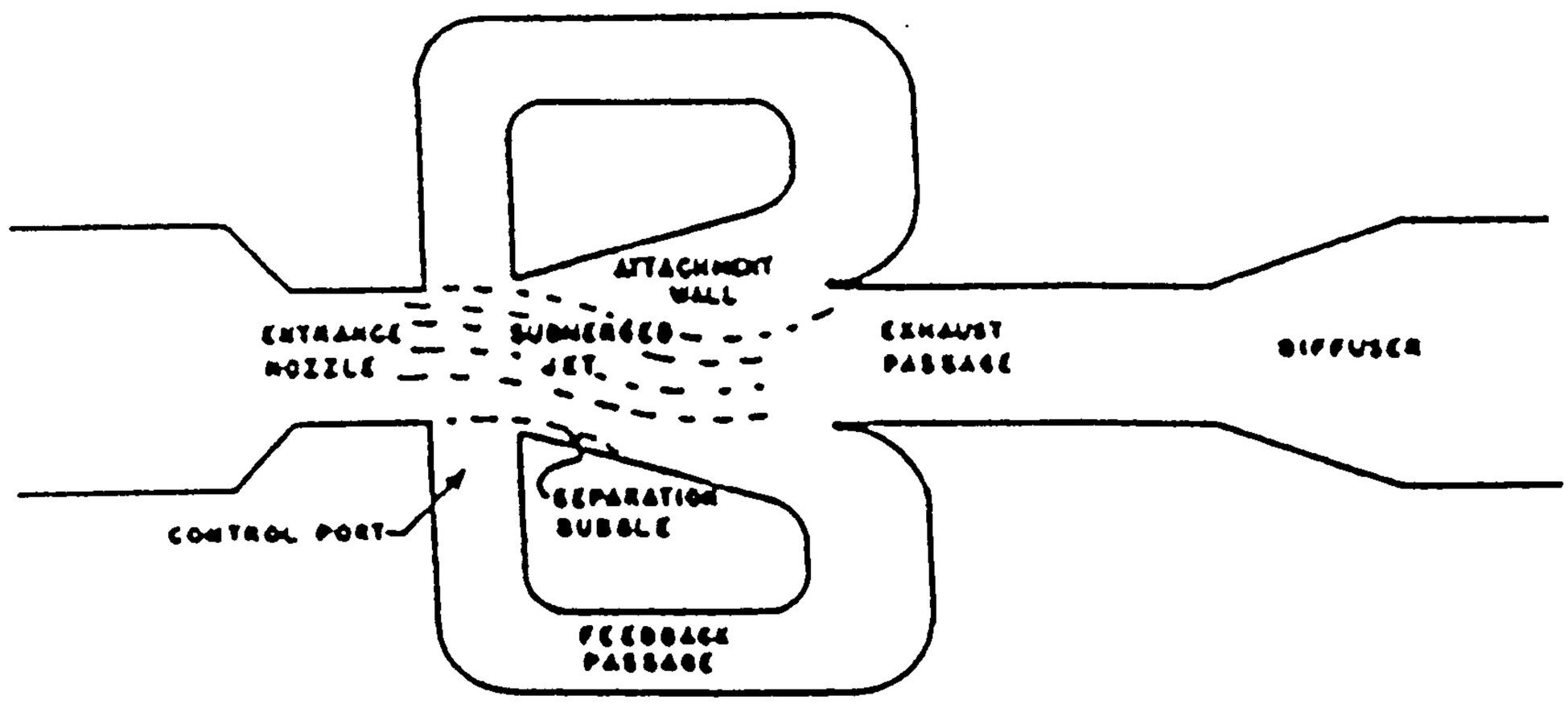

Figure 1.31: Feedback Oscillator Investigated By Beale and Lawler (1974).

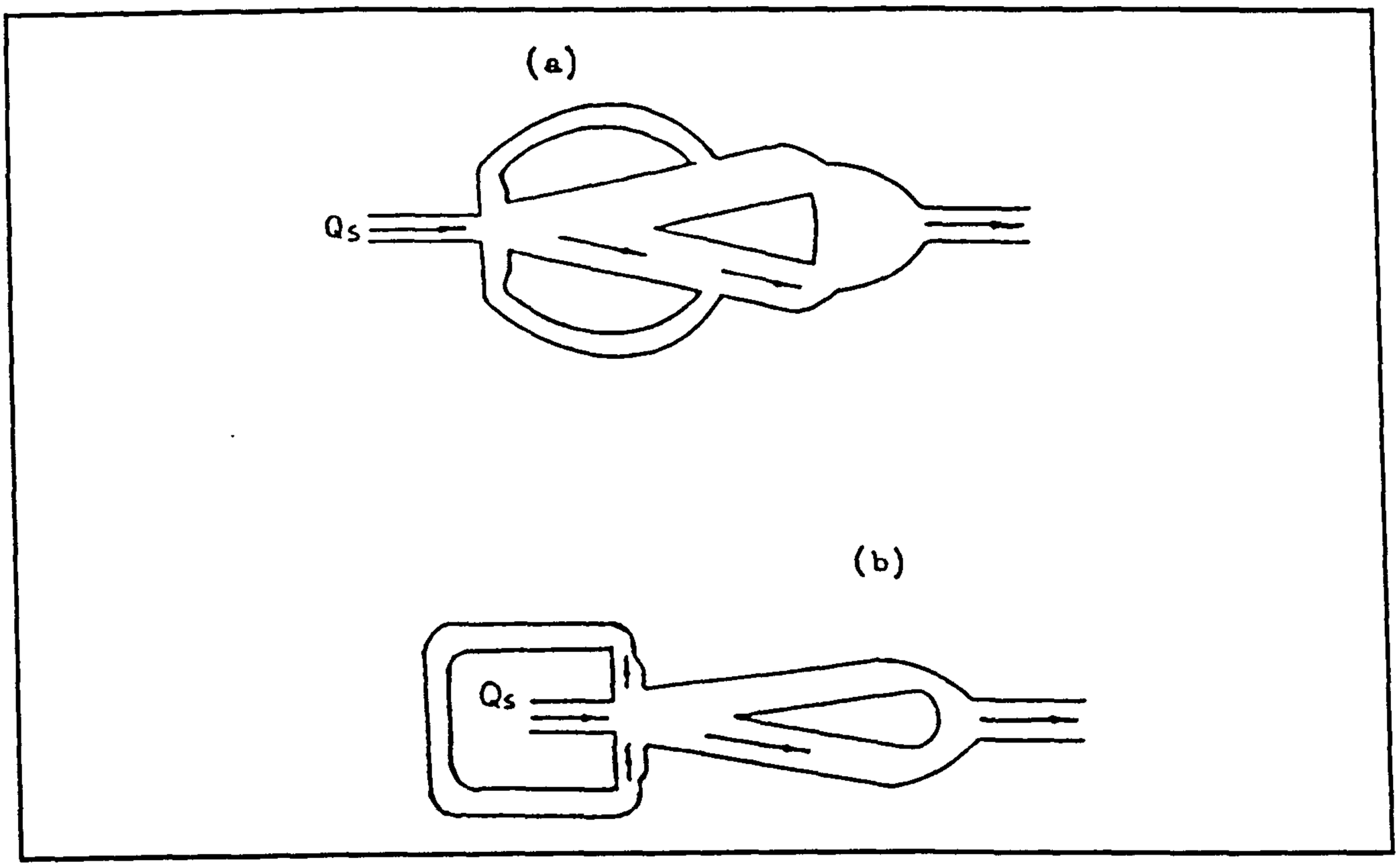

Figure 1.32: (a) Feedback Oscillator and (b) Relaxation Oscillator Investigated By Wu et al (1980).

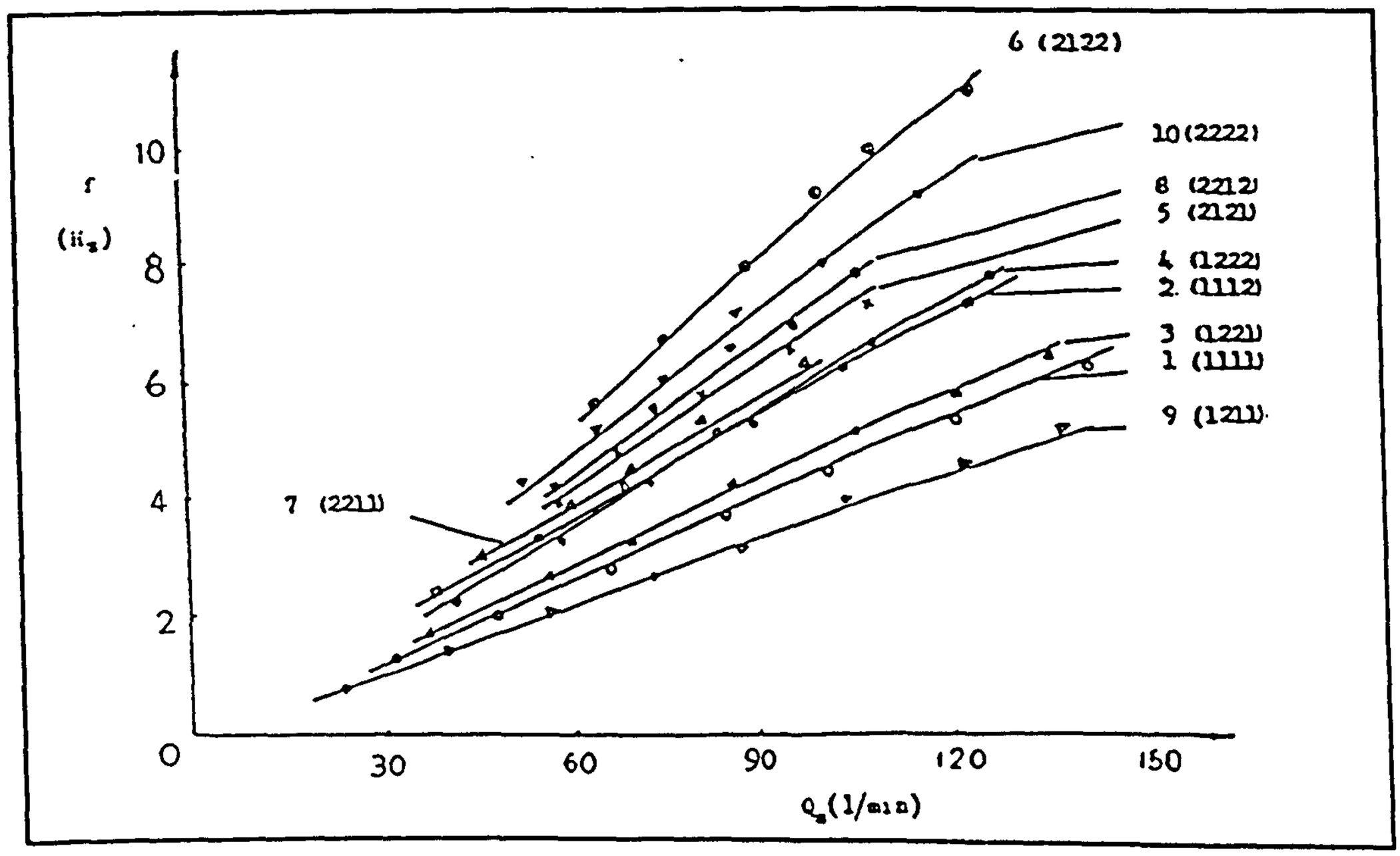

Figure 1.33: Effect On Oscillation Frequency Caused By Altering Design Parameters, Wu et al (1980).

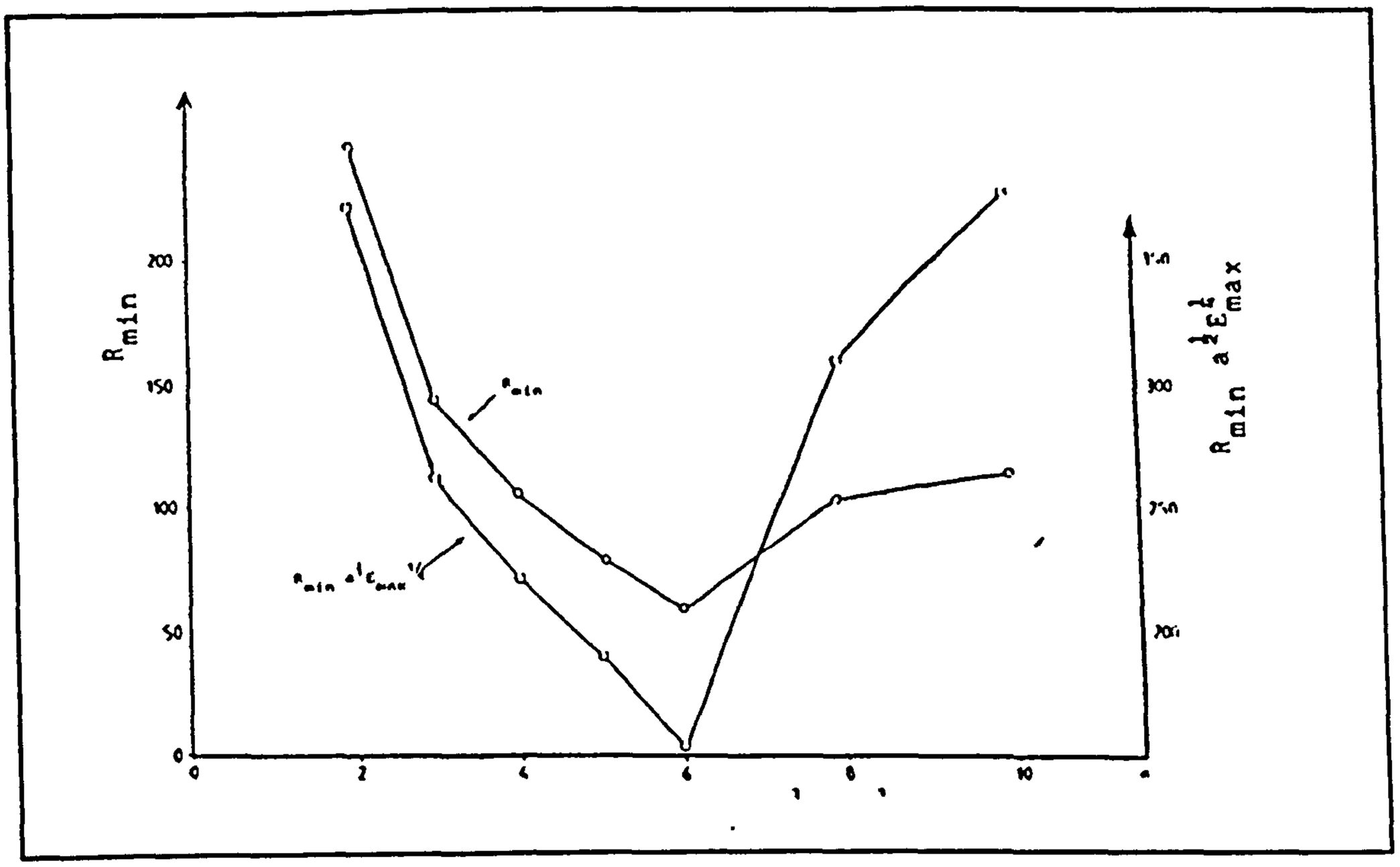

Figure 1.34: Minimum Reynolds Number Against Aspect Ratio For Fluidic Target Meter, Boucher and Mazharoglu (1988).

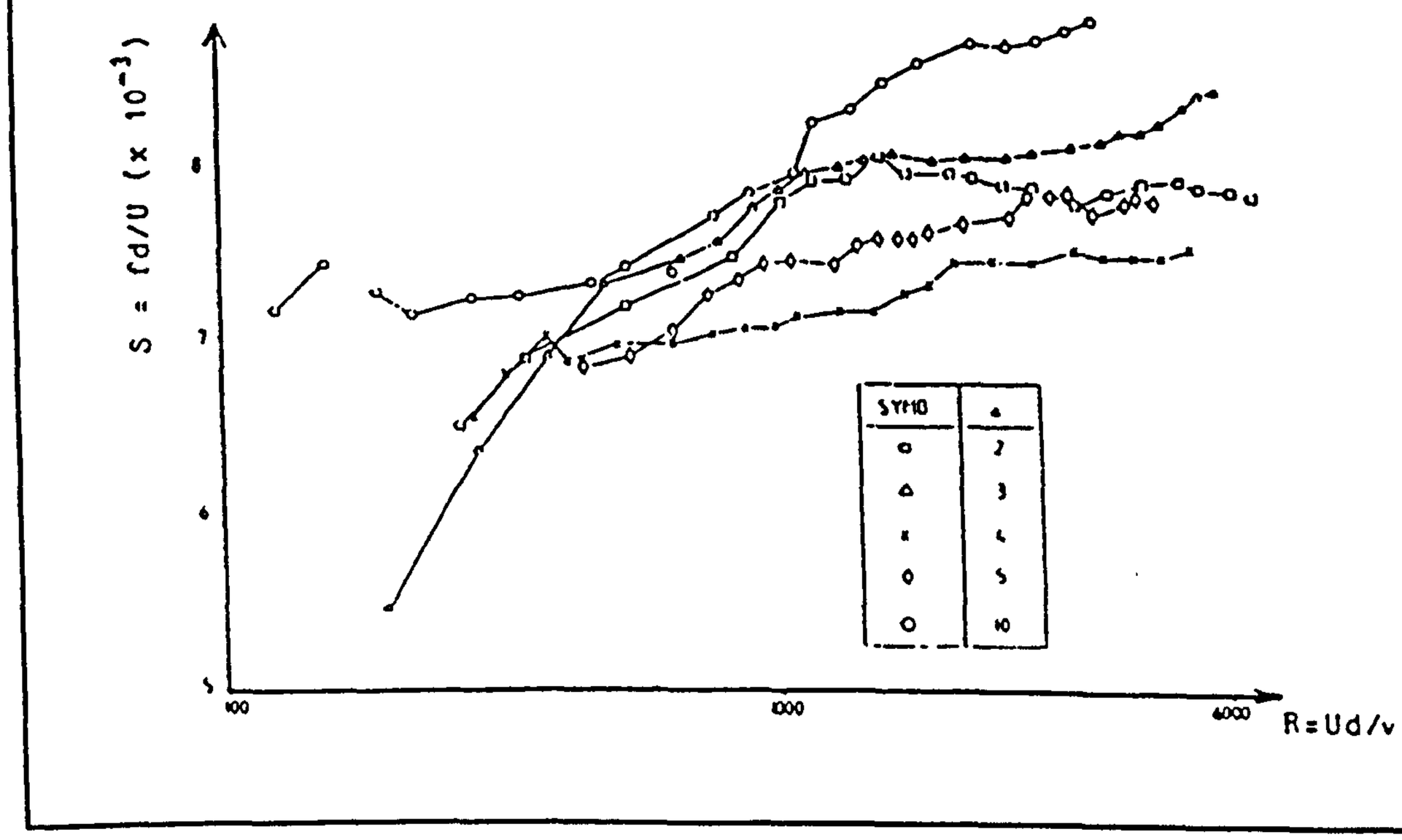

Figure 1.35: Strouhal Number Against Reynolds Number For Varying Aspect Ratios, Boucher and Mazharoglu (1988).

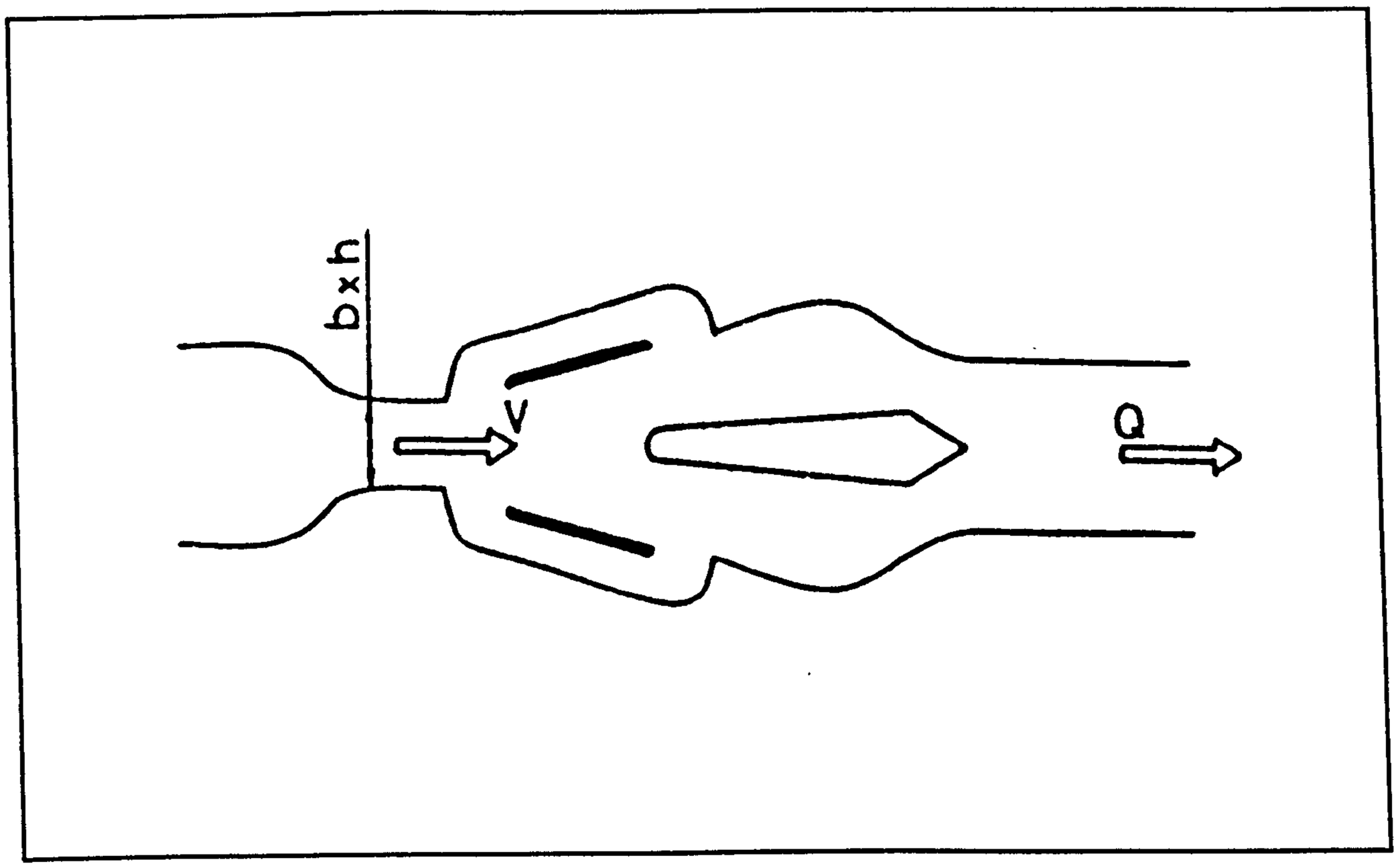

Figure 1.36: Thorn EMI Flow Measurement Meter U100.

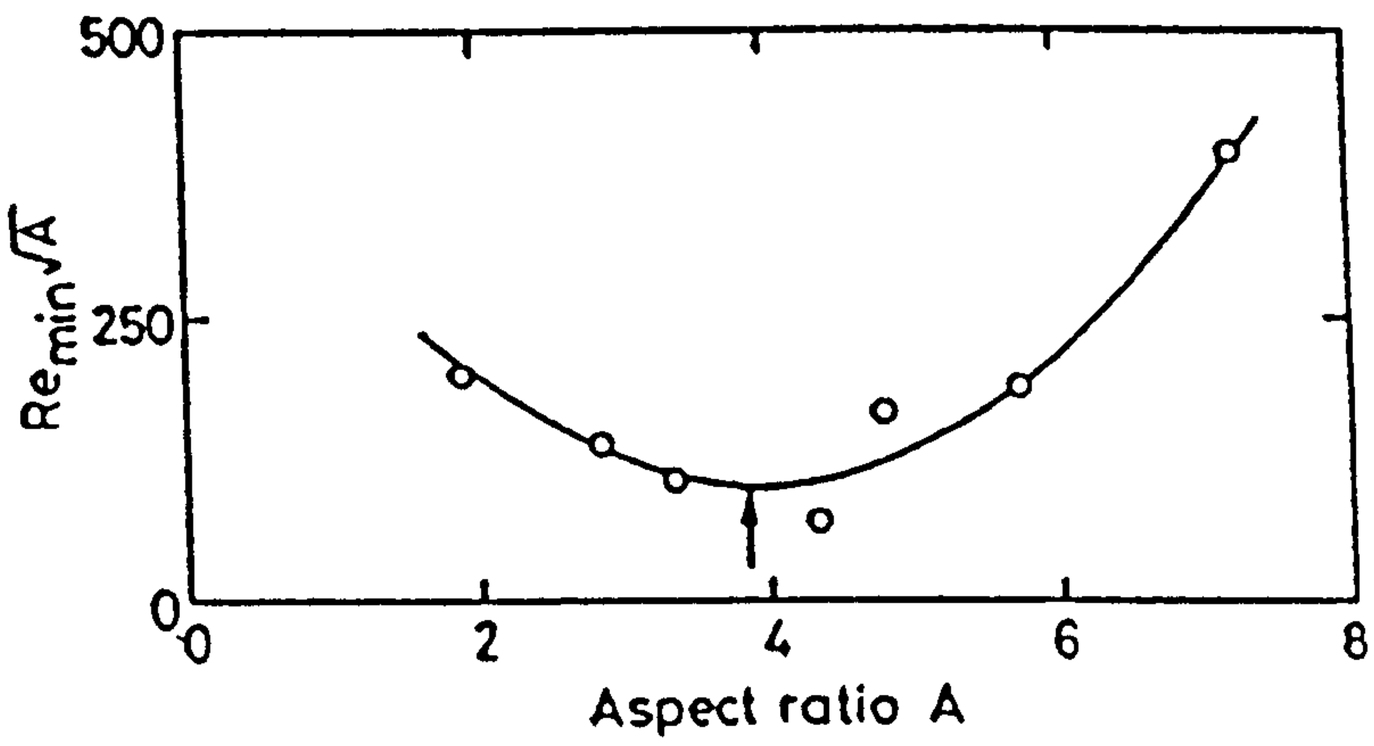

Figure 1.37: Minimum Flowrate Achievable Against Aspect Ratio, Kalsi et al (1988).

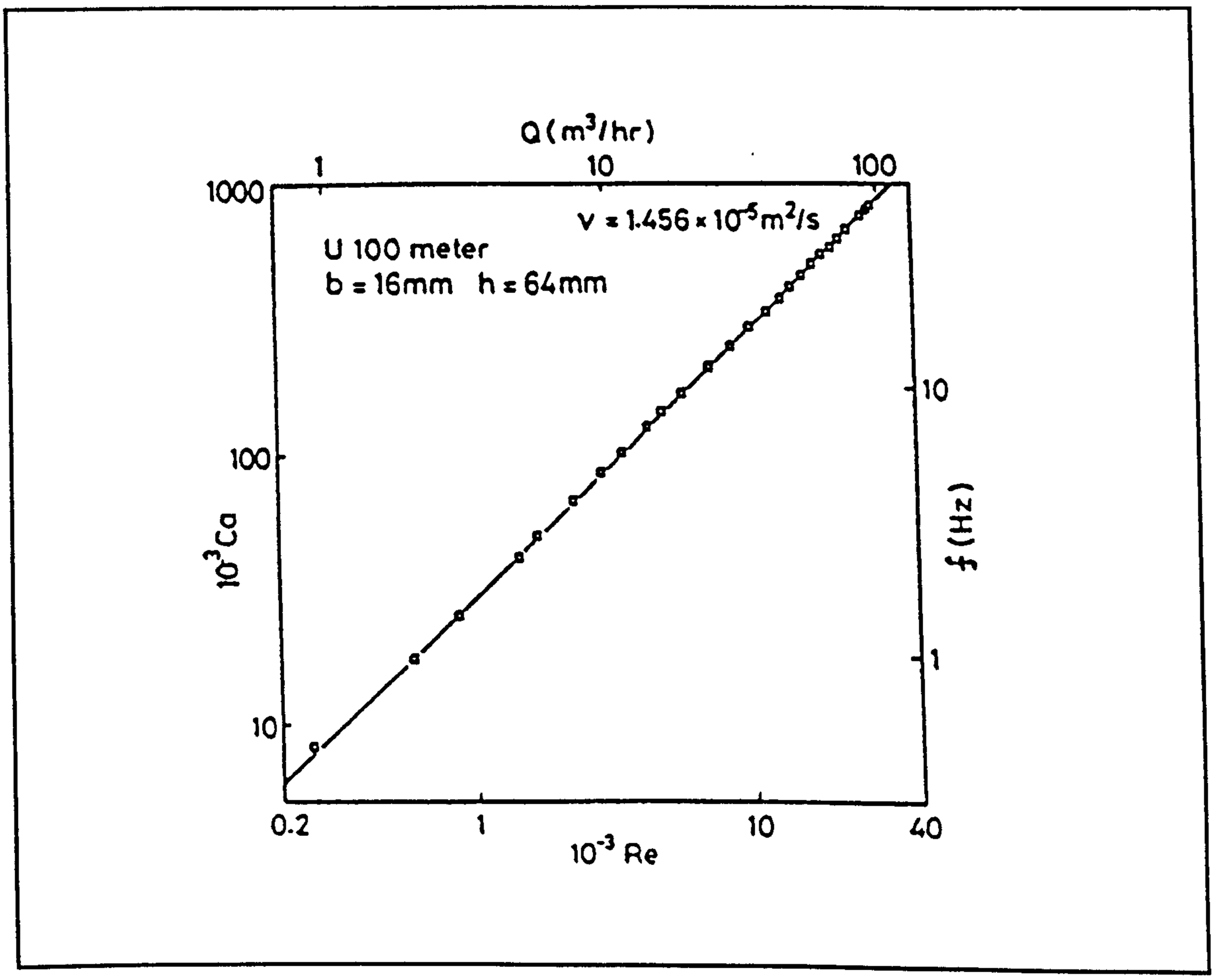

Figure 1.38: Linearity of Thorn EMI U100 Meter, Kalsi et al (1988).

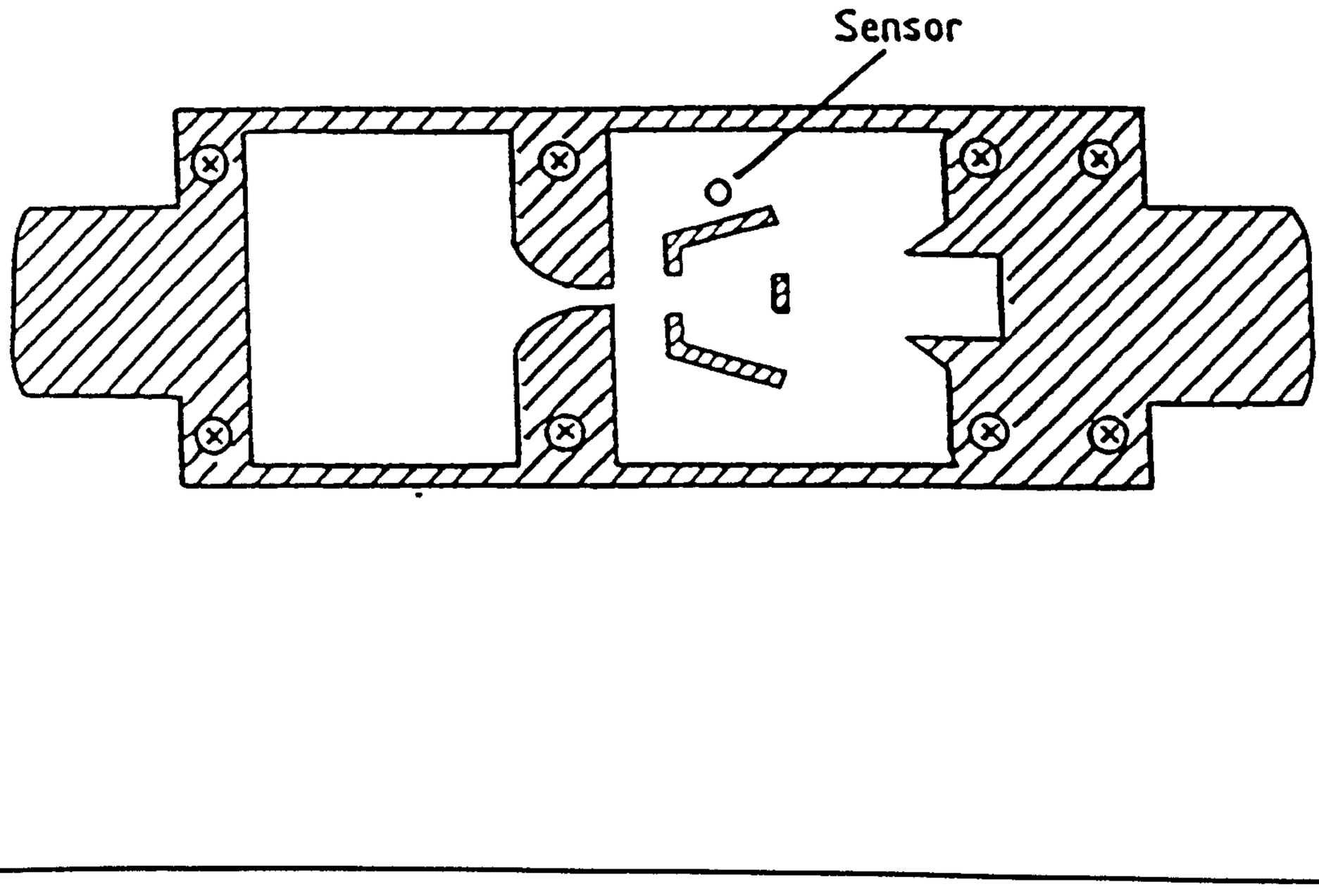

Figure 1.39: Fluidic Oscillator With Wider Range Than Conventional Types, Kawano et al (1985).

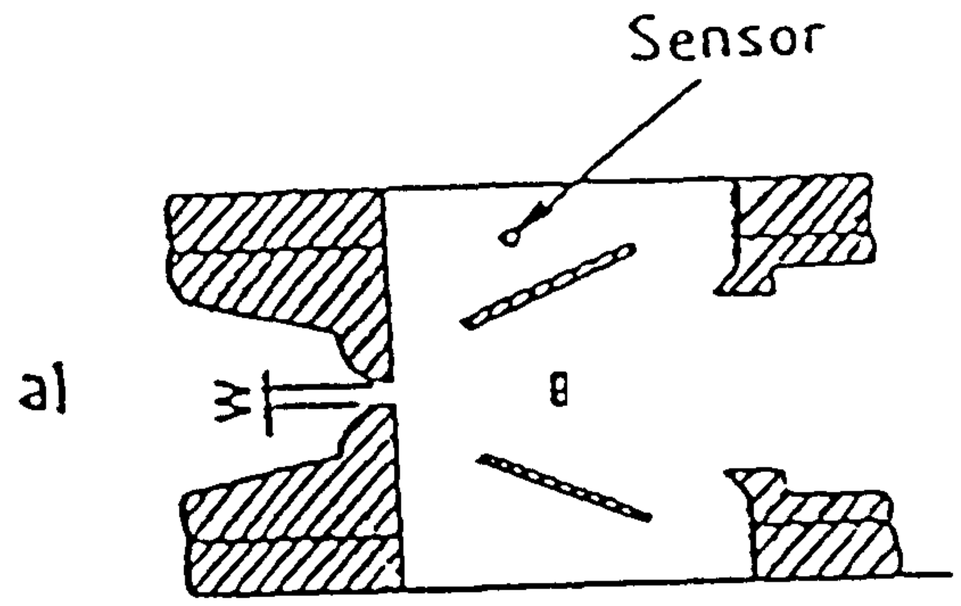

Figure 1.40: Stages of Transducer Development Carried Out By Kawano et al (1988).

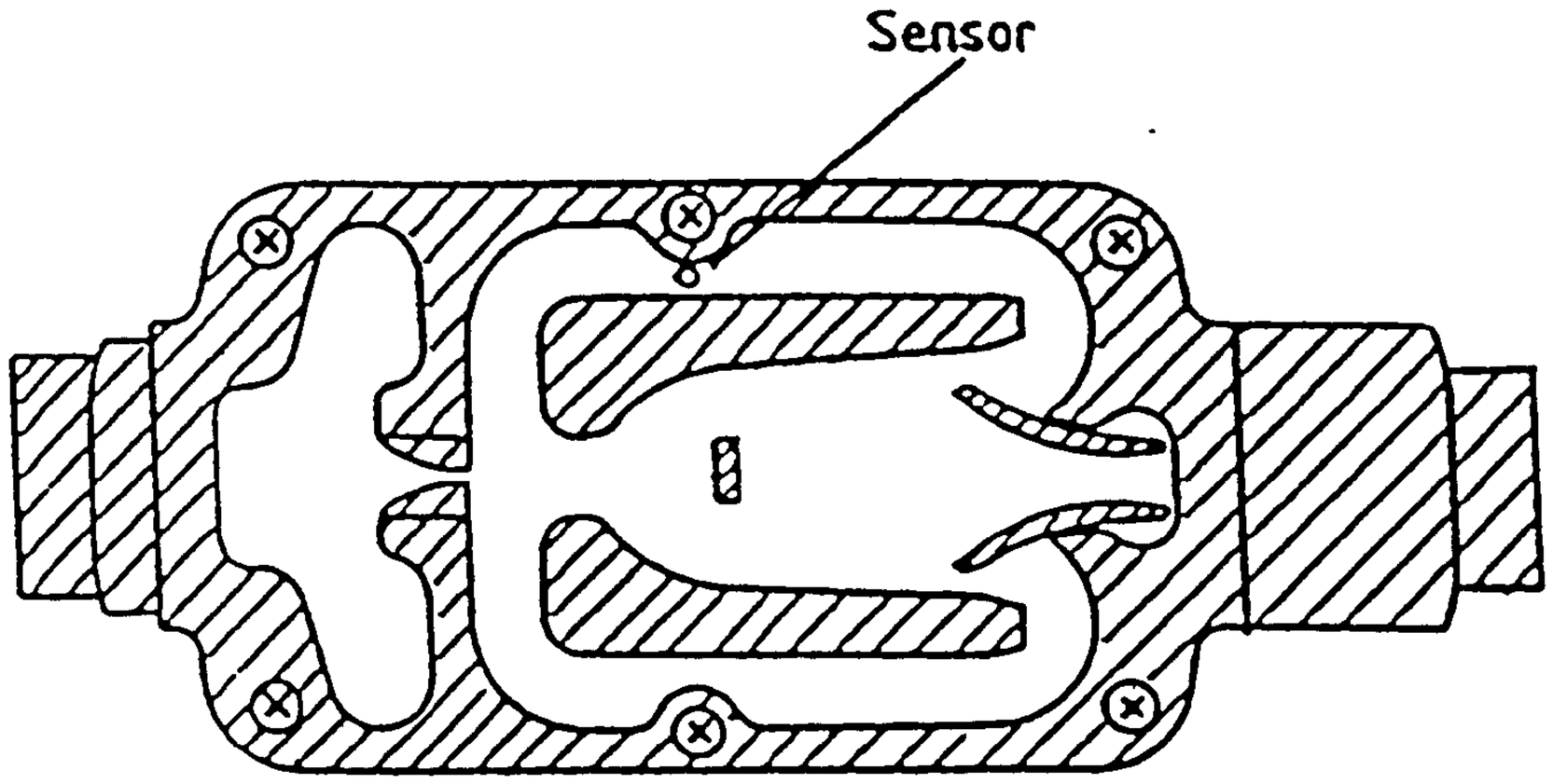

Figure 1.41: Configuration of Final Revised Meter Design, Kawano et al (1988).

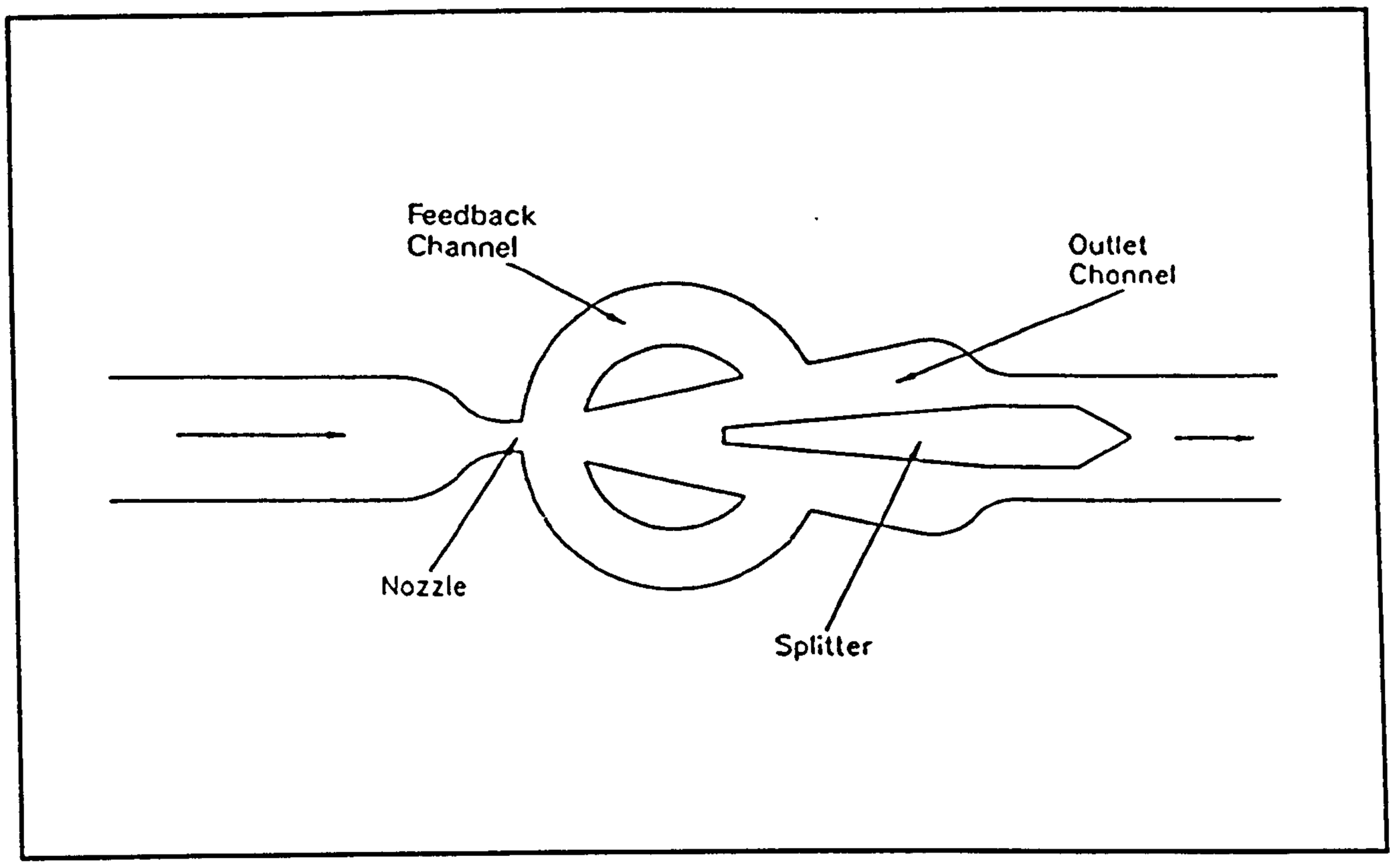

Figure 1.42: Fluidic Feedback Oscillator With Extended Range, Boucher (1995).

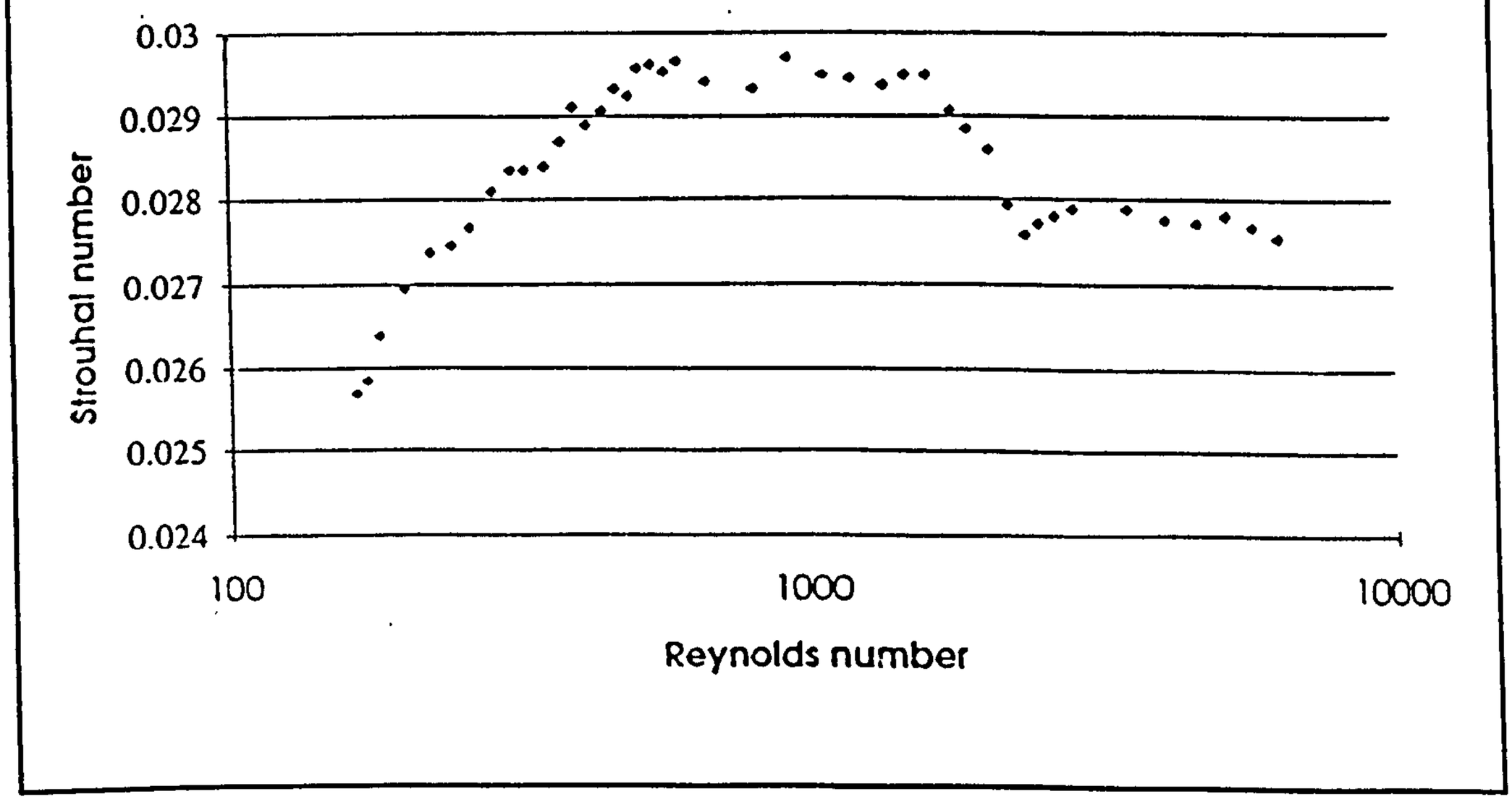

Figure 1.43: Strouhal Number Against Reynolds Number For Extended Range Feedback Meter, Boucher (1995).

Chapter 2

The Fluidic Oscillator Water Meter Calibration Rig.

2.1 Introduction.

This chapter describes the Cranfield Class D test rig and calibration procedure used to determine the linearity, range and pressure drop of the fluidic oscillator water meter. The rig can be used to calibrate the volumetric total flow output of the water meter, which is displayed as a total count on the LCD display, or the transducer signal may be calibrated directly. The transducer meterfactor calibration is derived directly from the transducer signal and is not compensated for temperature or linearity, thus a true transducer response is produced. The transducer response is later used to provide the data which is to be stored within the lookup table of the compensation scheme.

2.2 The Cranfield Class D Test Rig.

The experimental work described within this thesis and the calibration of fluidic oscillator designs was carried out using the Cranfield Class D test rig. The test rig determines a liquid flowrate by measuring the mass of liquid delivered into a weighing tank in a known time interval. Although the rig is not accredited it is designed around the methods of measurement of liquid flow in closed conduits using weighing and volumetric methods described in the British Standard BS6199 (1981). This method gives an absolute measurement of flow which is considered to be one of the most accurate methods of determining flowrate and is consequently often used as a calibration method.

The flow rig uses the static weighing method of flow measurement. The flow rig is adjusted to the approximate required flowrate, as indicated by reference turbine meters,

with all of the flow passing through the meter under test and then being returned to the sump tank. After steady flow is achieved the drain valve of the weighing tank is closed. The initial mass of the weigh tank plus any residual liquid is determined and recorded, or adjusted to zero. The diverter is then operated which actuates a timer to measure the duration of the filling time. The diverter diverts flow into the weighing tank until it contains sufficient quantity to attain the desired accuracy. The final mass of the tank plus the liquid collected in it is determined and the precise flowrate is then derived from the mass collected and the collection time.

Figure 2.1 shows a schematic for the test rig. The large sump tank is supplied with fresh tap water via a ball cock mechanism. There is a settling baffle in front of the main pump outlet to prevent air bubbles from being drawn into the main line by the pump which draws water from the tank into the main flow line. There is a bypass return loop from the main flow line which is fed directly back into the sump tank. The flow through the return loop is set by a control valve and is used to keep the pump operating at a constant rate. If the meter is to be tested at a high flowrate then the return flow is low and if the meter is to be tested at a low flowrate the return flow is high. This reduces any pulsations that may occur at low flowrates by throttling the pump so that it is operating below its optimum working range. The outlet flow from the main flow line may be directed in two possible ways using isolation valves.

One flow path directs the flow through the high flow line passing through a reference turbine and into a long straight section of inlet pipe which is connected to the inlet flange of the meter under test. Upstream of the inlet stage is the flow control valve.

The other flow path directs the flow into a constant level head tank. A weir is used to keep the level within the tank constant and an outlet pipe from the tank supplies flow at constant head into a smaller reference turbine. The flow then joins the long straight section of the meter inlet upstream of the flow control valve. The constant level head tank is used for the measurement of low flowrates and provides steady flow conditions at very low flowrates. During a meter calibration there is an overlap of calibration

points taken using both the constant head tank flow path and the direct line high flow path.

Downstream of the meter under test there is a temperature measurement probe and the outlet flange of the meter leads into a swan neck arrangement. Once the flow has travelled through the swan neck it passes through a control valve and into the nozzle of the diverter. The fish tail nozzle produces a thin flat jet of liquid which is returned to the sump tank or diverted into the weigh tank by means of the diverter. The diverter can be set to allow the flow to return straight to the sump tank or redirect the flow into the weighing tank. The diverter has an optical sensor connected which is used to operate the diversion timing mechanism.

The flow control valve upstream of the meter under test is used to set the flowrate through the meter and another control valve, downstream of the meter and above the fishtail diverter, is used to set the line pressure at the meter. A thermistor is used to measure the temperature of the water at the meter outlet. A drain tap is fitted to the highest point of the swan neck so that any air can be bled off from the system before a calibration takes place. There are pressure tappings upstream and downstream of the meter under test which are connected to a differential pressure gauge so that the pressure drop across the meter may be determined. The downstream tapping is also used to set the back pressure on the line to a desired value.

2.2.1 Description of Rig Components.

Nozzle. The diverter system consists of a fish tail nozzle which produces a thin flat liquid stream and the diverter plate. The nozzle is designed such that the jet is 60mm wide across and 2mm wide through the plane in which the diverter operates. Obviously these dimensions change depending on flowrate but in all cases the jet flow is clean with no splashing and no air is entrained within the jet. No air is drawn into the nozzle at low flowrates and for very high flowrates, for the calibration of larger meter sizes,

there is a larger replacement nozzle. The diverter nozzle is shown in figure 2.2.

Diverter. The diverter plate is pivoted around a horizontal axis and cuts across the thin liquid stream diverting the flow into the weigh tank through a section of conduit. The diverter is designed so that it cuts cleanly through the thin liquid sheet formed by the nozzle and does not cause splashing whilst diverting the flow. The motion of the diverter actuates an optical switch which is used to trigger the timer which measures the duration of the diversion. The optical switch is set to switch at the point when the diverter is in mid-travel position in the fluid jet. The diverter does not influence the flowrate within the circuit during any phase of the measurement procedure.

Diversion Timer. The optical switch connected to the diverter activates an electronic timer. The timer is started with the operation of the diverter and once enough water has been diverted to the weigh tank the diverter is returned to its original position turning off the timer. The time of diversion is then displayed until the timer is reset. The timer is a high accuracy device controlled by an oscillating crystal and is capable of accurate measurement to a resolution of 0.0001 seconds. The time of the diversion, T_{div}, and the mass of water collected during the diversion, m, are used to calculate the mass flowrate, Q_m.

Pulse Counter Timer. There is a second electronic timer and a digital pulse counter which are connected to the electronic pulse output of the fluidic oscillator meter under test. The second timer is necessary to prevent errors occurring in the meterfactor calculation due to missing fractions of pulses from the oscillator at the start and end of the diversion period. The pulse timer only starts to operate after the diverter is operated and the rising edge of the first flow pulse is received from the oscillator. The pulse timer continues to operate after the diverter has been returned to its original position until it receives the trailing edge of the last pulse from the fluidic oscillator. The pulse counter counts the number of complete pulses during this time. The time of pulses, T_{puls}, and the number of complete pulses, N_{puls}, gives a precise time for an exact number of complete pulses. Figure 2.3 shows a schematic of the operation of the two timing

mechanisms and shows how errors due to missing fractions of pulses at the start and end of the diversion are avoided.

The pulse timer and the pulse counter are used to calculate the precise oscillation frequency of the fluidic oscillator transducer. Using the volumetric flowrate and the oscillation frequency it is possible to calculate the volume flow per pulse or meterfactor, K, for the transducer at that precise flowrate.

Weighing Machine. The weigh tank is mounted on a digital scale weighing platform capable of measuring up to 50kg at a resolution of 0.1g. The outlet of the weigh tank has a drain valve which has an open outlet, so that the weigh tank is not physically connected to any other device, which when open drains the tank into a catch tray connected to the drain. Before each calibration the weigh tank is emptied, the drain valve is closed and the scales are set to zero.

Reference Turbines. There are two reference turbines used to set the flowrate to an approximate desired rate for a calibration. The high flow line has a larger turbine with an operating range which covers the high flowrates and the low flow line has a smaller turbine which covers the low flowrange. The operating ranges of the devices overlap which is useful for lower flowrate tests on the high flow line and higher flow tests on the low flow line. Both turbine meters are connected to a switchable digital display unit which has stored calibrations for both devices.

Flow Control Valves. The isolation and gate valves are standard devices but the two flow control valves upstream and downstream of the meter under test are modified by the manufacturers to give no valve clatter and to give greater and more precise flow control.

Temperature Probe. The temperature of the water is measured downstream of the meter under test using a thermistor probe with a digital display.

Inlet Stage. The internal diameter of the long straight section of inlet pipe is the same as the internal diameter of the fluidic oscillator water meter flanges as per the installation specifications. The depth of the threaded section is such that once correctly fitted there is only a very small internal step between the inlet pipe and the inside of the meter inlet flange.

Pressure Measurement Devices. A boss is fitted both upstream of and downstream of the threaded section into which pressure tappings are made for the differential pressure measurement across the meter under test. The downstream tapping is also used with a line pressure indicator to display the back pressure under which the meter is calibrated.

The Cranfield calibration rig is shown in figure 2.4.

2.3 Operational procedure of Test Rig.

The meter to be tested is installed within the flow rig. Before a meter may be calibrated it is necessary to remove any trapped air from the test rig. Initially the bypass loop control valve is fully opened and all other valves are closed. The pump is then switched on and left to circulate all flow through the bypass loop for a few seconds. The low flow path is then opened and the bypass loop control valve closed until a reasonable flow is seen to be entering the constant header tank. The flow control valves are then opened so that the fluidic oscillator is supplied with flow from the constant header tank. Once flow is seen from the fish tail nozzle the rig is left to run for a while whilst any trapped air within the low flow line is cleared. The low flow line is then closed at the outlet from the header tank first and then at the inlet line to the header tank.

The high flow line is then opened and run at maximum flowrate. The outlet control valve is adjusted so that a line pressure of 5p.s.i. is downstream of the meter and then the bleed valve is opened at the top of the swan neck. This is the highest point of the flow rig and any air that has not already been flushed from the system is trapped here.

The system is then run at this high flowrate for a few minutes and then the bleed valve is closed and the control valves are adjusted to maintain constant line pressure.

Once the rig is running at the desired flowrate under steady flow conditions the diverter is temporarily operated to wet the diverter and weigh tank so that the test is started under the same conditions as it ends. The diverter is then returned to its original position with the flow being returned to the sump tank. The tank is then drained and the drain valve closed. The initial mass of the tank plus any residual liquid is determined, or adjusted to zero using the weigh scales. The electronic diversion timer, pulse timer and pulse counter are all reset to zero. The diverter is then operated to divert flow into the weighing tank and the timers and pulse counters start counting.

The analogue and digital output from the fluidic oscillator transducer is monitored at all times during the calibration test using an oscilloscope to check for missing pulses or irregular sinusoidal flow patterns. The oscilloscope is also used to measure the magnitude of the analogue output from the fluidic oscillator transducer.

Once the weighing tank contains enough water for the required accuracy then the diverter is returned to its original position. The water is allowed a few seconds to settle and for the diverter to return to the same wetted conditions as at the start of the test and then the mass of water diverted is recorded. The time of the diversion, the number of pulses counted from the fluidic oscillator and the time of the pulse count are also recorded as are the line pressure, pressure drop across the meter and the temperature of the water. Once all the readings have been recorded the water within the weigh tank is emptied into the drain so that the sump tank is replaced with clean mains water and the flowrate is readjusted and the test repeated.

For a full meter calibration the flowrate is traversed from the minimum required flowrate to the maximum flowrate and then back down from Q_{max} to Q_{min}. A portable computer is used to enter the recorded data into a spreadsheet which calculates flowrate, oscillation frequency and meter factor. The calibration is displayed in the form of a

meterfactor against flowrate plot during the test. The portable computer is useful because it can be used to indicate the flowrates at which more data points are required, for example at a point where the meterfactor response curve is changing rapidly with flowrate. The data from the calibrations are stored on computer disk and hard copy printouts of meterfactor response curves.

2.4 Calculation of Meterfactor For Fluidic Oscillator Calibration.

For each test carried out the mass flowrate is calculated and hence volumetric flowrate determined. The oscillation frequency is then calculated for the fluidic oscillator under test which is then used to determine the meterfactor of the device at that particular flowrate. The calculations are carried out using a computer spreadsheet according to the following equations.

2.4.1 Calculation of Mass Flowrate.

The mean mass flowrate during the diversion time is obtained by dividing the real mass, m, of the water by the diversion time, T_{div}.

$$Q_m = \frac{m}{T_{div}}(1+\epsilon) \qquad (2.1)$$

The final term in this equation is a correction term introduced to take into account the difference in buoyancy exerted by the atmosphere on a given mass of liquid and on the equivalent mass in the form of weights used when calibrating the weighing machine.

$$\epsilon = \rho_{air}\left(\frac{1}{\rho}-\frac{1}{\rho_p}\right)$$

where ρ is density of the liquid, ρ_{air} is the density of air at 20°C and 1bar and ρ_p is the density of standard weights.

In the case where the liquid is water it is sufficient to calculate the correction factor, ε, from mean approximate values:

$$\rho = 1000 kg\ m^{-3}$$

$$\rho_{air} = 1.21 kg\ m^{-3}$$

$$\rho_p = 8000 kg\ m^{-3} \text{ (conventional mean value, OIML)}$$

Hence, $\varepsilon = 1.06 \times 10^{-3}$

2.4.2 Calculation of Volumetric Flowrate.

The volume flowrate, Q_v, is calculated using the mass flowrate calculated in equation (2.1) and from the density of the liquid, ρ, at the temperature of operation, as read from standard tables.

$$Q_v = \frac{Q_m}{\rho} \qquad (2.2)$$

2.4.3 Calculation of Oscillation Frequency of Fluidic Oscillator.

The oscillation frequency of the fluidic oscillator is determined using the number of complete pulses associated with the diversion time, N_{puls}, and the time of pulses, T_{puls}, for the complete pulses associated with the diversion time. The number of complete flow pulses associated with the time of diversion is measured using the pulse output from the fluidic oscillator, the count starts on first rising edge received after the diverter is activated and finishes on first trailing edge after diverter is closed.

$$f = \frac{N_{puls}}{T_{puls}} \qquad (2.3)$$

This method reduces any inaccuracies caused by fractions of a pulse which would not be counted at the start and end of the diversion time if pulses were measured during the diversion only.

2.4.4 Calculation of Meterfactor.

The volume flow per pulse meterfactor, K, is calculated using the volumetric flowrate, Q_v, and the oscillation frequency, f.

$$K = \frac{Q_v}{f}$$

The meterfactor value is calculated at a range of frequencies and indicates the variation of the slope of flowrate against frequency and hence meter linearity. The meterfactor calibration for the fluidic transducer may be stored within a lookup table access scheme so that the response may be compensated for linearity. Figure 2.5 shows a typical meterfactor against frequency plot for a fluidic oscillator transducer with no flow conditioning or linearity compensation. The precise flowrate at any frequency is given by multiplying the frequency by the meterfactor value, taken from the plot at that frequency.

2.4.5 Calibration Check of Overall Meter Performance.

The Class D flow rig may also be used to calibrate the total volume flow output of the water meter by using the rig in a standing start arrangement. The flow rig is set to run at a known flowrate, using the flying start method described above, and then the flow is shut off with a rapid acting solenoid valve. The total volume indicated on the LCD display of the water meter is then recorded and the weigh tank set to zero. The diverter is set to divert the flow into the weigh tank and the solenoid valve is opened. As the flow restarts the counter on the water meter begins to count volume flow and the weigh tank fills. Once sufficient mass has been collected the solenoid valve is shutoff and the mass of water collected and the new volume flow indicated on the L.C.D. display are recorded.

The mass collected is used to calculate the volume flow which is compared against the difference in recorded volume flow on the meter display. The error is expressed as a percentage at that flowrate. This is a check on the performance of the complete metering system, including linearisation and temperature compensation, rather than a calibration of the transducer performance.

2.5 Accuracy of measurement.

The weighing method gives an absolute measurement of flow requiring only mass and time measurements and is considered to be one of the most accurate methods of determining flowrate. Assuming there is no leakage in the flow circuit, between the meter and the diverter nozzle, then the accuracy of the measurement depends upon the accuracy of the weigh scales, the losses due to splashing spray etc. and errors due to the switch over time at the start and end of the diversion timing mechanism. The BS 6199 (1981) standard states that strictly speaking the time measurement shall be started, or stopped, at the instant when the hatched areas in figure 2.6, which represents the flow variation with time, are equal. In practice it is generally accepted that this corresponds to the mid travel position of the diverter in the fluid stream. The position of the optical switch fitted to the diverter of the Cranfield test rig is adjustable and is set so that it activates as the diverter passes through the centre of the nozzle jet.

The errors due to actuation of the diversion timer may be considered to be negligible provided that the time of passage of the diverter through the nozzle stream is negligible in comparison with the period of diversion to the tank. At the maximum flowrate, which is the worst case for error, the 50kg tank still takes 90 seconds to fill. The diverter is hand operated but can still be expected to reach a velocity of at least 1m s^{-1} at mid travel. The width of the nozzle jet increases with increasing flowrate but is still less than a maximum of 8mm wide at the maximum flowrate. Therefore the time of travel through the stream is 0.08 seconds and the worst possible error due to the diverter is 0.088% if the tank takes 90 seconds to fill.

Another possible source of error is the splashing caused when the diverter breaks the high velocity nozzle stream, however, the mass of liquid lost through spray is very small in comparison to the 50kg collected in the weigh tank. At lower flowrates less mass is collected due to the excessive time taken to fill the tank but at the lower flowrates there is also less splashing due to the lower velocity nozzle stream.

The weigh scales are supplied with a calibration certificate after being calibrated against standard weights. The weigh scales used are the Mettler FB60 platform scales which has certification to the Organisation of Legal Metrology (OIML). The FB60 has a measurement resolution of 0.1g and an accuracy of ±1.0g.

The BS 6199 (1981) standard states that when the installation is carefully constructed, maintained and used, an uncertainty of ±0.1% (with 95% confidence limits for the random part of that uncertainty) can be achieved. Owing to its high potential accuracy, this method is often used as a primary method for calibration of other methods or devices for mass-flowrate measurement or volume-flow measurement provided that the density of the liquid is known accurately.

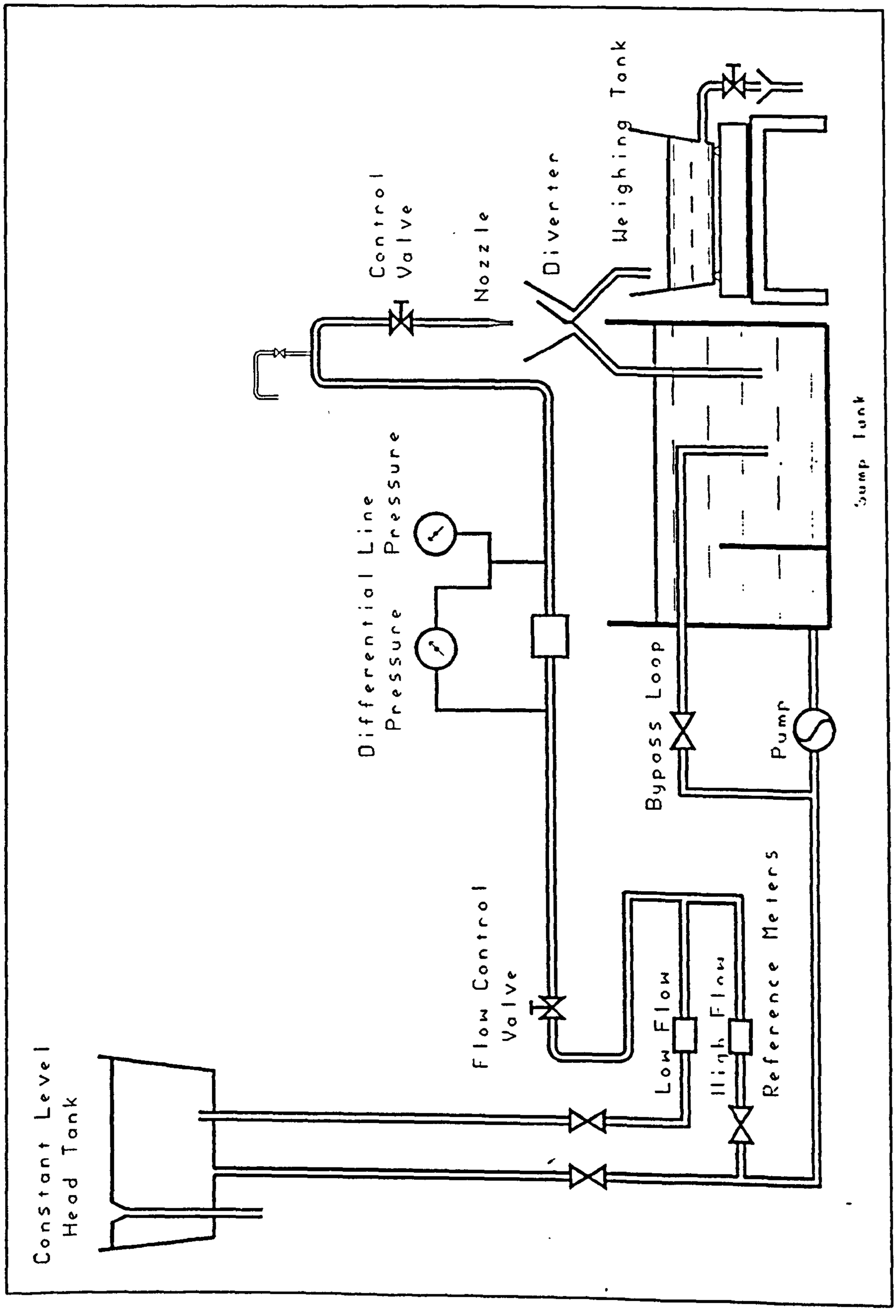

Figure 2.1: Schematic of Fluidic Oscillator Calibration Rig.

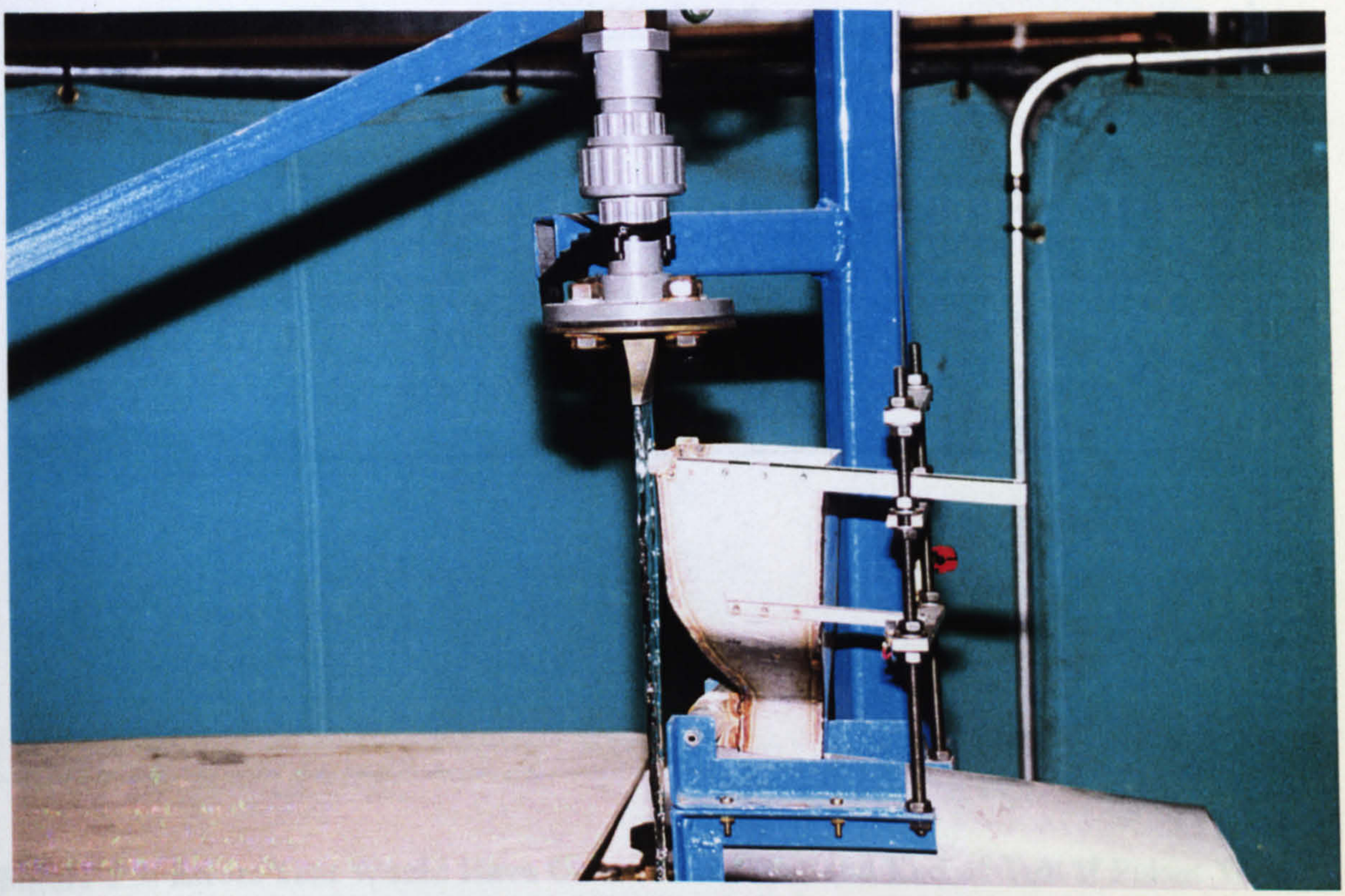

Figure 2.2: Fish Tail Diverter Nozzle.

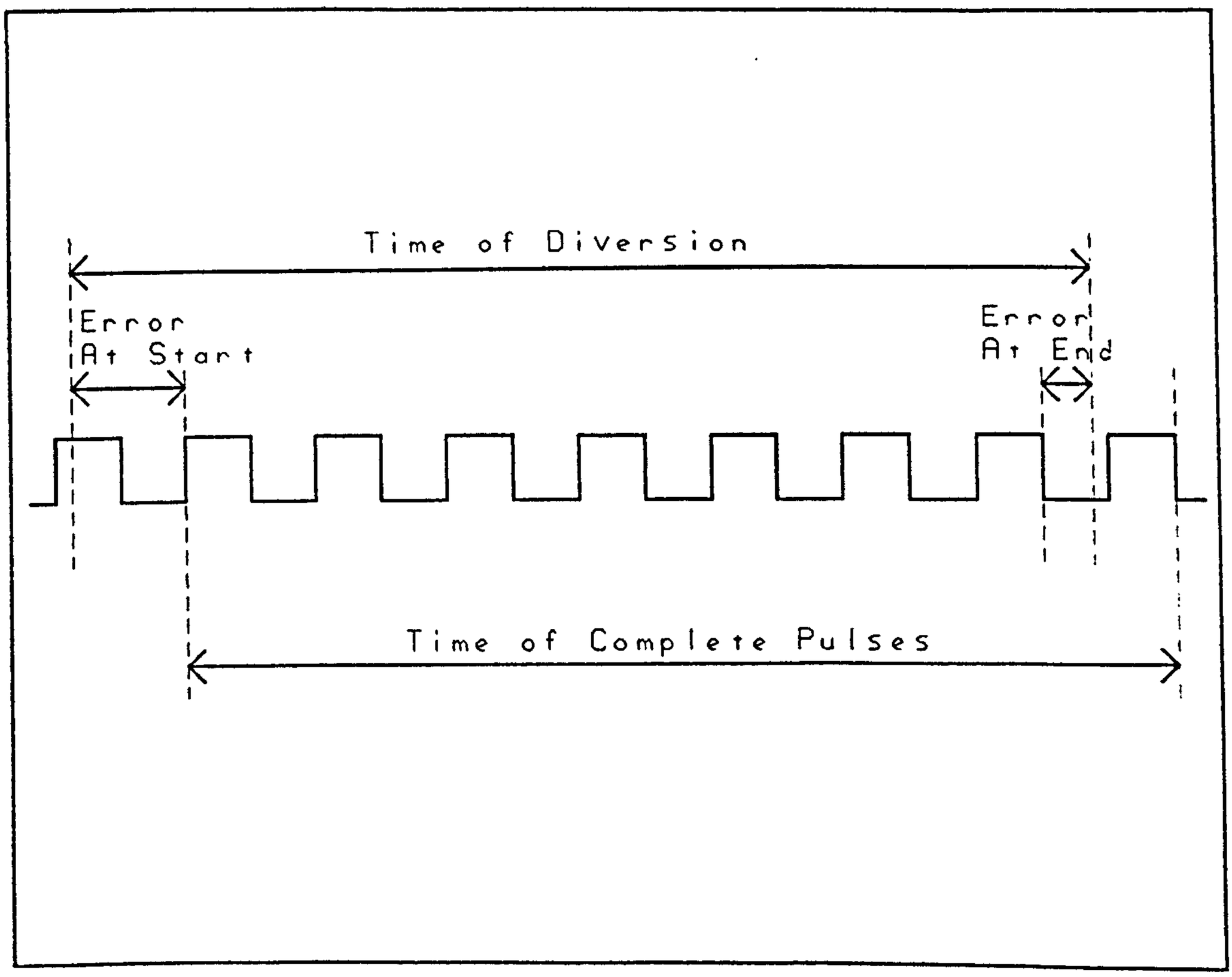

Figure 2.3: Errors That Would Have Occurred At Start and End of Test If Pulses Were Counted During Time of Diversion Only.

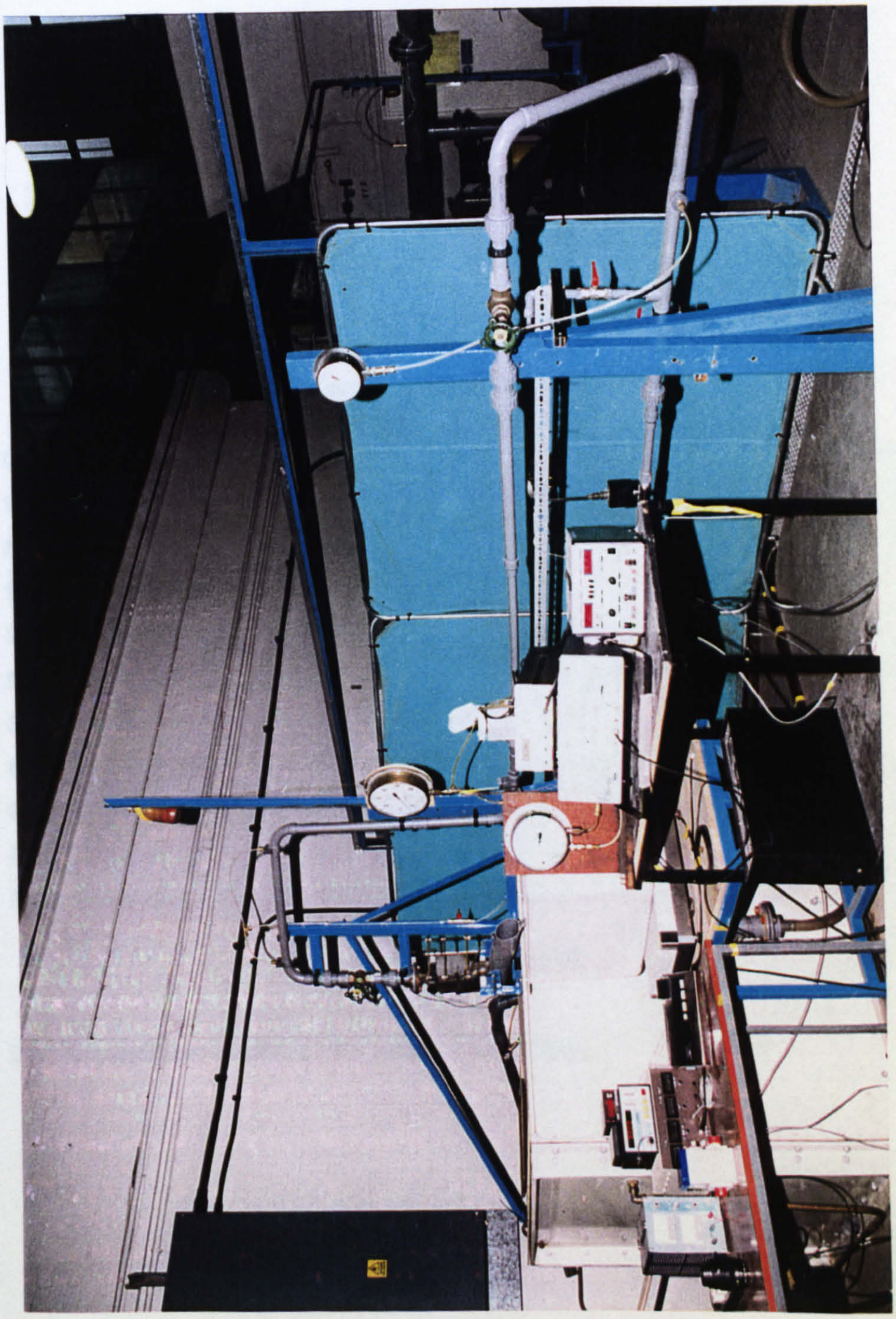

Figure 2.4: The Fluidic Oscillator Calibration Rig.

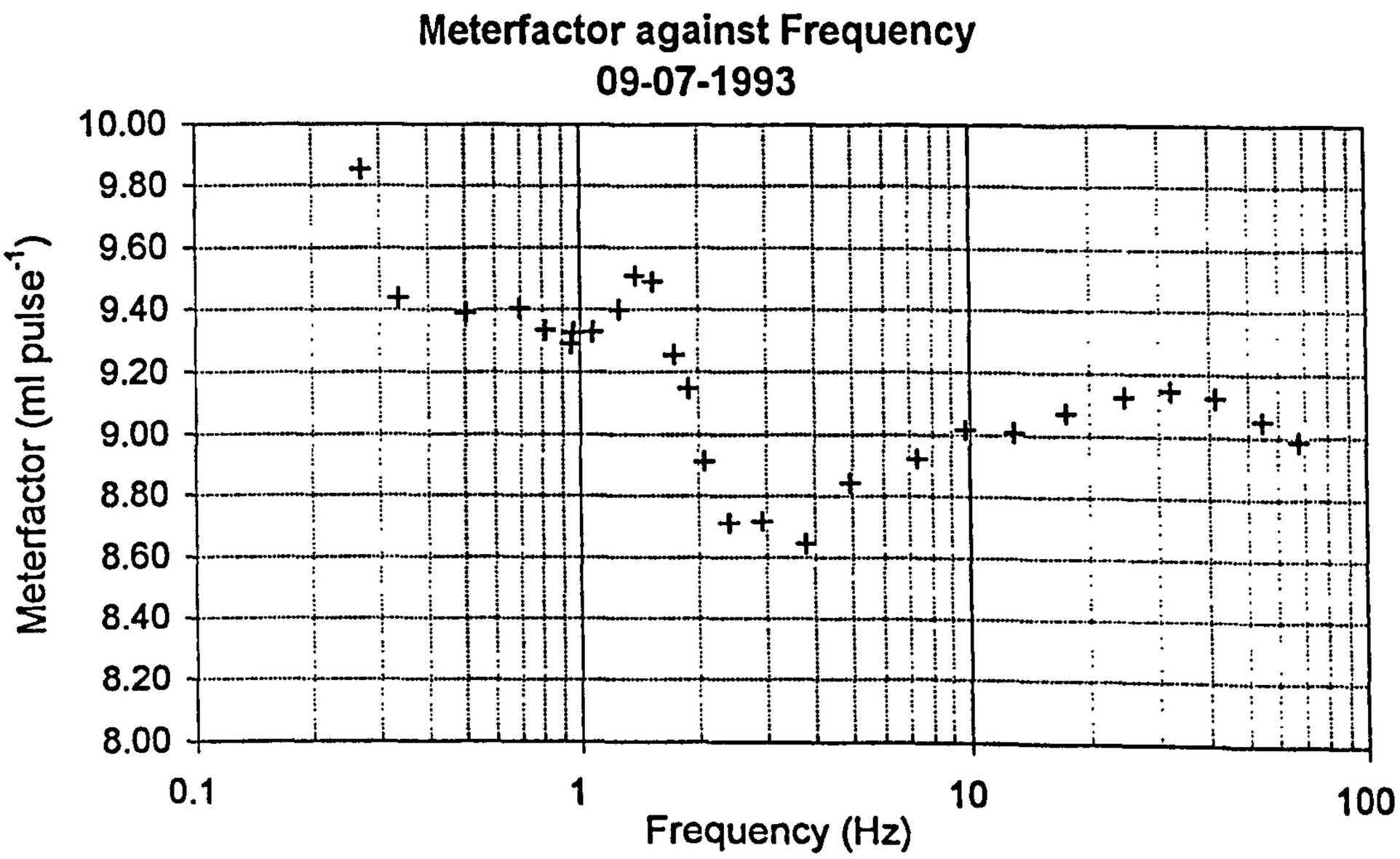

Figure 2.5: Meterfactor Against Frequency Calibration.

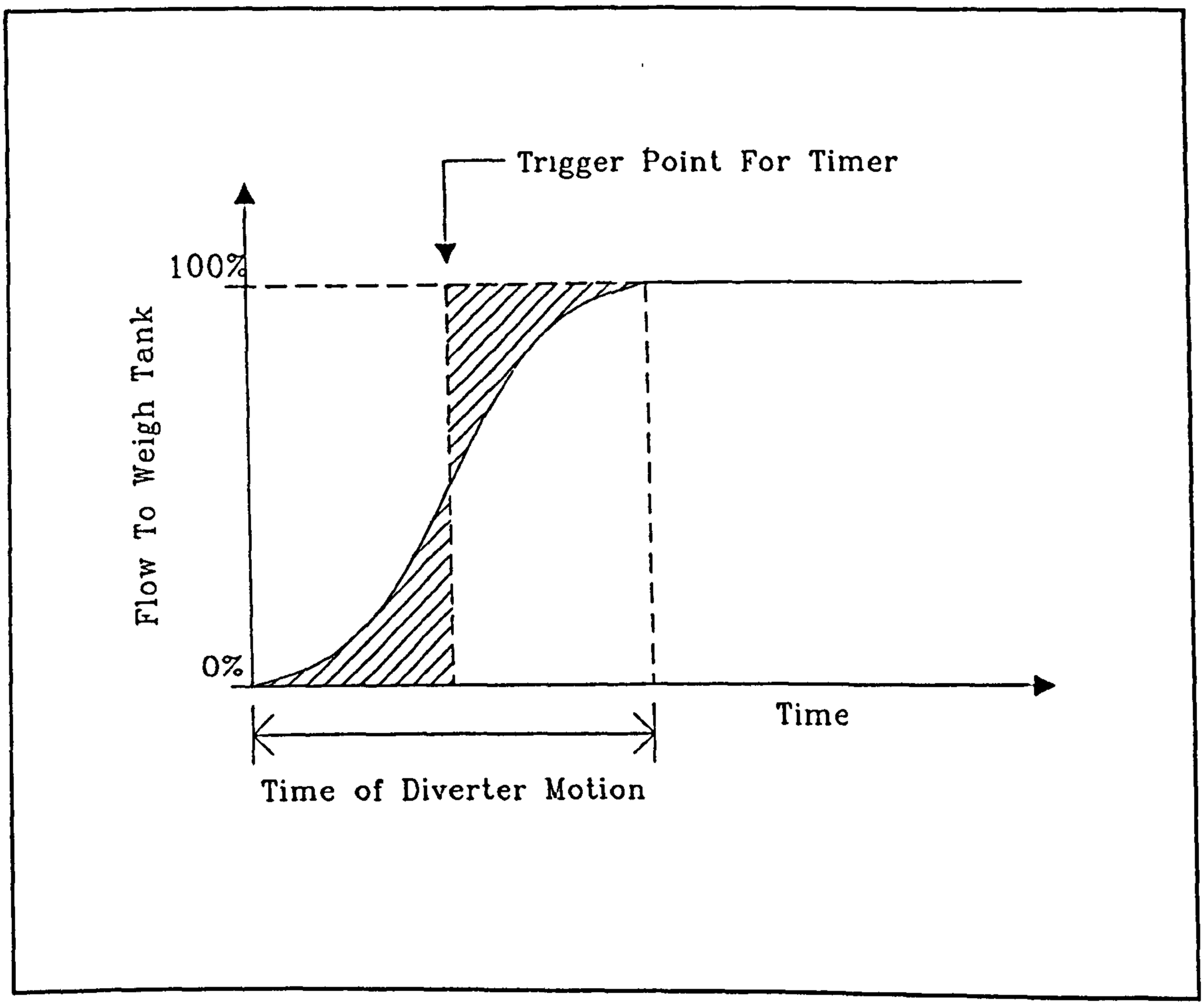

Figure 2.6: Flow Variation With Time During Operation of Diverter.

Chapter 3

Signal Strength and Pressure Drop.

3.1 Introduction.

This chapter describes the work carried out to enhance the design of the prototype fluidic oscillator water meter so that electronic detection of the oscillation is possible at low flowrates and that the device is within the maximum allowable pressure drop specification at the maximum flowrate.

Several electromagnetic induction sensing configurations were considered for the detection of oscillations within a constant magnetic field provided by two permanent magnets. Commercial considerations including the cost of magnetic material, manufacture problems and meter assembly were taken into account whilst developing the sensing configuration. The mechanisms which reduce the sensitivity of the fluidic oscillator at low flowrates were investigated and predicted sensitivities were compared with experimental results. Also the effects on meter sensitivity caused by incomplete switching of the jet at low flowrates were investigated.

To limit the pressure drop of the fluidic oscillator meter to within the domestic water meter specification the dimensions of the inlet nozzle were experimentally investigated. These dimensions determine the area of the transducer which is most critical to the pressure losses across the fluidic oscillator. The dimensions of the inlet nozzle are also critical to the velocity of the jet flow and therefore signal strength and the minimum point of oscillation.

A nozzle geometry is described which maintains the pressure drop of the device below the maximum allowed within the specifications and is still capable of operating at the required minimum flowrate.

3.2 Electromagnetic Sensing.

The oscillations within the fluidic oscillator water meter can sensed using electromagnetic induction because water is a conducting fluid. The basis of the electromagnetic sensor is described by Faraday's Law of electromagnetic induction as shown in figure 3.1.a. If a conductor of length, l, moves with velocity, v, through a magnetic field of strength , B, than an e.m.f., e, is induced across its length given by:

$$e = B.l.\mathrm{v} \tag{3.1}$$

If the conductor is a liquid moving in a rectangular channel with uniform B field as shown in figure 3.1.b then the same e.m.f. is generated between the sensing electrodes given by:

$$e = B.\mathrm{v}.h \tag{3.2}$$

where v is the mean velocity of the flow and h is the height of the channel.

Electromagnetic flowmeters incorporating permanent magnetic fields cannot measure flows which have no time varying component, however the oscillatory nature of the switching flow in a fluidic oscillator employing a constant magnetic field produces an alternating e.m.f. which can be detected using sensing electrodes.

3.3 Location of Magnet and Sensors.

Three possible locations for the electromagnetic sensor are possible as shown in figure 3.2. The first configuration shown senses the flow in the feedback channels, the second senses the flow in the main jet flow and the third senses the flow through the meter outlet port. The sensing of the flow in the main jet and in the feedback channels were investigated as described by Furmidge and Sanderson (1993).

The sensor consists of a pair of permanent magnets, together with backing plates to boost the field, which create a magnetic field orthogonal to the direction of the flow. Flow through the magnetic field induces an e.m.f. in the flow itself which is sensed using stainless steel electrodes mounted in the surface of the flow chamber. Earthing electrodes are provided upstream and downstream of the measurement volume in the form of stainless steel rings mounted between the inlet flange and meter body and the outlet flange and meter body.

3.3.1 Magnetic Field Configuration.

The magnetic materials which were considered for use within the sensing arrangement include sintered ferrite, bonded neodymium which is capable of being injection moulded for ease of manufacture, and sintered neodymium. The relative strengths of these materials are related to their remanence B_r, measured in tesla. The B_r values for the three materials are 0.37T, 0.7T, and 1.2T respectively. The sintered neodymium provides a field strength approximately three times greater than that provided by sintered ferrite using the same amount of magnetic material. The cost of sintered neodymium is considerably greater than that of sintered ferrite however, but the price per unit is considerably reduced for the numbers required by production runs of domestic water meters.

The remanence, B_r, which is roughly equal to the saturation magnetism of which the magnetic material is capable, is a measure of the materials magnetic dipole strength per unit volume when fully magnetised. This is not a measure of the magnetic field strength, B, produced by the material because a magnet always produces some field in the direction which tends to demagnetise itself. The strength of the demagnetising field depends upon the geometry of the magnet and the configuration of the rest of the magnetic circuit which it energises.

Coercive force is a measure of a magnets resistance to demagnetisation, as well as the resistance to magnetisation when unmagnetised. Magnetic materials such as ferrite or neodymium withstand demagnetisation in the worst geometric configuration which is a flat slab of the material in air magnetised through the thickness of the material, rather than through the length.

For a slab of magnetic material with remanence B_r the field strength produced by the magnet is given by:

$$B = k.B_r \tag{3.3}$$

where k is some constant depending on the geometry of the magnet.

By backing the magnetic material with a mild steel backing plate the field in the centre of the front face of the magnet is almost the same as that created by having a magnet of twice the thickness. Therefore the magnetic field strength produced by a 6mm slab of magnetic material would be the same as that produced by a 3mm thick slab of the same material backed with mild steel.

The field strength across the front face of a 6mm thick slab of sintered ferrite separated by 7.5mm from a second magnet of the same dimensions in the arrangement shown in figure 3.3 was measured using a Hall probe. Figures 3.4 and 3.5 show plots of the field strength measurements in a horizontal and vertical direction across the face of the magnet respectively. Figure 3.5 shows that the field strength produced by a 6mm thick ferrite slab is approximately 0.12 tesla through the region occupied by the height of the jet flow.

Given that the remanence of sintered ferrite is 0.37 tesla then for the magnet geometry described above equation (3.3) can be written as:

$$B = 0.32\ B_r \tag{3.4}$$

Equation (3.4) is also correct for a 3mm thick slab of magnetic material, of the same height and width dimensions, backed with a mild steel backing plate.

The field strength produced by a 3mm thick slab of sintered neodymium, B_r value 1.2 Tesla, backed with a mild steel backing plate, in the same arrangement as shown in figure 3.3, is therefore calculated to be 0.39 tesla.

3.4 Sensitivity in Feedback channel.

Measurement of the frequency of oscillation using flow in the feedback channel depends on the sensing of the fluctuations in flow which occur in the feedback channel as a result of the switching of the main jet flow. If the flow being sensed has uniform velocity profile over the cross section of the channel with a time variation given by:

$$v_{(t)} = \sum_{n=1}^{\infty} V_n \cos(n\omega t + \varphi_n) \qquad (3.5)$$

where ω is the fundamental frequency of fluctuation and v_2, v_3,.... etc. represent the harmonic content of the velocity fluctuation then using equation (3.2):

$$e_{(t)} = Bhv_{(0)} + Bh \sum_{n=1}^{\infty} V_n \cos(n\omega t + \varphi_n) \qquad (3.6)$$

Thus the waveform of the fluctuating component of the e.m.f. will have the same shape as the velocity waveform. It is not possible to distinguish the d.c. component of the velocity from electrochemical e.m.f.s. However the fluctuating component can be distinguished as long as its magnitude is sufficiently large compared to the electrochemical noise at the sensors. The rectangular cross section of the feedback channel with a large height to width ratio, together with a uniform magnetic field and electrodes almost completely filling the width of the channel, provides a configuration which is almost ideal, ie. the generated e.m.f. is independent of velocity profile and depends only on the mean flow.

The typical width of the channel in the feedback section of a $Q_N1.0$ meter is 4.5mm. Assuming a material wall thickness of 1.5mm, this was later increased to 3mm to prevent enlargement of the flow chamber under high back pressure, then the poles of the magnet are separated by 7.5mm. The field produced across this gap if two pieces of magnetic material of thickness 3mm are used in conjunction with a mild steel backing plate is estimated to be $0.32B_r$ tesla as described in the previous section.

With electrodes on the top and bottom of the channel the sensitivity, S_f, of the configuration in μV ml s^{-1} for flow in the feedback channel is given by:

$$S_f = \frac{0.32\ B_r}{W_f} \tag{3.7}$$

where W_f is the width of the feedback channel.

The sensitivity of the configuration, S_m, with respect to the main flow is approximately 0.05 of that measured with respect to the feedback channel, since the feedback flow is approximately 5% of the main flow. The expected sensitivity, S_m, of the feedback flow configuration is $4.27\mu V$ ml s^{-1}, using sintered neodymium as the magnetic material. This sensitivity is low compared with the main jet sensitivity.

If the relative positions of the electrodes and the magnetic field are swapped, ie. the magnets are located at the top and bottom of the feedback channel with electrodes at each side of the feedback channel, then there is no gain in signal strength. This is because the strength of the magnetic field would be lower, due to the increased spacing of the magnets, and the shorter path length between the electrodes results in a smaller generated e.m.f.

3.5 Sensitivity in the Main Jet.

The velocities in the main jet are significantly higher than those in the feedback channel, and therefore it appears to be attractive to place magnetic material within the diffuser wall sections of the oscillator and detect the fluctuations due to the jet moving from one diffuser wall to the other. The exact sensitivity in this configuration is difficult to estimate because of the presence of the splitter post and the non-uniformity of the magnetic field caused by the angle at which the magnets are installed and the varying gap width across the diffuser section.

The model which has been used to estimate the sensitivity is shown in figure 3.6 where 2a is the width of the channel, d is the width of the electrode and 2b is the channel height. The model is two dimensional and assumes a uniform magnetic field in the regions close to the side wall, electrodes in the corners of the channel, a jet which switches fully from side to side with stagnant fluid everywhere else, and no splitter post. It can be seen that the arrangement has a maximum sensitivity to flows near the electrodes, but still some residual sensitivity when it is near the wall furthest away from the electrodes.

The change in sensed e.m.f. of such a configuration can be determined by calculating the outputs when the jet is in a position close to the sensing electrodes, U_n, and when the jet is on the diffuser wall away from the electrodes, U_f. The amplitude of the voltage detected between the electrodes as the jet switches is then given by $U_n - U_f$.

The equation to be solved for the potential U is:

$$\frac{\partial^2 U}{\partial x^2} + \frac{\partial^2 U}{\partial y^2} = 0 \qquad (3.8)$$

Subject to the boundary conditions determined from the field and flow conditions given above.

It can be shown that the solution is given by:

$$U = Bvy + \sum_{n\ odd}^{\infty} A_n \cosh\frac{n\pi x}{2b} \cdot \sin\frac{n\pi y}{2b} \qquad 0 \le x \le d \qquad (3.9)$$

and

$$\sum_{n\ odd}^{\infty} B_n \cosh\frac{n\pi(x-2a)}{2b} \cdot \sin\frac{n\pi y}{2b} \qquad d \le x \le 2a \qquad (3.10)$$

where the A_n's and B_n's are found by requiring continuity of $\frac{\partial U}{\partial x}$ and U at x = d.

The potential developed between the two electrodes when the jet is at the wall nearest to them, U_{jn} is given by:

$$U_{jn} = 2Bvb\left[1+\frac{8}{\pi^2}\sum_{n\ odd}^{\infty}\frac{1}{n^2}\cdot\frac{\sinh n\pi\frac{(d-2a)}{2b}}{\sinh\frac{n\pi 2a}{2b}}\right] \qquad (3.11)$$

and the potential that is developed between the electrodes when the jet is at the wall furthest from the electrodes, U_{jf} is given by:

$$U_{jf} = \frac{16Bvb}{\pi^2}\sum_{n\ odd}^{\infty}\frac{1}{n^2}\cdot\frac{\sinh\frac{n\pi d}{2b}}{\sinh\frac{n\pi 2a}{2b}} \qquad (3.12)$$

the change in potential as the jet fluctuates from side to side is thus given by:

$$U = U_{jn} - U_{jf} \qquad (3.13)$$

In the case of a uniform jet flow, ie fully developed flat profile, with complete switching, the sensitivity is given by:

$$S_m = \frac{0.3\ B}{w} \tag{3.14}$$

where w is the jet width and B is the field strength.

The sensitivity is reduced by two effects. When the jet is close to the measuring electrodes the e.m.f. generated is shorted by the surrounding stagnant fluid and when the jet is on the far wall a signal is still picked up by the sensing electrodes. These both have the effect of reducing the signal detected as the jet switches from side to side.

Comparisons have been made between the predicted sensitivity, using the model, and the signal detected in the oscillator. In an oscillator employing sintered neodymium magnets the average field strength close to the wall in the region of the electrodes was measured with a Hall probe and found to be 0.22 T. Equation (3.14) gives the predicted sensitivity to be 27.5μV ml s^{-1}. The experimentally measured sensitivity was 24.0μV ml s^{-1} which is sufficient to allow electronic detection of the jet oscillation over the range required for a Q_N1.0 domestic water meter.

3.5.1 Alternative Sensing Configuration.

An alternative sensing arrangement for the measurement of flow in the main jet is shown in figure 3.7. In this configuration the magnetic field is applied to the upper and lower faces of the flow chamber and the electrodes are mounted within the diffuser walls. In order for this scheme to work there has to be a change in sign of the magnetic field between the two sides of the body. The length of the conductor now corresponds to the width of the jet. The amount of shorting out of the signal depends on the penetration depth of the magnetic field.

The sensitivity, S_m, of this configuration is given by:

$$S_m = \frac{k\,B}{b} \tag{3.15}$$

where B is the field strength in Tesla, 2b is the height of the flow chamber and k depends upon the penetration depth of the field.This alternative configuration, even with a high field strength and a reasonable penetration depth, eg. 6mm, only gives a sensitivity equal to that of the standard configuration in the main jet. In practice it is unlikely that a penetration depth of 6mm can be achieved and therefore the most suitable sensing configuration is the sensing of the main jet flow with magnetic material mounted within the diffuser walls of the fluidic oscillator.

3.6 Effect of Incomplete Jet Switching on Sensitivity.

At low flowrates approaching Q_{min} the jet oscillations weaken due to viscous damping and the jet switches across the post only and not completely from one diffuser wall to the other. As the flowrate is reduced further the jet only partially switches across the post and at even lower flowrates oscillation ceases as the jet becomes stable and simply splits around the post reforming downstream.

The sensitivity calculation model described above can be used to predict the reduction in sensitivity as the jet moves away from the diffuser walls and towards the splitter post as the oscillation weakens at low flowrates. Figure 3.8 shows the prediction of the reduction of sensitivity as the jet switching moves away from the diffuser walls. It can be seen that as the jet moves away from the diffuser wall there is a considerable reduction in sensitivity of the flowmeter. If the jet switches 1mm away from the diffuser wall then the sensitivity is reduced by 43% compared to that of full jet switching.

This rapid reduction in sensitivity occurs because of two effects. When the jet moves

away from the diffuser wall the signal detected at that wall is reduced and, because the jet is nearer to the sensing electrode on the opposite diffuser wall, the signal detected at the opposite wall is greater. When the jet becomes stable and splits evenly around the splitter post the device has zero sensitivity.

A modification enhancement to the geometry of the fluidic oscillator, described in Chapter 5, involves a concave recess machined into the upstream face of the splitter post. The modification was developed to improve the low flow performance of the fluidic oscillator but also significantly improves the strength of oscillation at low flowrates and results in more complete switching. This more complete switching significantly boosts the signal strength at low flowrates. The splitter post modification also has the advantage that it does not alter the linearity of the fluidic oscillator but increases the oscillation frequency throughout the range which is beneficial. The modification is easily tooled for the production version of the fluidic oscillator domestic water meter and has been incorporated within the Class C Q_N1.0 meter. The mechanisms behind the improved oscillation switching are described in more detail in Chapter 5.

3.7 Relative Sensitivity of Fluidic Oscillator Water Meter.

The relative sensitivity of a Q_N1.0 Class C fluidic oscillator sensor over a range of flowrates up to 80ml s^{-1} is shown in figure 3.9. It can be seen that the graph displays the characteristics described above. At flowrates above 40ml s^{-1} the sensitivity is constant. 40ml s^{-1} corresponds to a Reynolds number of 2000 within the jet, above Reynolds numbers of 2000 the jet flow is in the fully turbulent flow regime. As the flow reduces to 10ml s^{-1} there is a reduction in sensitivity of approximately 60%. This corresponds to the transition from fully turbulent to laminar flow conditions within the jet. At flowrates below 3ml s^{-1} there is a further rapid reduction in sensitivity as the oscillation weakens and the jet switching becomes only partial. At 2ml s^{-1} the sensitivity of the jet is estimated to be 6μV ml s^{-1}, which provides a detectable signal of 12μV.

3.8 Pressure Drop Across Fluidic Oscillator Flowmeter.

The British Standard BS5728 (1979) states that the maximum allowable pressure drop for a Q_N1.0 water meter is 1 bar, 14.7 p.s.i., at the maximum flowrate, Q_{max}.The inlet nozzle of the fluidic oscillator is the region which is most critical to the pressure drop of the fluidic oscillator.

The maximum pressure drop, Δp_{max}, of a fluidic oscillator meter is given by:

$$\Delta p_{max} = E_{max} \frac{1}{2} \rho \frac{Q_{max}^2}{\alpha^2 w^4} \qquad (1.3)$$

where ρ is the density of the measured fluid, E is the Euler number and α is the aspect ratio of the fluidic oscillator defined as the ratio of nozzle height, h, to nozzle width, w.

Equation (1.3) shows that the pressure drop of the fluidic oscillator is inversely proportional to w^4. This implies significant changes in pressure drop are achievable with only small changes in the nozzle width dimension.

The pressure drop of the meter components must also be considered when attempting to maintain the pressure losses across the flowmeter to within the B.S.I. specification. The fluidic oscillator is not capable of reading reverse flows therefore the device must be fitted with a non-return valve which will have a fixed pressure drop at Q_{max}. Any additional filtering or flow conditioning device within the meter unit will also add to the pressure losses across the flowmeter.

3.9 Nozzle Width.

Early fluidic oscillator water meter transducer designs had a nozzle width, w, of 2.4mm. The internal height of the flow chamber is 20mm resulting in a nozzle aspect ratio, α, of 8.33. Pressure drop tests showed that the fluidic oscillator flow chamber with a jet gap of 2.4mm fitted with a flow conditioner, a strainer of 1mm pitch, and a non-return valve did not meet the required maximum pressure drop specification.

To reduce the pressure drop of the device two test meters were modified to have increased nozzle widths. The nozzle of the first test meter was increased by 10% to 2.64mm. The nozzle of the second meter was enlarged by a further 10% wider than the previously enlarged test meter to 2.9mm. The nozzle widths were enlarged using computer numerical controlled machining techniques to ensure high quality material surface finishes and accurate sizing and alignment.

The meters were tested with all fitted components including a fine filter, of 1mm pitch, a flow conditioner plate and a non-return valve. Figure 3.10 shows the pressure drop curves for the three jet widths, 2.4mm, 2.64mm, and 2.9mm tested with all fitted components.

An improvement of 3.06 p.s.i. in pressure drop is seen after increasing the jet gap from 2.4mm to 2.64mm whilst the pressure drop is reduced by 4.16 p.s.i. after increasing the jet gap to 2.9mm. The reduction in pressure drop after increasing the jet gap from 2.64mm to 2.9mm is not as great as that as increasing the gap from 2.4mm to 2.64mm. This is because the distance between the splitter post and the diffuser wall becomes the limiting factor rather than the width of the nozzle gap.

Figure 3.11 shows a comparison between the pressure drops produced by a meter with a 2.4mm wide nozzle and a 2.64mm wide nozzle. Both meters were tested without any other additional meter components.

3.10 Pressure Drop Investigations

Tests were carried out to determine the pressure drop due to each of the meter components as described by Furmidge (1992). Figure 3.12 shows the results of the pressure drop experiments carried out.

Curve A :- 2.64mm nozzle with open inlet and outlet.

Curve B :- 2.64mm nozzle and flow conditioner.

Curve C :- 2.64mm nozzle, flow conditioner and filter.

Curve D :- 2.64mm nozzle, flow conditioner, filter and non-return valve.

The increase in pressure drop due to each meter component of the fluidic oscillator meter at the maximum flowrate is shown in table 3.1.

Meter Component	Pressure Drop At Q_{max} (p.s.i.)
1mm Filter	2.65
Flow Conditioner	1.47
Non-return Valve	0.88

Table 3.1 Pressure drop due to meter components.

The pressure drops created by the filter and flow conditioner are dependent on their blockage ratio. A filter is only required for flow conditioners with small holes as the fluidic oscillator itself is capable of passing debris through the device and requires no filter. The development of flow conditioner plates with low pressure losses that require no form of filtering is described in Chapter 4. The pressure drop of the non-return valve is dependant on the type used, however 0.88 p.s.i. would seem an acceptable low value.

3.11 Minimum Point of Oscillation and Signal Strength.

Increasing the width of the fluidic oscillator nozzle gap reduces the pressure drop across the meter but both the velocity of the jet flow and the distance between each jet oscillation and its opposite electrode pair are also reduced. The velocity of the jet flow and the distance between the jet and its opposite electrode pair are proportional to signal strength as described earlier in this chapter. Also the Reynolds number within the jet is lower at equivalent flowrates. Lowering the Reynolds number causes the jet flow to be more stable at equivalent flowrates which results in a higher minimum point of oscillation. Increasing the minimum point of oscillation makes the Q_{min} specification difficult to achieve which is particularly significant at low temperatures, where the minimum flowrate for oscillation is increased due to the increased viscosity of the water.

3.12 Pressure Drop Conclusions.

A nozzle width of 2.64mm provides sufficient signal strength at low flowrates, using neodymium magnetic material, and is capable of maintaining oscillation at flowrates low enough to reach the $Q_N1.0$ Class C minimum flowrate specification at 10°C. Increasing the nozzle width to 2.9mm increases the minimum point of oscillation and reduces the signal strength at low flowrates whilst giving only marginal benefits in pressure drop over a nozzle width of 2.64mm. The improvements in pressure drop following the increase in jet width to 2.64mm are such that with careful design of the flow conditioner the fluidic oscillator water meter is within the maximum pressure drop specification at the maximum flowrate.

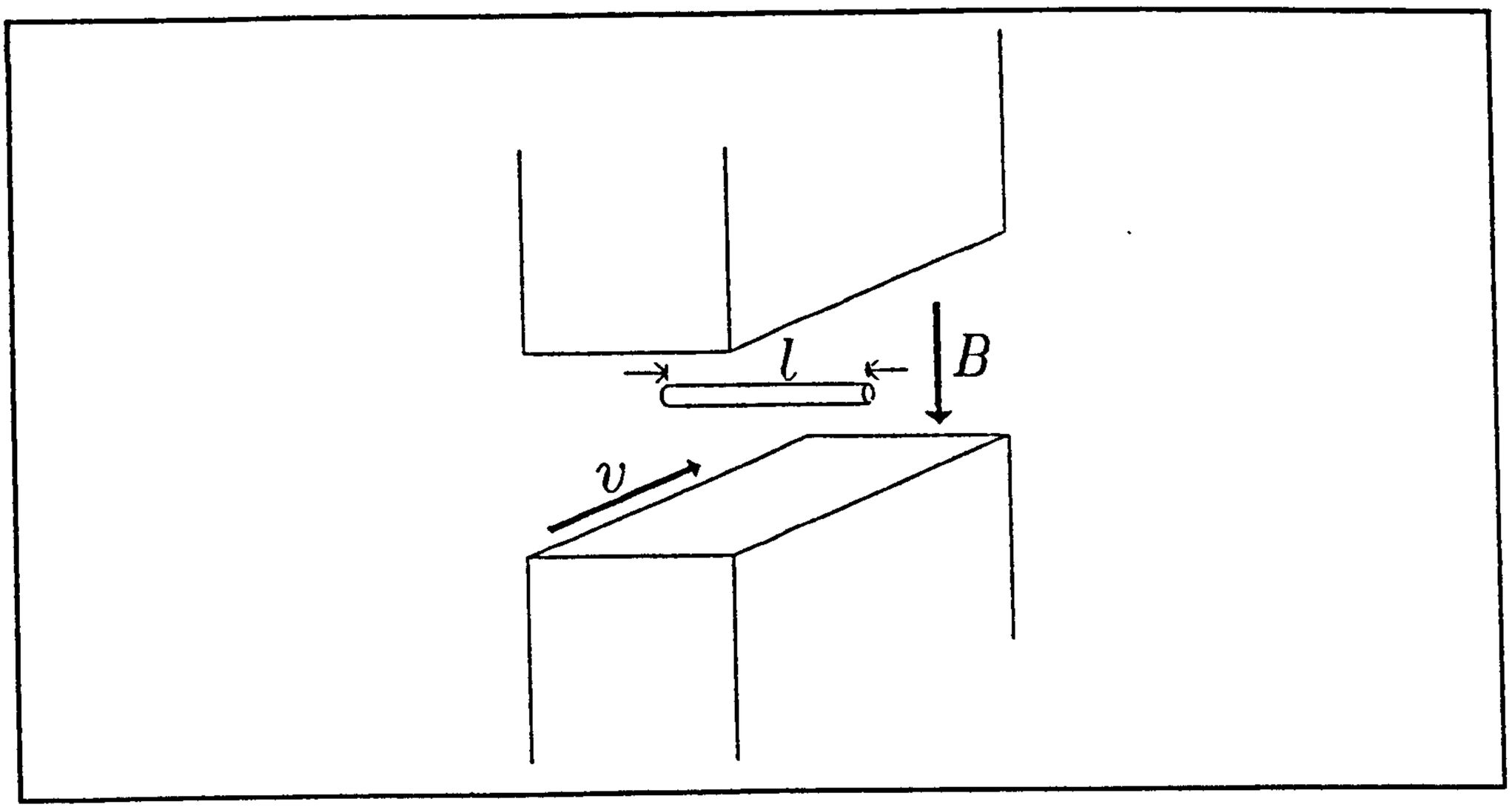

Figure 3.1a: Conductor Moving Through Magnetic Field.

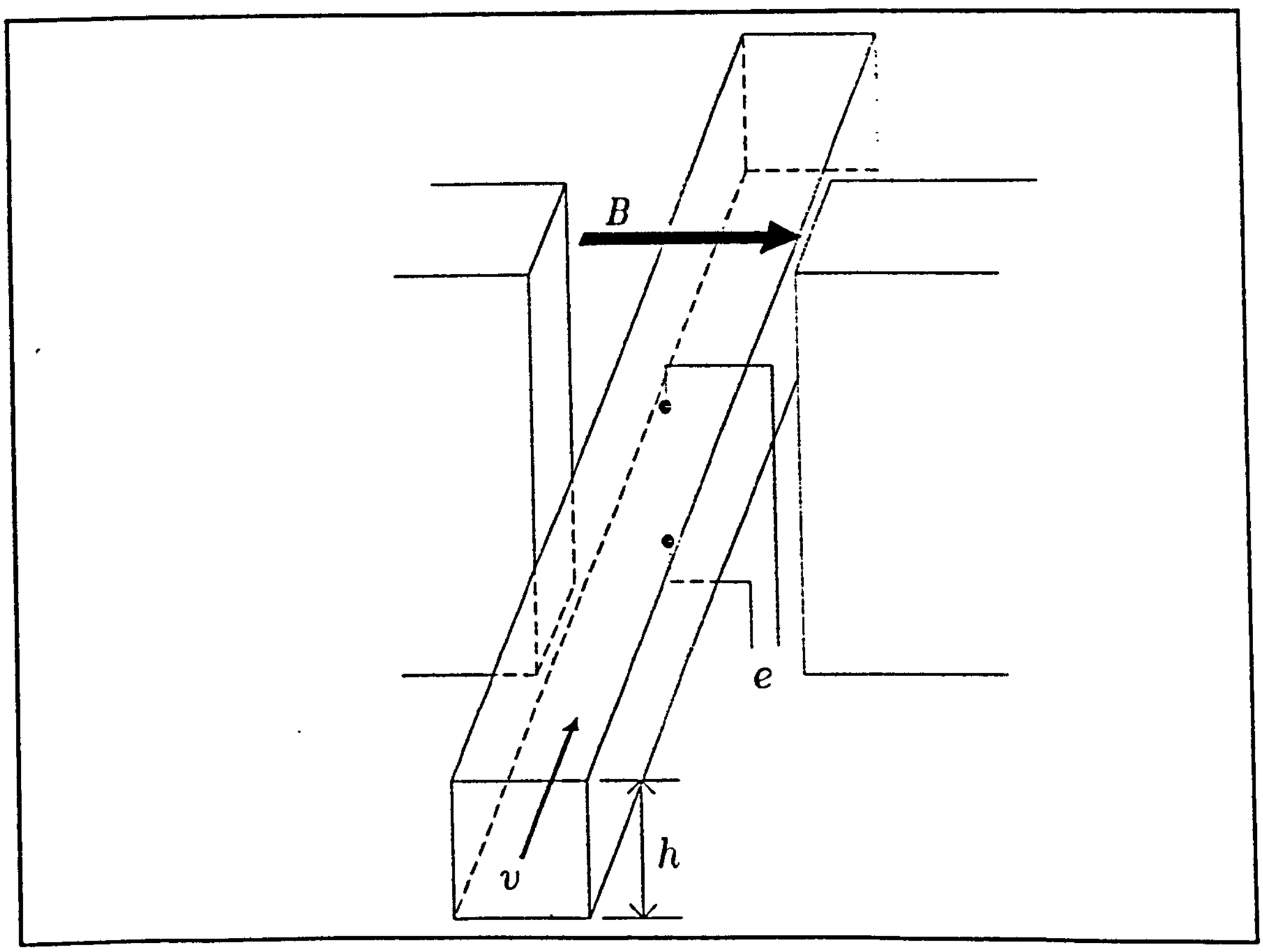

Figure 3.1b: Conducting Liquid Flowing in Channel Through Magnetic Field.

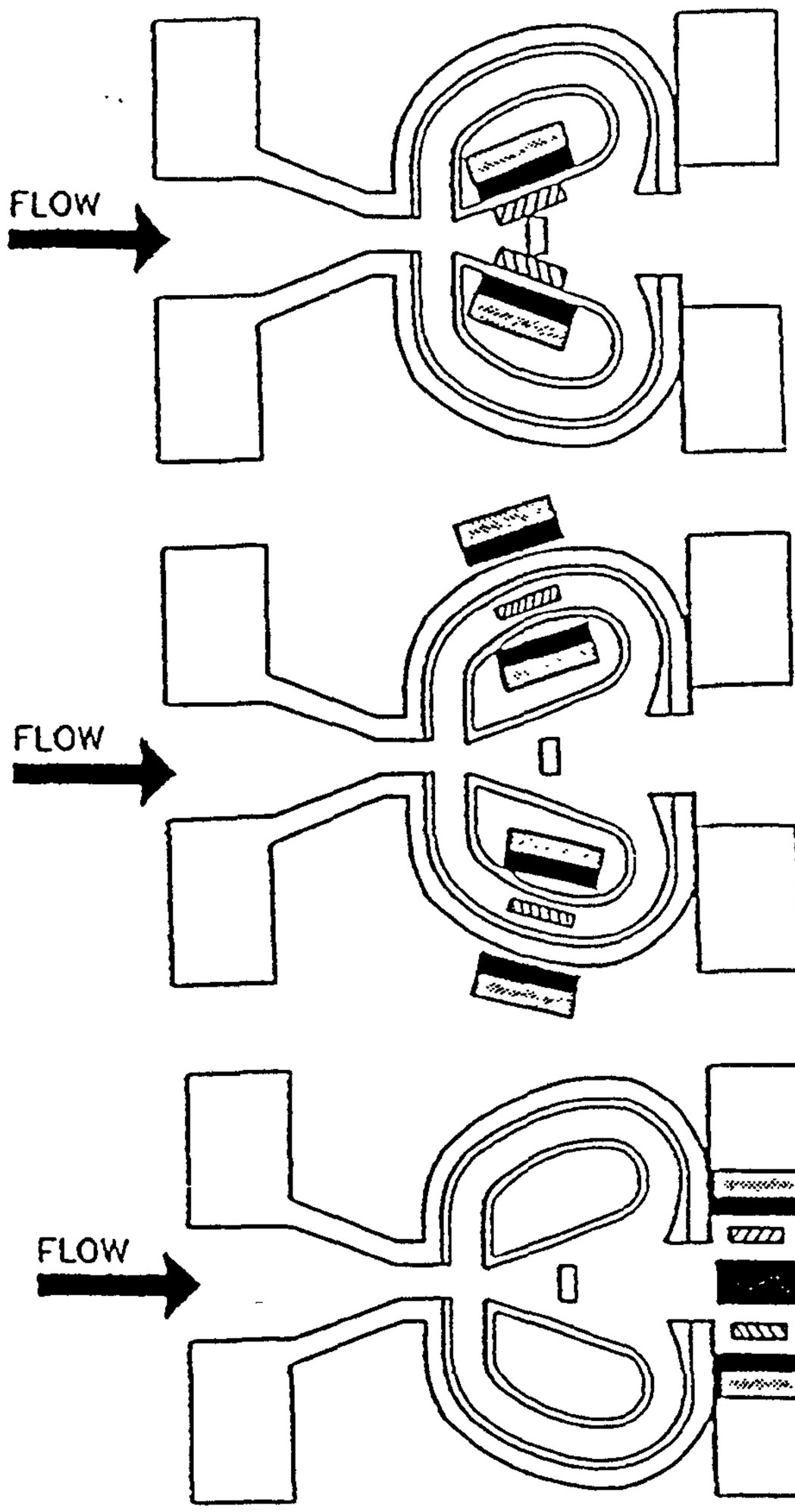

Figure 3.2: Possible Locations For Electromagnetic Sensor.

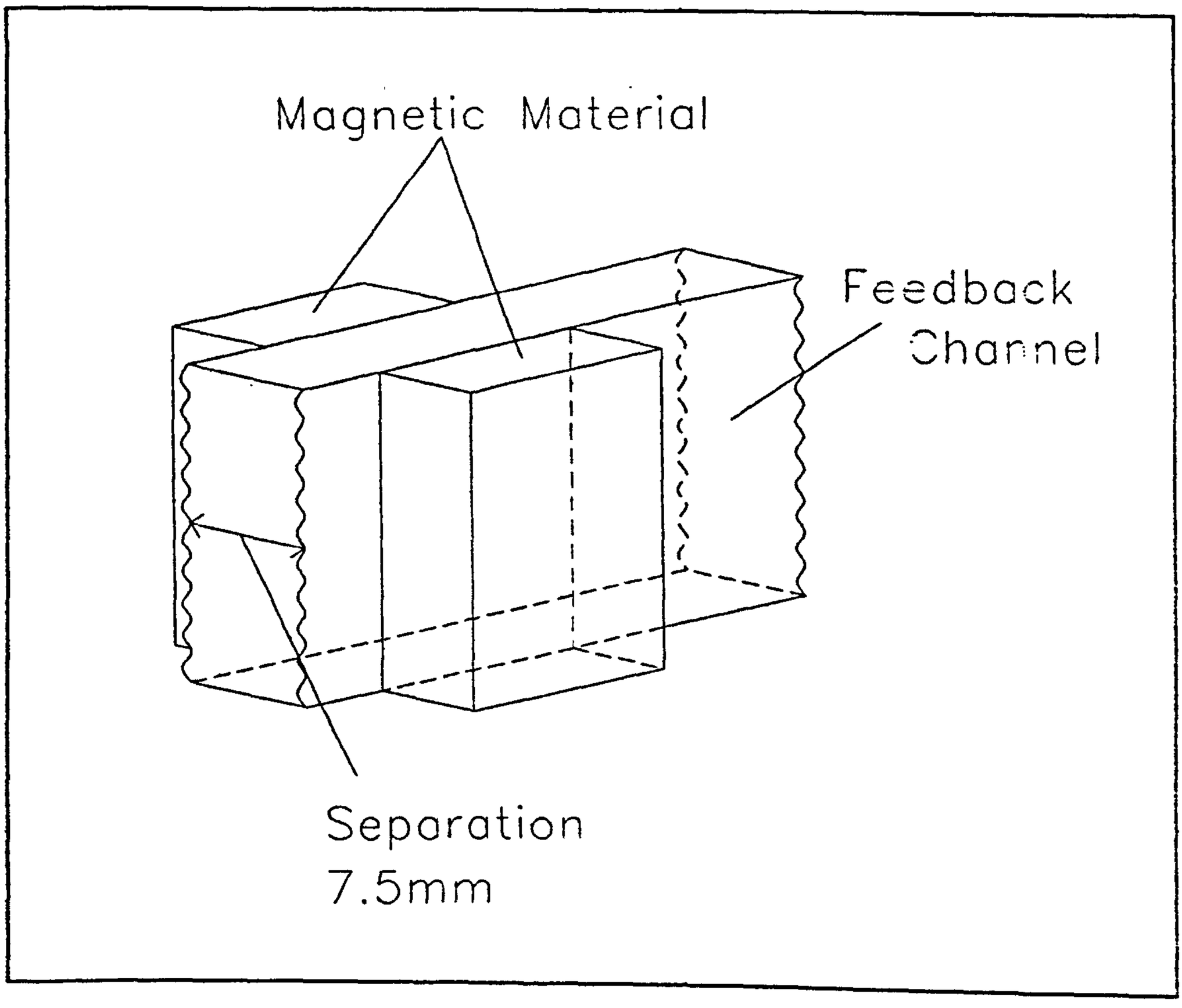

Figure 3.3: Magnetic Configuration.

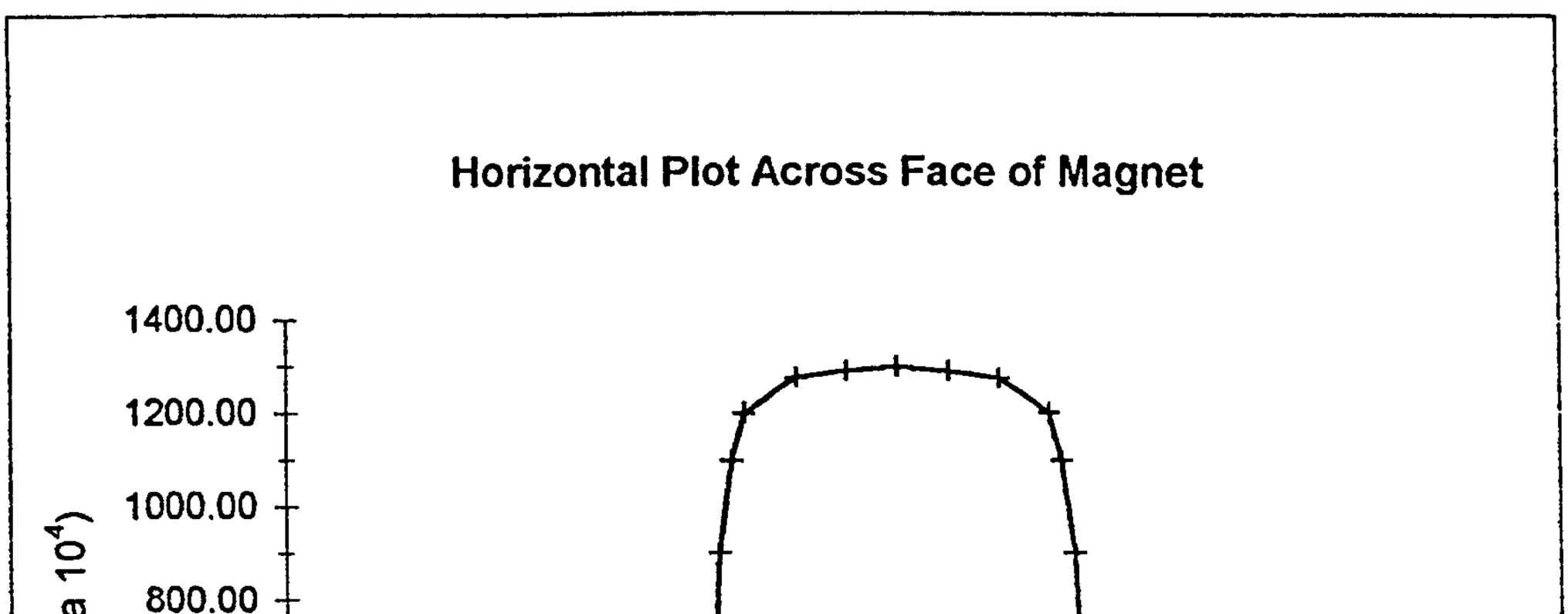

Figure 3.4: Measured Field Strength In Horizontal Direction.

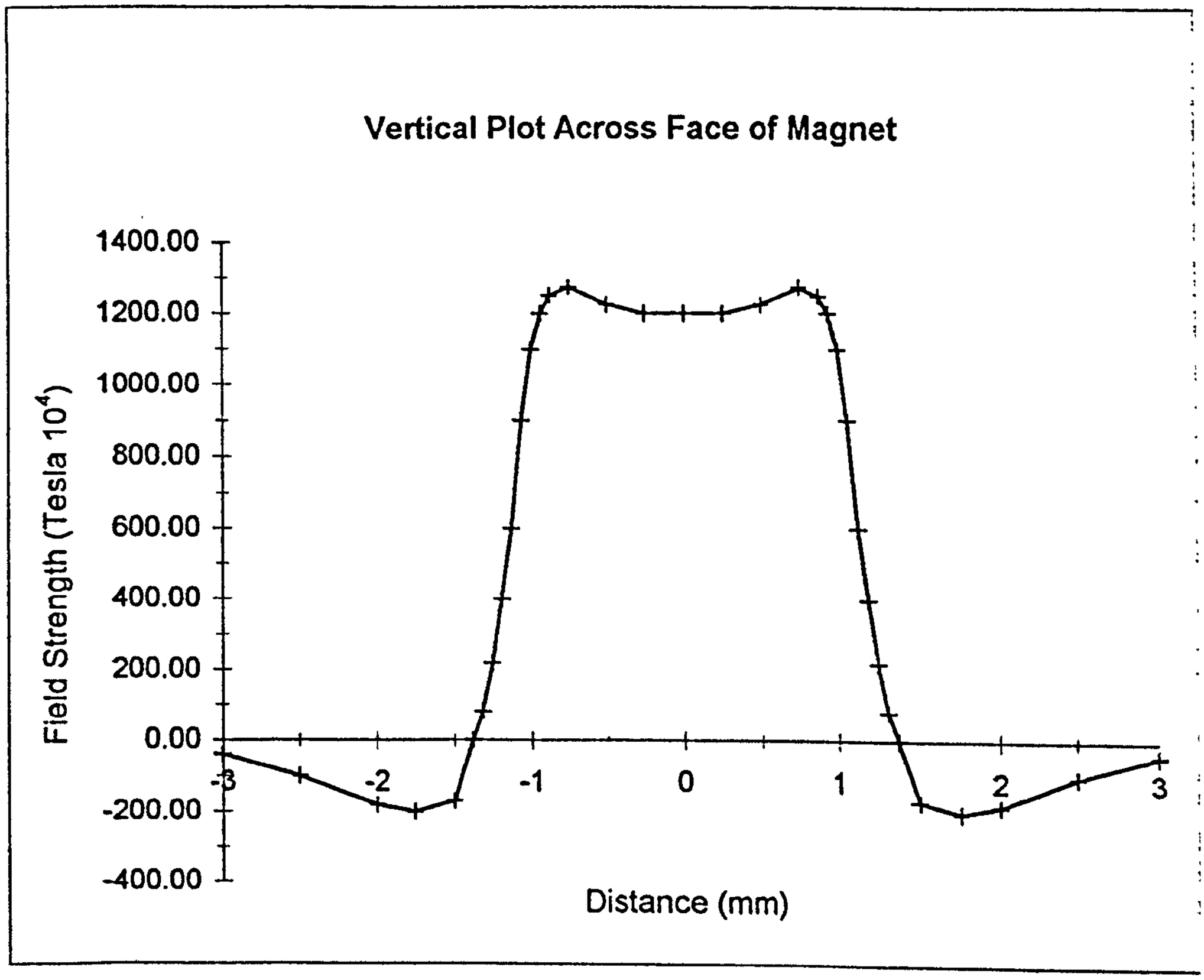

Figure 3.5: Measured Field Strength In Vertical Direction.

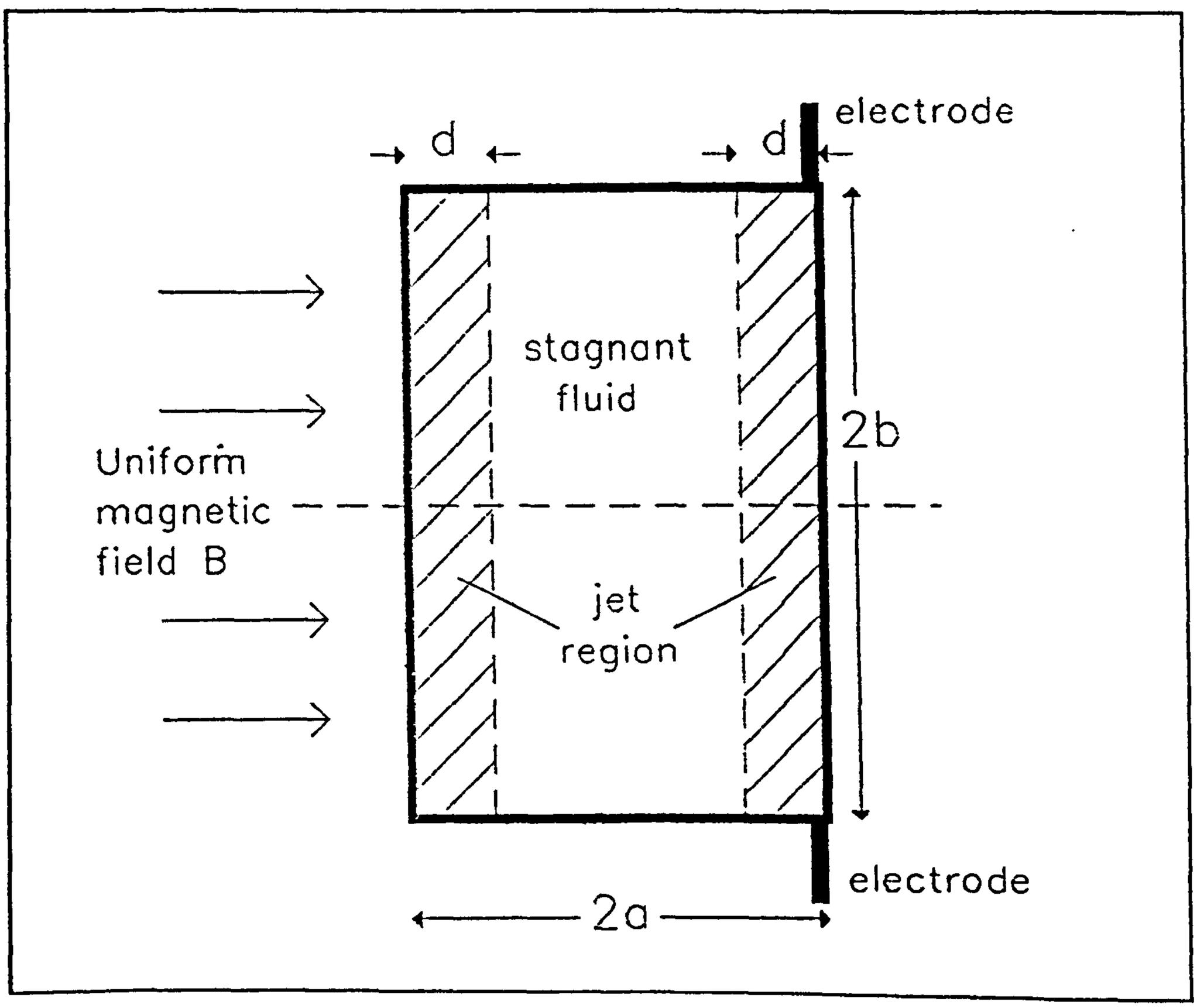

Figure 3.6: Model Used To Estimate Sensitivity In Main Jet.

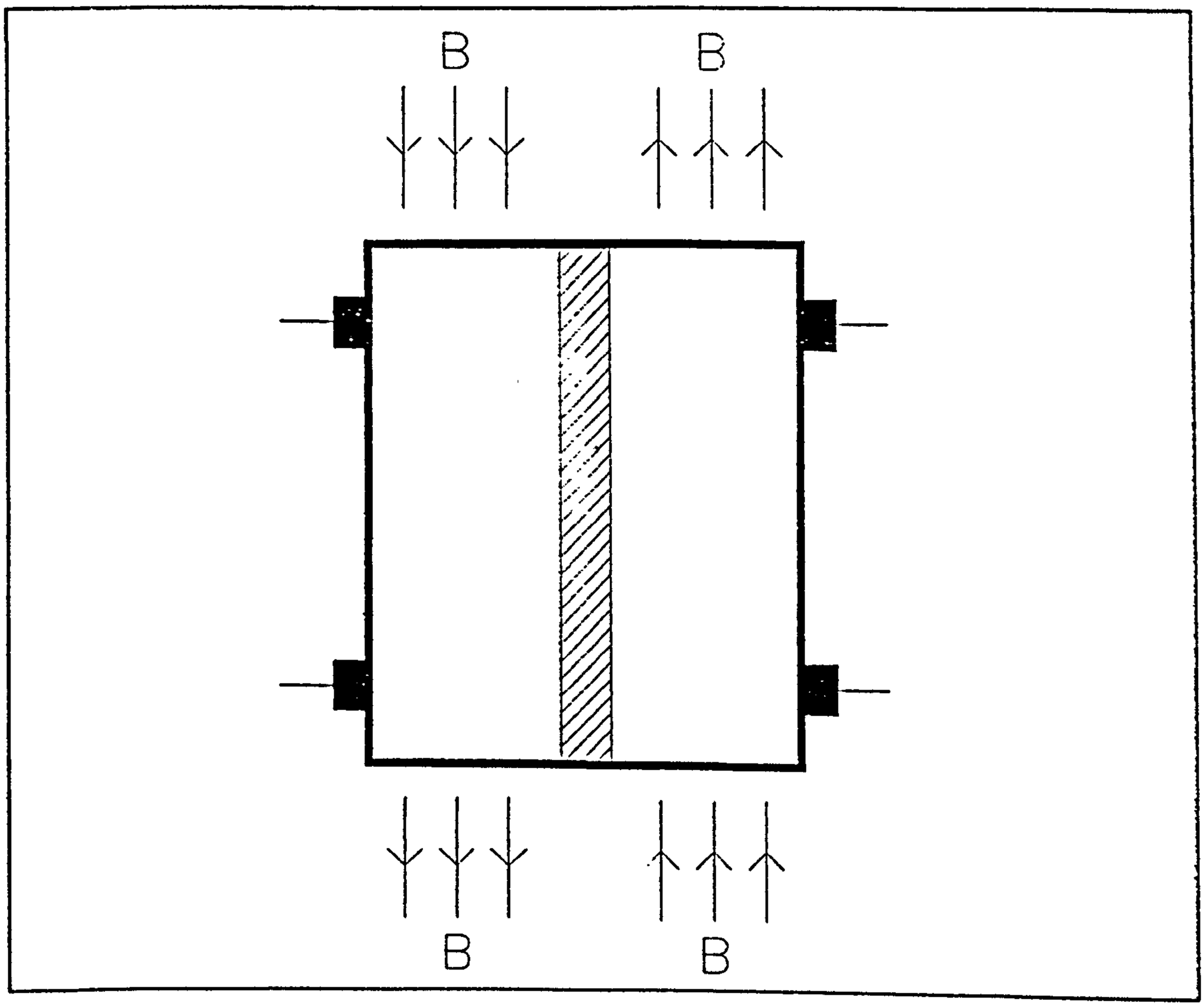

Figure 3.7: Alternative Sensing Arrangement.

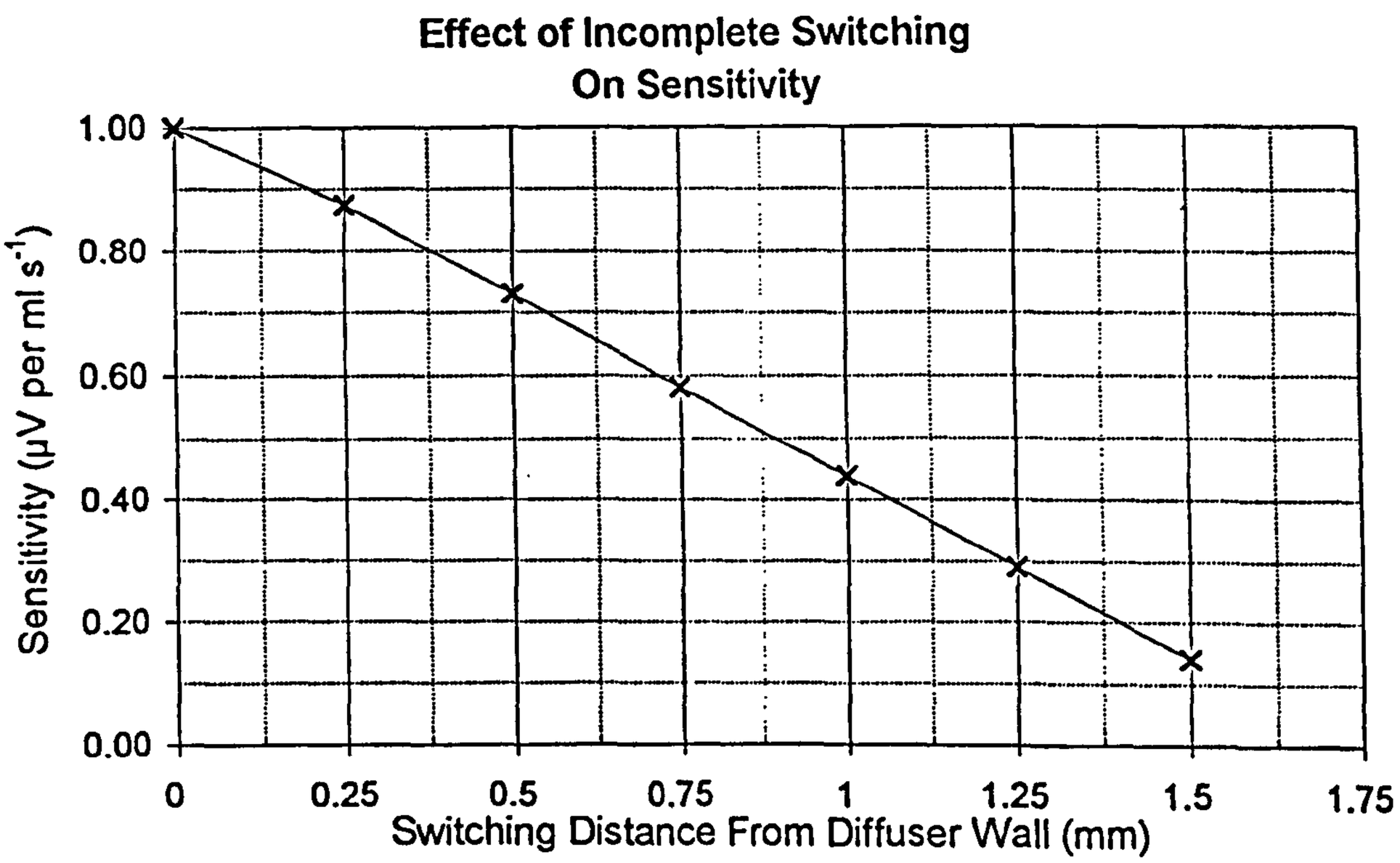

Figure 3.8: Reduction In Sensitivity As Jet Moves Away From Diffuser Wall.

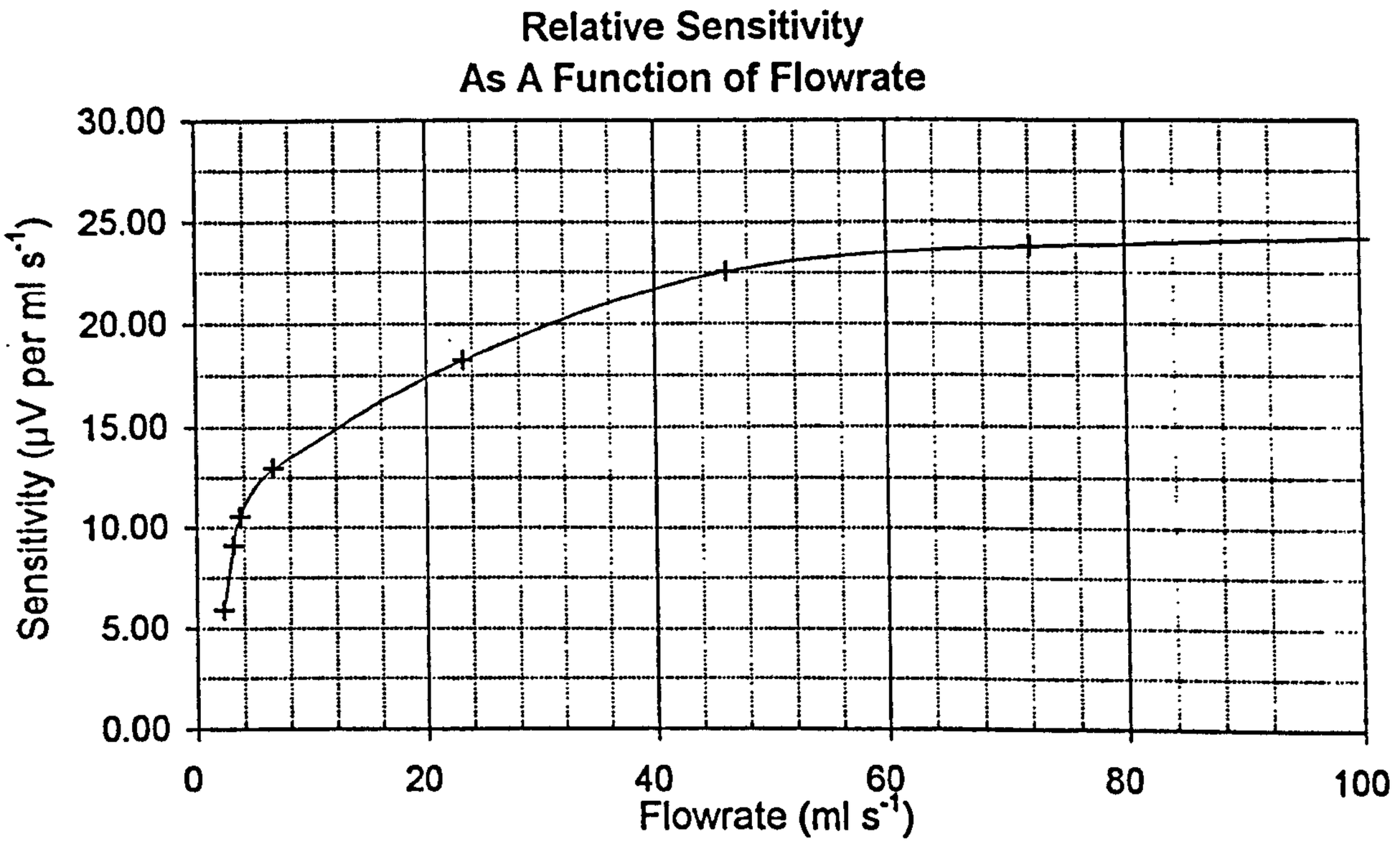

Figure 3.9: Relative Sensitivity Over Range of Flowrates.

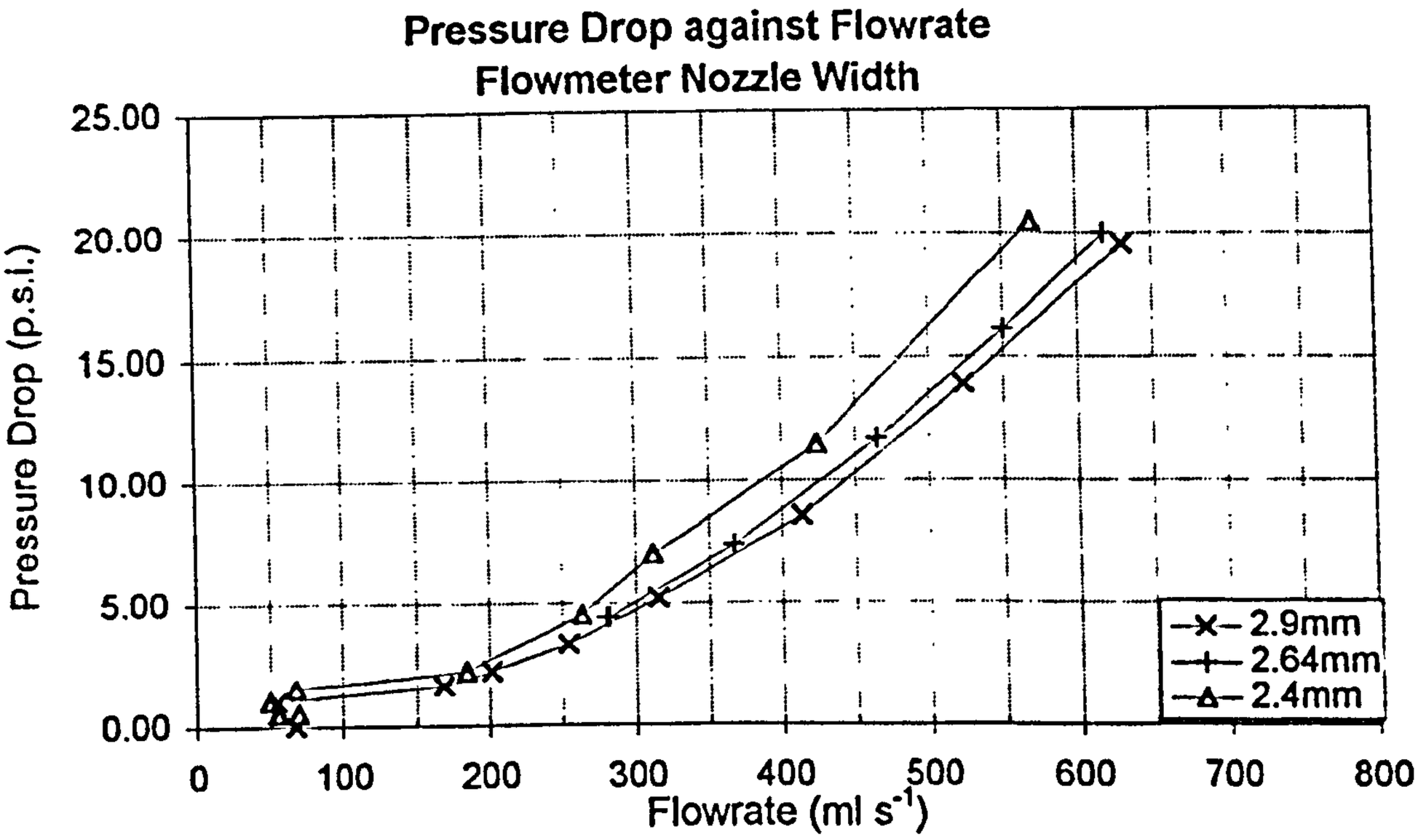

Figure 3.10: Pressure Drop of Fluidic Oscillator Meter With Varying Nozzle Widths.

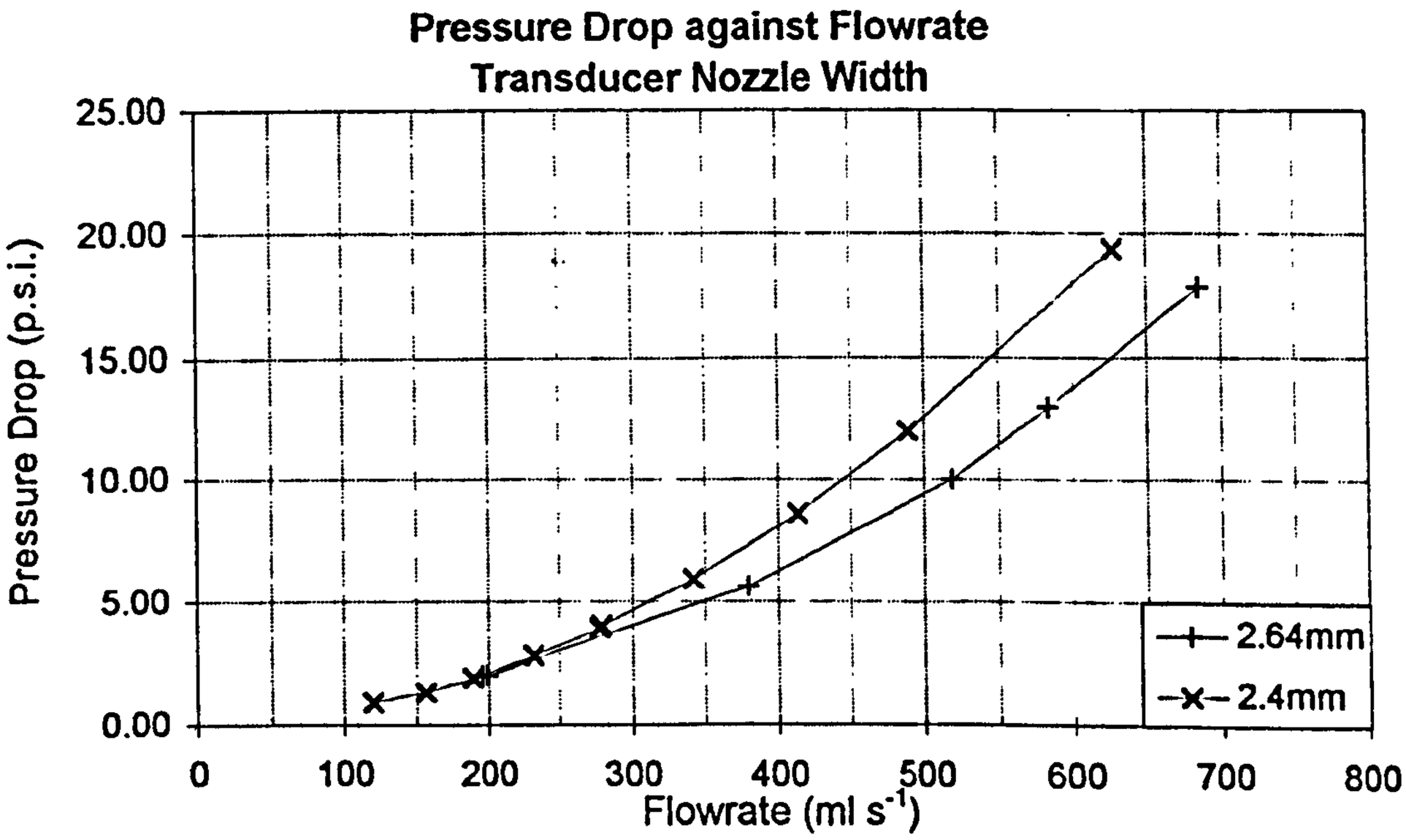

Figure 3.11: Pressure Drop of Transducer With Varying Nozzle Widths.

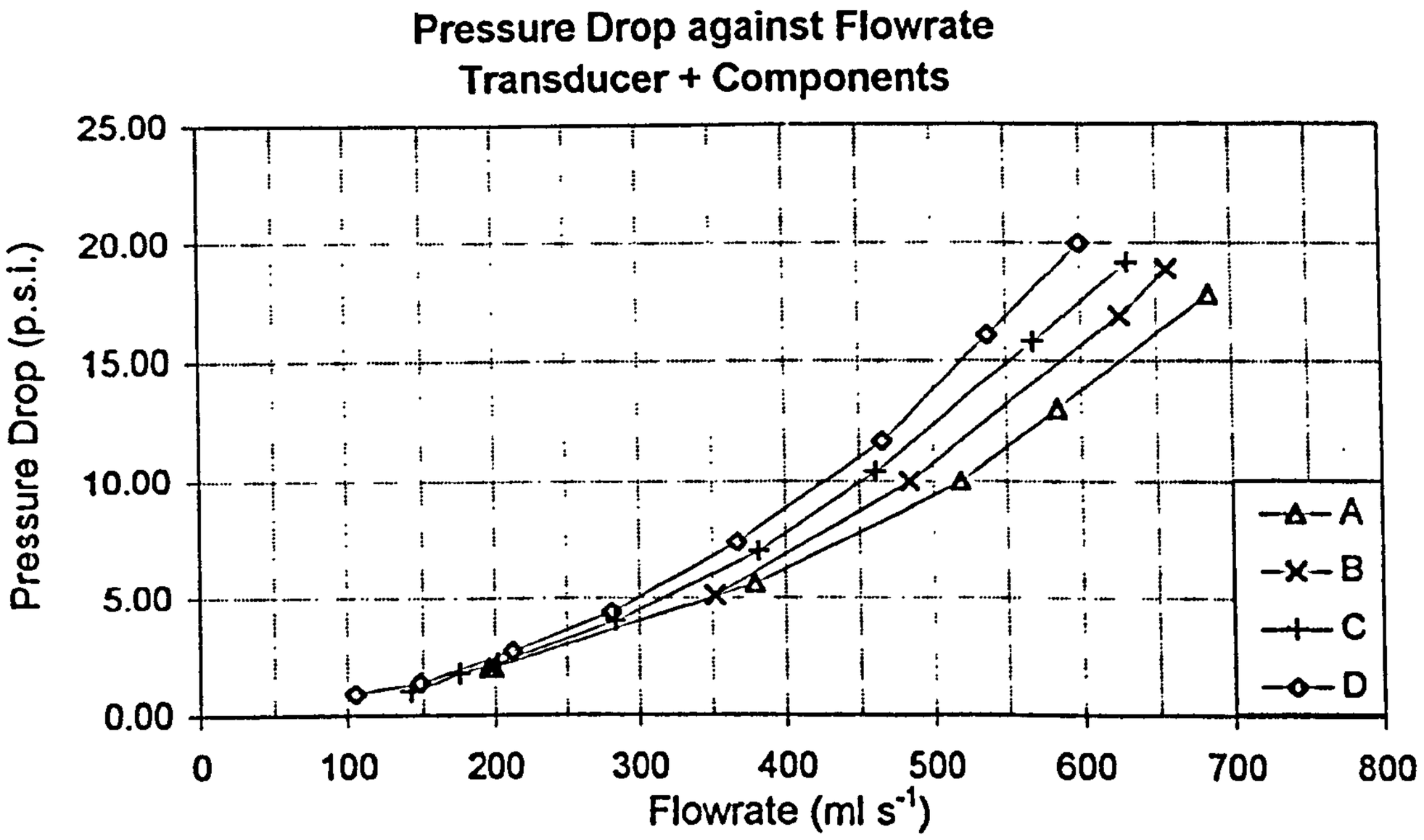

Figure 3.12: Pressure Drop Due To Individual Meter Components.

Chapter 4

Increased Linearity Over Full Flow Range.

4.1 Introduction.

The effects of flow conditioning carried out to improve and optimise the linearity of the fluidic transducer are described in this chapter. The fluidic oscillator water meter is equipped with linearisation and temperature compensation, however, the compensation scheme is restricted in its complexity by the limitations of a low power microprocessor based algorithm. The compensation scheme requires that the meterfactor response curve of the fluidic oscillator be as linear as possible with variations in meterfactor occurring through smooth transitions rather than rapid step changes.

In practice this is difficult to achieve because, to meet the water meter performance specifications, the meter is required to operate over a very wide flow range covering varying flow conditions. The changing flow patterns during these varying flow conditions cause the fluidic oscillator to behave in a non-linear way with abrupt rapid changes in meterfactor response throughout the flow range. However, the linearity of the flowmeter can be significantly improved by altering the velocity profile of the inlet flow during transitional and laminar flow regimes using flow conditioning upstream of the converging nozzle.

Several flow conditioning configurations were investigated and the effects on the linearity of the fluidic oscillator, expressed as meterfactor against flowrate plots, were compared and discussed. The investigations led to the development of a flow conditioner design with a meterfactor response that is acceptable for use with the linearisation and temperature compensation scheme used by the fluidic oscillator domestic water meter. The flow conditioner also has a low pressure drop and is capable of passing debris without causing blockage problems.

4.2 Flowmeter Performance Specifications.

The performance specifications required for Class C and Class D domestic water meters are described in Chapter 1. The metrological specifications according to BS5728 (1979) are given in tables 1.1 and 1.2. For a flowmeter of nominal flowrate, Q_N, between the transitional flowrate, Q_t, and the maximum flowrate, Q_{max}, the meter has to be accurate to within ±2%. Between the minimum flowrate, Q_{min}, and Q_t it must be accurate to within ±5%. This results in an accuracy envelope as shown in figure 1.1.

4.3 Linearity Over Flow Range.

The oscillation frequency of the fluidic oscillator is given by:

$$f = S\frac{v}{w} \tag{1.4}$$

where f is the frequency of oscillation, S is the Strouhal number, v is the velocity of the jet and w is the width of the jet.

If frequency is plotted against flowrate, figure 4.1, then the performance of the fluidic oscillator appears to be linear, however, a more accurate way to evaluate the performance of the flowmeter is to plot the variation in Strouhal number with Reynolds number. This is a measure of the variation of the slope in figure 4.1 and emphasizes the non-linearity of the device.

If the meter were truly linear then the Strouhal number would not vary with Reynolds number over the flowrange of the meter. This is not the case for the fluidic water meter because the operational range of the meter requires Reynolds numbers which span from fully turbulent jet flow, through a transitional region, and into a fully laminar jet flow. The changing flow patterns during these varying flow conditions and viscous effects

result in the Strouhal number changing with Reynolds number, R_e, given by equation (1.5).

Figures 4.2 and 4.3 show the variation in Strouhal number with Reynolds number for the fluidic oscillator water meter transducer and for the extended range feedback oscillator, investigated by Boucher (1995), over the range required for a domestic water meter.

At Reynolds numbers of greater than 2500, in the fully turbulent flow regime, both plots are relatively flat, the variation in Strouhal number is within ±1%, as the oscillators are behaving in a linear manner. At Reynolds numbers of between 700 and 2500, during the transitional stage from laminar to turbulent flow conditions, both plots have a maximum peak which drops off with increasing Reynolds number until the flow is turbulent. The peak is flatter for the extended range feedback meter investigated by Boucher (1995) but is greater in magnitude. Also the slope of the change in Strouhal number during the transitional stage is steeper for the fluidic water meter transducer. At low Reynolds numbers the Strouhal number decreases as the oscillation frequency decreases, due to the effects of viscous damping, until oscillations cease.

The aspect ratio of the fluidic oscillator, α, is defined as the ratio of nozzle height, h, to nozzle width, w. Equation (1.4) can thus be written as:

$$S = \frac{f\alpha w^3}{Q} \tag{4.1}$$

where Q is the volumetric flowrate.

Equation (4.1) shows that Strouhal number is directly proportional to the number of cycles per second per volume flow, ie. f/Q the meterfactor. The volume flow per pulse, Q/f, is a more useful indication for a volume flow flowmeter and is also termed meterfactor or more correctly K-factor.

Figure 4.4 shows the volume flow per pulse plotted against flowrate for the fluidic oscillator water meter transducer. The meterfactor response curve has rapid step changes with steep gradients in the slope of the curve and is far from being within the required accuracy specification shown in figure 1.1 The variation in linearity can be overcome by using a meterfactor calibration stored electronically in memory, however, as Reynolds number varies with viscosity then the temperature of the water must also be measured. Although the variations in linearity can be overcome using laboratory instrumentation, production water meters would be limited to relatively simple microprocessing power. The complexity of the linearisation and temperature compensation algorithm would be restricted by the limitations of a low power microprocessor based compensation algorithm.

The meterfactor response curve of the fluidic oscillator water meter transducer shown in figure 4.4 is too complex for a simple compensation algorithm. The variation of Strouhal number with Reynolds number, and hence linearity of the flowmeter, can be significantly improved by altering the jet flow pattern during transitional and laminar flow regimes using flow conditioning upstream of the converging nozzle. The meterfactor response can therefore be improved so that it is acceptable for use with a simple compensation algorithm. Conditioning of the jet flow also makes the meter less susceptible to upstream disturbances and more tolerant of installation conditions.

4.4 Temperature and Linearity Compensation Scheme.

The temperature and linearity compensation scheme of the fluidic oscillator water meter uses a look-up table of discrete frequency bins stored electronically in memory. Each entry within the look-up table contains a representation of the theoretical volume flow at 0°C, a temperature correction volume and the sign of the temperature correction volume.

The volume flow stored within the table is calculated using the oscillation frequency

and an experimentally derived volume flow per pulse meterfactor at that frequency. Before the flow volume is stored it is temperature shifted to a theoretical volume flow at 0°C. The temperature correction volume is derived from the best straight line approximation of a meterfactor against temperature plot for each frequency used within the table.

The output from the fluidic oscillator transducer head amplifier is in the form of flow pulses. The number of pulse edges, N, of the flow pulse signal counted within an integration period, P, is used to determine a centre frequency, f_c, for the oscillations. P is of fixed duration set by the processor clock and starts with the detection of the first edge. N includes the counting of the first edge therefore there are a minimum of N-1 complete half cycles within period P.

4.4.1 Calculation of Centre Frequency.

A range of frequencies can give N edges in a period P. The oscillation frequency lies in the range $f_{min} < f < f_{max}$ where:

$$f_{max} = \frac{N}{2P} \quad : \quad f_{min} = \frac{N-1}{2P}$$

The centre frequency, f_c ,which is used as an approximation for all these frequencies is stored in the lookup table and is given by:

$$f_c = \frac{N-0.5}{2P} \tag{4.2}$$

4.4.2 Lookup Table Access Scheme.

An integration period doubling scheme is used to enable a wide range of frequencies to be measured whilst keeping the number of edges counted to between 5 and 12.

The shortest integration period is 70.3125ms derived from the 32768Hz system clock. The integration period is started on the detection of an edge. If less than 5 edges are counted in this period then the integration period is doubled and the count continued. This process continues until 5 or more edges are counted. If less than 5 edges have been counted and the integration period has been doubled 8 times, to 18 seconds, then no flow is registered and the process restarts on the detection of the next edge.

If 12 edges are counted then the hardware halts the integration period and the flow associated with the 12 edges in the complete integration period is recorded. This introduces a slight error into the system but will only occur during a rapid transition from low to high flowrates. With the exception of very high flowrates continuous flows will be recorded with between 5 and 9 edges in an integration period.

The size of the lookup table is equal to the 9 different integration periods multiplied by the 8 different number of edges that can be counted. Each of the 72 entries in the lookup table contains a 16 bit number. The least significant 11 bits represent the volume flow at 0°C, the next 4 bits represent the temperature correction volume and the most significant bit represents the sign of the temperature correction volume. The fluidic oscillator look-up table data centre frequencies are shown in appendix.a.

4.4.3 Calculation of Stored Volume Flow.

The number of complete flow oscillation cycles, M, associated with the integration period, ie. that occur between the start of the integration period and the start of the next integration period, is given by:

$$M = \frac{N}{2} \tag{4.3}$$

For a continuous signal this number is exact as it covers the time from the start of the integration period, an edge, to the start of the next integration, another edge, so there are no fractions of pulses lost in the time between integration periods.

The total flow volume, V, occurring between the start of the integration period and the start of the next integration period is given by:

$$V = \frac{K}{M} = \frac{2K}{N} \qquad (4.4)$$

where K is the experimentally derived meterfactor in ml pulse^{-1} at the centre frequency, f_c.

The volume, V, is temperature shifted to a theoretical volume flow at 0°C and stored in the lookup table which is accessed when this number of edges occur in this length of integration period.

The stored volume is scaled to give flow totals between 0 and 100ml. This gives a single bit resolution of:

$$\frac{100ml}{2^{11}} = 48.8\mu l$$

The temperature correction volume is stored to the same resolution.

4.4.4 Calculation of Temperature Correction Volume.

The meterfactor against frequency characteristic for the fluidic oscillator shifts along the frequency axis with changes in temperature due to the change in viscosity of the water.

A meterfactor value K at a frequency f_1 at a temperature T_1 will shift to frequency f_2 at temperature T_2 according to:

$$f_2 = \left(\frac{\nu_2}{\nu_1}\right) f_1 \tag{4.5}$$

where ν_1 and ν_2 are the kinematic viscosities of water at temperatures T_1 and T_2.

The temperature compensation scheme approximates this shift of the meter factor against frequency characteristic with a linear shift in meterfactor with temperature at each centre frequency. The magnitude of the shift is different at each centre frequency and is calculated and stored within the lookup table for each centre frequency.

To calculate the lookup table values the experimentally derived meterfactor against frequency plot is normalised to 15°C and the shape of the curve is then approximated by a series of straight lines to give a best fit through the data points on the characteristic. This best straight line approximation is then temperature shifted along the frequency axis between 0°C and 30°C in 1°C steps. This produces 31 best fit response plots, one for each temperature, from which the meterfactor value is recorded at each centre frequency. Figure 4.5 shows an example of a best straight line approximation of a typical meterfactor response curve.

The meterfactor value at each centre frequency is tabulated against temperature. For each centre frequency a plot of meterfactor value against temperature was produced in the range of 10°C to 20°C. A best fit straight line approximation is then made to the plots indicating the change in meterfactor value with change in temperature at each frequency bin. The slope of this line is determined and matched to the nearest possible slope allowed by the resolution of the temperature compensation slope at that particular centre frequency. The resolution of the slope depends upon the length of the integration period and the number of edges detected at that centre frequency.

4.4.5 Operation of Algorithm.

The contents of the fluidic oscillator water meter lookup table are shown in appendix.a. The values stored in the lookup table are the meterfactor value and the meterfactor per °C multiplied by the meterfactor multiplier, M, which is equal to the number of oscillation cycles in a measurement period. The multiplier is between 2.5 and 6 in 0.5 steps, ie. between 5 and 12 half cycles or edges.

The temperature correction volume is multiplied by the water temperature in an integer degrees Celsius and added to or, depending on the sign bit, subtracted from the 0°C volume to give the total temperature compensated volume flow during a total integration period. This value is then stored within memory and incremented with each further entry as a continuous flow volume count. This is displayed on the L.C.D. meter display and transmitted when a radio read request is received by the automatic meter reading system.

Figure 1.12 shows a block diagram schematic of the operation of the linearisation and temperature compensation scheme. While this temperature compensation scheme works well for the sections of the meterfactor characteristic with constant slope it is a poor approximation at the sections where the slope of the meterfactor against temperature graph varies most with temperature and can even change sign. The compensation scheme requires that the meterfactor response curve be as linear as possible with variations in meterfactor occurring through smooth transitions rather than step changes. Any variations in slope that occur must be smooth and separated by linear sections along the curve.

4.5 Flow Conditioning.

The upstream and downstream pipework of a flowmeter installation are critical to meter performance. Most flowmeters are calibrated with ideal inlet conditions, that is a fully

developed non-distorted flow profile which is free from swirl. Meter manufacturers quote both practical and recommended minimum lengths of upstream and downstream pipe in their specifications and they are also set down as part of flowmeter installation standards.

In practice, normal plant piping contains pipe fittings, reducers, expanders, strainers, valves and elbows which all affect profile. If the upstream disturbances are in the same plane, i.e. a single elbow, two elbows in the same plane or a partially opened gate valve, they will distort the profile but will only impart a small rotational flow in the pipe. If elbows are arranged so that the flow changes direction twice in succession through different planes then swirl flow is introduced causing the profile to corkscrew down the pipe.

Low energy fluid moving from the inside of the first elbow to the inside of the second elbow causes the swirl action and any bends in perpendicular planes that intersect between 30° and 90° will produce swirl. If having two bends in perpendicular planes is unavoidable then the situation can be improved by separating the bends by five or more diameters of straight pipe. The worst case for swirl generation is when the intersecting elbow planes form an angle of 60°. This case has the greatest interaction between bends allowing the slower moving fluid to take the shortest path between the elbows causing rotation of the fluid.

Swirl is difficult to remove and requires many upstream diameters, over 100 in severe cases, before it reduces to a level which is acceptably low enough not to affect meter performance. Profile distortion disappears more quickly but can still require around 30 upstream diameters for the undisturbed profile to reform.

Flow straighteners are used in installations where there is insufficient upstream lengths of straight pipe. They are used to remove swirl and provide a flow profile free from distortion at the meter inlet. Flow straighteners are used to remove swirl but the profile is not brought into symmetry. Examples of flow straighteners used to remove swirl are

shown in figure 4.6.

Profile distortion is removed, or an acceptable profile produced, using perforated plates. Perforated plates have a higher headloss than flow straighteners but have the advantage that they can easily be fitted between flanges. Combinations of flow straightener and perforated plate have been developed that remove swirl and provide a non-distorted flow profile. The Zanker (1969) conditioner is a combination of tube bundle and perforated plate, shown in figure 4.7. The Mitsubishi conditioner removes swirl and improves profile but can still be installed within flanges. The device is a thick perforated plate which has the holes machined with bevelled edges to reduce pressure drop. The Mitsubishi conditioner design is shown in figure 4.8.

4.6 Fluidic Oscillator Water Meter Flow Conditioning.

Flow conditioners are conventionally used to restore standard flow conditions after some disturbance in the pipework upstream of a flowmeter. Generally the meter is required to operate in only one flow regime, that is fully turbulent flow. To achieve the flowrange required to meet domestic water metering specifications the fluidic water meter must be capable of operating at a range of flow conditions which span from fully turbulent jet flow, through a transitional region, and into a fully laminar jet flow.

Early experimental work using machined perspex prototype fluidic flowmeters showed that the meterfactor characteristic of the fluidic oscillator flowmeter could be altered by using some form of flow conditioning at the inlet of the meter. At low flowrates the velocity of the fluid is not the same at all points across the pipe because of frictional effects at the pipe wall, this leads to a parabolic laminar flow profile. As the flow velocity increases turbulence starts to develop within the flow and at sufficiently high flowrates the flow profile becomes flat across the pipe. The turbulent to laminar flow transition at the inlet of the meter causes the flow patterns within the fluidic oscillator to vary significantly and result in the Strouhal number changing suddenly with Reynolds

number.

The linearity and temperature compensation scheme requires that the meterfactor response curve of the fluidic oscillator be as linear as possible with variations in meterfactor occurring through smooth transitions rather than rapid step changes.

4.7 Development of Fluidic Water Meter Flow Conditioner.

The research undertaken to identify a suitable flow conditioning configuration for the fluidic oscillator water meter has been a mostly intrinsic process. Each conditioner developed has been based around the results of previously tested designs leading to an optimum design with a desirable meterfactor response which is practical for ease of manufacture, has a low pressure drop and is capable of passing debris without causing blockage.

4.7.1 No Flow Conditioning.

The volume flow per pulse meterfactor against flowrate response for the fluidic oscillator transducer with no form of flow conditioning is shown in figure 4.4. At flowrates greater than 100ml s^{-1} the response is relatively flat and the device is behaving in a linear manner. This corresponds to a fully turbulent flow regime in the jet. At flowrates between 30ml s^{-1} and 100ml s^{-1} the curve steadily rises as the jet condition changes from transitional to fully turbulent. At flowrates between 10ml s^{-1} and 30 ml s^{-1} the meterfactor response has a maximum peak and a minimum peak with a rapid step change between the two. This is caused by the transition from fully laminar to transitional flow conditions within the jet. At flowrates below 10ml s^{-1} the flow condition is fully laminar and the meterfactor rises steadily with reduction in flow. This is due to the oscillation frequency reducing, because of the effects of viscous damping, until the flowrate is so low that oscillation ceases and the jet becomes stable.

The average meterfactor value at high flowrates is 9ml pulse^{-1}. This is for a flowmeter tested with a nozzle width of 2.64mm. Meters with smaller 2.4mm nozzle widths have a lower volume flow per pulse due to the increased jet velocity resulting in a higher oscillation frequency.

4.7.2 Inlet Trip.

Whilst testing early prototype fluidic oscillators one particular meter had a meterfactor response that was more linear than other similar meters. On closer examination it was found that the some of the sealant used to assemble the perspex 'building block' type meter had leaked between both the top and base of the meter and the perspex section which forms the converging nozzle. This excess sealant formed an inlet trip mechanism which shed vortices and helped to separate and disturb any boundary layers which develop along the wall of the of nozzle at low flowrates. This develops a more disturbed, turbulent type, flow profile and introduces instability into the jet flow at low flowrates. Instability of the jet helps to maintain oscillation at low flowrates and smooth the transition from the laminar flow regime to turbulent flow thus improving the linearity and contour of the meterfactor factor response curve.

A production moulded fluidic oscillator was modified to incorporate a 1mm × 1mm perspex section installed inside the flowmeter inlet. A perspex strip was mounted across each wall of the nozzle contraction forming an inlet trip at 15mm upstream of the outlet. A gauze of 1mm mesh was mounted upstream of the inlet flange to provide an inlet reference flow profile similar to that produced by a filter.

The meter was calibrated according to the test procedure described in Chapter 2 and the meterfactor curve for the meter is shown in figure 4.9 (November 11th 1991). The minimum peak to maximum peak deviation during the transitional flow range, 10ml s^{-1} to 30ml s^{-1}, is significantly smaller for the meter with the inlet trip. The change from transitional to fully developed flow conditions is similar but occurs at lower flowrates

in the range 10ml s^{-1} to 70ml s^{-1}. The fully turbulent linear range is therefore extended with the inlet trip flow conditioning, however, the deviations in linearity during transitional conditions make the curve unacceptable for use with the linearisation and temperature compensation algorithm.

4.7.3 Standard Profile Conditioner Plate.

A conditioner plate design used to produce a standard fully developed flow profile was installed between the inlet flange and the fluidic meter inlet. The conditioner was constructed in brass and sealed and mounted using 1mm cork gasket material. Figure 4.10 shows the geometry and hole pattern of the standard profile conditioner which consists of 12 1.5mm diameter holes on an 8mm radius, 6 2.5mm diameter holes on a 4mm radius and a 3mm diameter hole in the centre.

The standard profile conditioner configuration was calibrated according to the test procedure described in Chapter 2 and the meterfactor response curve is shown in figure 4.11 (November 12th 1991). The meterfactor response produced using the standard profile flow conditioner design is similar to that produced using the inlet trip. However, the magnitude of the maximum peak to minimum peak deviation during the change from fully laminar to transitional flow condition is greater.

4.7.4 Nine Hole Conditioner Pattern.

The nine hole conditioner plate is a very simple design based loosely around the standard profile conditioner pattern, ie. a large hole in the centre surrounded by smaller holes. The conditioner plate was manufactured using 1mm thick perspex and mounted using cork gasket material. Figure 4.12 shows the geometry and hole pattern of the nine hole conditioner. The centre hole is 6mm in diameter and the 8 outer holes are 4mm in diameter on a 7mm radius.

The nine hole conditioner was calibrated and the meterfactor response curve is shown in figure 4.13 (November 14th 1991). The meterfactor response produced using the 9-hole conditioner design has a larger fully turbulent flow range and a much smaller transitional to fully turbulent range. This is because the flow conditioner is able to sustain turbulent type flow conditions within the jet at flowrates where the jet flow would normally be transitional. There is a rapid step change between the minimum and maximum peaks during the change from fully laminar to transitional flow conditions. The magnitude and the slope of the change in meterfactor make the response unusable by the simple linearity and temperature compensation scheme.

4.7.5 Contoured Conditioner.

Flow conditioners are used to restore a distorted flow profile back to a fully developed turbulent profile following some disturbance in the flow. Plate conditioners generally have a contoured hole pattern with rings of smaller holes surrounding a larger centre hole. A conditioner plate was developed for the fluidic transducer with a contoured hole pattern using larger holes on the outer radius rather than in the centre. The contoured conditioner is a dense pattern of holes in a uniform arrangement with 0.5mm diameter holes at its centre increasing to 2mm diameter holes at an 8mm radius.

The very small diameter of the centre holes of the contoured conditioner would make it impractical for domestic metering applications, however, the device was constructed and tested to investigate the effect of using a conditioner plate with the hole contour in the opposite notation. The concept is to use a conditioner plate to disturb the inlet flow profile in a controlled manner rather than attempting to restore a conventional profile. The fluidic water meter inlet has a contraction upstream of the nozzle which itself will distort the profile of the inlet jet as the pipe section reduces in width. The conditioner is mounted immediately upstream of the inlet contraction so that the contraction will amplify, and add to, the distortion produced by the contoured conditioner.

The contoured conditioner was calibrated and the meterfactor response curve is shown in figure 4.14 (November 13th 1991). The response curve produced using the contoured design has a much smoother change from fully laminar to transitional flow conditions. The magnitude of the deviation between maximum and minimum peaks, which typify the change from fully laminar to transitional flow conditions, is much smaller using this conditioner. The change from transitional to turbulent flow conditions is still quite large and occurs over a narrowed flow range, 40ml s^{-1} to 70ml s^{-1}, resulting in a steep gradient.

4.7.6 Multi-Hole Pattern Conditioners.

The 9-hole conditioner pattern improves the change from transitional to turbulent conditions whilst the contoured conditioner improves the change from laminar to transitional conditions. A hybrid design incorporating a contoured hole scheme, with larger holes surrounding the outside of the conditioner rather than the centre, and a similar hole to plastic ratio as the 9-hole conditioner was developed. The 17-hole conditioner plate had a 1mm diameter centre hole, 8 1mm diameter holes on a 3mm radius and 8 4mm diameter holes on a 7mm radius.

Two further conditioner designs similar to the 17-hole design were developed, a 25-hole and 41-hole conditioner. The 25-hole conditioner had a further 8 1mm diameter holes surrounding the inner ring and the 41-hole conditioner had 32 more 1mm diameter holes. The hole pattern for each of the configurations is shown in figures 4.15 to 4.17.

The three conditioners were calibrated and the meterfactor response curves are shown in figures 4.18 to 4.20 respectively (November 19th, 21st, 22nd 1991). All three of the multi-hole pattern conditioners produced a very linear meterfactor response at flowrates above 15ml s^{-1}. These conditioner designs therefore appear capable of sustaining turbulent type flow conditions over a very wide range down to flowrates where the jet flow would normally be under almost laminar flow conditions. The transition from fully

laminar to turbulent flow conditions occurs as rapid change in slope at around 7ml s^{-1}. The magnitude of the minimum peak to turbulent steady meterfactor level is smaller for the designs with a higher number of 1mm diameter centre holes.

4.7.7 Conditioner Discs.

The fluidic transducer used for the conditioner testing was a moulded prototype and had not been designed to incorporate a flow conditioner. The results of the flow conditioning research showed that some form of conditioning would be necessary for the production fluidic oscillator water meter. The design of the production fluidic oscillator transducer was modified to incorporate a flow conditioner as a disc mounted within a moulded recess at the inlet stage of the flow meter body.

Four conditioner designs were developed which were based around the hole pattern of the best previously tested design, the 41 hole conditioner plate. The conditioner discs were made from relatively thick 2mm, perspex plate, an idea borrowed from the mitsubishi conditioner design, in the form of 22mm diameter discs. They were fabricated using computer numerical control, CNC, manufacturing techniques to ensure accurate hole location and high quality surface finishes to the entrance, exit, and internal lining of each hole.

4.7.8 Conditioner Disc Descriptions.

Figures 4.21 to 4.24 shows the hole pattern and disc geometry for the four conditioner discs CD1, CD2, CD3, and CD4 respectively.

Conditioner Disc CD1 - The previously tested conditioner plate which gave the most linear meterfactor response was the 41 hole conditioner plate. This conditioner incorporates a centre hole and inner ring of holes which are only 1mm in diameter.

Using holes of this diameter is likely to lead to blockage problems in a domestic installation and produce a high pressure loss across the conditioner. The hole pattern for the conditioner disc CD1 is based around the equivalent hole to blockage ratio of the 41 hole conditioner but uses inner holes of 2mm in diameter. CD1 consists of 8 4mm diameter holes on a 7mm radius, 8 2mmm diameter holes on a 3.5mm radius, and a 2mm diameter centre hole.

Conditioner Disc CD2 - The 41 hole conditioner was manufactured using hand operated machine tools and was made using only 1mm thick perspex plate. Conditioner disc CD2 has the same hole pattern as the 41 hole conditioner plate but is 2mm thick and made using CNC manufacturing techniques. Attention was given to the surface finishes of the conditioner face and the entrance, exit and lining of each hole of the conditioner disc designs. CD2 consists of 8 4mm diameter holes on a 7mm radius, 8 1mm diameter holes on a 3mm radius, 16 1mm diameter holes on a 4.25mm radius, 8 1mm diameter holes on a 5.5mm radius and a 1mm diameter centre hole.

Conditioner Disc CD3 - CD3 is a variation of CD2 but without the 8 1mm diameter holes on a 5.5mm radius.

Conditioner Disc CD4 - CD4 is a variation of CD2 without the 8 1mm diameter holes on a 5.5mm radius and only 8 1mm diameter holes on a 4.25mm radius, as opposed to 16, and these are centred symmetrically between the 8 1mm diameter holes on the inner ring.

A test meter was calibrated after being fitted with each conditioner disc and the meterfactor response curves are shown in figures 4.25 to 4.28 respectively (December 12th, 13th, 16th, 17th 1991). The meterfactor response produced using conditioner disc CD1 has large maximum peak to minimum peak deviation during the transitional flowrange. The meterfactor response curve produced using CD2 has a much smaller maximum peak during the transitional flowrange but the magnitude of the minimum peak is greater. Conditioner disc CD4 produced a meterfactor response curve with a

very large, turbulent, linear range. The magnitude of the minimum peak is not as great as that produced by CD2 but is still relatively large, however the transition is somewhat smoother from laminar to turbulent flow conditions.

The meterfactor response produced by conditioner design CD3 has very smooth changes from laminar to transitional flow and from transitional to turbulent jet flow. The magnitude of the minimum peak during the change from laminar to transitional conditions is relatively small and if a centre line for the meterfactor response curve is carefully selected the response is within ±2% over most of the range, except at very low flowrates. The shape of the response is such that a best straight line model of the curve could satisfactorily be used by the simple linearisation and temperature compensation scheme described earlier.

4.8 Fluidic Oscillator Jet Width.

It was at this stage of the flow conditioner development that pressure drop experiments showed that the fluidic oscillator body with a nozzle width of 2.4mm fitted with conditioner disc CD3, a filter of 1mm pitch, and a non-return valve did not meet the required minimum pressure drop specification at Q_{max}.

As described by Furmidge (1992), a nozzle width of 2.64mm was found to have a satisfactorily low pressure drop whilst providing sufficient signal strength at low flowrates, using neodymium magnetic material, and is capable of maintaining oscillation at flowrates low enough to achieve the Q_N1.0 Class C minimum flowrate specification.

4.9 Conditioner Disc Rotation Angle.

Variations in the results of testing the 2.64mm nozzle width fluidic oscillator fitted with conditioner disc CD3 led to investigations into the effect of conditioner angle of

rotation on meterfactor response. The angle of rotation had not been considered during earlier investigations because all of the conditioners tested had symmetrical hole patterns. This is acceptable for flow through circular pipe section but the inlet contraction and nozzle are not circular therefore there is a dependency on the symmetry of the hole pattern relative to the geometry of the nozzle.

To give accurate and repeatable angular adjustment location marker holes were machined into the outer radius of the conditioner disc CD3 at 0, 5, 10, 15, and 20 degrees to the vertical. The conditioner design CD3 is symmetrical about eight, equally spaced, axis and therefore adjustments of greater than 22.5 degrees repeat symmetry.

A datum pin was fitted at 0 degrees vertical, with respect to the nozzle geometry, at the top of the conditioner recess on the inlet face of the test meter. The marker holes seat on the datum pin only when the conditioner is aligned at the correct angle. The 2.64mm jet width fluidic oscillator unit was calibrated with conditioner CD3 positioned at each of the respective location marker holes according to the test procedure described in Chapter 2 and the collected data displayed in meterfactor versus flowrate graphs.

Figures 4.29 to 4.33 show the meterfactor response curves produced by the 2.64mm jet width fluidic oscillator fitted with conditioner disc CD3 installed at 0, 5, 10, 15, and 20 degrees to the vertical (January 27th,28th,29th, February 3rd, 4th 1992). The average high flow meterfactor value is greater for these tests than previous tests because the nozzle width has been enlarged from 2.4mm to 2.64mm. The meterfactor response curves are very similar for each rotation angle of the conditioner except for during the transitional flow stage.

For the conditioner mounted at 0° vertical with respect to the jet the response has a significant minimum and maximum peak during the transitional flow stage. The magnitude of the difference between the peaks is reduced when the conditioner is mounted at 5° and reduced further still when mounted at 10°. With the conditioner mounted at 15° to the vertical the transition from fully laminar flow conditions to fully

turbulent is very smooth. When the conditioner is mounted at 20° there is no minimum peak but the maximum peak during the transitional stage reappears.

With the conditioner disc CD3 mounted at 15° the changes in meterfactor with increasing flowrate are very smooth and could be modelled by a best straight line representation within the lookup table described earlier. The meterfactor response is linear over most of the flowrange, except for the very low flowrates, and would be within ±2% over this range.

The differences in meterfactor response with change in angle of rotation would appear to be caused by the variation in symmetry of the hole pattern of the flow conditioner with the flow nozzle. If viewed through the nozzle then at 15° the hole pattern of the conditioner would allow most flow through the top right and bottom left of the nozzle. This may introduce swirl flow into the inlet contraction as well as shedding vortices helping to create even greater disturbances and instability within the jet flow thus smoothing the transition from laminar to turbulent flow conditions. Of the rotation angles tested a rotation angle of 15° displays the greatest level of asymmetry with respect to the nozzle. Figure 4.34 shows the end view of the conditioner hole pattern and nozzle outlet at 0° and 15°.

4.10 Plastic Moulded conditioners.

A production moulding tool for the CD3 conditioner disc was manufactured and the fluidic oscillator production mould tool was modified to give a jet width of 2.64mm. A batch of 2.64mm jet width fluidic meters and moulded conditioner CD3 were manufactured for field trial purposes.

The meters were tested and found to have low levels of meter to meter repeatability. Some of the meterfactor responses were very linear with smooth transitions. The meters with linear meterfactor responses were inspected and it was found that the plastic

moulded flow conditioner had deformed due to the pressure of the 'o' ring conditioner mounting which is a compression fitting. The amount of compression and conditioner deformation depends on the torque and procedure used to tighten the inlet flange bolts during meter assembly.

A forming tool was manufactured to cold form the moulded conditioners to a controlled deformation similar to that of the meters with a linear response. A batch of meters was assembled with cold formed conditioners and the linearity of the meters was acceptable, however, the meter to meter repeatability levels were still low because consistent forming of the conditioner was difficult and the conditioner form altered once fitted due to plastic relaxation.

Any single meterfactor response could have been stored and used in a lookup table but because of meter to meter variations one lookup table curve would not have been adequate for all of the meterfactor curves produced by the batch of meters. For this reason it was decided to use the CD3 conditioner in field trials using a lookup table with data based on the average of the meterfactor response curves but to continue research into flow conditioners which could be made more consistently and with larger holes, to reduce the risk of particle blockage and lower the pressure drop of the device.

4.11 Effect of Hole Size On Conditioner Performance.

Before developing further conditioner designs with larger hole sizes, to reduce blockage and pressure losses, the effects of hole size on conditioner performance was investigated. The aim of the work was to determine if the actual hole size is a critical factor in conditioner performance, rather than the geometry of the hole pattern, and if useful conditioners could be developed with larger hole sizes.

Experiments were carried out using a disc of wire gauze as a conditioner with increasing pitch size and then conditioner plates with increasing hole size were tested.

The holes were arranged in uniform patterns with no variation in hole density across the conditioner.

4.11.1 Gauze Conditioners.

To determine the effect of conditioner hole size on linearity three wire gauze conditioners of regular mesh spacing were tested. Gauze of 0.5mm pitch, 1.0mm pitch and 1.5mm pitch were tested. Figures 4.35 to 4.37 show the meterfactor response plots produced by the three sizes of gauze conditioner respectively (May 17th, 24th, June 2nd 1993).

The linearity of the response curves is far worse than for those of previously investigated multi-hole pattern conditioner plates. Also the spread of data points on the plot is far greater indicating lower levels of repeatability for the meters tested with gauze conditioners. The magnitude of the deviations in meterfactor during the transitional flow stage become larger with increasing hole size. This indicates that smaller hole sizes do smooth the transition from laminar to turbulent flow conditions for fluidic oscillators fitted with gauze conditioners.

4.11.2 Conditioner Plates With Increasing Hole Size.

Conditioner plates with increasing hole size were tested. The holes were arranged in uniform patterns with no variation in hole density across the conditioner. Although the test is for hole size only it was still necessary to determine a notation for the hole pattern to maintain consistent testing and therefore all lines of holes were centred and aligned vertically with respect to the nozzle.

The conditioner plate hole sizes tested were 1.08mm, 2.1mm, 2.34mm, 3.0mm and 3.2mm in diameter. The meterfactor response plots produced using the conditioners are

shown in figures 4.38 to figure 4.42 (June 15th, 8th, 10th,16th, 14th 1993). All of the meterfactor responses produced during the hole size investigation are very non-linear in comparison to the flow conditioners investigated earlier. The conditioner consisting of 1.08mm holes has the smoothest transition from laminar to turbulent flow conditions, the next smoothest response is produced using the conditioner with 2.34mm holes.

The results of the hole size test indicate that smaller holes do improve the transition from laminar to turbulent flow conditions but the geometry contour of the conditioner hole pattern is more significant to overall meter linearity than hole size.

4.12 Slot Conditioners.

During the flow conditioner hole size test the conditioner with 2.34mm diameter holes produced a meterfactor response with a relatively smooth transitional flow region, for a conditioner plate with large diameter holes. The hole pattern for this conditioner was aligned vertically with respect to the nozzle forming vertical columns of holes. The spaces between the holes were removed to form vertical slots and the experiment repeated. The slot conditioner produced an improved response compared to the original hole pattern and has a lower pressure loss and is less susceptible to particle blockage. The meterfactor response produced by the prototype slot conditioner is shown in figure 4.43 (July 5th 1993).

Six slot conditioner designs based around the prototype were developed and tested to determine the optimum width and spacing, or blocking region, of the slots. The slot conditioner designs which produced the most linear meterfactor response curves were conditioners SLOT5.DC2 and SLOT6.D2. The geometries of these designs are shown in figures 4.44 and 4.45, both have slots of 3.2mm in width. The slots are spaced by 2.8mm blocking regions for SLOT5.DC2 and 3.2mm blocking regions for SLOT6.DC2.

The meterfactor response plots for these conditioners are shown in figures 4.46 and 4.47 (July 23rd and 22nd 1993). Both of these curves are very flat with very smooth transitions between fully laminar and turbulent flow conditions. The response produced by SLOT6.DC2 has slightly less scatter of the data points within the transitional stage than that produced by SLOT5.DC2. The response is linear over a very wide flowrange from 10ml s^{-1} to Q_{max} requiring linearity compensation only at low flowrates where the meterfactor rises with reducing flowrate, due to viscous damping effects which reduce oscillation frequency. The slope of the meterfactor response at low flowrates and the smooth transition through varying flow conditions result in the meterfactor response being acceptable for use with the linearity and temperature compensation scheme described earlier.

The slot conditioner design SLOT6.DC2 was tooled and production mouldings of the conditioner developed. As well as being able to pass debris, and therefore not requiring a filter or strainer, the slot conditioner has a lower pressure drop than CD3. Figure 4.48 (July 22nd 1993) shows the pressure drop against flowrate plot for the fluidic oscillator transducer fitted with conditioner design SLOT6.DC2. The pressure drop of the complete meter fitted with the slot conditioner is 12.5 psi at Q_{max} which is within the maximum specification of 14.7 p.s.i.

4.13 Meterfactor Repeatability.

Accuracy calibrations showed that the repeatability of production meters, fitted with the slot conditioner, was unacceptable for pattern approval submission. A programme of controlled work was undertaken to improve production meter repeatability.

Fusion Meters manufactured a batch of meter bodies maintaining all moulding variables constant throughout the batch. Fifty of the mouldings were accurately measured by Disc GB Ltd. using a coordinate measuring machine. The measurements were taken using an insertion probe at a series of critical positions to determine the variation in meter

geometry due to the moulding process. The location of the probe measurements is shown in figure 4.49. The mouldings were then fitted with lids and returned to Disc GB Ltd to determine the variation in geometry due to the lid weld process, however, some measurement points were inaccessible to the insertion probe following the lid weld operation. The measurements taken showed that moulding repeatability is very consistent and variations due to the lid weld process are minor with inlet steps, the step formed between the jet exit and the inside face of the meter lid which are critical to meterfactor, of less than 0.02mm. A tooling problem was demonstrated, however, in that the inlet core of the mould tool was not aligned at true vertical.

Meters were selected which had no measurable inlet step and were then assembled using the slot conditioner and tested for repeatability. The meterfactor response curves for the meters were linear with relatively small peak to peak deviation in meterfactor, through the transition region. All of the responses were acceptable for use with the linearisation and temperature compensation scheme, however, the meterfactor curves were different from each other in that the centre line through the plots occurred at different values of meterfactor. The differences are such that it would not be possible for one lookup table to be used by all of the meters. The geometry data for the meters with the most similar meterfactor curves was compared with that of the meters with the most different, but no correlation between geometry variation and meterfactor could be seen.

During the repeatability testing the mould tool was adjusted to ensure alignment of the inlet and outlet cores and a batch of improved meters was produced. Three of the meters were constructed using the plastic slot conditioner and tested for repeatability. The meterfactor response curves had large peak to peak deviation in the transition region and were very dissimilar from each other. Closer examination of the complete meter assembly showed deformation of the plastic slot conditioner. The conditioner is installed within an 'o' ring which is compressed under tightening of the four flange screws.

To investigate the effect on meterfactor response due to variation in conditioner installation a conditioner was manufactured using brass which will not deform under compression. With the brass conditioner fitted to each meter the meterfactor response curves are much more consistent and of similar shape. The coordinate measurement data shows that moulding variation is minimal indicating that the meterfactor variations are due to the assembly of the meter components in particular the inlet flange and installation of the conditioner.

The coordinate measurement investigations and the tracing of the assembly process and component installations that are critical to meterfactor response was a very important stage in the development of more repeatable consistent meter manufacture. Twenty slot conditioners were manufactured using Computer Numerical Control, C.N.C., techniques from stainless steel. The steel conditioners were fitted to seventeen of the meters, that had a large amount of data available concerning the geometry, moulding, and lid weld consistency of the meters. All screw torques were kept constant for the meter assemblies and the conditioners were centred, with respect to the jet, using a jig tool during assembly. Also the non-return valves were selected to have consistent spring strengths.

The controlled assembly meters showed much higher levels of repeatability than any other test run. Meters with meterfactor responses that were dissimilar from the standard curve were found to have an improved response after disassembling and rebuilding the meter. Using a stainless steel version of the slot conditioner and controlled meter assembly techniques the linearity and repeatability of the fluidic oscillator water meter was acceptable for pattern approval submission.

4.14 Discussion of Flow Conditioning Mechanism.

The operation of the fluidic oscillator relies on the action of the coanda effect to amplify instabilities within the jet flow causing the jet to attach to a diffuser wall. As

the flowrate is reduced the jet flow becomes increasingly stable as the flow condition within the jet tends towards the laminar regime. The varying levels of jet stability and altering flow patterns within the oscillator cause variations in oscillation frequency with flowrate. This results in a nonlinear meterfactor response because the operational range of the fluidic water meter requires Reynolds numbers within the jet which span from fully turbulent jet flow, through a transitional region and into full laminar flow.

The greatest variations in meterfactor occur during changes from one flow conditioner to another. Throughout the flowrange required for the water meter the flow condition within the jet flow proceeds through several stages with increasing flowrate. The three different flow regimes of the fluidic oscillator jet result in four flow stages throughout the range of the water meter as follows:

. Fully laminar conditions.
. Change from fully laminar to transitional conditions.
. Change from transitional to turbulent conditions.
. Fully turbulent conditions.

Flow conditioning of the fluidic oscillator inlet flow is capable of increasing the linearity of the device over the required flowrange. This is achieved through the flattening and smoothing of the contour of the meterfactor response by reducing the severity of the changes in jet flow condition. The transition from one flow stage to another is improved by disturbing the jet flow so that turbulent conditions are sustained at lower flowrates thus reducing the definition of the two distinct flow conditions over a narrower range than the transition normally occurs.

Reynolds has shown that with great care it is possible to sustain laminar flow conditions at higher flowrates provided the system is not disturbed. Once the system becomes disturbed the laminar flow condition breaks down rapidly and the system becomes turbulent. It therefore follows that intentionally disturbing a system can cause laminar flow conditions to break down at lower flowrates, or Reynolds number, over a greater

flowrange producing a less rapid change from one condition to another.

Improving the meterfactor response of the fluidic oscillator transducer is not as simple as merely altering the Reynolds number at which transition from one flow condition to another occurs because there are many other processes occurring within the fluidic oscillator, all of which are dependent to some extent on the condition of the jet flow. These processes include the coanda effect, the build up and separation of boundary layers along the diffuser walls and internal faces of the flow chamber, the velocity and flow profile of flow within the feedback channels, the entrainment of feedback flow and the stability of the jet. The inlet flow condition must be tuned to match and enhance the operational characteristics of the fluidic oscillator in a similar manner to which an electrical signal may be may be prefiltered before being fed into an amplifier to give the desired output response.

Using flow conditioners it is possible to generate a disturbance at the meter inlet which is amplified as it travels through the contraction. This introduces instability into the jet flow where the flow would ordinarily be under fully laminar conditions. Instabilities of the jet flow are amplified by the coanda effect and help to simulate the flow conditions under which the meter would be operating during the turbulent flow regime. Maintaining turbulence in the jet flow during the transitional and laminar flow regimes reduces the variation in Strouhal number with Reynolds number across the range of the flow transition. The large hole pattern conditioners, the nine hole conditioner for example, extend the linear range of the fluidic oscillator, which would normally occur under fully turbulent conditions, by sustaining turbulent like flow conditions at lower flowrates where the jet would normally be under laminar or transitional flow conditions. Flow visualisation experiments showed large regular eddies shedding from the flow conditioner and travelling down the contraction of the meter inlet and into the nozzle. This creates a more disturbed jet flow which is similar to the jet flow that occurs under turbulent conditions thus extending the range where the fluidic oscillator behaves linearly at high flowrates. The magnitude of the peak to peak deviations in meterfactor response that occur during transitional flow conditions are not improved, and can be

made larger, whilst being compressed into a narrow band of flowrates causing steeper gradients.

The small hole pattern conditioners smooth the transition from laminar to transitional and transitional to turbulent conditions and also increase the linear range, though not to as great an extent as the nine hole conditioner. Flow visualisation experiments using small hole condition patterns showed small turbulent eddies shed at a high rate producing very disturbed flow stream lines through the contraction. The smaller holes appear to produce a much greater mixing of the inlet flow even at low flowrates. The contoured multi-hole pattern conditioners combine both of these effects to produce a more linear meterfactor response over the entire flowrange. For the conditioner CD3 installed at 15° the meterfactor is very flat without peak to peak deviations in meterfactor through the transitional flow stage. With the conditioner disc installed at this angle there is asymmetry between the conditioner pattern and the nozzle which may be introducing swirl into the jet flow thus creating even greater instability.

The optimum design of slot conditioner has a meterfactor response as linear as that produced by conditioner CD3 but has lower pressure drop and is less likely to cause blockage. The geometry of the slot conditioner pattern is such that vortices are shed from the blocking regions between the slots in the form of tall vortices. Each vortex will be the height of the blocking region and travel through the contraction creating severe disturbances at the jet nozzle. The geometry of the slot conditioner differs from the contoured conditioner designs in that the geometry of the slot design is constant in the vertical dimension. It would seem that the slot conditioner affects the profile of the inlet flow in the horizontal plane to a greater extent than the vertical plane, however, the contraction of the fluidic oscillator is itself two-dimensional because the pipe diameter is only reduced in the horizontal plane through the contraction. The contraction will therefore distort the velocity profile in the horizontal plane thus amplifying the disturbances caused by the conditioner.

4.15 Conclusions.

Flow conditioners are conventionally used to restore a standard velocity flow profile after some disturbance in a flow line. The novel concept described within this thesis involves using flow conditioning techniques to alter the performance characteristics of an oscillating device to improve the linearity of the meter.

A flow conditioning system has been developed that dramatically improves the linearity of the fluidic oscillator transducer. The meterfactor response of the same fluidic transducer fitted with and without the flow conditioning device is shown in figure 4.50. When fitted with the flow conditioner the linearity of the fluidic oscillator is such that the meterfactor response may be used by a simple linearity and temperature compensation scheme.

The flowmeter has an acceptable low pressure drop when fitted with the flow conditioning device and is capable of passing debris through the meter without causing blockage problems.

Determining the source of meter non-repeatability through investigation of the meter mouldings and component assembly was a significant step in speeding up the development time of flow conditioners and improving the consistency of results.

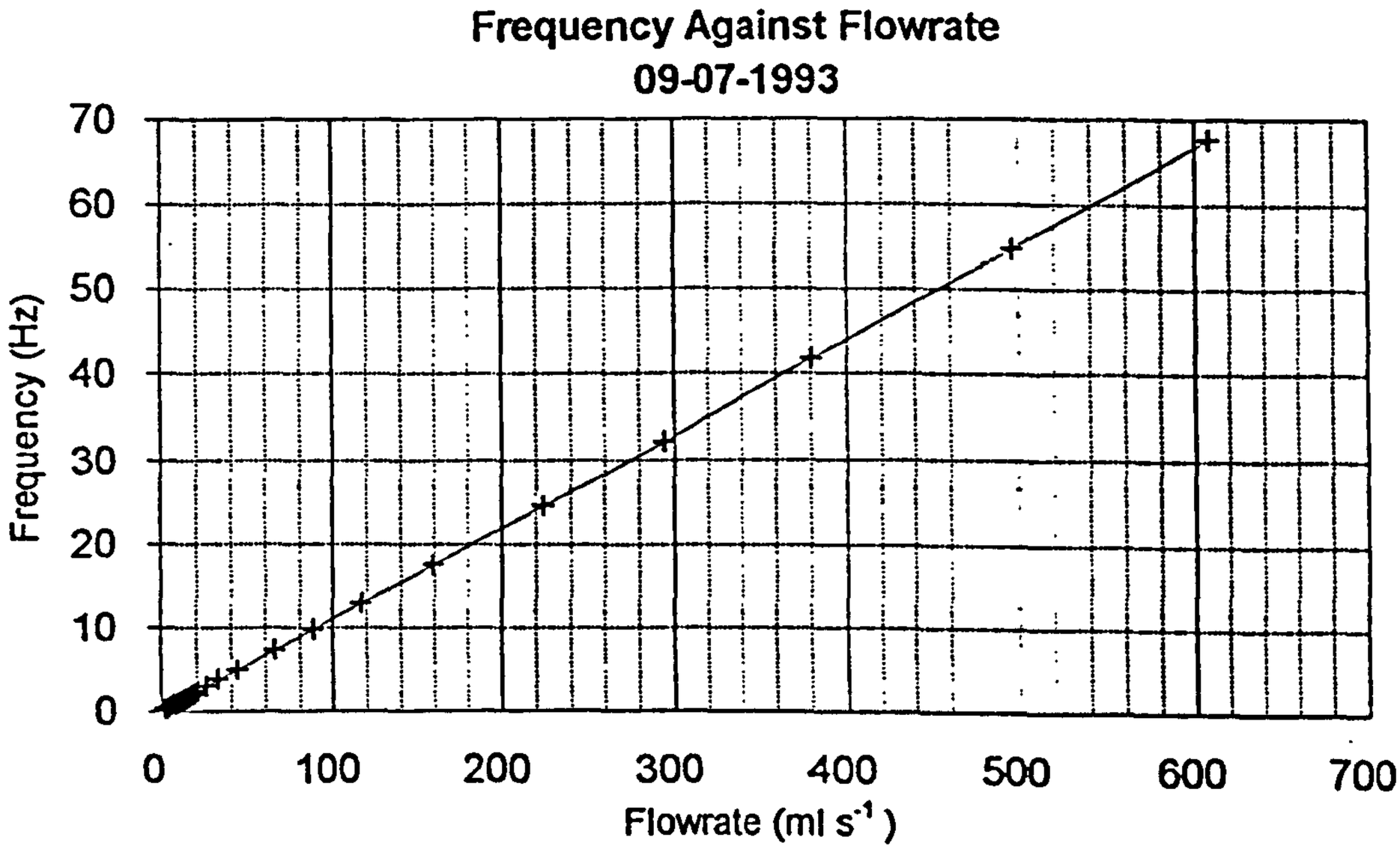

Figure 4.1: Frequency Against Flowrate For Fluidic Oscillator.

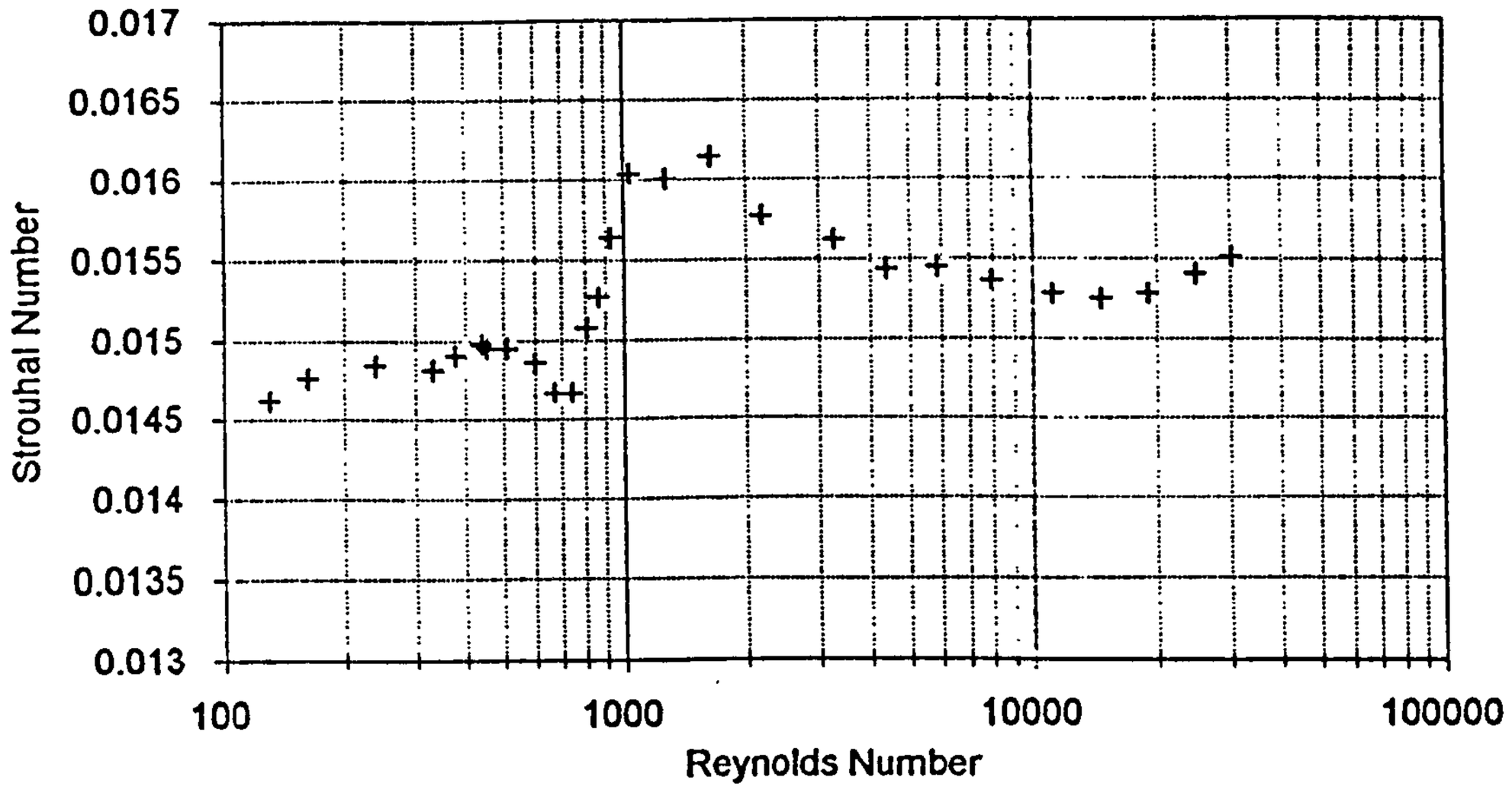

Figure 4.2: Variation of Strouhal Number With Reynolds Number For Fluidic Oscillator Water Meter.

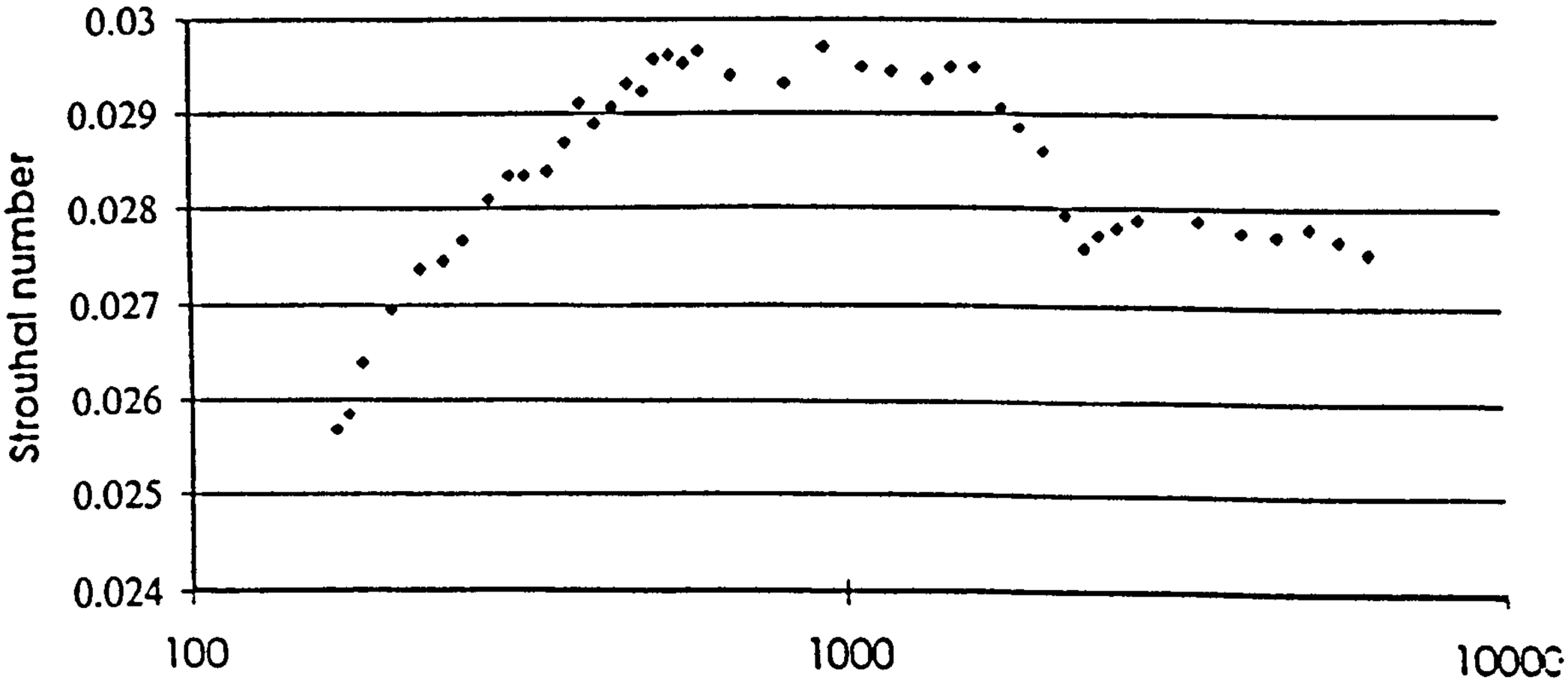

Figure 4.3: Variation of Strouhal Number With Reynolds Number For Extended Range Feedback Oscillator, Boucher (1995).

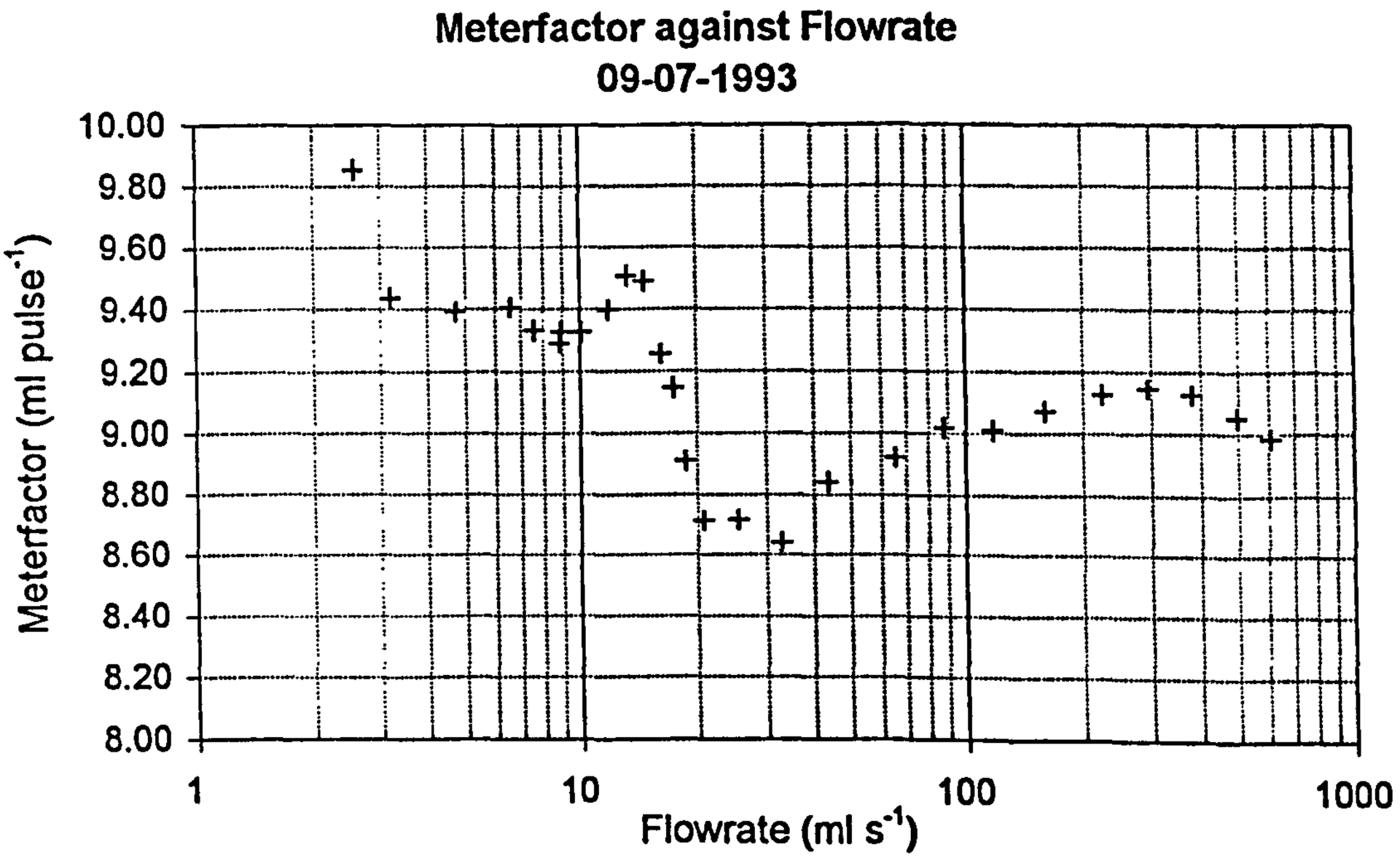

Figure 4.4: Meterfactor Response of Fluidic Oscillator Transducer.

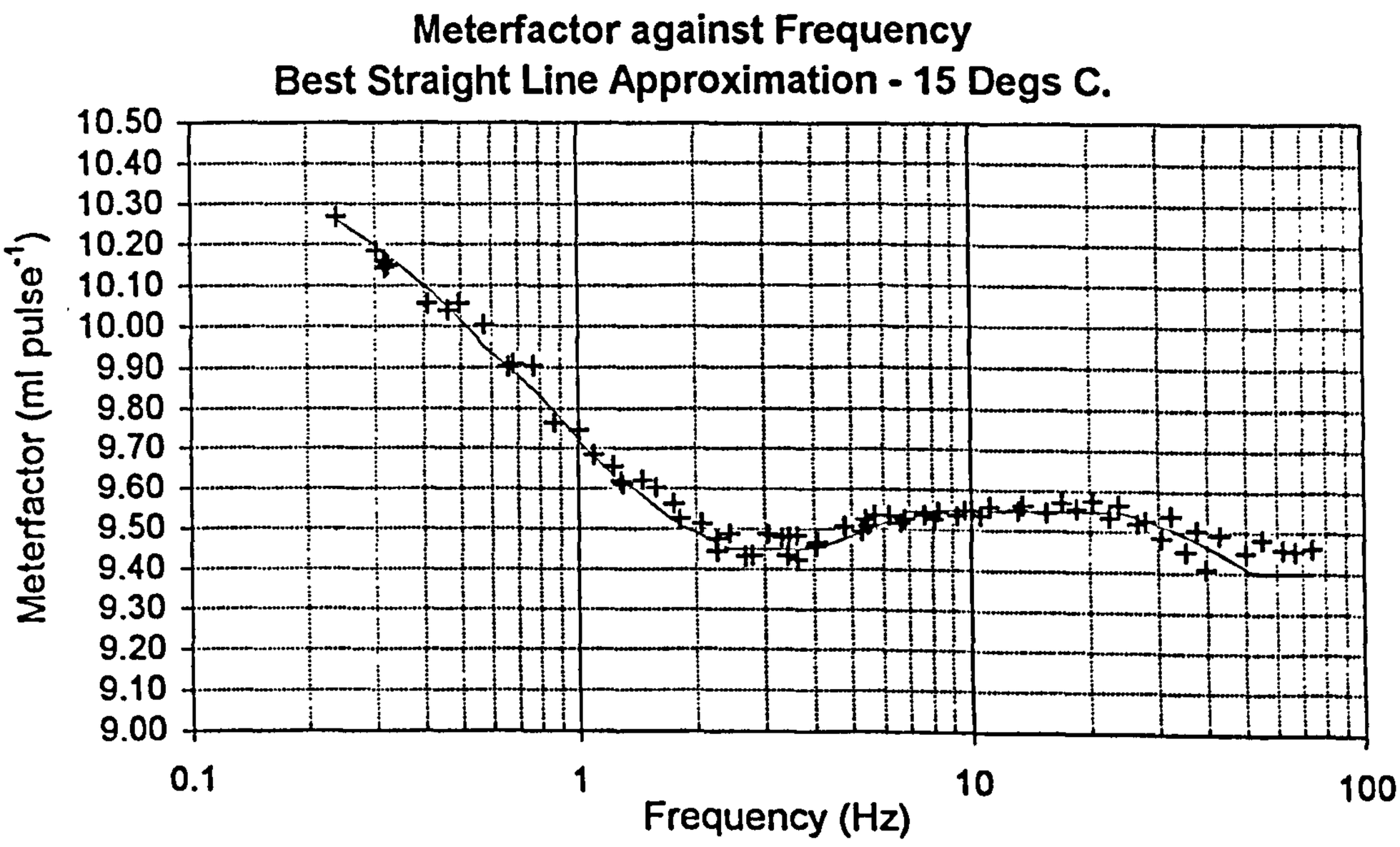

Figure 4.5: Best Straight Line Approximation of Meterfactor Response.

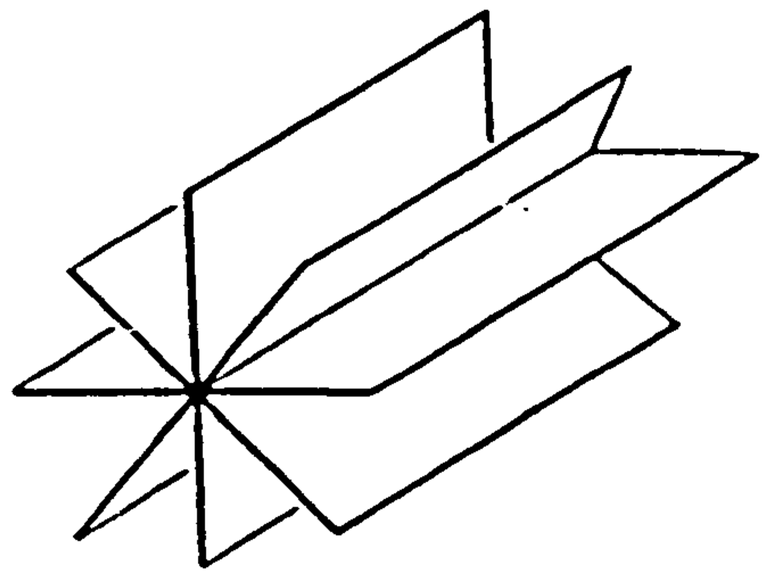

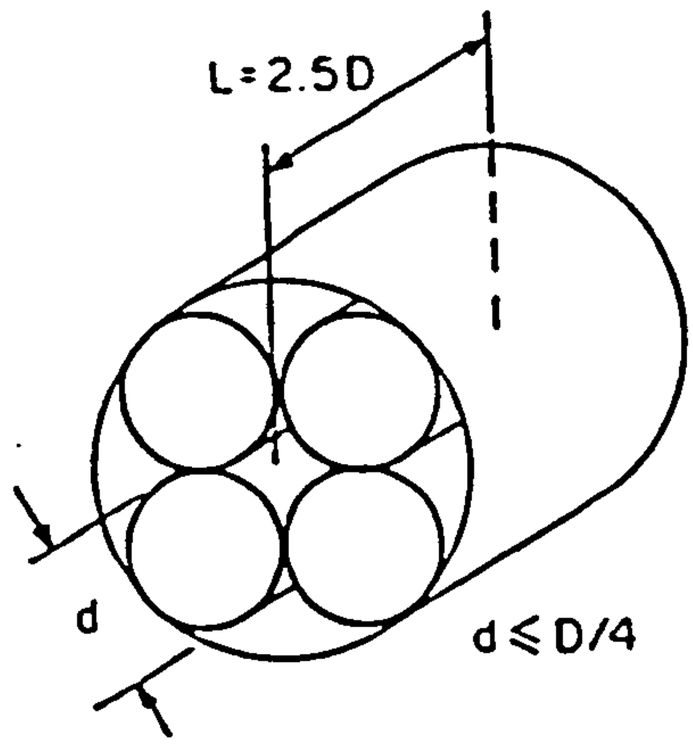

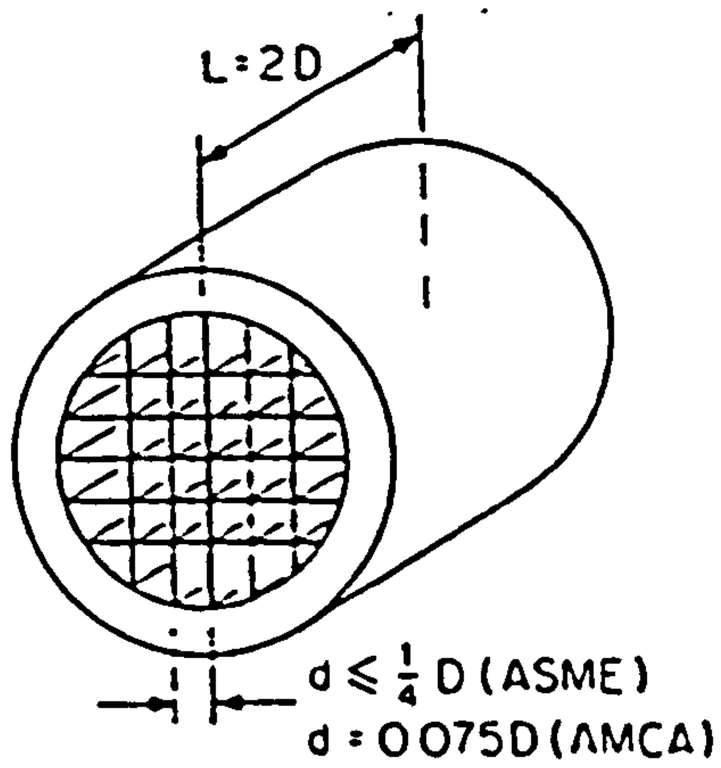

Figure 4.6: Examples of Flow Straighteners.

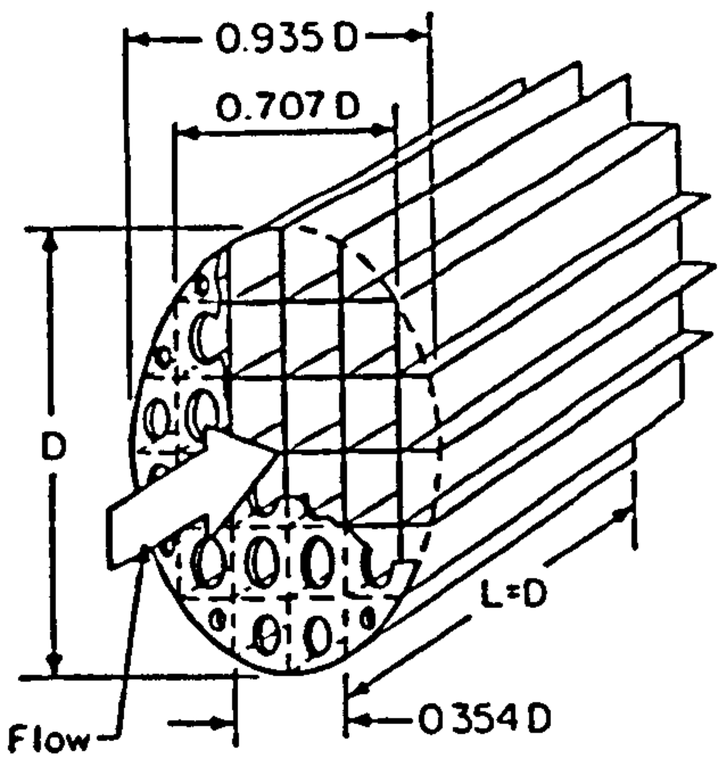

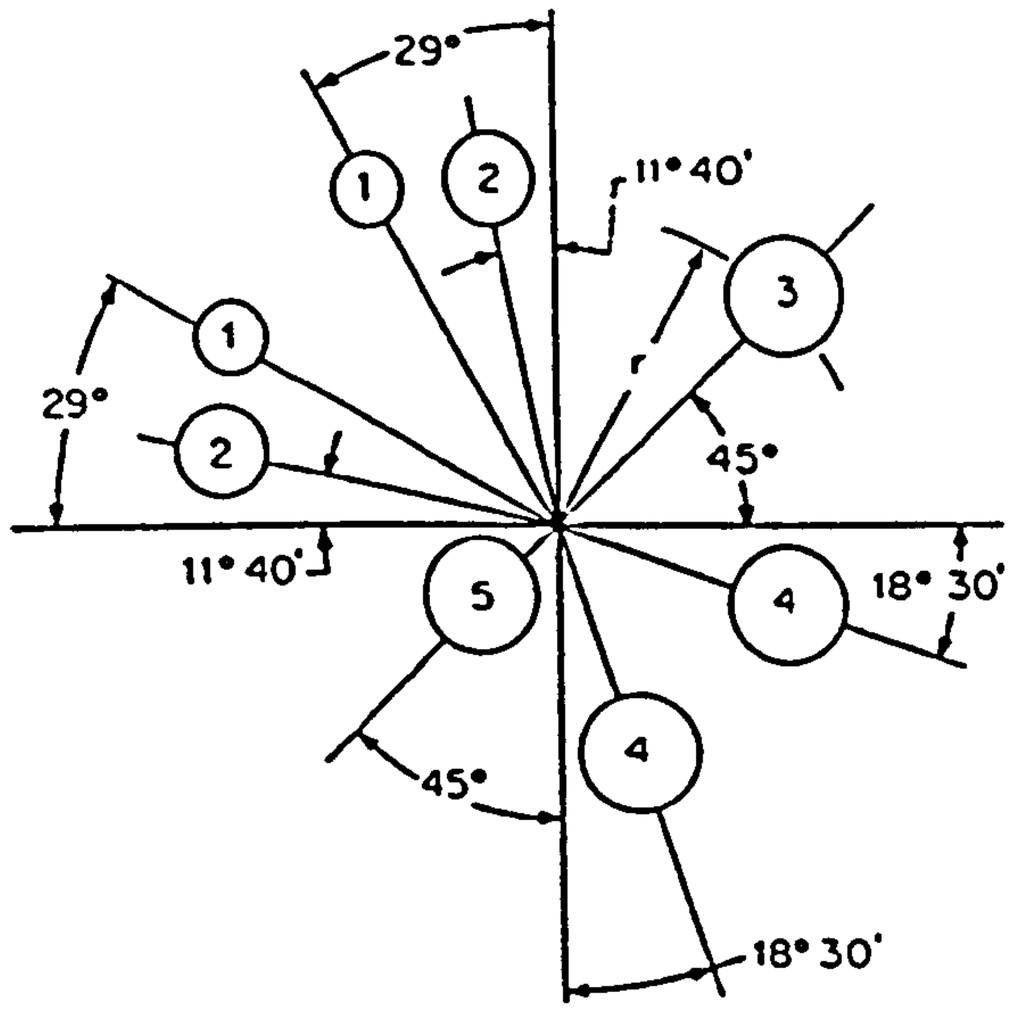

	Hole number				
	1	2	3	4	5
Hole diameter	0.077D	0.110D	0.1365D	0.139D	0.141D
Radius to hole (r)	0.045D	0.425D	0.375D	0.28D	0.125D
Number of holes	8	8	4	8	4

Figure 4.7: The Zanker Flow Conditioner.

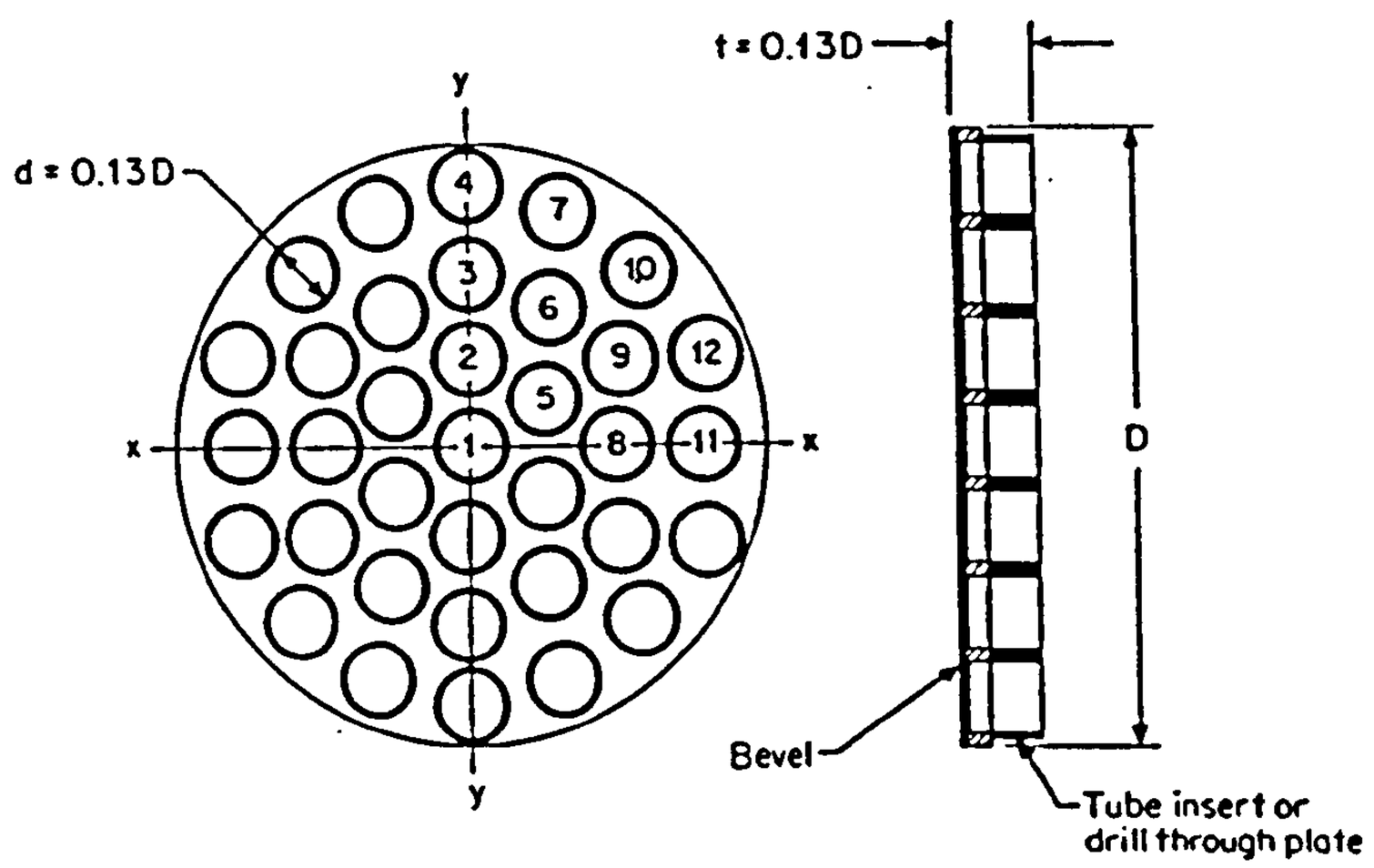

	Hole number											
Coordinate	1	2	3	4	5	6	7	8	9	10	11	12
x	0	0	0	0	0.129D	0.134D	0.156D	0.252D	0.255D	0 288D	0.396D	0.400D
y	0	0.142D	0.283D	0 423D	0 078D	0.225D	0.381D	0	0.146D	0.288D	0	0 151D
Number of holes	1	2	2	2	4	4	4	2	4	4	2	4

Figure 4.8: The Mitsubishi Flow Conditioner.

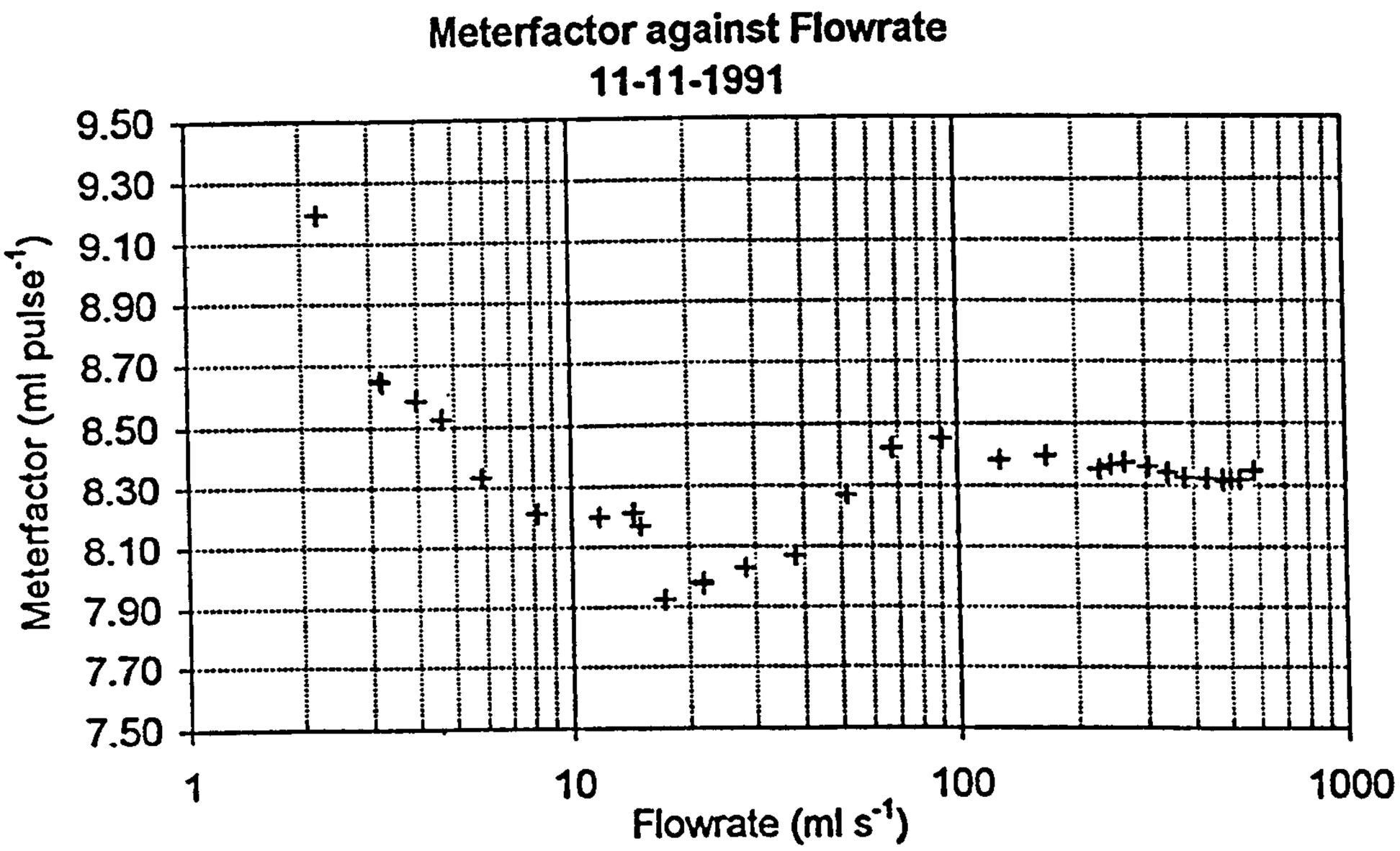

Figure 4.9: Meterfactor Response of Fluidic Oscillator Fitted With Inlet Trip.

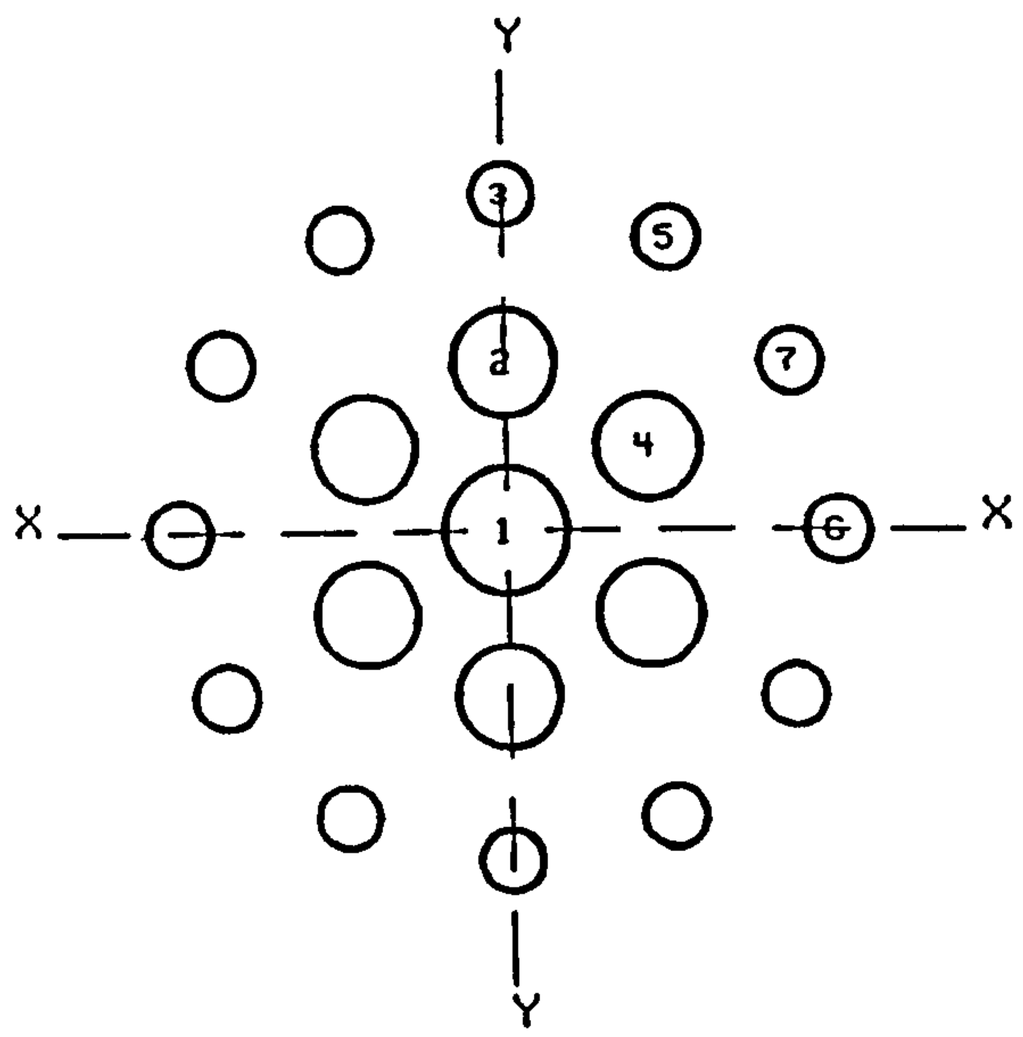

Hole Number	1	2	3	4	5	6	7
Coordinate x	0	0	0	3.46	4	8	6.93
Coordinate y	0	4	8	2	6.93	0	4
Diameter	3	2.5	1.5	2.5	1.5	1.5	1.5
Number of Holes	1	2	2	4	4	2	4

Figure 4.10: Geometry of Standard Profile Flow Conditioner Plate.

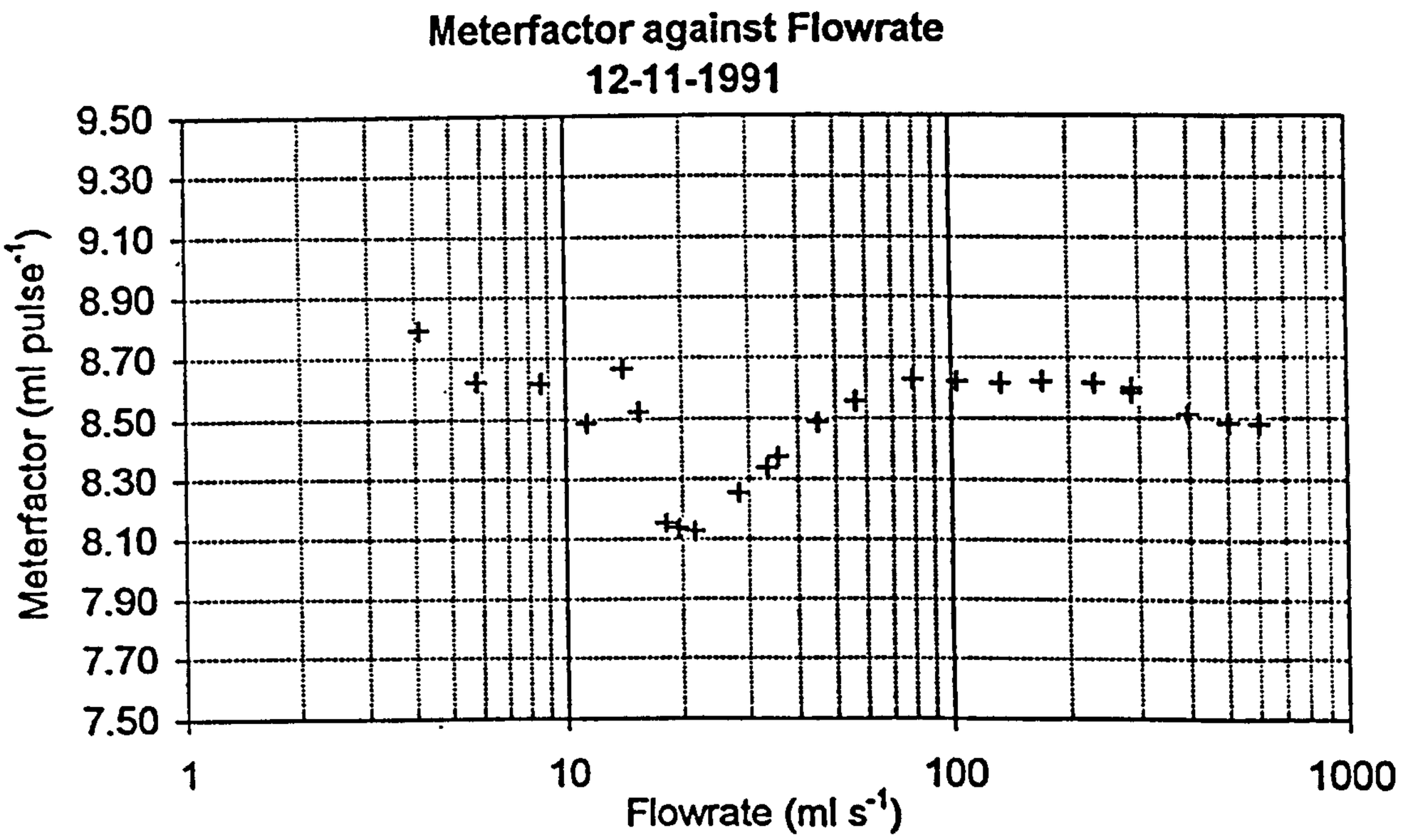

Figure 4.11: Meterfactor Response of Fluidic Oscillator Fitted With Standard Profile Conditioner Plate.

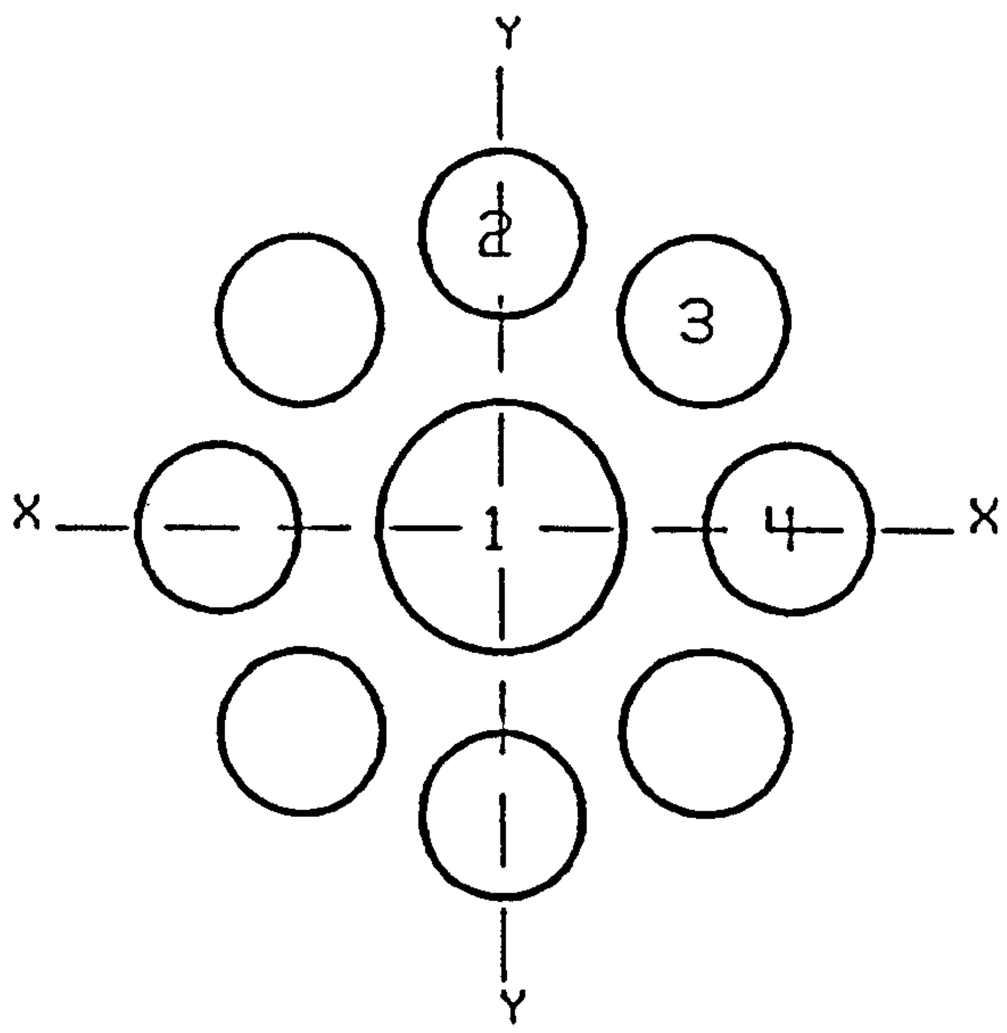

Hole Number	1	2	3	4
Coordinate x	0	0	0	3.46
Coordinate y	0	4	8	2
Diameter	3	2.5	1.5	2.5
Number of Holes	1	2	2	4

Figure 4.12: Geometry of Nine Hole Conditioner Plate.

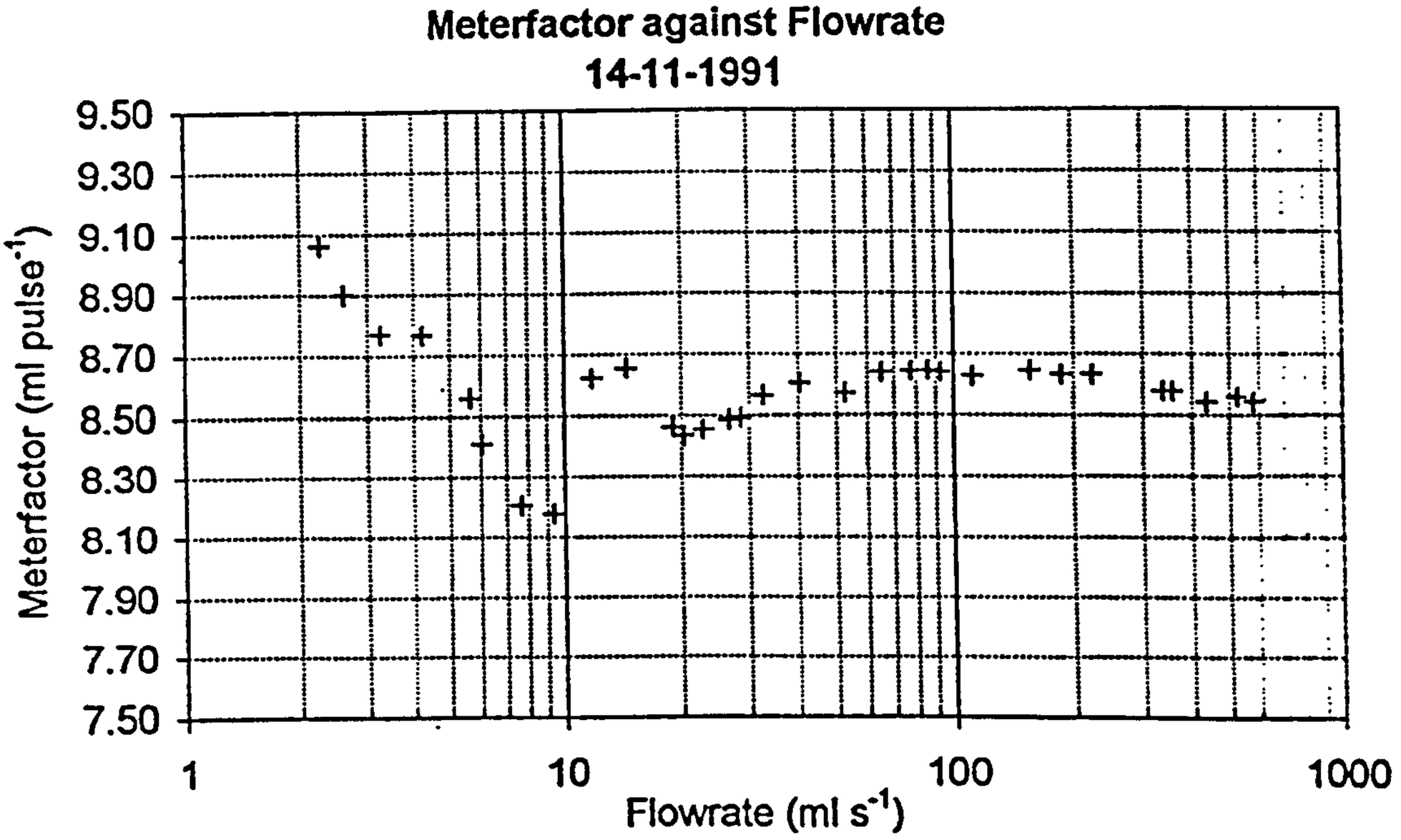

Figure 4.13: Meterfactor Response of Fluidic Oscillator Fitted With Nine Hole Conditioner Plate.

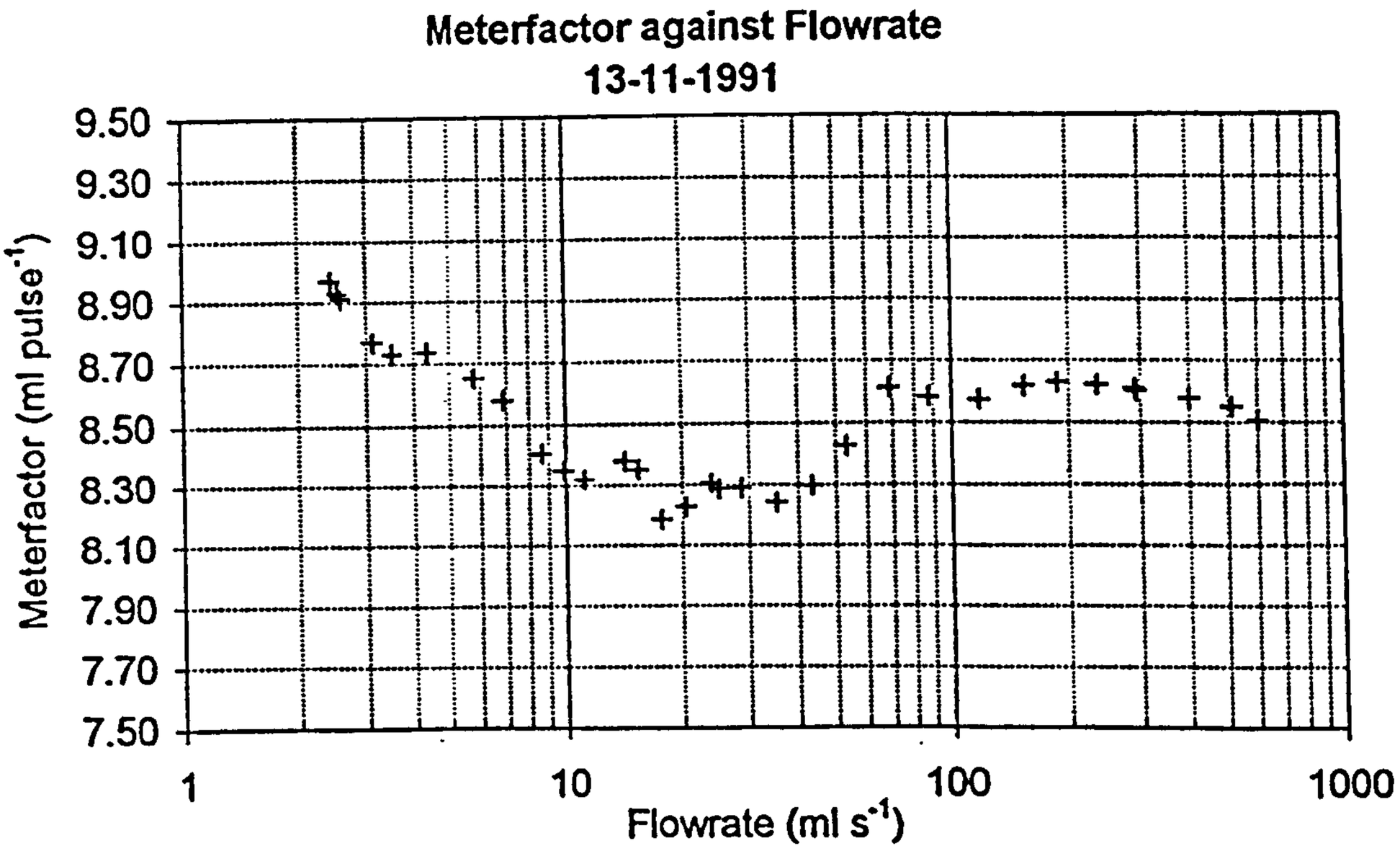

Figure 4.14: Meterfactor Response of Fluidic Oscillator Fitted With Contoured Hole Pattern Conditioner Plate.

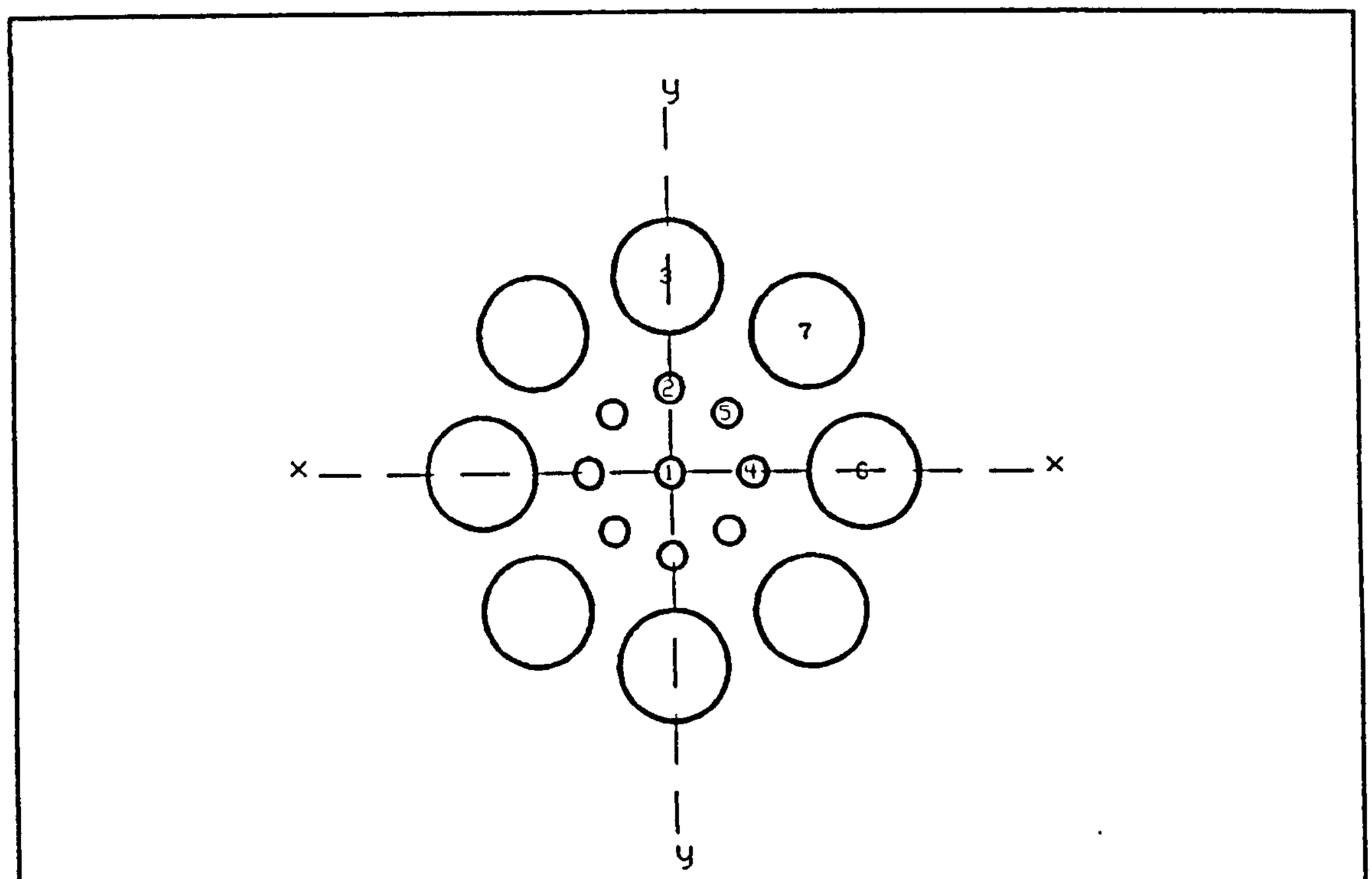

Hole Number	1	2	3	4	5	6	7
Coordinate x	0	0	0	3	2.1	7	5
Coordinate y	0	3	7	0	2.1	0	5
Diameter	1	1	4	1	1	4	4
Number of Holes	1	2	2	2	4	2	4

Figure 4.15: Geometry of 17-Hole Conditioner Plate.

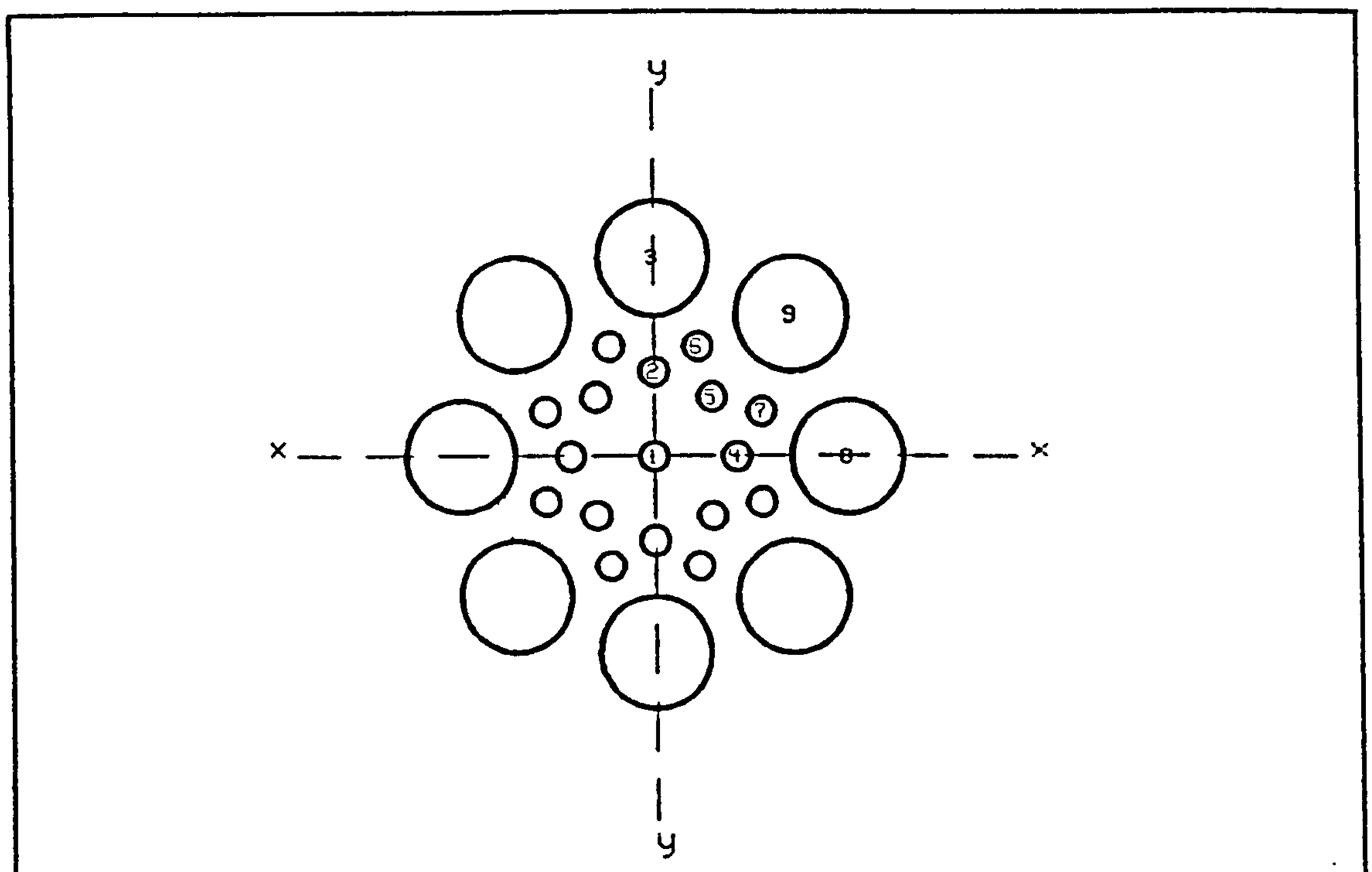

Hole Number	1	2	3	4	5	6	7	8	9
Coordinate x	0	0	0	3	2.1	1.6	3.9	7	5
Coordinate y	0	3	7	0	2.1	3.9	1.6	0	5
Diameter	1	1	4	1	1	1	1	4	4
Number of Holes	1	2	2	2	4	4	4	2	4

Figure 4.16: Geometry of 25-Hole Conditioner Plate.

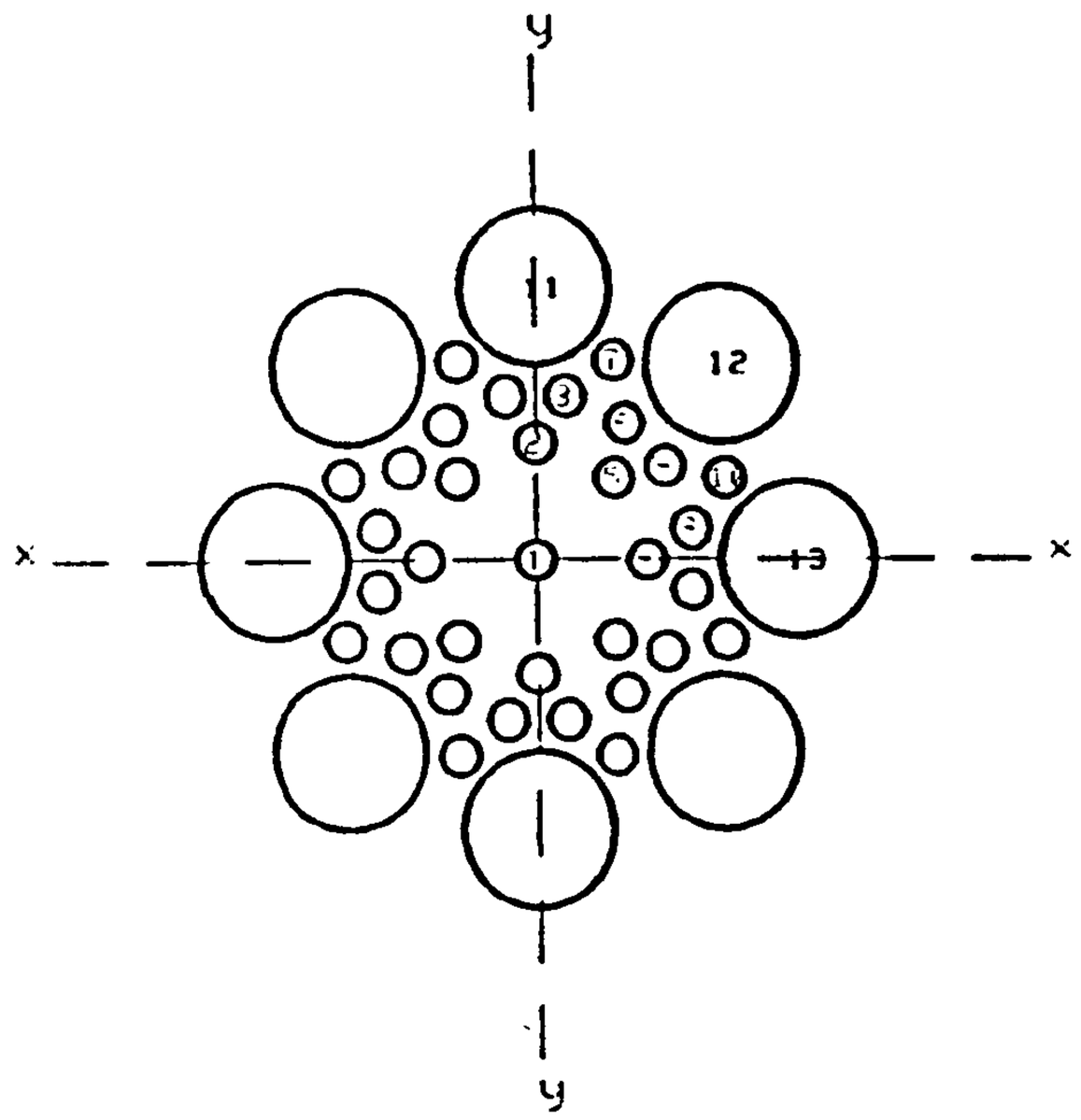

Hole Number	1	2	3	4	5	6	7	8	9	10	11	12	13
Coordinate x	0	0	0.8	3	2.1	2.4	2.1	4.2	3.5	2.1	0	5	7
Coordinate y	0	3	4.2	0	2.1	3.5	5.1	0.8	2.4	5.1	7	5	0
Diameter	1	1	1	1	1	1	1	1	1	1	4	4	4
Number of Holes	1	2	4	2	4	4	4	4	4	4	2	4	2

Figure 4.17: Geometry of 41-Hole Conditioner Plate.

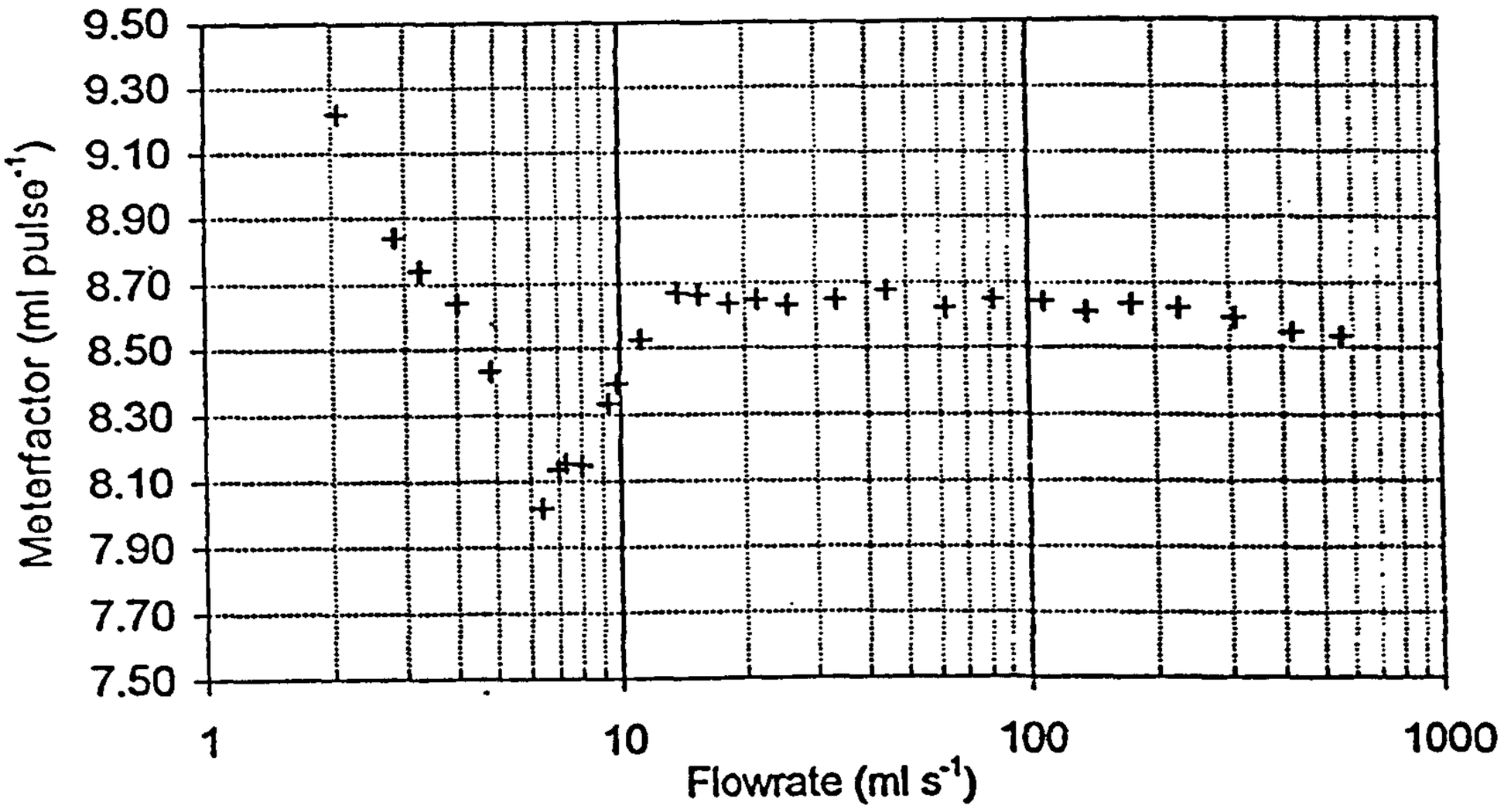

Figure 4.18: Meterfactor Response of Fluidic Oscillator Fitted With 17-Hole Conditioner plate.

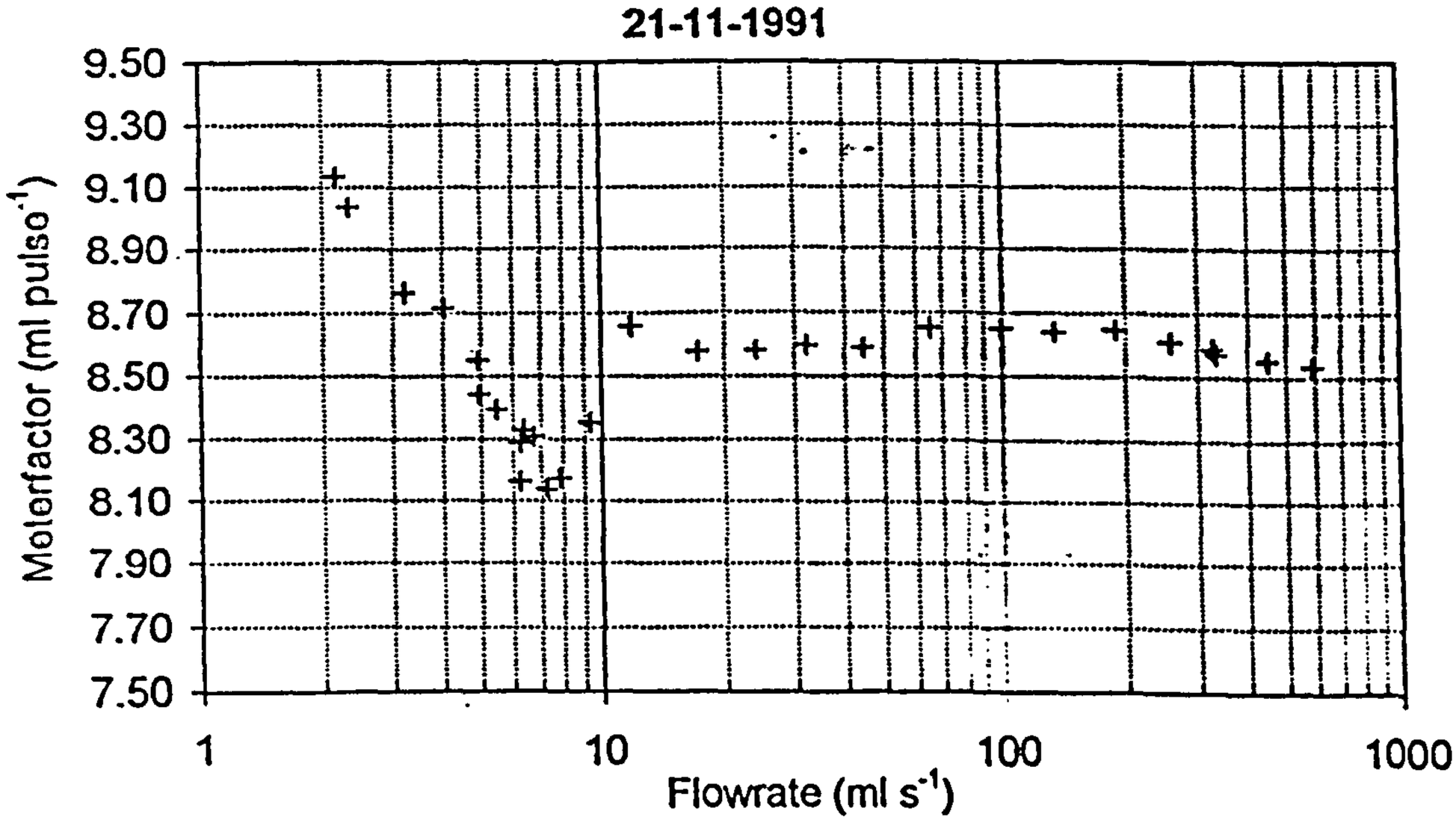

Figure 4.19: Meterfactor Response of Fluidic Oscillator Fitted With 21-Hole Conditioner plate.

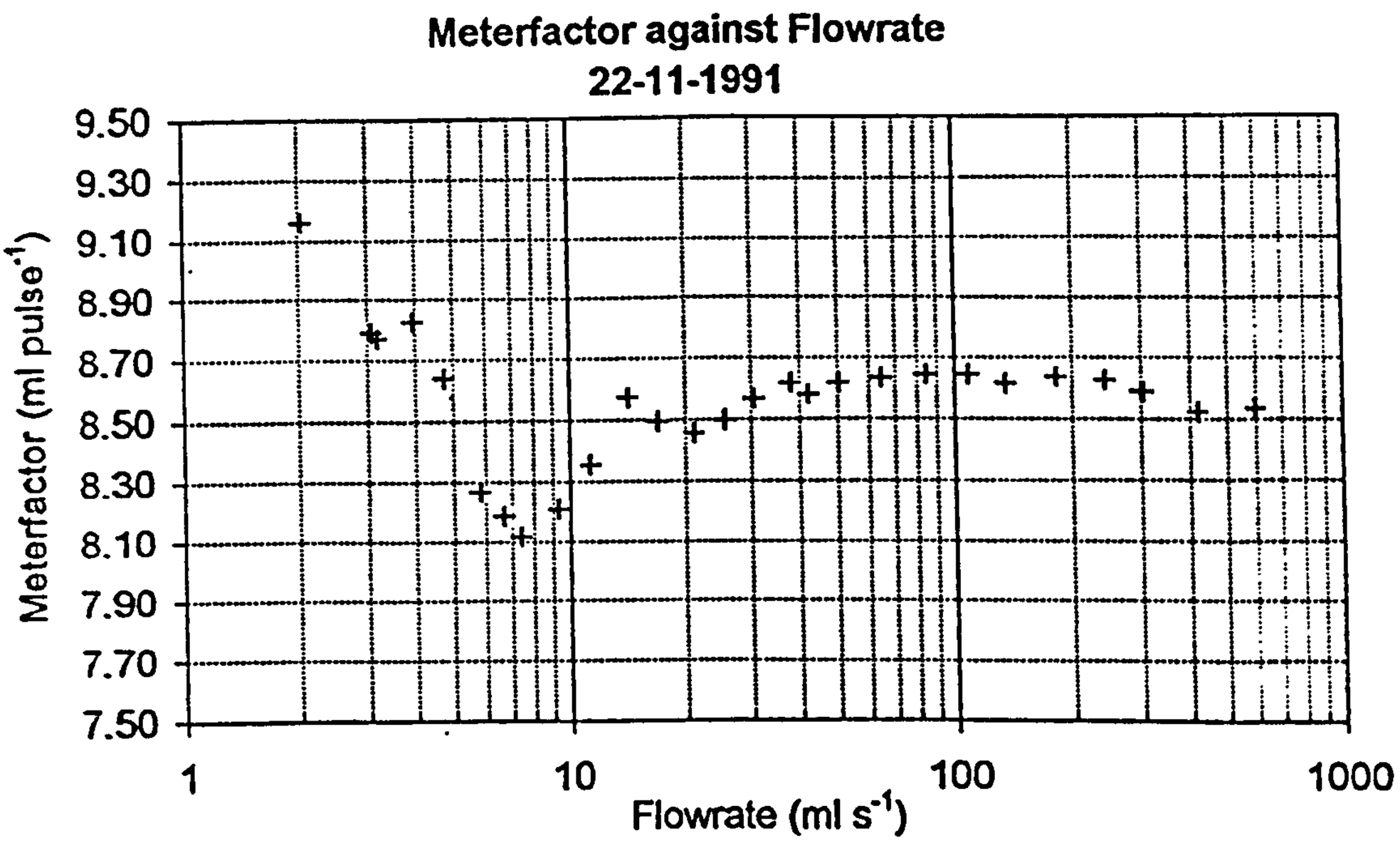

Figure 4.20: Meterfactor Response of Fluidic Oscillator Fitted With 41-Hole Conditioner Plate.

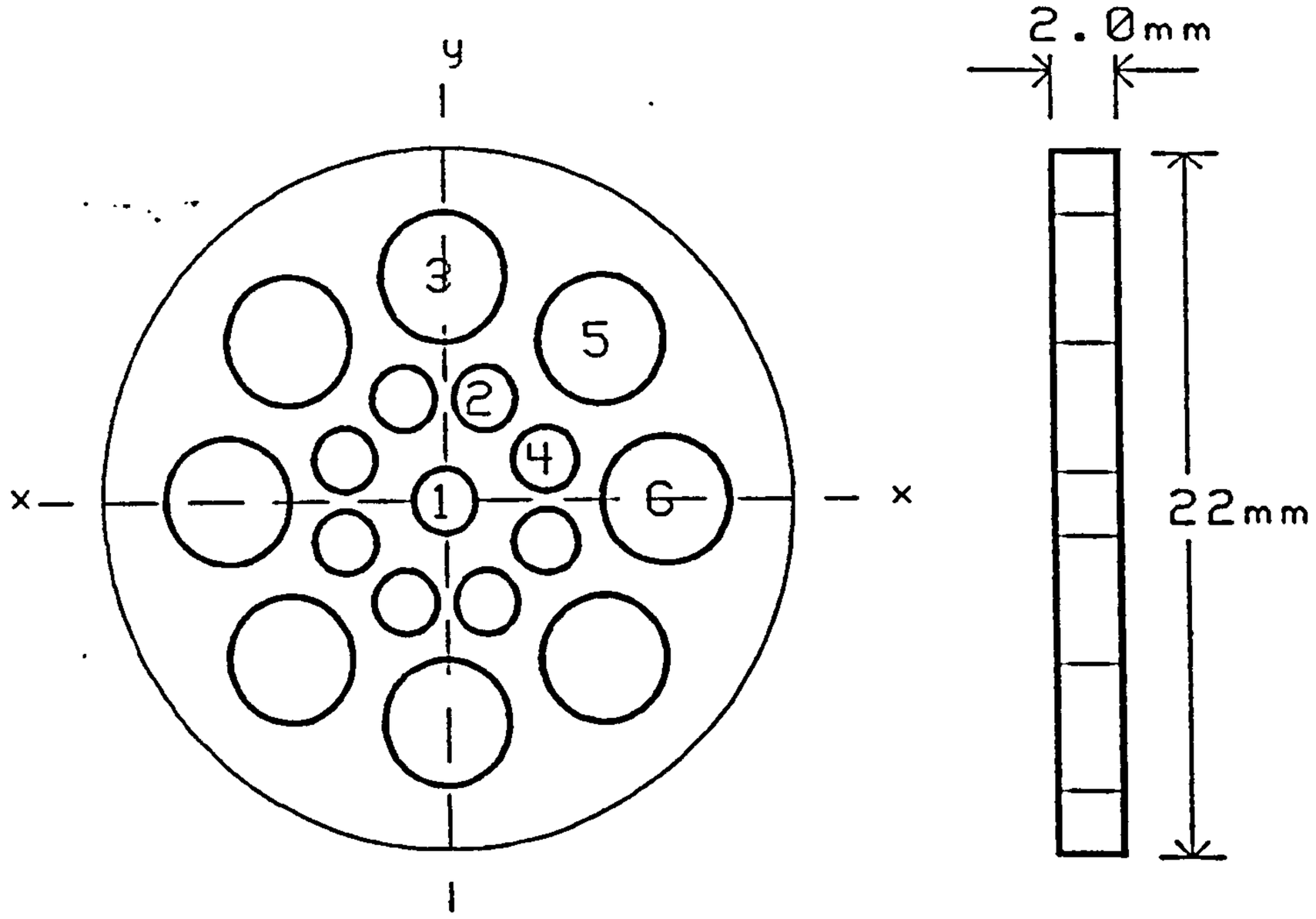

Hole Number	1	2	3	4	5	6
Coordinate x	0	1.3	0	3.2	5	7
Coordinate y	0	3.2	7	1.3	5	0
Diameter	2	2	4	2	4	4
Number of Holes	1	4	2	4	4	2

Figure 4.21: Geometry and Hole Pattern of Conditioner Disc CD1.

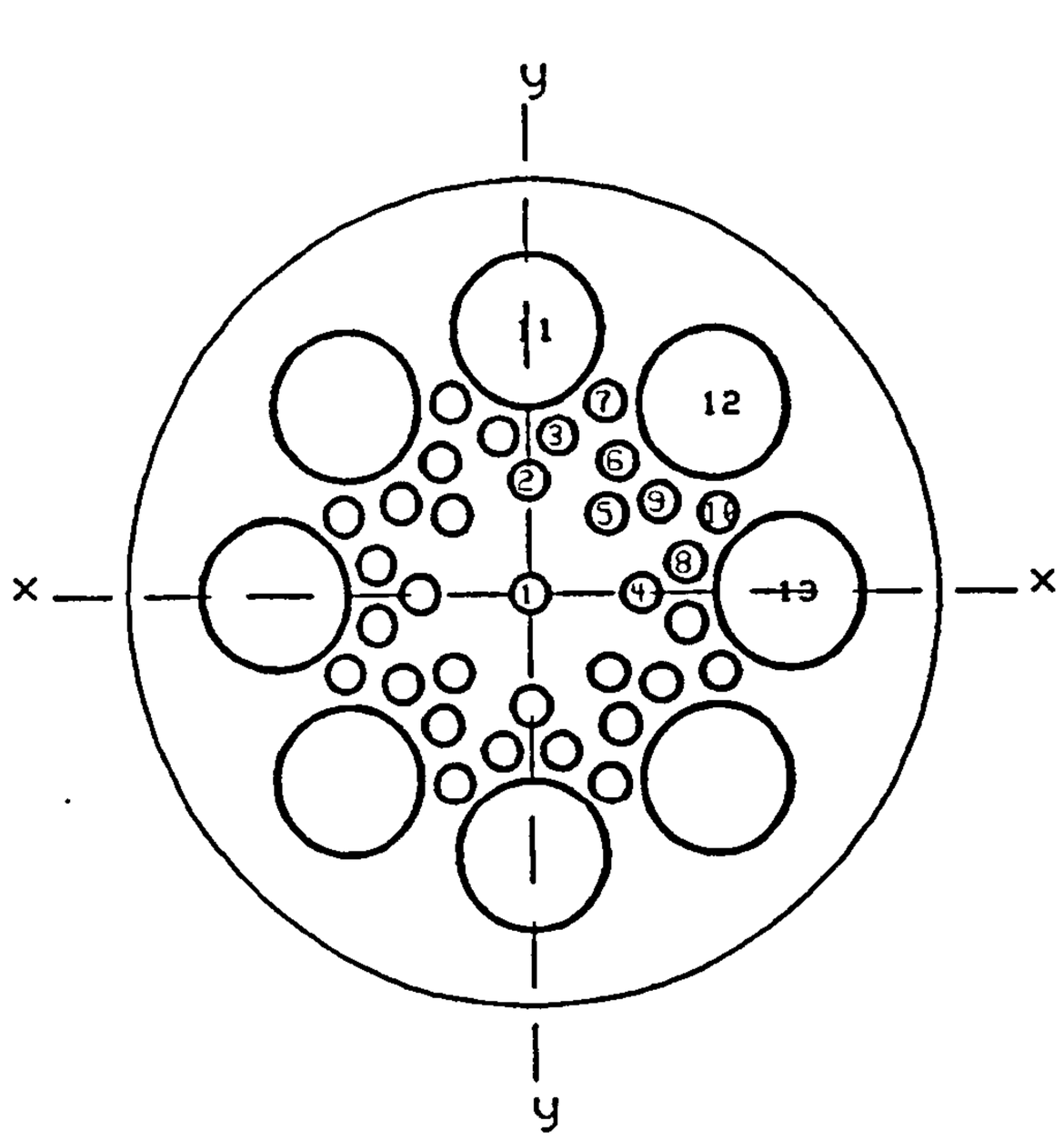

Hole Number	1	2	3	4	5	6	7	8	9	10	11	12	13
Coordinate x	0	0	0.8	3	2.1	2.4	2.1	4.2	3.5	2.1	0	5	7
Coordinate y	0	3	4.2	0	2.1	3.5	5.1	0.8	2.4	5.1	7	5	0
Diameter	1	1	1	1	1	1	1	1	1	1	4	4	4
Number of Holes	1	2	4	2	4	4	4	4	4	4	2	4	2

Figure 4.22: Geometry and Hole Pattern of Conditioner Disc CD2.

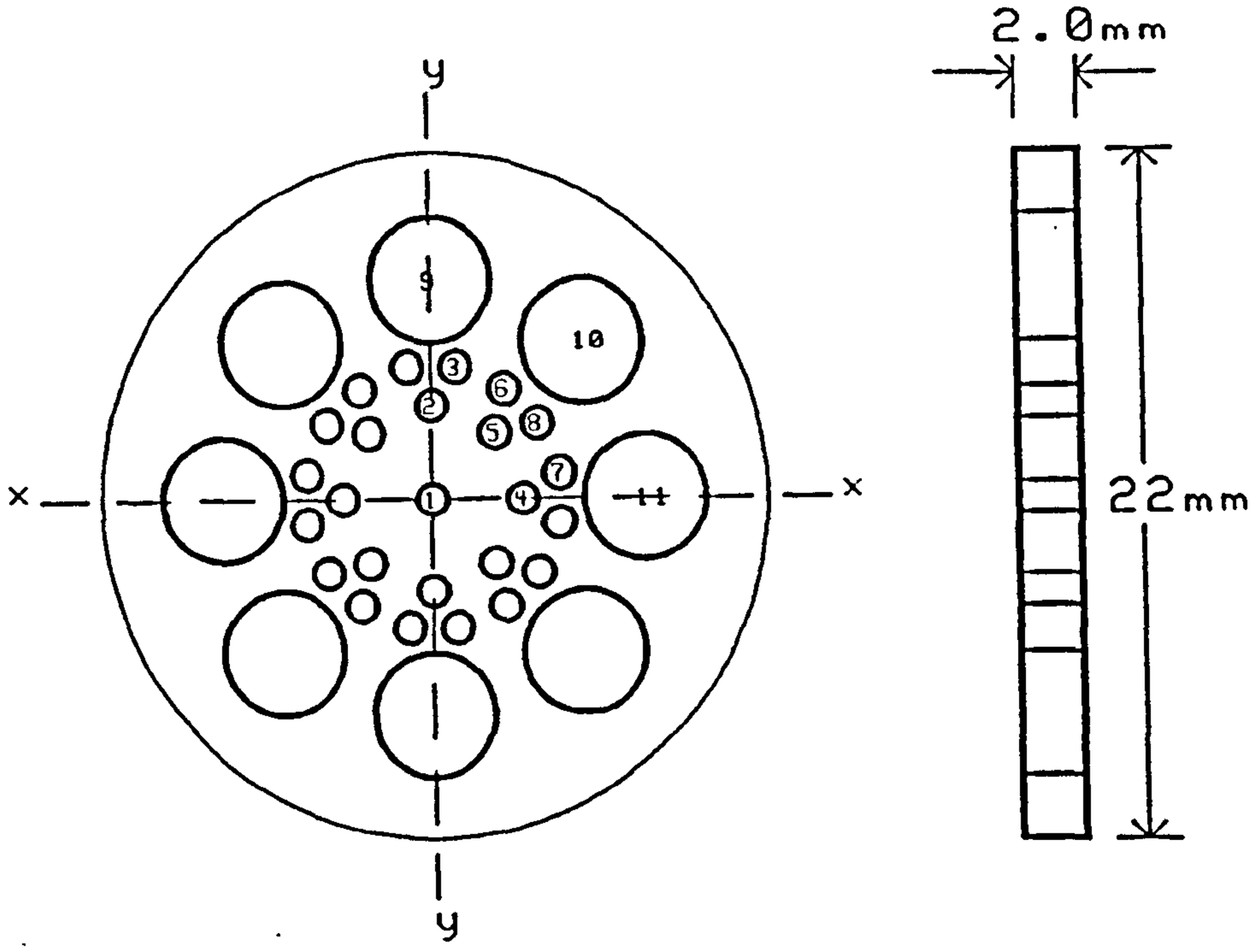

Hole Number	1	2	3	4	5	6	7	8	9	10	11
Coordinate x	0	0	0.8	3	2.1	2.4	4.2	3.5	0	5	7
Coordinate y	0	3	4.2	0	2.1	3.5	0.8	2.4	7	5	0
Diameter	1	1	1	1	1	1	1	4	4	4	4
Number of Holes	1	2	4	2	4	4	4	4	2	4	2

Figure 4.23: Geometry and Hole Pattern of Conditioner Disc CD3.

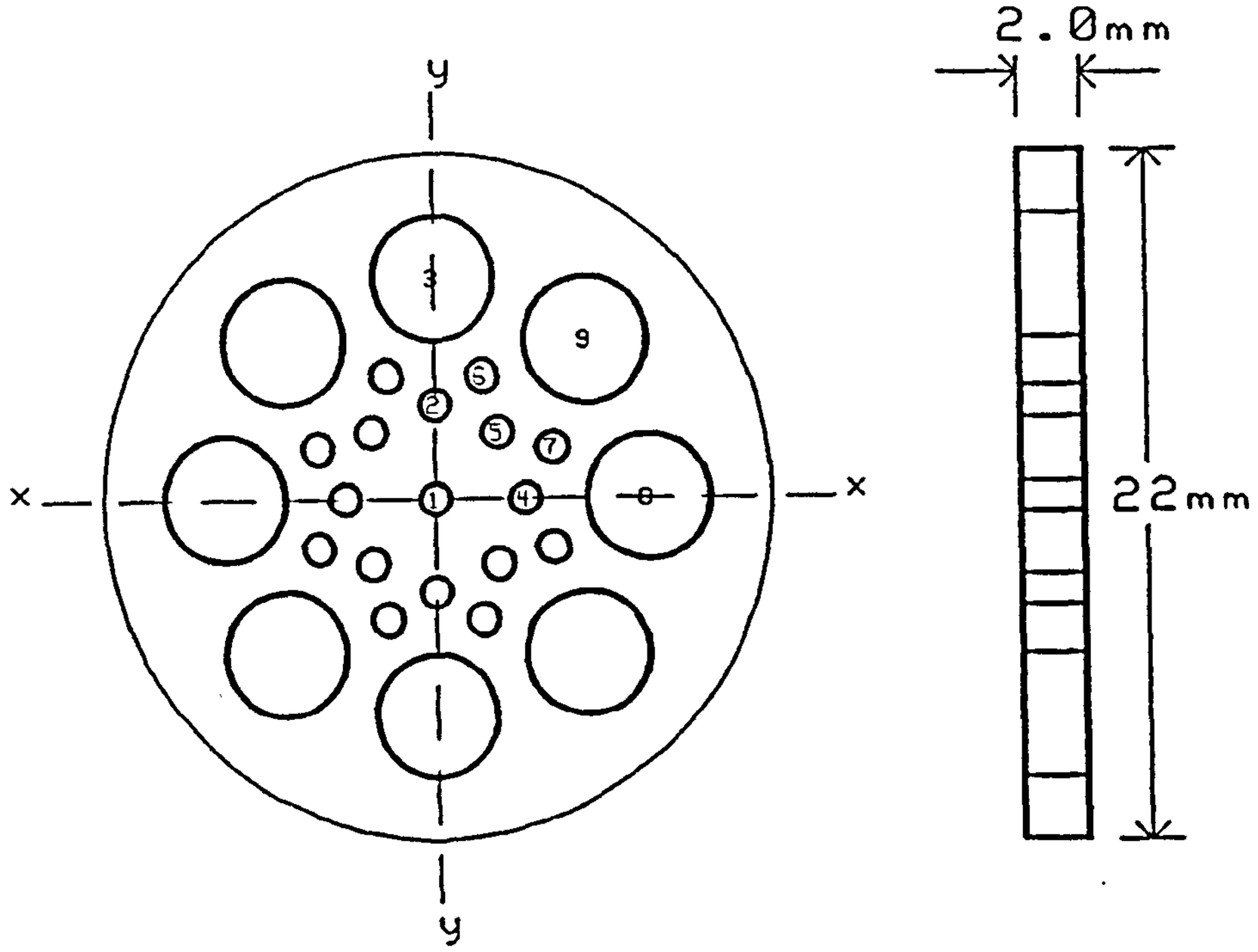

Hole Number	1	2	3	4	5	6	7	8	9
Coordinate x	0	0	0	3	2.1	1.6	3.9	7	5
Coordinate y	0	3	7	0	2.1	3.9	1.6	0	5
Diameter	1	1	4	1	1	1	1	4	4
Number of Holes	1	2	2	2	4	4	4	2	4

Figure 4.24: Geometry and Hole Pattern of Conditioner Disc CD4.

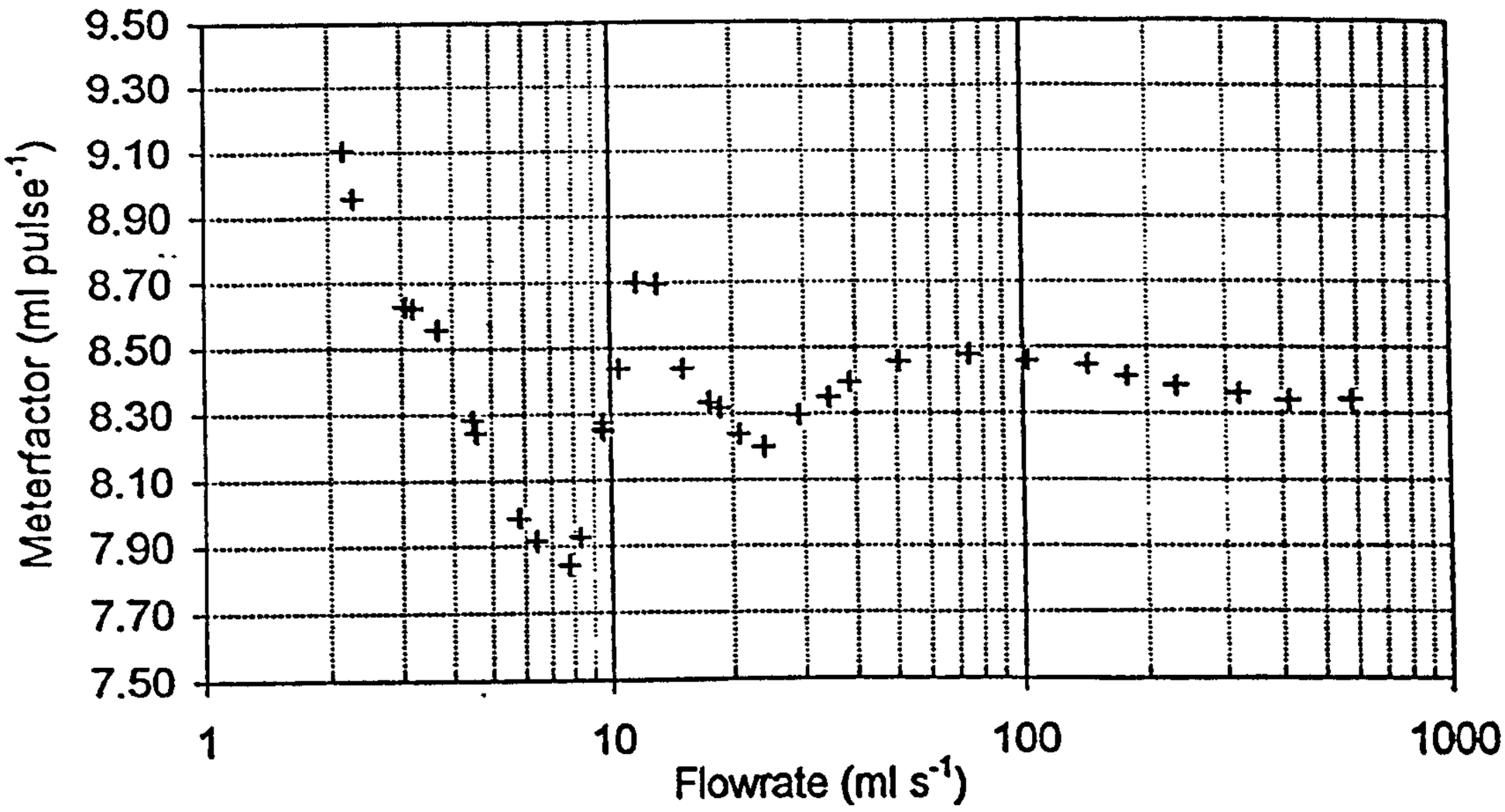

Figure 4.25: Meterfactor Response of Fluidic Oscillator Fitted With Conditioner Disc CD1.

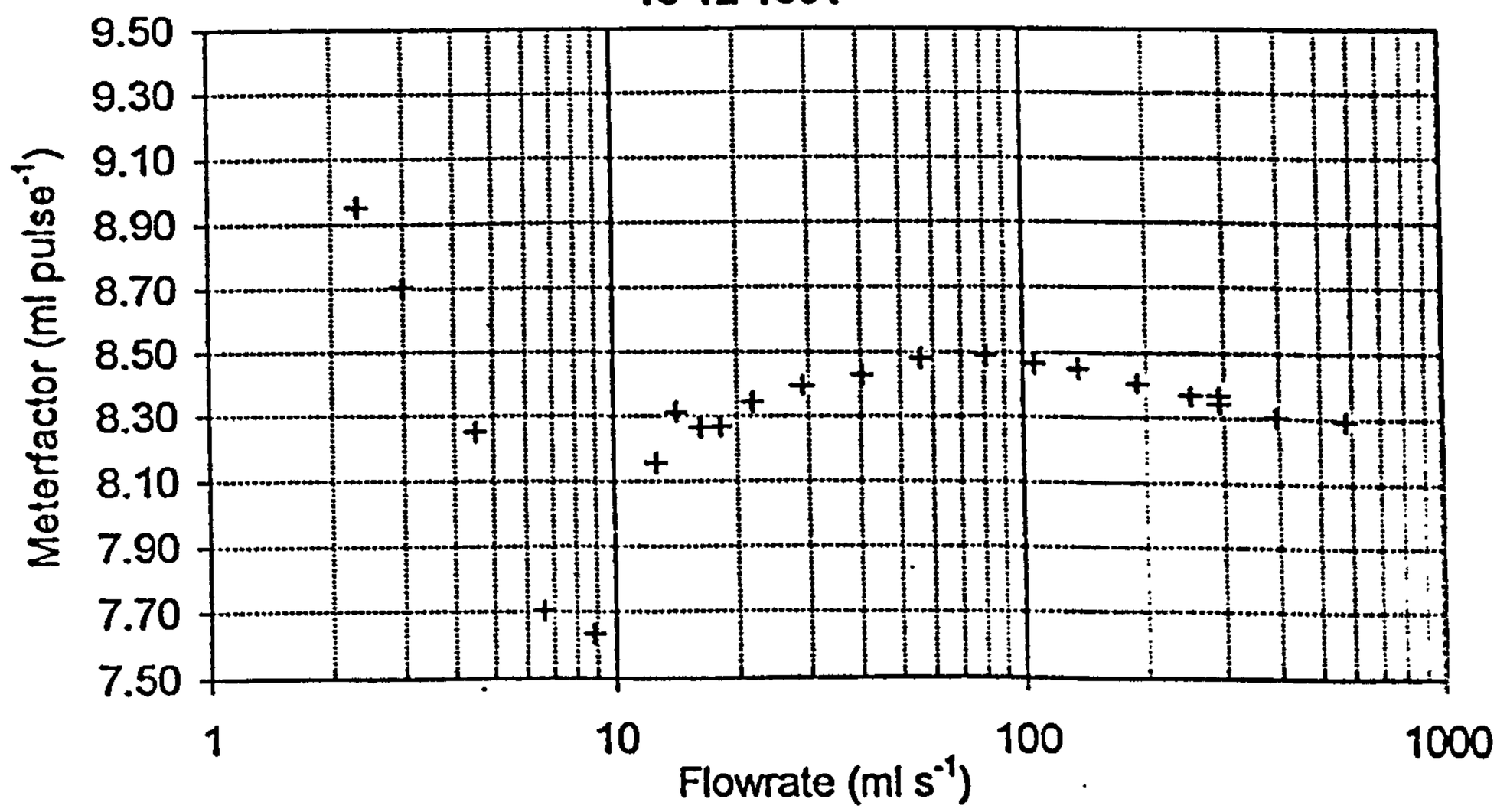

Figure 4.26: Meterfactor Response of Fluidic Oscillator Fitted With Conditioner Disc CD2.

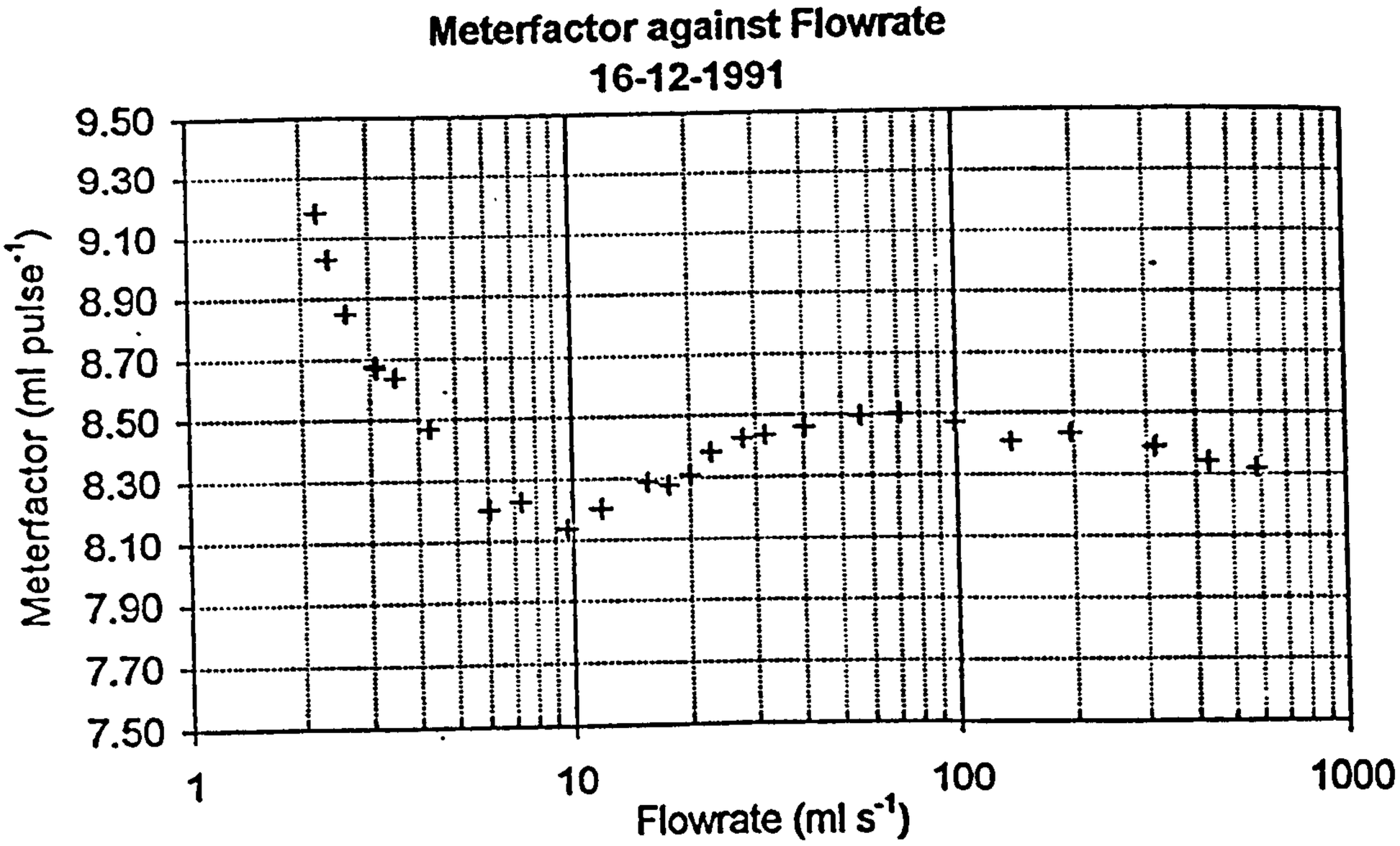

Figure 4.27: Meterfactor Response of Fluidic Oscillator Fitted With Conditioner Disc CD3.

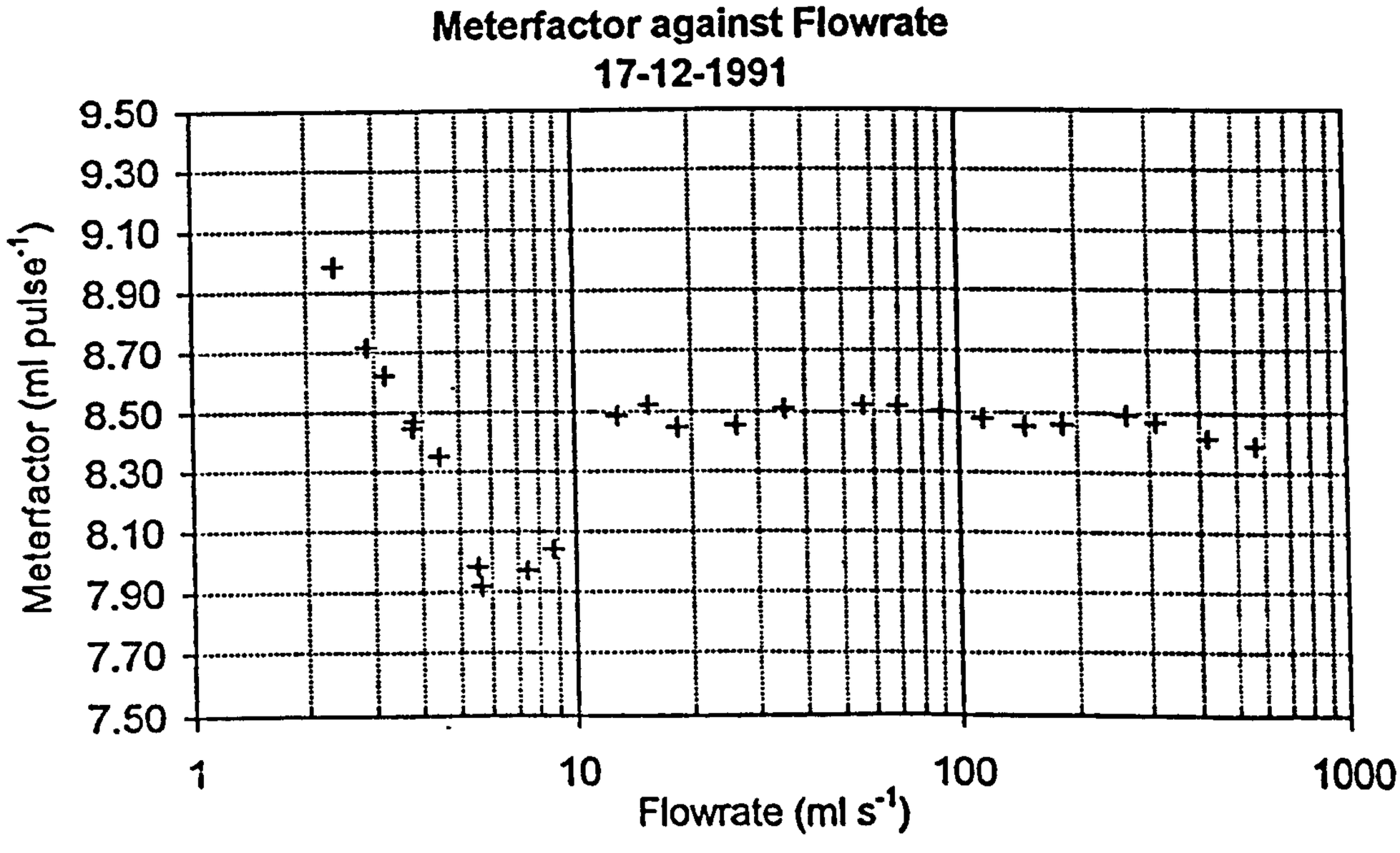

Figure 4.28: Meterfactor Response of Fluidic Oscillator Fitted With Conditioner Disc CD4.

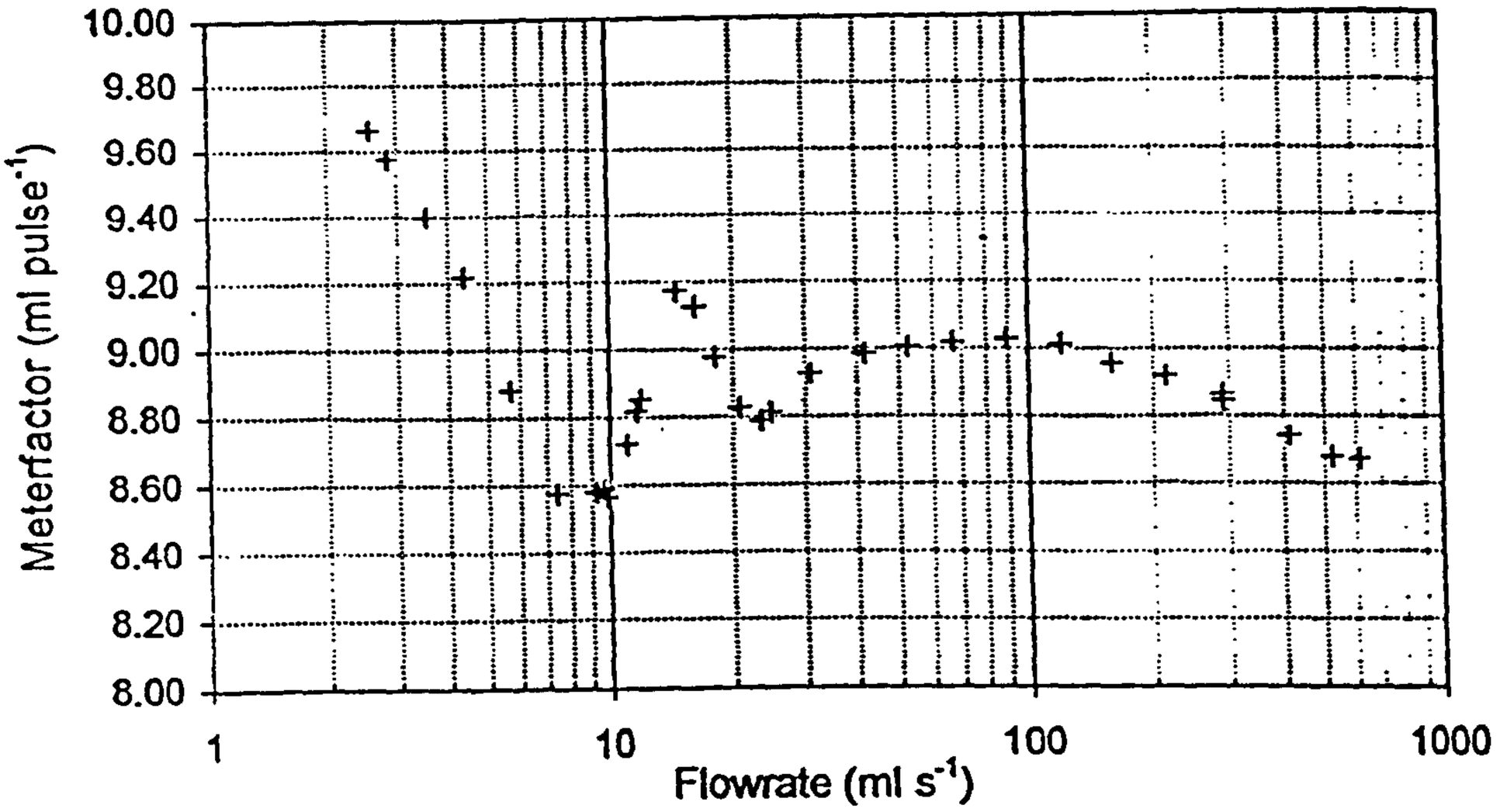

Figure 4.29: Meterfactor Response of Fluidic Oscillator Fitted With Conditioner Disc CD3 at 0°.

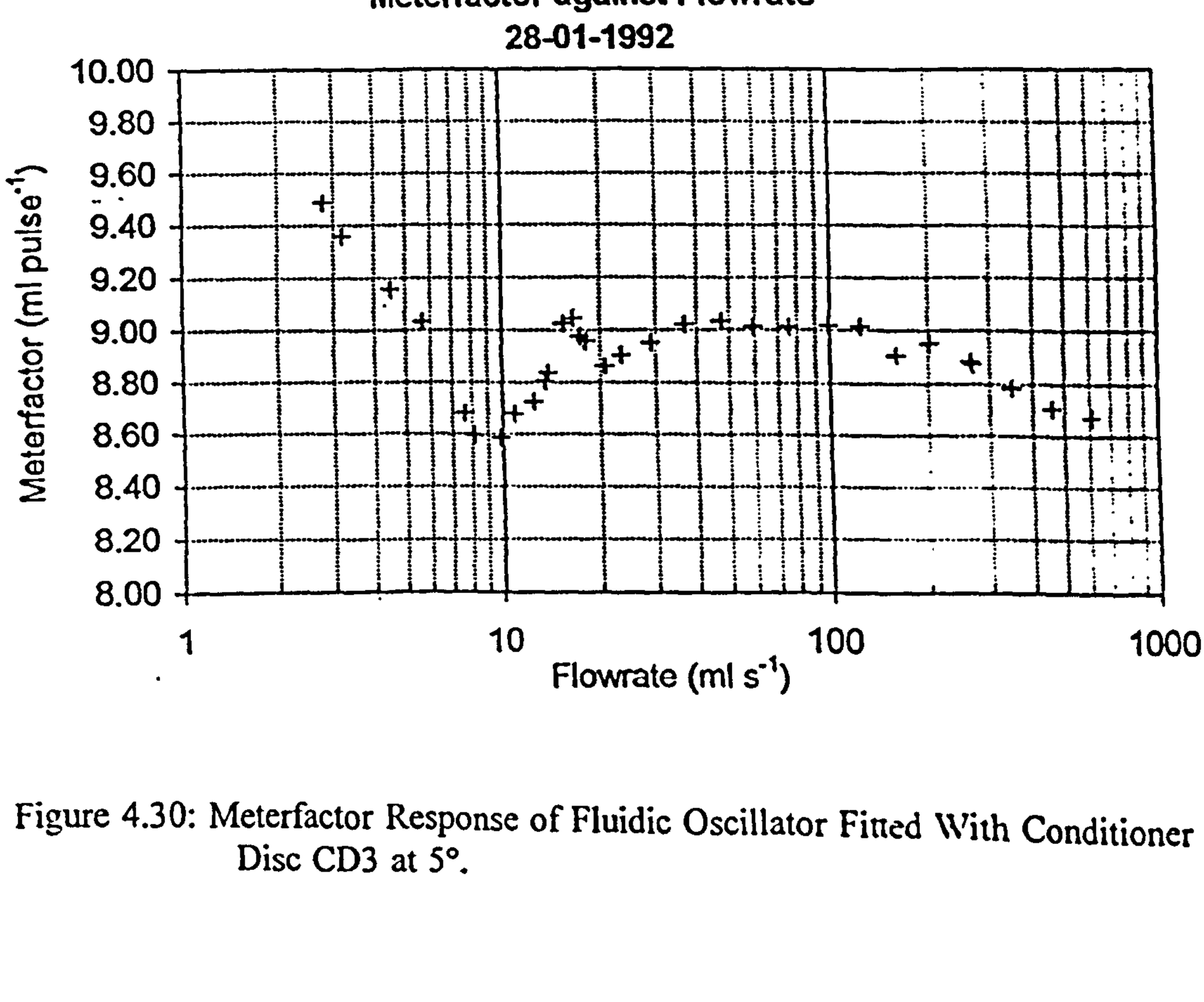

Figure 4.30: Meterfactor Response of Fluidic Oscillator Fitted With Conditioner Disc CD3 at 5°.

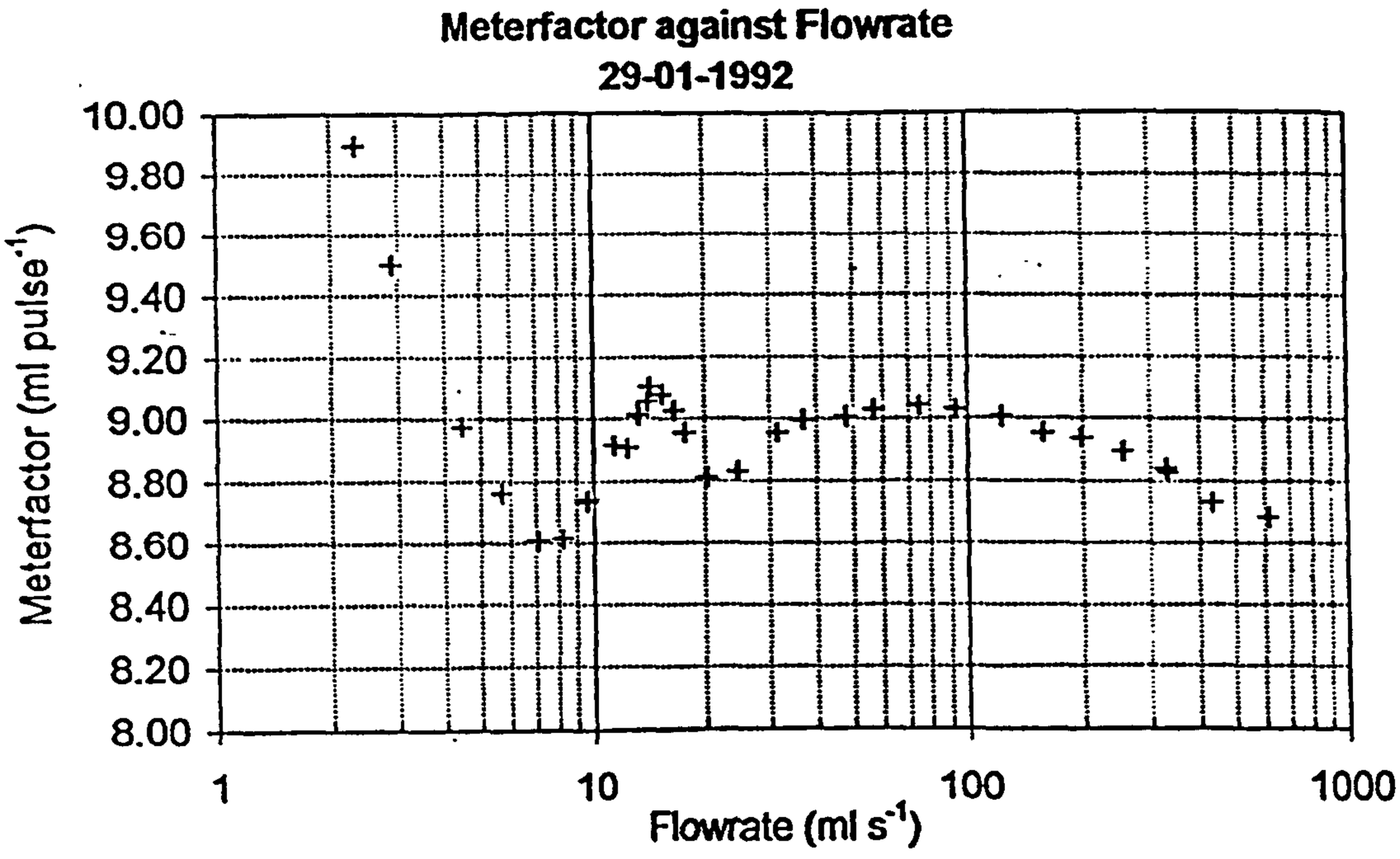

Figure 4.31: Meterfactor Response of Fluidic Oscillator Fitted With Conditioner Disc CD3 at 10°.

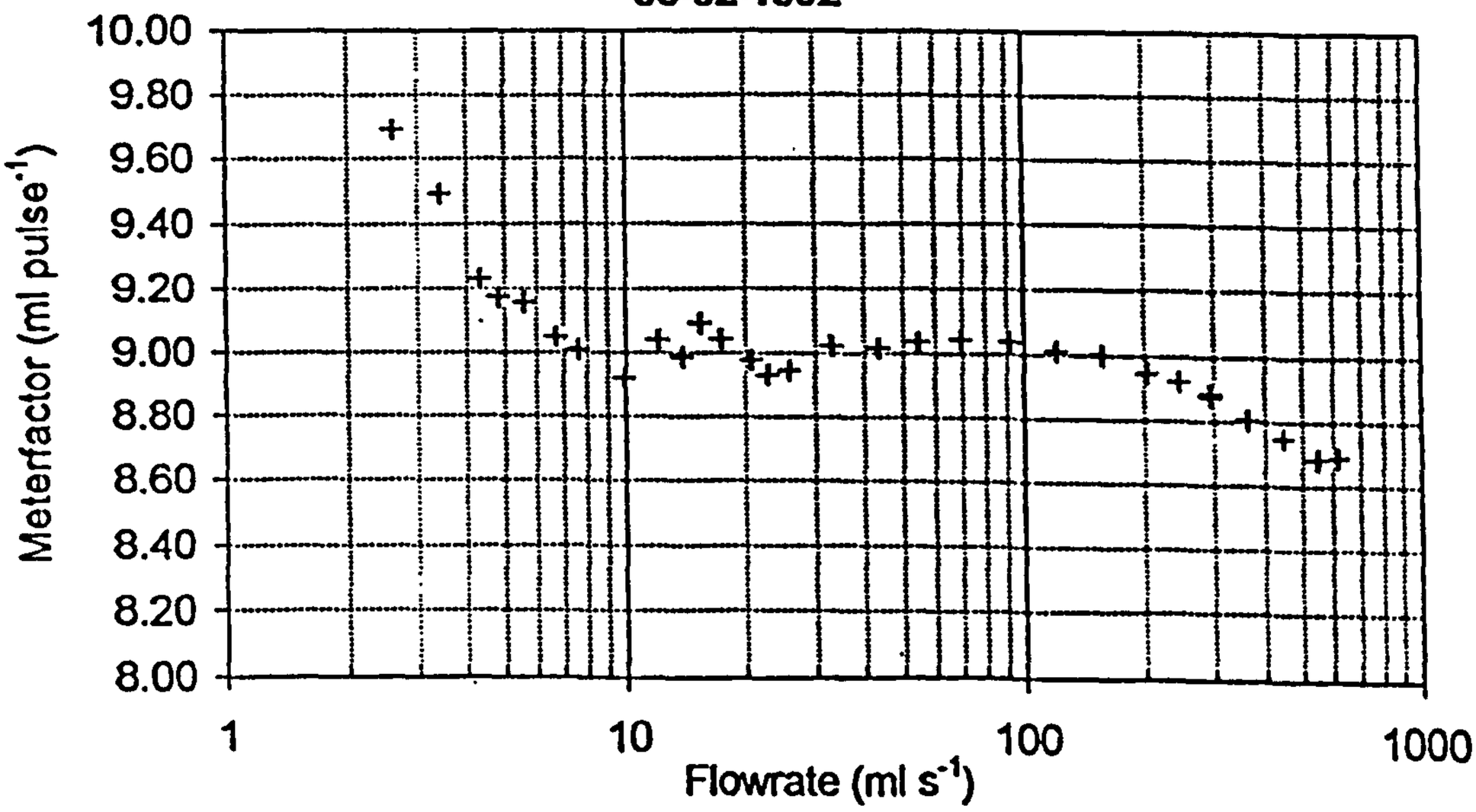

Figure 4.32: Meterfactor Response of Fluidic Oscillator Fitted With Conditioner Disc CD3 at 15°.

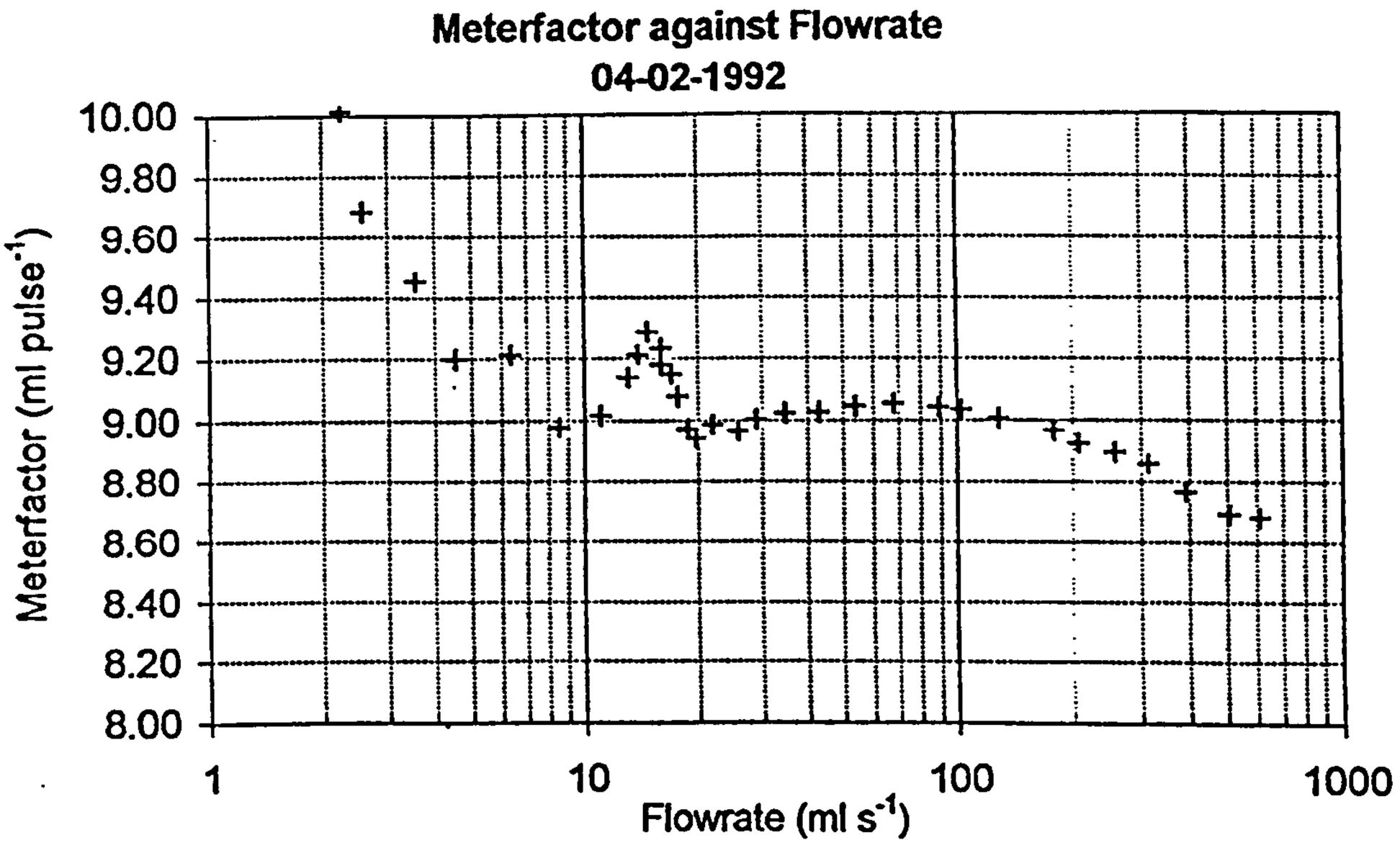

Figure 4.33: Meterfactor Response of Fluidic Oscillator Fitted With Conditioner Disc CD3 at 20°.

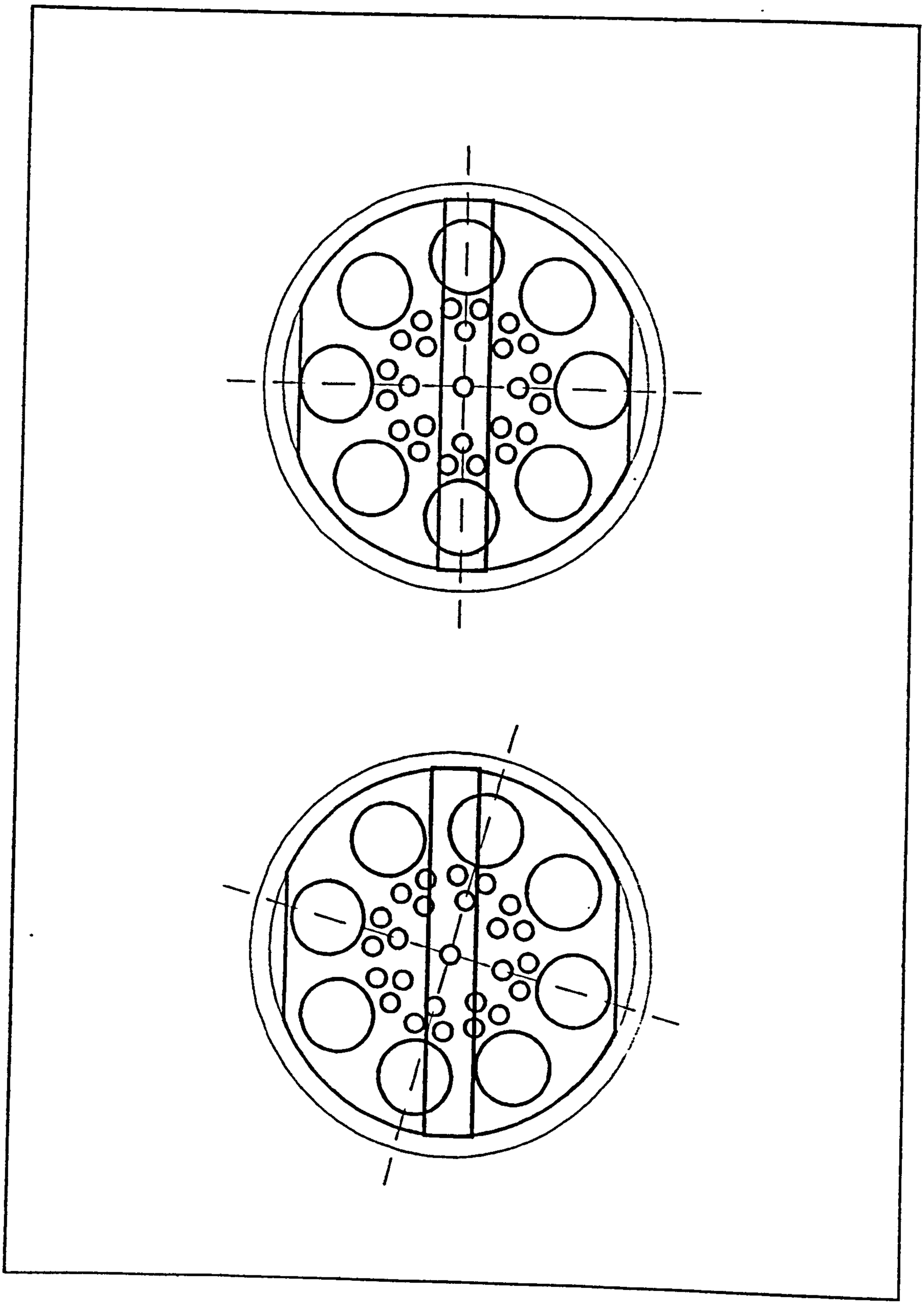

Figure 4.34: End View Through Nozzle Outlet of Conditioner Hole Pattern at 0° and 15°.

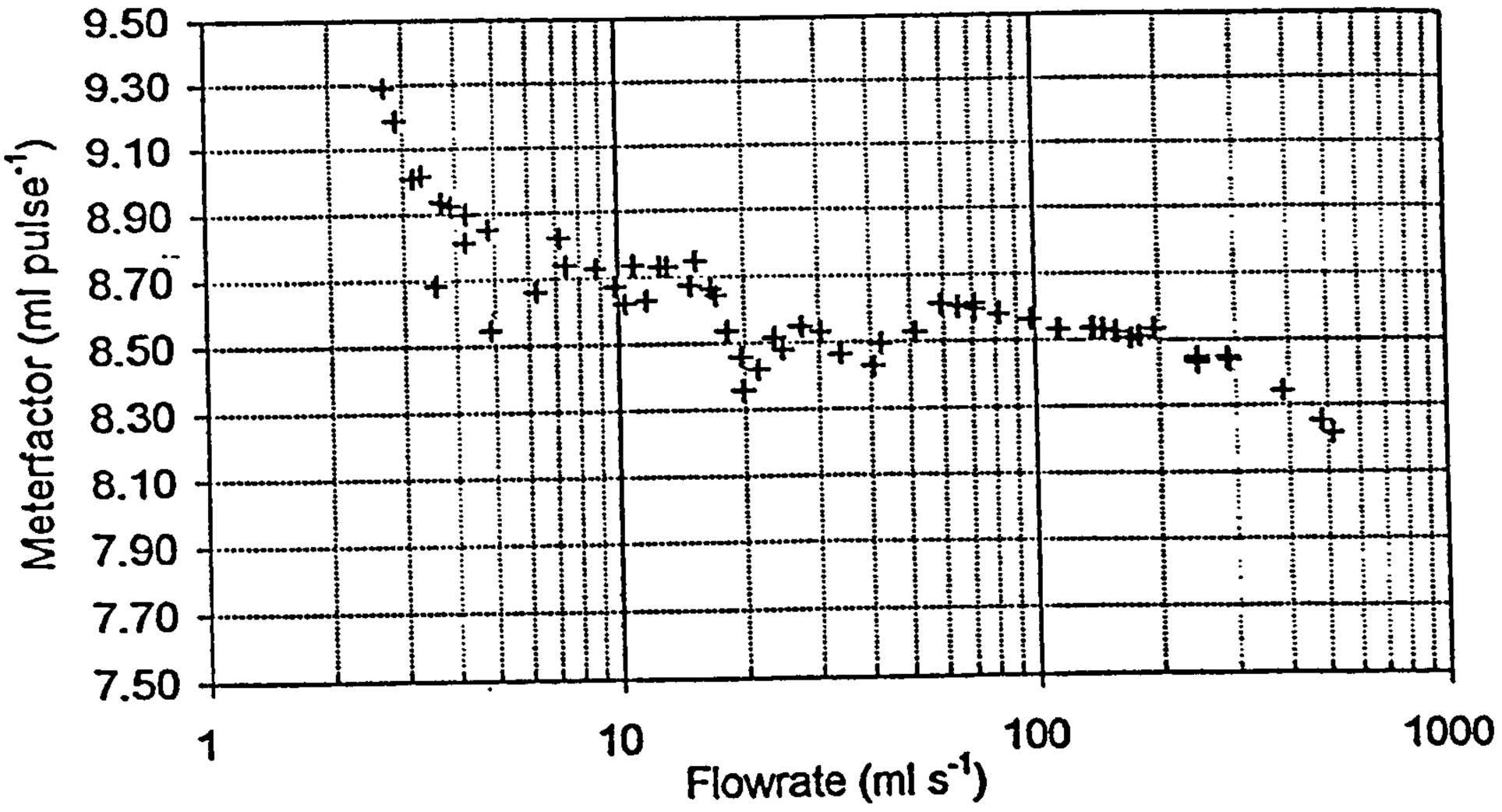

Figure 4.35: Meterfactor Response of Fluidic Oscillator Fitted With 0.5mm Gauze Conditioner.

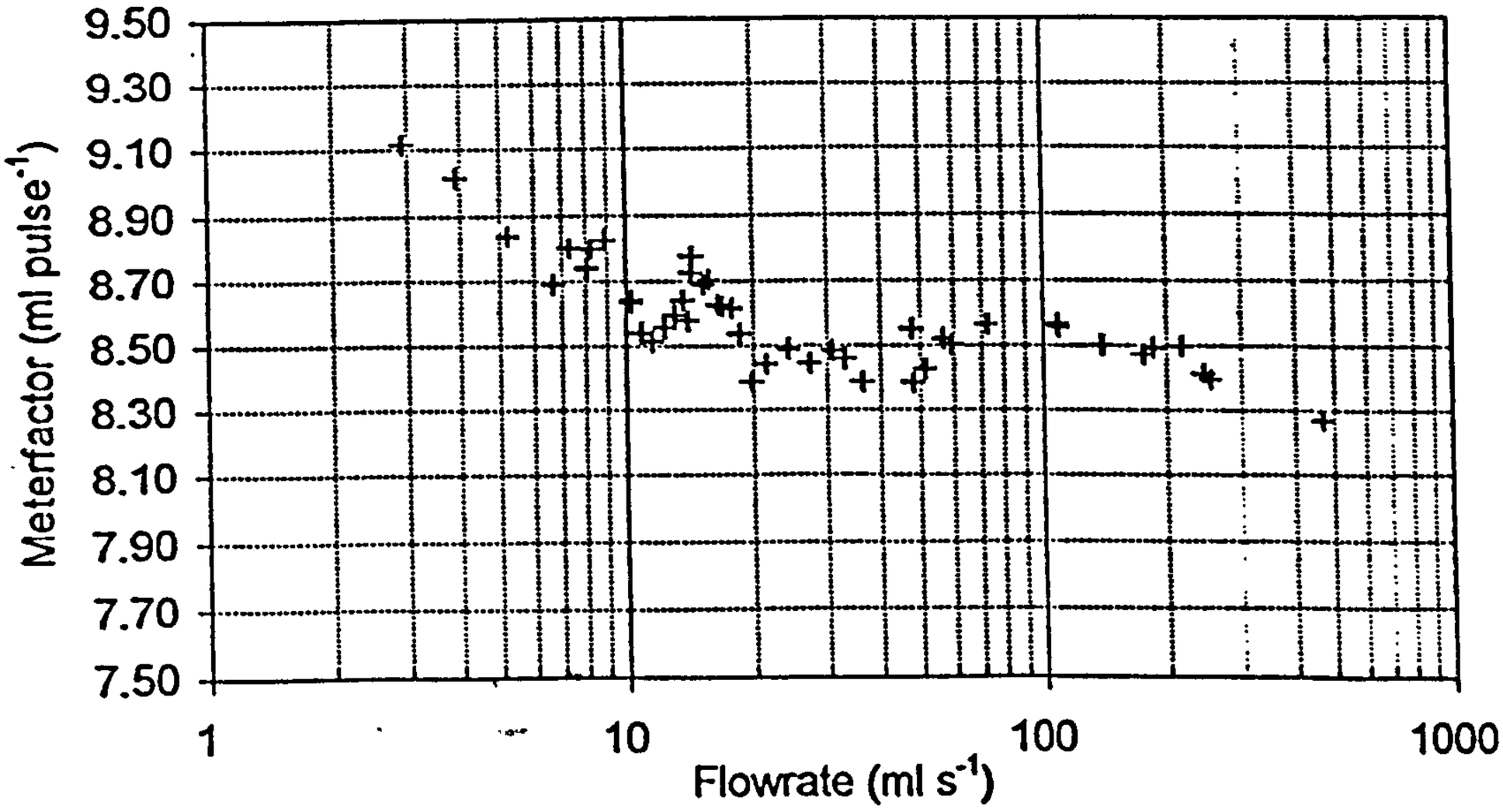

Figure 4.36: Meterfactor Response of Fluidic Oscillator Fitted With 1.0mm Gauze Conditioner.

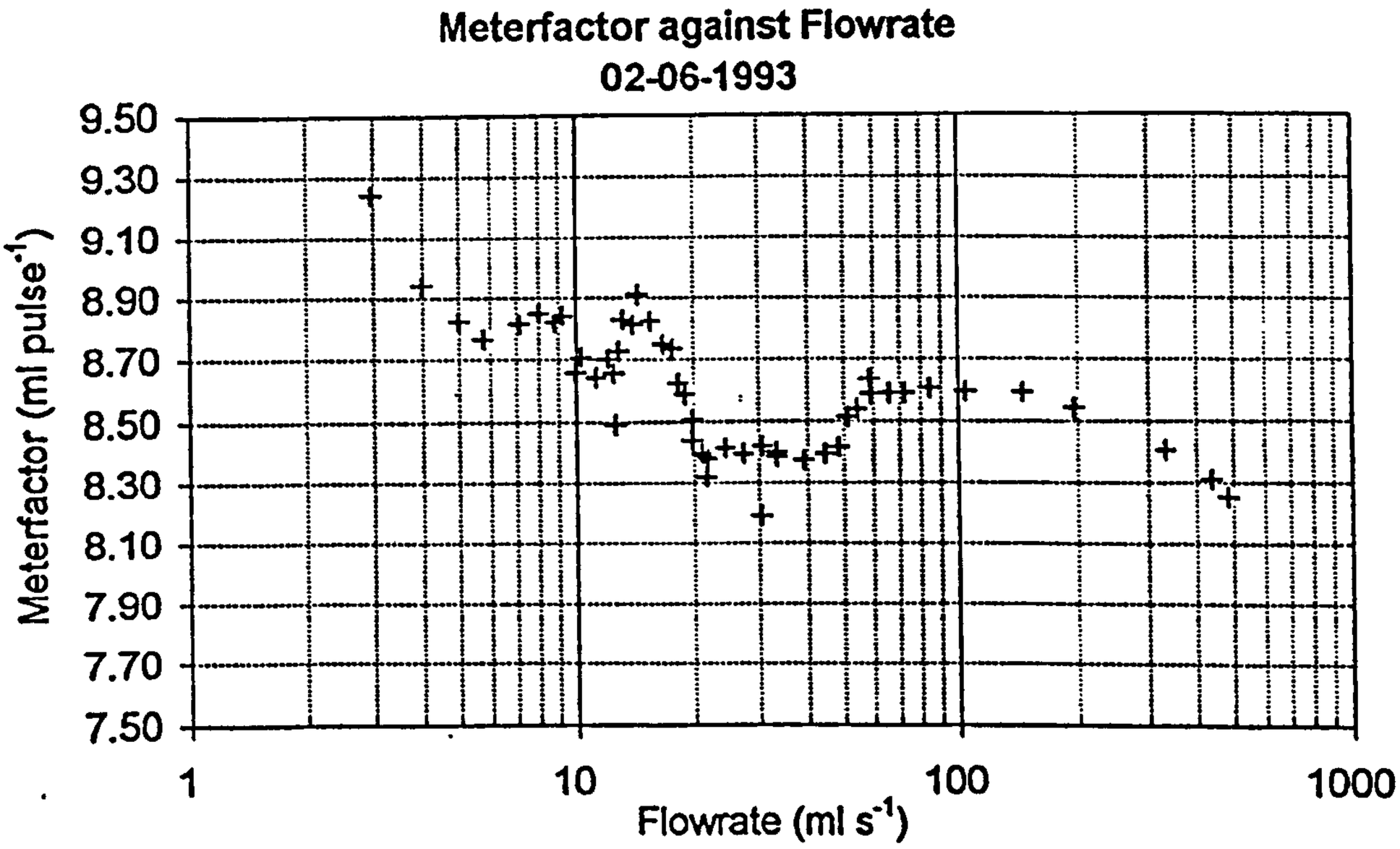

Figure 4.37: Meterfactor Response of Fluidic Oscillator Fitted With 1.5mm Gauze Conditioner.

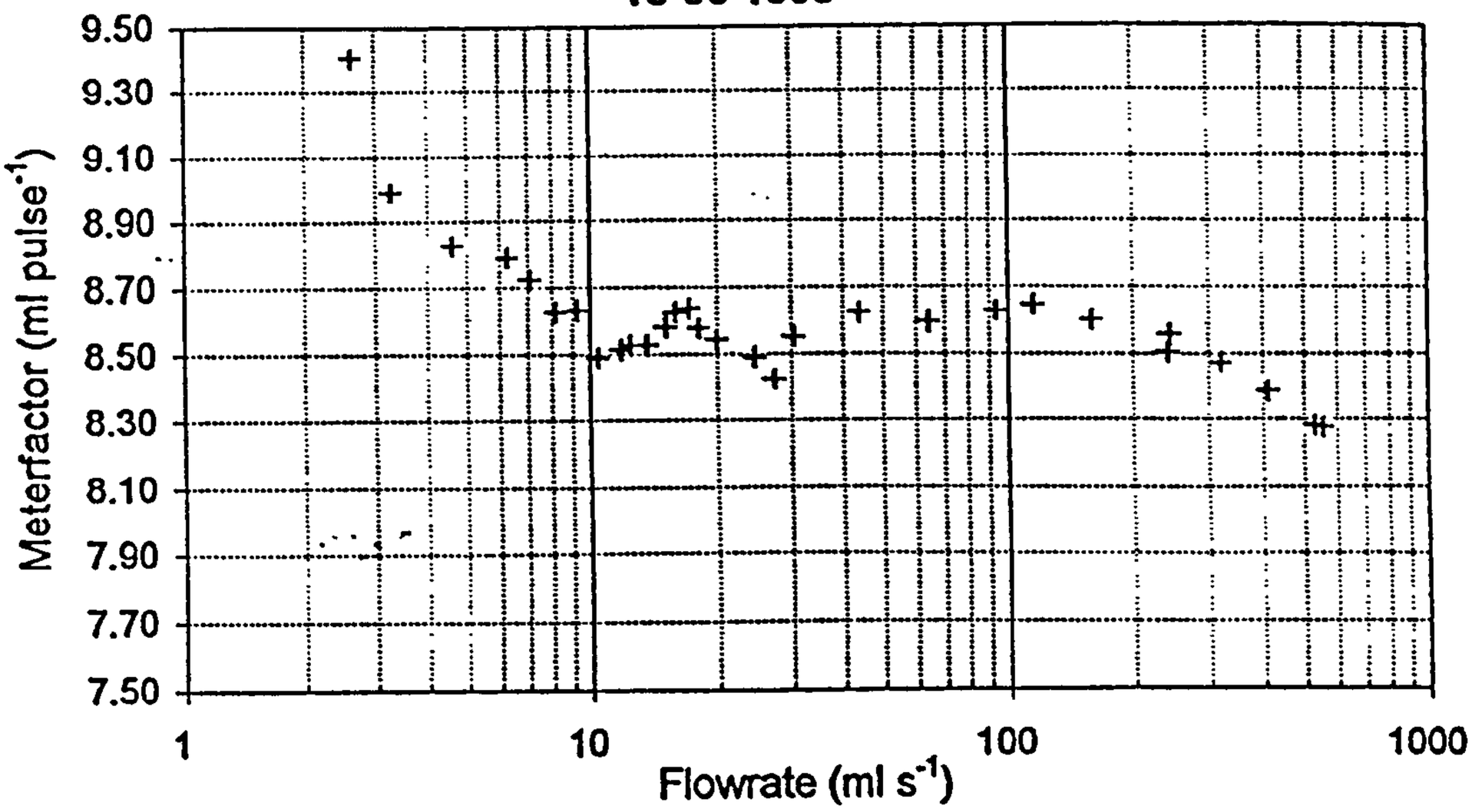

Figure 4.38: Meterfactor Response of Fluidic Oscillator Fitted With 1.08mm Hole Size Conditioner.

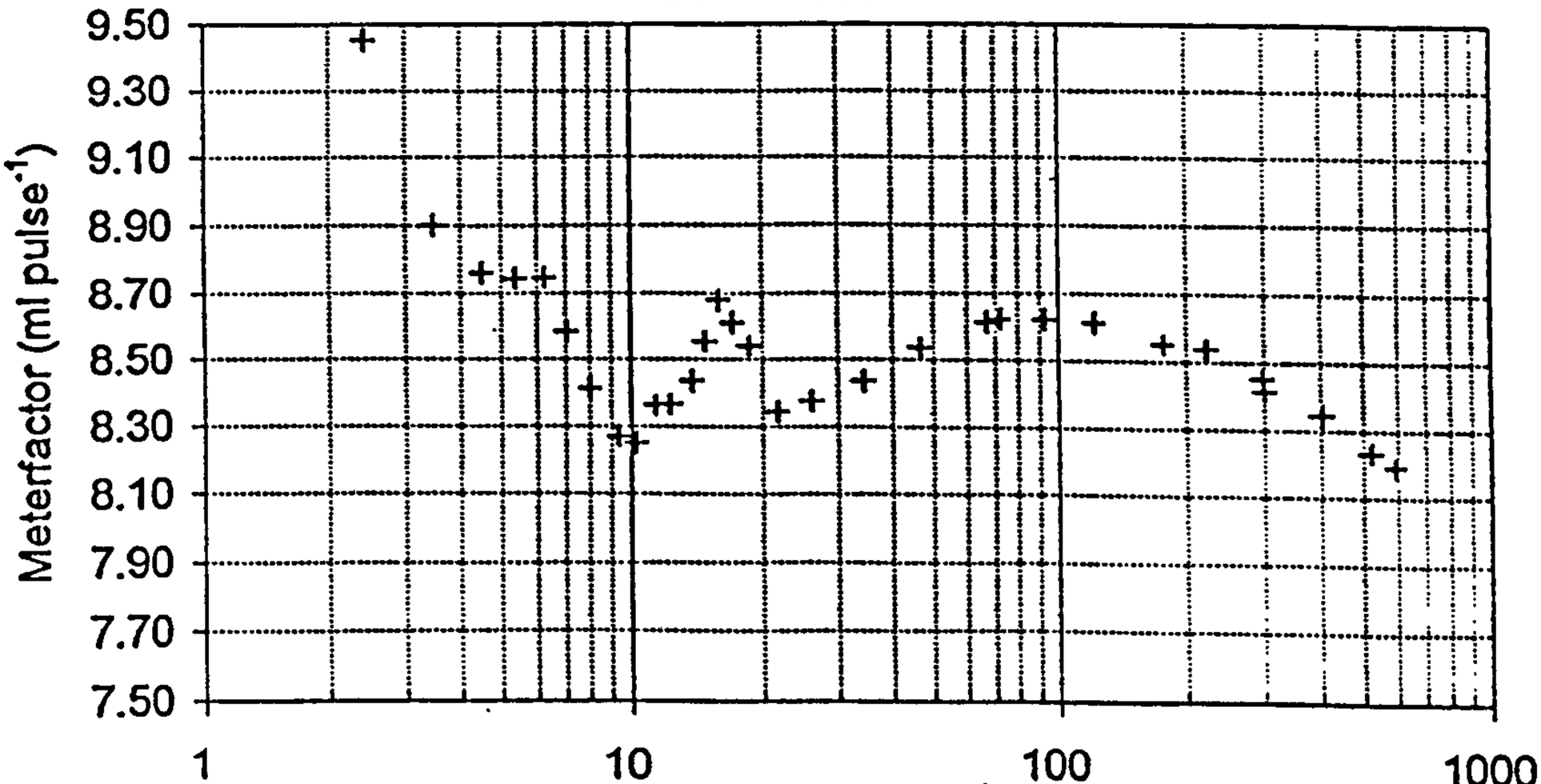

Figure 4.39: Meterfactor Response of Fluidic Oscillator Fitted With 2.1mm Hole Size Conditioner.

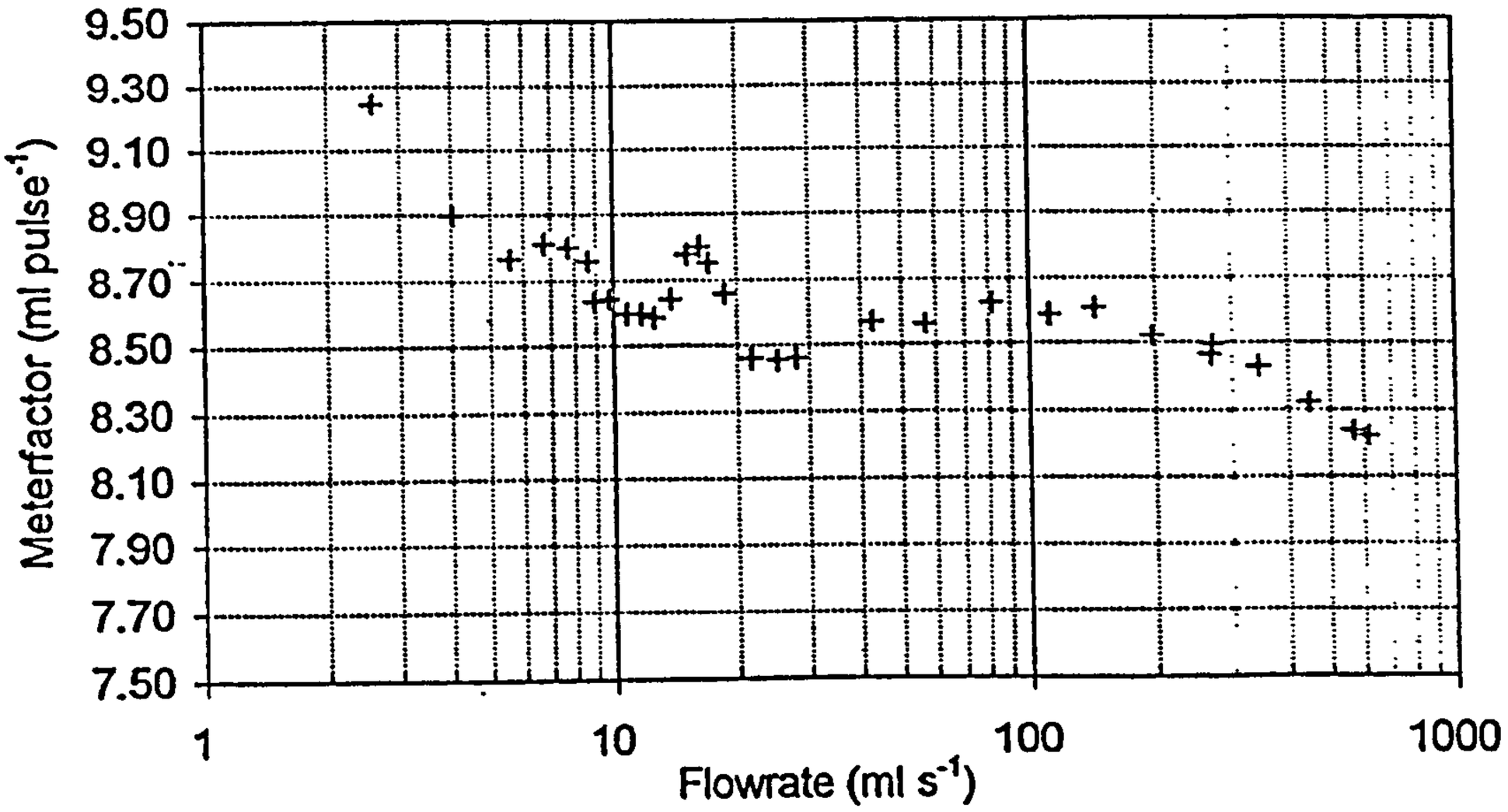

Figure 4.40: Meterfactor Response of Fluidic Oscillator Fitted With 2.34mm Hole Size Conditioner.

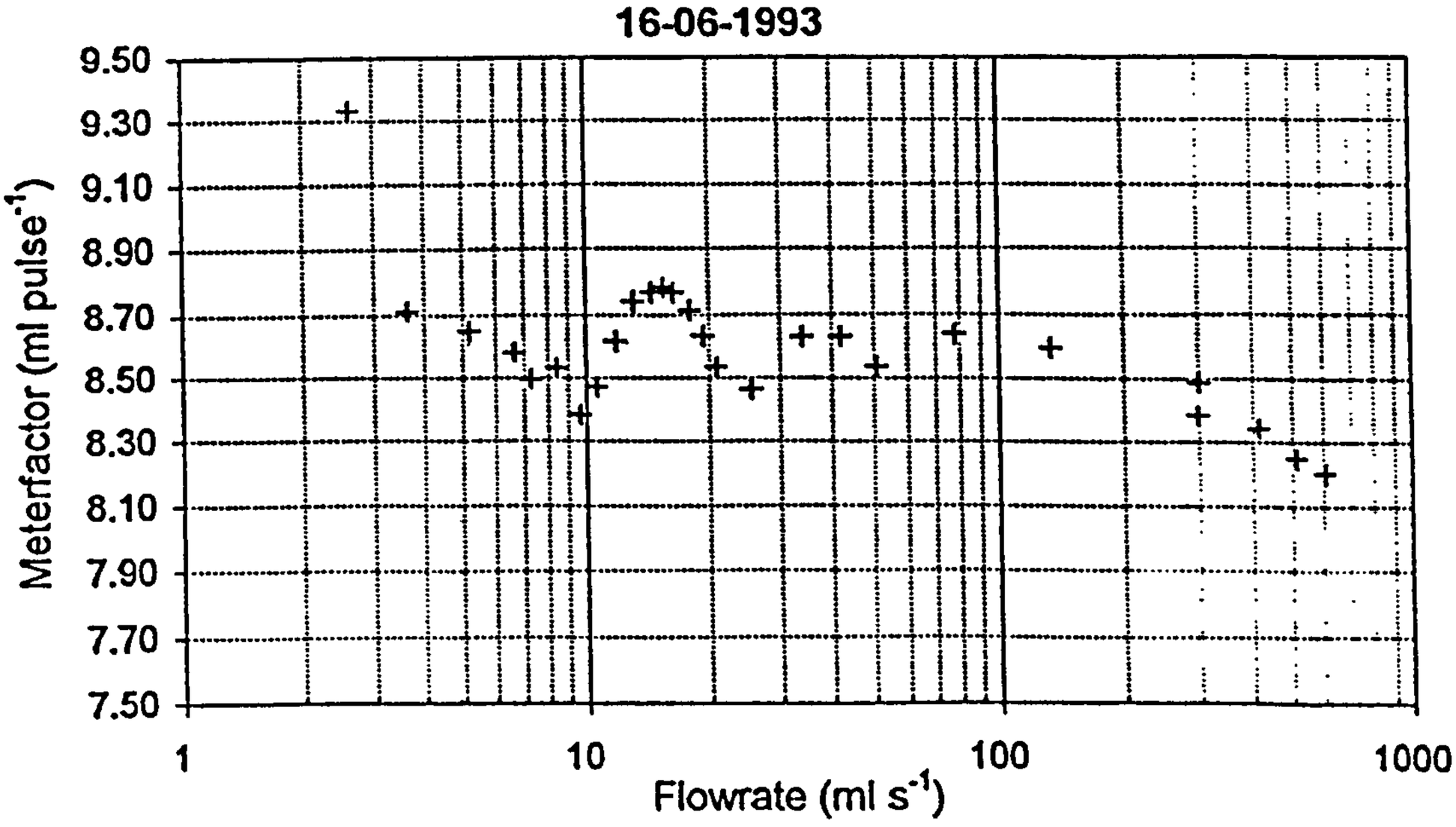

Figure 4.41: Meterfactor Response of Fluidic Oscillator Fitted With 3.0mm Hole Size Conditioner.

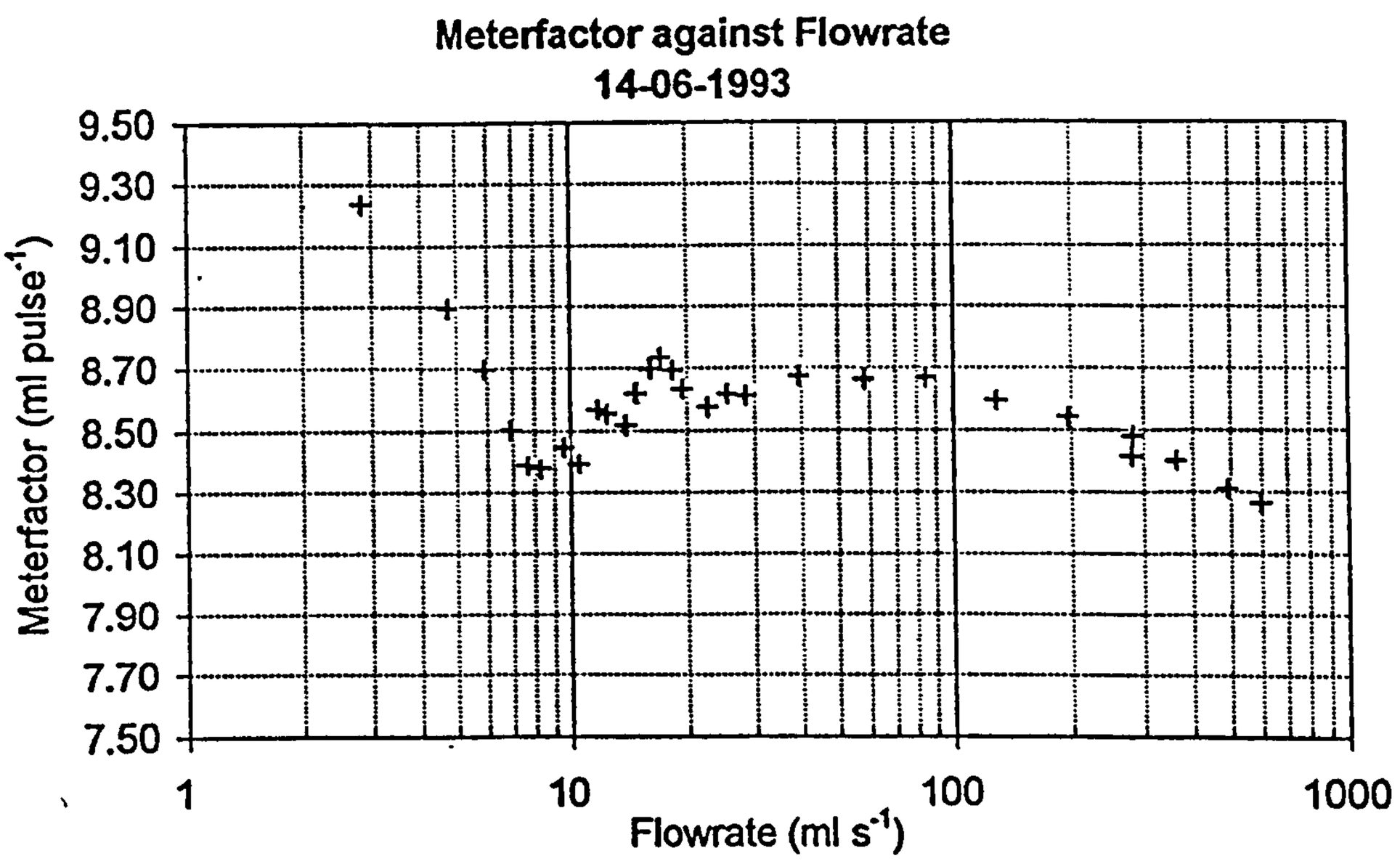

Figure 4.42: Meterfactor Response of Fluidic Oscillator Fitted With 3.2mm Hole Size Conditioner.

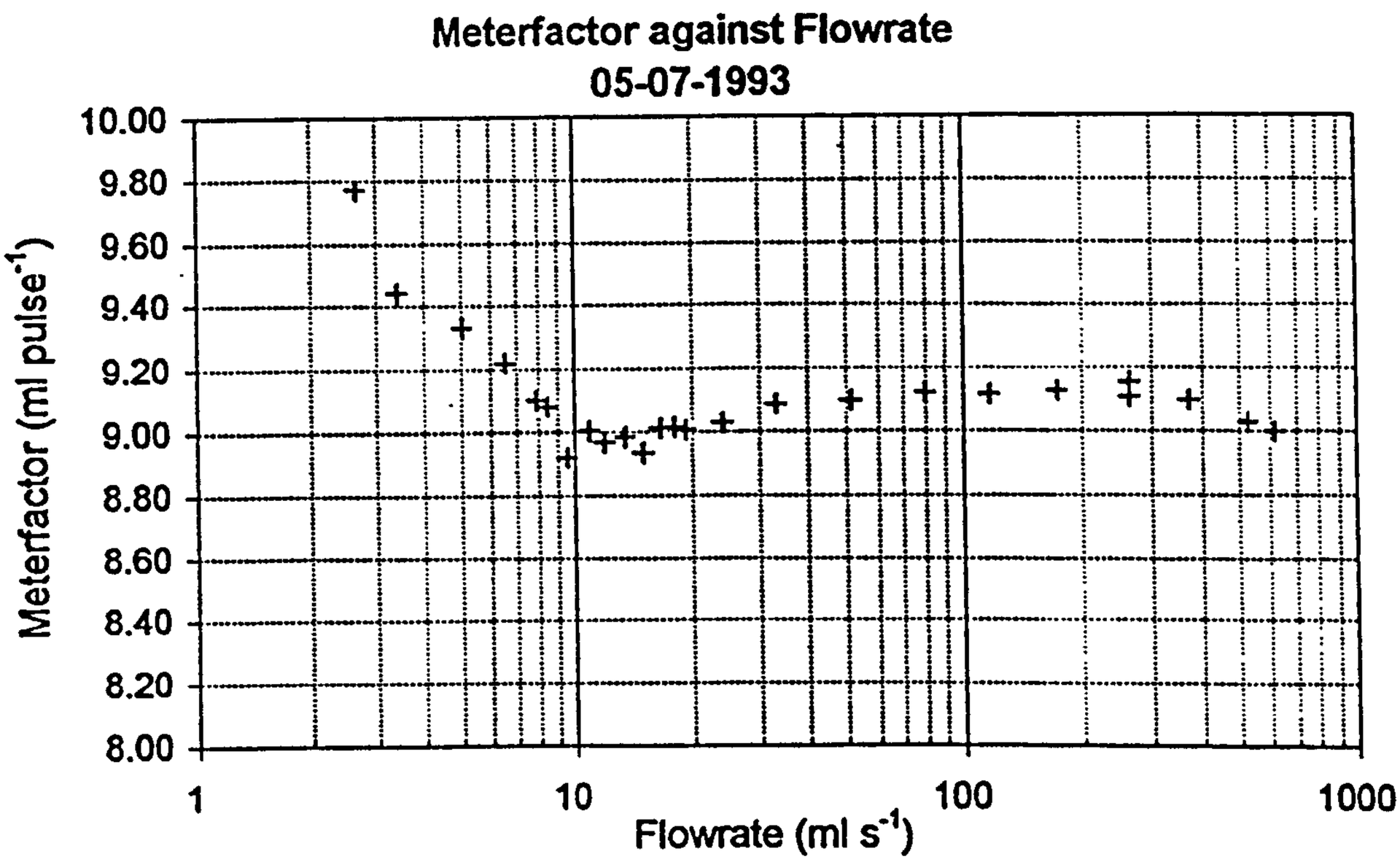

Figure 4.43: Meterfactor Response of Fluidic Oscillator Fitted With Prototype Slot Conditioner.

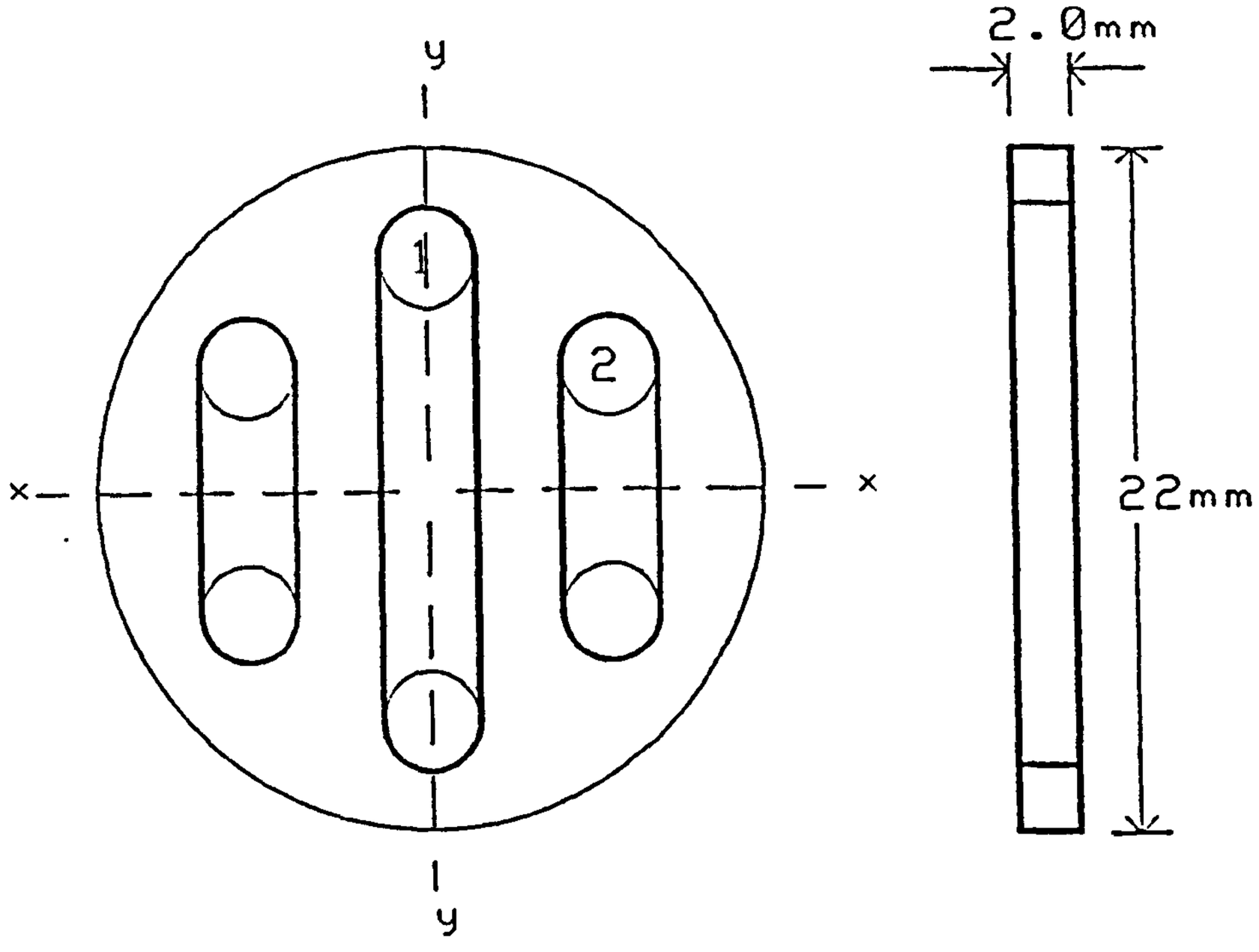

Hole Number	1	2
Coordinate x	0	6
Coordinate y	7.5	4
Diameter	3.2	3.2
Number of Holes	2	2

Figure 4.44: Geometry of SLOT5.DC2 Slot Conditioner Design.

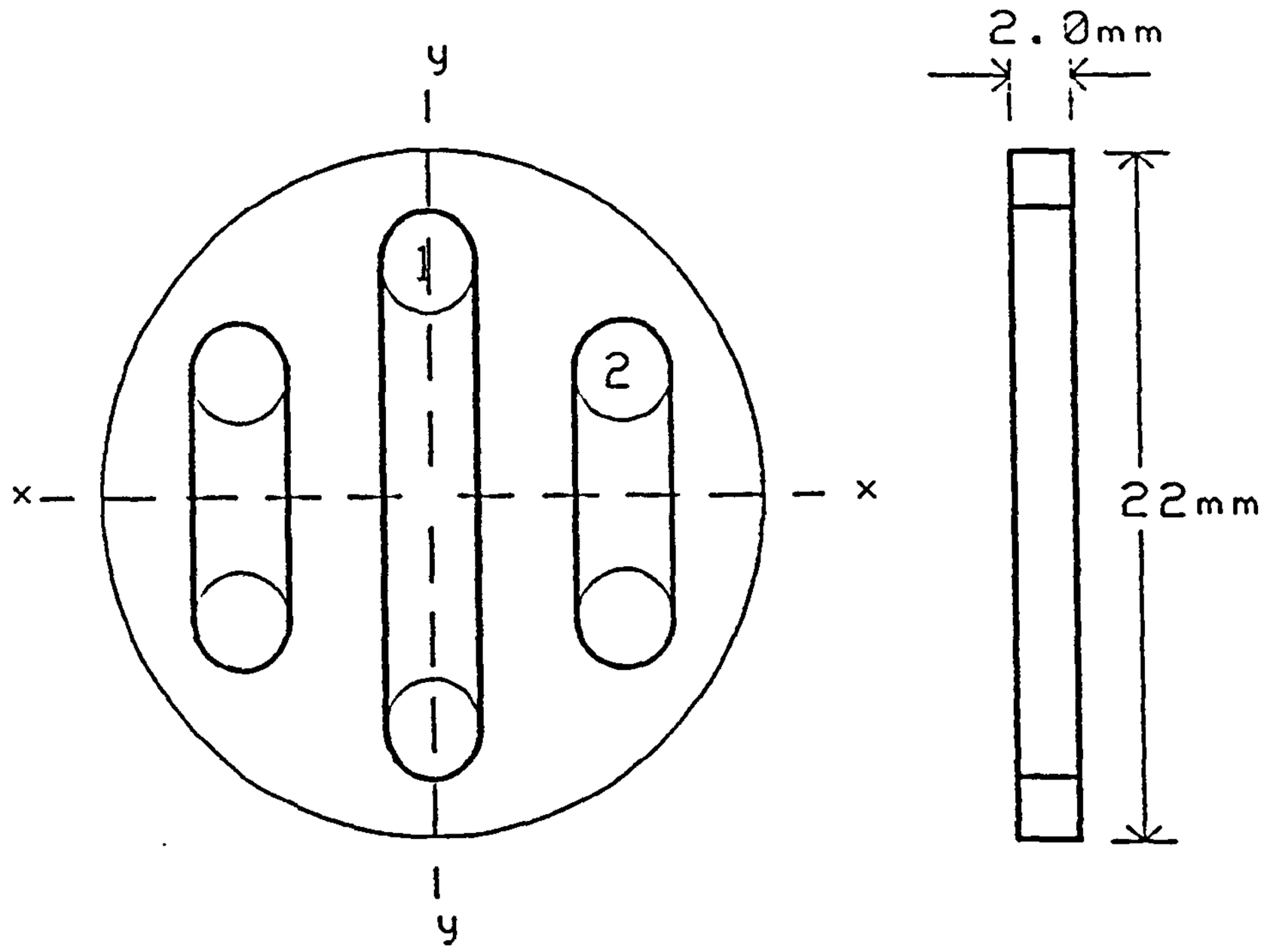

Hole Number	1	2
Coordinate x	0	6.4
Coordinate y	7.5	4
Diameter	3.2	3.2
Number of Holes	2	2

Figure 4.45: Geometry of SLOT6.DC2 Slot Conditioner Design.

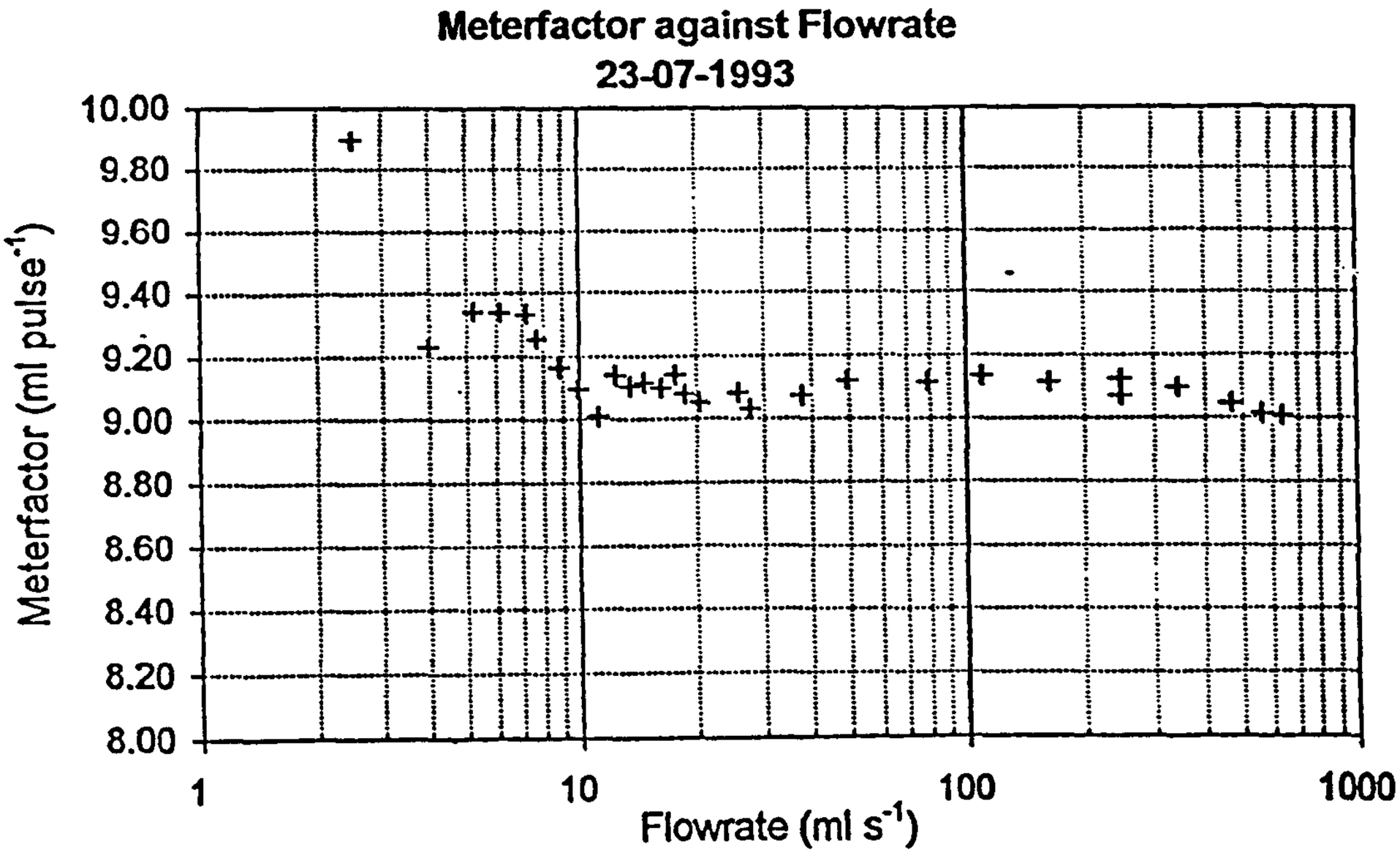

Figure 4.46: Meterfactor Response of Fluidic Oscillator Fitted With Conditioner Disc SLOT5.DC2.

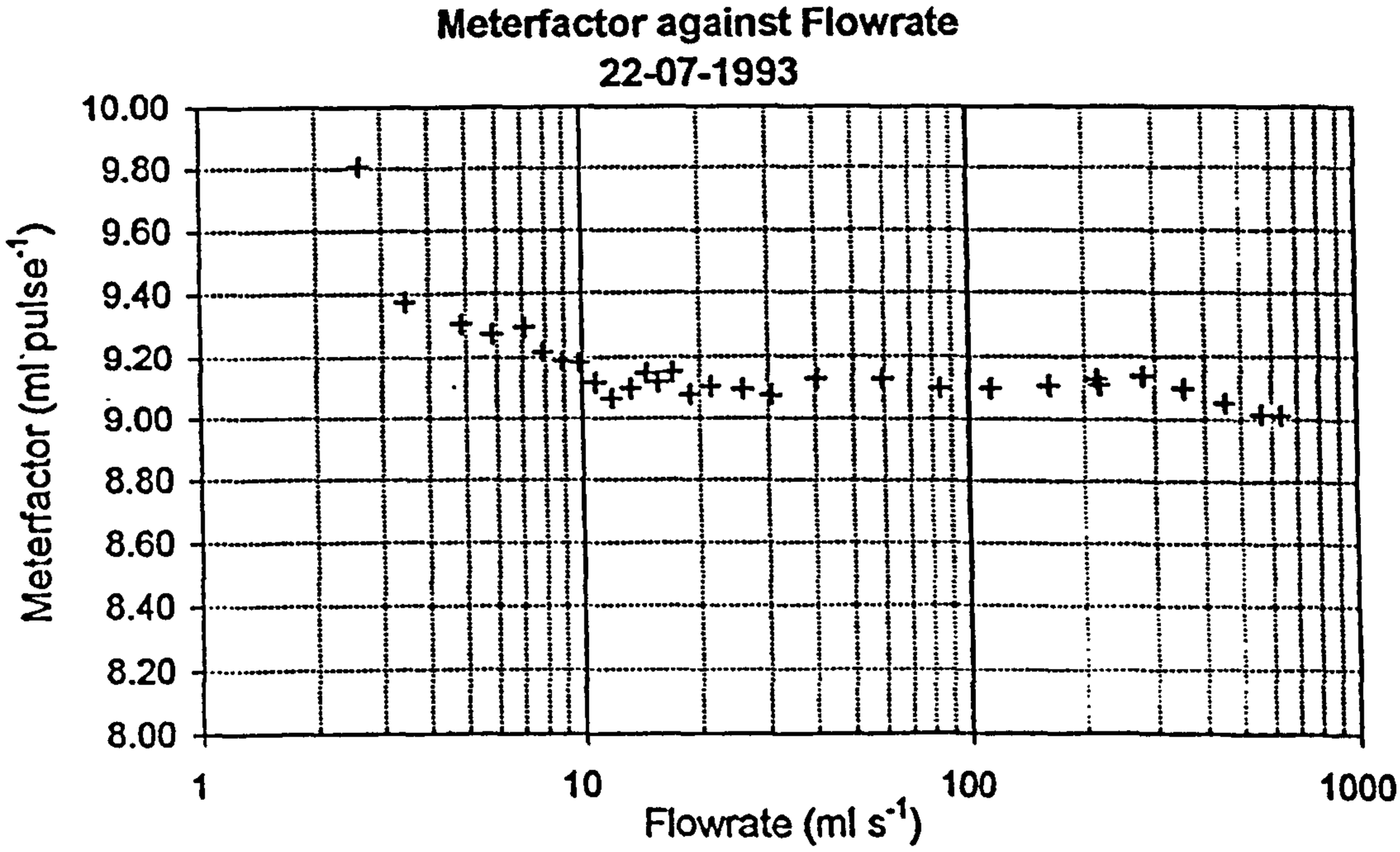

Figure 4.47: Meterfactor Response of Fluidic Oscillator Fitted With Conditioner Disc SLOT6.DC2.

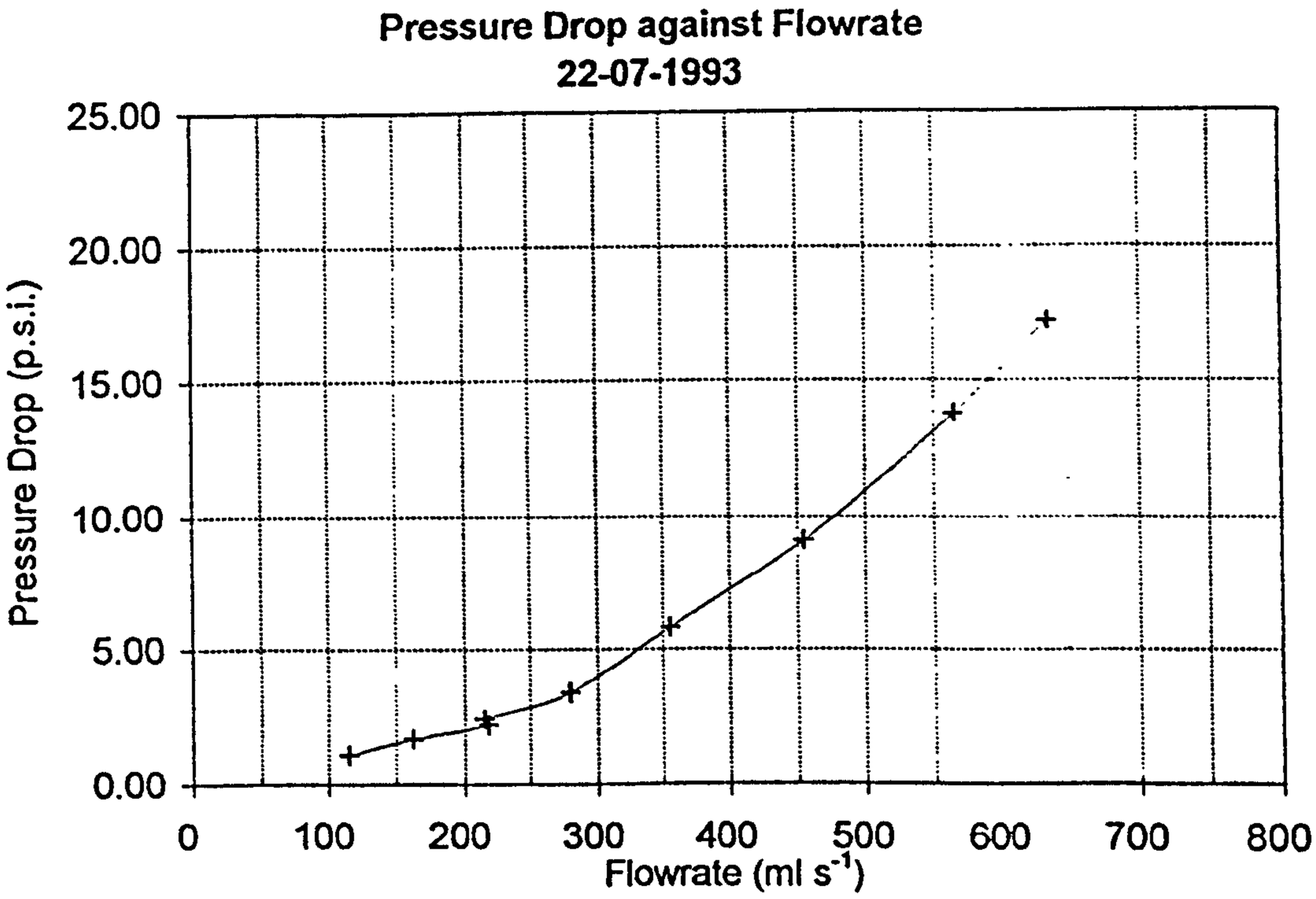

Figure 4.48: Pressure Drop of Fluidic Oscillator Fitted With Conditioner Disc SLOT6.DC2.

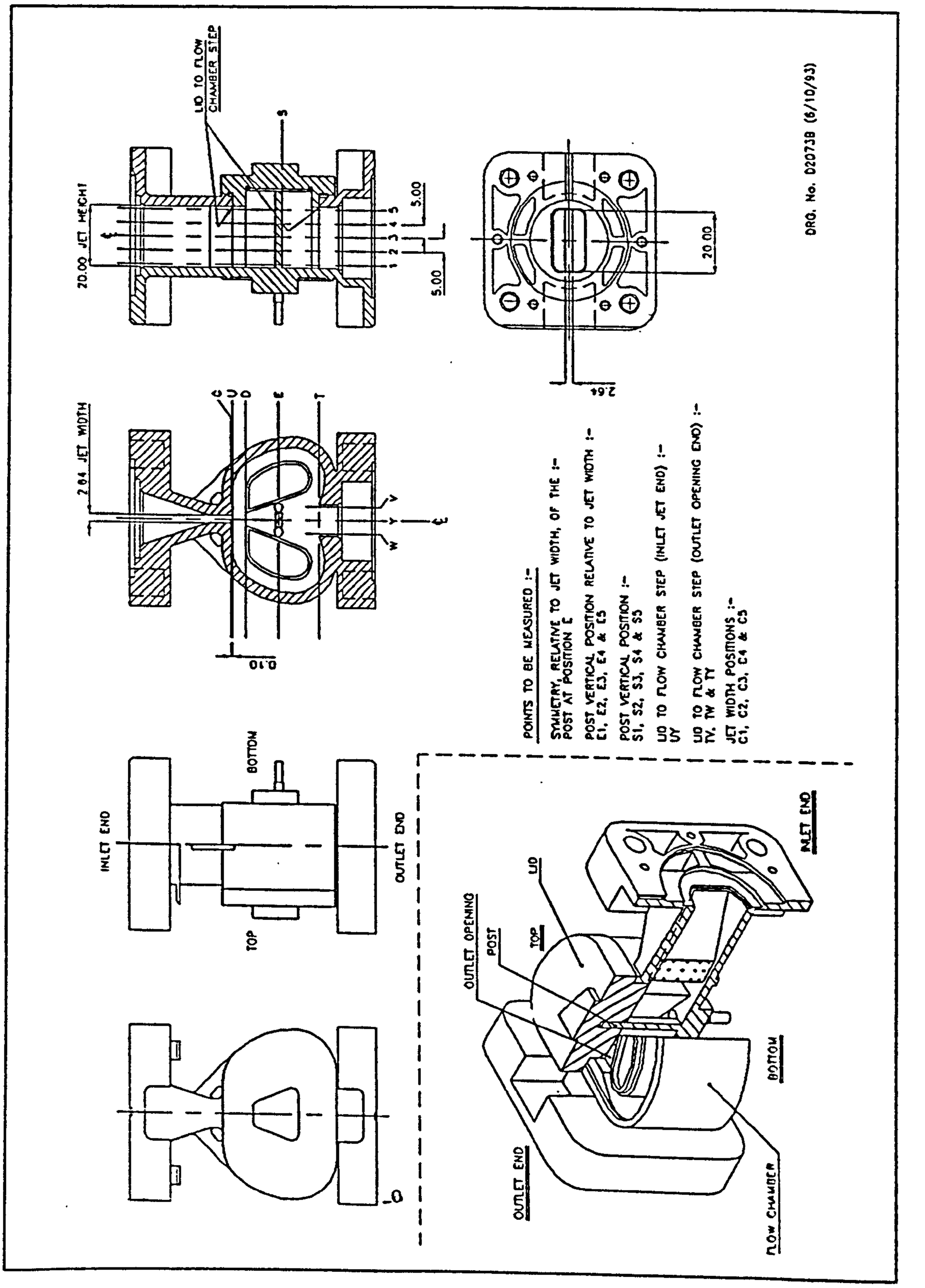

Figure 4.49: Location of Insertion Probe Measurements.

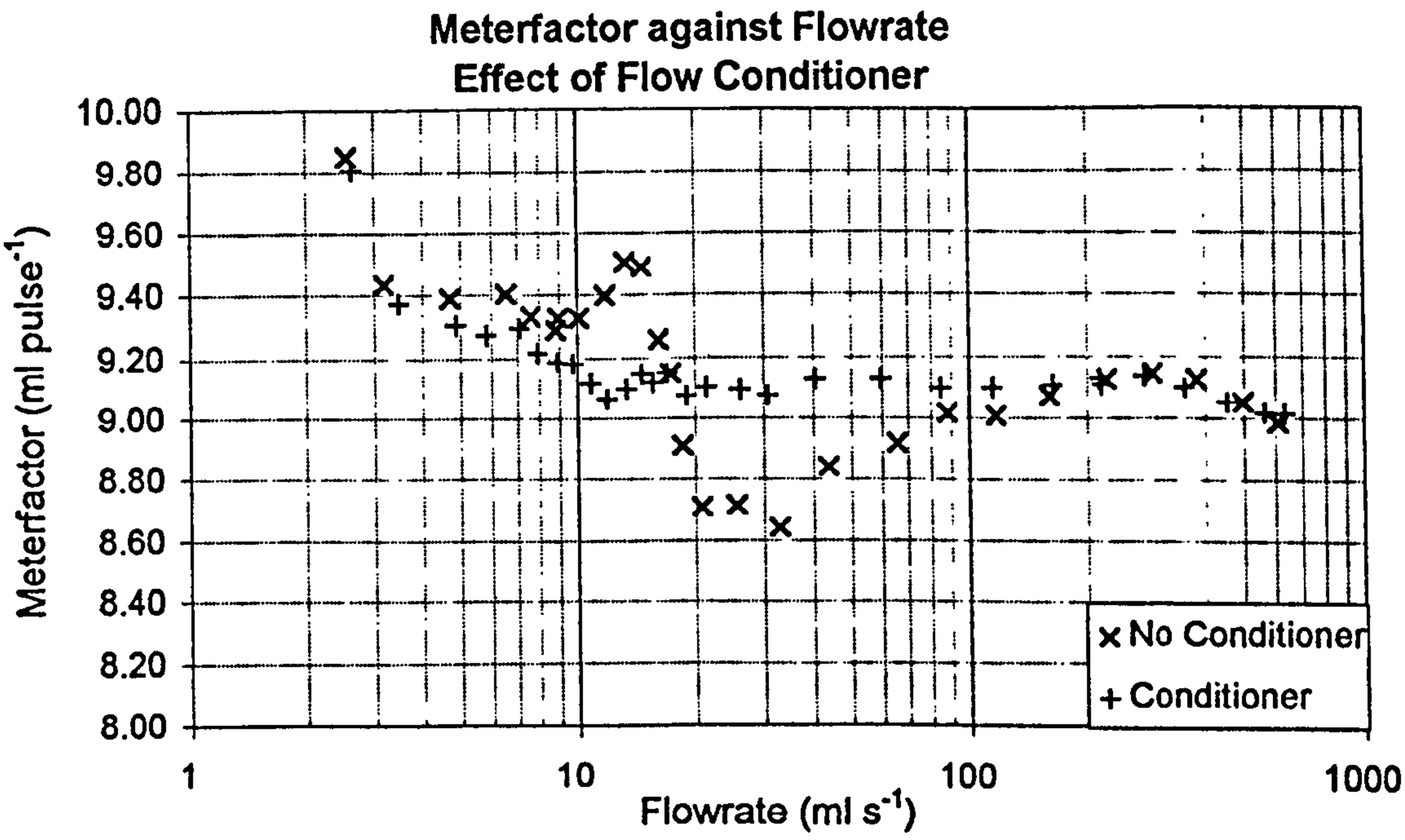

Figure 4.50: Comparison of Meterfactor Response of Fluidic Oscillator With and Without Flow Conditioning.

Chapter 5

Achieving Class D Minimum Flowrate Specification.

5.1 Introduction.

The transitional and minimum flowrate specifications for Class D flowmeters occur at lower flowrates than for Class C meters as shown earlier in Chapter 1. This chapter describes the performance enhancements developed to increase the turndown range of the fluidic oscillator water meter so that the $Q_N1.0$ Class D minimum flowrate specification is achievable using fluidic oscillatory techniques.

At very low Reynolds numbers, for example less than 200, the small fluctuations in the jet flow become too small to be amplified by the coanda effect. This causes the jet to become stable and the fluidic oscillator ceases to operate. At these low Reynolds numbers the jet flow splits evenly around the splitter post and stabilises. The minimum flowrate at which the flowmeter is capable of operation is determined by the minimum Reynolds number at which oscillation is maintained before the jet stabilises. With careful design the fluidic oscillator can sustain oscillation at low Reynolds numbers.

In this chapter modifications to the areas of the fluidic oscillator geometry which are most critical to low Reynolds number performance are investigated and the successful methods of reducing the minimum point of oscillation are described. Also geometry modifications which bring about increased sensitivity and signal strength at low flowrates by generating more complete switching of the jet flow are identified.

The mechanisms which bring about the reduction in minimum Reynolds for oscillation are discussed and the reductions in minimum flowrate that have been achieved are presented.

5.2 Minimum Flow Performance Criteria.

As described in Chapter 1 the minimum flowrate at which the meter continues to operate is determined by the minimum Reynolds number for oscillation given by:

$$Re_{\min} = \frac{vw}{\nu} \tag{1.6}$$

where v is the velocity of the jet, w is the width of the nozzle and ν is the kinematic viscosity.

As flow velocity is proportional to flowrate then:

$$v = \frac{Q}{wh} \Rightarrow Re_{\min} = \frac{Q_{\min}}{\nu h} \tag{1.7}$$

where Q_{min} is the minimum achievable volumetric flowrate and h is the height of the jet.

Including the fluidic oscillator aspect ratio, α defined as the nozzle height to nozzle width, equation (1.7) becomes:

$$Re_{\min} = \frac{Q_{\min}}{\nu \alpha w}$$

$$\Rightarrow w = \frac{Q_{\min}}{Re_{\min} \alpha \nu} \tag{5.1}$$

The size of the meter is given by the nozzle width dimension and is determined using the maximum allowable pressure drop at the maximum flowrate given by:

$$\Delta p_{\max} = E_{\max} \frac{1}{2} \rho \frac{Q_{\max}^2}{\alpha^2 w^4} \tag{1.3}$$

Rearranging equation (1.3) gives the expression for the fluidic oscillator jet width dimension:

$$w = \left(\frac{1}{2}\rho\frac{E_{max}}{\alpha^2}\right)^{1/4} \frac{Q_{max}^{1/2}}{\Delta p_{max}^{1/4}} \tag{1.8}$$

Substituting equation (5.1) for w in equation (1.8) gives:

$$\frac{Q_{min}}{Re_{min}\alpha w} = \left(\frac{1}{2}\ \rho\ \frac{E_{max}}{\alpha^2}\right)^{1/4} \frac{Q_{max}^{1/2}}{\Delta p_{max}^{1/4}}$$

$$\Rightarrow\ Q_{min} = \left(\frac{\rho E_{max}}{2\alpha^2}\right)^{1/4} \frac{Q_{max}^{1/2}}{\Delta p_{max}^{1/4}}\ Re_{min}\ \alpha\ w \tag{5.2}$$

Rearranging equation (5.2) gives the expression for the minimum flowrate achievable:

$$Q_{min} = \left(\frac{\rho Q_{max}^2}{2\Delta p_{max}}\right)^{1/4} \nu\ Re_{min}\ \alpha^{1/2}\ E_{max}^{1/4} \tag{1.9}$$

Q_{max} and Δp_{max} are given in the meter specifications and the density and kinematic viscosity are determined by the fluid. The minimum flowrate for oscillation is therefore set by lowest value of Re_{min} achievable and the product of $\alpha^{1/2}$ and $E_{max}^{1/4}$.

5.3 Minimum Reynolds Number Required.

The required turndown range, Q_{max} to Q_{min}, is 200:1 for a Q_N1.0 Class C domestic water meter and 267:1 for a Class D meter. The Class D minimum flowrate specification is $7.5\times10^{-3}m^3\ hr^{-1}$ or 2.083ml s^{-1} for a Q_N1.0 water meter. The minimum detectable flowrate achieved by the standard production meter fitted with a flow conditioner is 2.2ml s^{-1} at 20°C. This allows a reasonable margin of safety for the Class C flowmeter but is considerably higher than the Class D minimum flow specification.

The Euler number for the fluidic oscillator is nearly constant at high flowrates and $E_{max}^{1/4}$ is close to unity. The aspect ratio of the fluidic oscillator water meter with a nozzle width of 2.64mm and chamber height of 20mm is 7.576. Using equation (1.9) and given that the kinematic viscosity of water is $1.0019\times10^{-6}m^2\ s^{-1}$ and that the density of water is 998.202kg m^{-3} at 20°C then the minimum Reynolds number achieved by the $Q_N1.0$ Class C meter is 127.3.

Using equation (1.9) the minimum Reynolds number within the jet flow required to meet the $Q_N1.0$ Class D minimum flowrate specification is found to be 120.6 at 20°C. At 10°C the kinematic viscosity and density of water is $1.3071\times10^{-6}m^2\ s^{-1}$ and 999.699kg m^{-3} respectively, indicating that a minimum Reynolds number for oscillation of 92.4 is required to achieve the Class D Q_{min} specification at 10°C . These are very low Reynolds numbers for a fluidic oscillator to maintain oscillation but reductions in Re_{min} are possible through design modifications which enhance the low flow performance of the oscillator.

5.3.1 Minimum Flowrate Required At Low Temperatures.

As the temperature of the water is reduced the minimum point of oscillation is increased. Therefore to meet the minimum flowrate specification, Q_{min}, at low temperatures then the meter must be capable of measuring less than Q_{min} at the standard operating temperature. If oscillation is to be maintained at a flowrate of 2.08ml s^{-1} at 10°C then the required minimum point of oscillation at room temperature may be calculated using the minimum Reynolds number for oscillation given in equation (1.7):

$$Re_{\min} = \frac{Q_{RT}}{h\nu_{RT}} = \frac{Q_2}{h\nu_2} \tag{1.7}$$

$$\Rightarrow \quad Q_{RT} = \frac{Q_2 \nu_{RT}}{\nu_2} \tag{5.3}$$

where Q_{RT} is the flowrate at room temperature, ν_{RT} is the kinematic viscosity at room temperature, Q_2 is the flowrate required at temperature T_2, and ν_2 is the kinematic viscosity at T_2.

The kinematic viscosity of water is $1.0019\times10^{-6}m^2\ s^{-1}$ at 20°C and $1.3071\times10^{-6}m^2\ s^{-1}$ at 10°C. If the fluidic oscillator water meter is required to meet the minimum flowrate specification, Q_{min}, at 10°C then, using equation (5.3), the fluidic oscillator must be capable of operation at a flowrate of $1.597ml\ s^{-1}$ at room temperature. This indicates that a reduction in actual minimum flowrate of over 27% is required to achieve the Class D Q_{min} specification at 10°C.

5.4. Experimental Procedure.

To determine the precise minimum point of oscillation and compare oscillation strength, flow visualisation techniques were used rather than signal detection. This allows a true comparison of oscillation strength rather than introducing the variables of electrode surface quality, magnetic field strength and electronics integrity associated with signal strength detection and comparison.

The inlet pipe of the Class D test rig was adapted to incorporate a hypodermic needle which was positioned 30mm upstream of the meter inlet flange and with the needle outlet in the centre of the pipe cross section. The hypodermic needle was gravity fed through a control valve with a tracer dye solution. The tracer dye used was fluorescein

which travels through the meter inlet and into the main flow chamber where it is illuminated with a narrow plane of light. There are no errors caused by the slightly increased flowrate due to the addition of dye solution because the dye flow is fed upstream of the meter and collected along with the outlet flow, therefore it is included within the total flow calculations. For all flow visualisation work the constant head tank was used to set up very steady flow conditions.

The plane of light is produced from a projector beam passing through a narrow slit and is focused horizontally across the centre line of the flow chamber. The illuminated tracer dye provides a visual representation of the flow patterns within the fluidic oscillator through a single narrow section of the meter when observed from above. A video camera was used to record the oscillations at a range of flowrates and frame by frame playback was utilised to determine the strength of oscillation and the minimum point of oscillation. Figure 5.1 shows flow visualisation photographs produced using this technique of an early experimental perspex meter and figure 5.2 shows an oscillation cycle for a transparent polycarbonate moulding of a production meter.

5.5 Areas of Investigation.

To reduce the minimum point of oscillation for the fluidic oscillator water meter the critical design parameters such as the nozzle geometry, diffuser wall design, feedback channels, feedback entrance region, feedback channel exit or jet contact region and the splitter post geometry were experimentally investigated.

The aim of the work was to determine the correct combination of these parameters required for the fluidic oscillator to maintain oscillation at reduced flowrates, where the jet flow is normally stable, and to determine the effects on oscillation frequency and meterfactor response caused by altering the design parameters. Figure 5.3 shows the location of the critical design parameters that were experimentally investigated.

5.6 Modifications To Nozzle Geometry.

To investigate the effects of altering the nozzle geometry the perspex 'building block' $Q_N1.5$ prototype fluidic oscillator was used, as shown in figure 5.4. Although the perspex meter is not a true geometric scaling of the moulded production meter the operating principals are intrinsically similar so that the effects on the performance may be used to predict the effects on performance of the production meter. The perspex meter has advantages in that it is clear and may be polished to allow high quality flow visualisation and because of its block construction it has an inherent ease of modification to individual meter components.

Work carried out to improve the linearity of the Class C fluidic oscillator water meter demonstrated that flow conditioning helped to reduce the minimum flow rate at which oscillations occur. Flow visualisation showed that turbulent eddies were generated downstream of the conditioner which travel through the contraction and cause the jet to become unstable helping to induce oscillation. Below the minimum point of oscillation the turbulent eddies are not sustained through the contraction and the flow is perfectly laminar at the nozzle entrance generating a stable jet flow. For disturbances to be maintained at the exit of the jet then the source of the disturbance may be moved closer to the nozzle exit or within the parallel section of the nozzle. This section describes the geometry modifications made to the fluidic oscillator nozzle to reduce stability within the jet flow.

5.6.1 Standard Perspex Meter.

The perspex meter was initially tested without any modification and then disassembled so that the inlet blocks which form the contraction and nozzle region could be duplicated and modified. Figure 5.5 shows the geometry of the standard inlet nozzle configuration. The standard perspex meter was capable of maintaining oscillation at a minimum flowrate of 2.6ml s^{-1} when fitted with a flow conditioner. The oscillations

ceased at a flowrate of 2.5ml s^{-1} with the jet splitting evenly around the post.

5.6.2 Parallel Nozzle Section.

The fluidic oscillator uses the coanda effect to amplify small disturbances in the jet flow, therefore, a stable jet flow is undesirable when attempting to reduce the minimum point of oscillation. The parallel section of the jet nozzle, following the contraction, of the fluidic oscillator develops a rectangular jet flow which is beneficial for signal detection and profile uniformity but may also allow stabilisation of the flow passing through this section. The inlet of the prototype meter was modified to remove the parallel section of the nozzle thus making the inlet contraction end sharply at the nozzle exit as shown in figure 5.6.

The meter with no parallel section within the nozzle was tested using flow visualisation techniques and was found to oscillate at a minimum flowrate of 2.9ml s^{-1}, which is higher than for the standard meter. This indicates that the formation of rectangular jet flow is beneficial to meter low flow performance.

5.6.3 Asymmetric Nozzles.

At flowrates lower than the minimum point of oscillation the jet flow splits around the splitter post and reforms downstream of the post with two recirculating loops of fluid within the feedback channels. The flow patterns are perfectly symmetrical at each side of the meter. To determine if the introduction of slight asymmetry to the meter nozzle helps to induce an initial switching of the jet, followed by the feedback process from which oscillation results, the nozzle region was machined with a slight radius on the edge of the nozzle exit as shown in figure 5.7.

The meter with the asymmetric nozzle was tested using flow visualisation techniques and the minimum point of oscillation was found to be 2.9 ml s^{-1}. This is higher than for the standard meter and the oscillations were very irregular and unstable, particularly at higher flowrates. As the jet flow becomes stable it is always biased to the side of the flow chamber which has the radius on the nozzle outlet. This indicates that perfect symmetry is desirable for oscillation at low flowrates and is a criteria for production fluidic flowmeters.

5.6.4 Chamfered Nozzle.

The prototype meter was fitted with a pair of matched nozzle blocks, as used singularly in the asymmetric nozzle experiments, to investigate the effect of a chamfered nozzle outlet on the minimum point of oscillation. The chamfered nozzle outlet is shown in figure 5.8.

The meter with the chamfered nozzle exit was tested using flow visualisation techniques and the minimum point of oscillation was found to be 3.1ml s^{-1}. Reverse flow patterns were observed within the feedback channels originating from the chamfered nozzle exit indicating that a sharp square edged nozzle exit is desirable for low flow performance and is a criteria for production flowmeters.

5.6.5 Nozzle Modification Results.

The results of the nozzle modifications to the inlet of the Cranfield Q_N1.5 perspex prototype meter are shown in table 5.1.

Nozzle Modification	Minimum Oscillation ml s^{-1}	Temperature °C	Minimum @ 20 °C ml s^{-1}	% Change in Minimum Oscillation
Standard Nozzle	2.6	19.9	2.6	-
No Parallel Section	2.9	22.3	3.03	+16.41
Asymmetric Nozzle	3.1	22.8	3.32	+27.69
Chamfered Nozzle	3.1	23.2	3.35	+28.84

Table 5.1 Nozzle Modification Results.

5.6.6 Nozzle Modification Conclusions.

All of the modifications made to the geometry of the inlet nozzle of the Cranfield $Q_N1.5$ prototype meter increased the minimum point of oscillation. The experimental work did highlight the geometric areas of the fluidic transducer that are critical to meter low flow performance and demonstrates the optimum desired nozzle geometry. The results indicated that the meter design must be as symmetrical as possible with a sharp square edged exit to the nozzle for enhanced low flow performance. Also the parallel section of the nozzle is required for effective rectangular jet flow formation.

5.7 Vortex Ring Methods.

A technique reported by Yamasaski et al (1991) uses a ring of slots around the fluidic oscillator nozzle to produce a two dimensional jet flow profile. The simple target fluidic oscillators are two dimensional devices, having constant dimensions in the vertical plane, and they suggest that it is therefore desirable to have a two dimensional jet flow profile. This may not be the case for complex fluidic oscillators particularly when using flow conditioning techniques and velocity flow profile to improve meter linearity. The profile of the simple oscillator jet flow tends to become three dimensional due to the drag caused by boundary layers along the top and base of the meter. The concept they describe uses a ring of slots to form a stationary vortex of constant angular velocity around the nozzle outlet. As faster moving fluid passes through the nozzle it is decelerated by the vortex and gives energy to the vortex. As slower moving fluid passes through the nozzle the vortex provides energy to the fluid which is accelerated thus equalising the velocity profile of the jet flow.

They carried out tests on two simple target meters as shown in figure 1.24 with both a single slot and double slot configuration. The length of the inlet nozzle of the simple target meter used is ten times the width. The slot machined into the nozzle outlet of the oscillator in which the stationary vortex is developed is shown in figure 1.25. Their results indicate that a flatter jet profile is produced using vortex rings at the nozzle outlet and that reductions in minimum flowrate of almost 40% are achieved for the simple target meter.

To investigate the effect of vortex rings on the fluidic oscillator water meter slot configurations were machined into the parallel section of the inlet nozzle of the Cranfield $Q_N1.5$ perspex prototype design. The effects on jet flow velocity profile caused by slots in the inlet nozzle and nozzle aspect ratio were also investigated by James (1994) using Computational Fluid Dynamics (CFD) techniques.

5.7.1 Vortex Slot configurations.

A square duct of 1mm × 1mm was machined vertically into each of the sidewalls of the parallel nozzle section of the perspex meter. Figure 5.9 shows the configuration of the nozzle with the slot located at 3mm from the nozzle exit. Three variations were constructed with the centre of the slot located at 1mm, 3mm, and 5mm from the nozzle exit respectively.

A similar single slot configuration was assembled using 2mm × 2mm vertical slots at each side of the parallel section of the nozzle, as shown in figure 5.10. The centre of the slots were located at 3mm from the nozzle exit.

A double slot configuration was constructed with a pair of 1mm × 1mm vertical slots at each side of the parallel section of the nozzle. The configuration of the double slot nozzle is shown in figure 5.11. The centre of the slots were located at 3mm and 5mm from the nozzle exit.

A complete ring of slots was developed with a 1mm × 1mm slot surrounding the outlet nozzle at 3mm from the nozzle exit. The geometry of the sidewalls of the nozzle were the same as for figure 5.9, however both the lid and base of the meter were machined with a 1mm × 1mm slot also to complete the vortex ring.

A nozzle configuration was assembled using standard sidewalls but with slots in the top and base of the inlet nozzle only. The slots were located at 3mm from the jet exit.

5.7.2 Vortex Slot Configuration Results.

Each of the nozzle configurations described above was experimentally investigated using flow visualisation techniques to determine the minimum point of oscillation. The results of the vortex slot modifications to the inlet nozzle of the Cranfield $Q_N1.5$ perspex

prototype meter are shown in table 5.2.

Nozzle Modification	Minimum Oscillation ml s^{-1}	Temperature °C	Minimum @ 20°C ml s^{-1}	% Change in Minimum Oscillation
Standard	2.6	19.9	2.6	-
Side Slot @ 1mm	2.6	20.2	2.61	+0.49
Side Slot @ 3mm	2.4	21.2	2.47	-5.0
Side Slot @ 5mm	2.5	21.9	2.62	+0.77
2mm Side Slot	2.5	21.0	2.56	-1.49
Double Slot @ 5mm & 3mm	2.6	20.8	2.65	+1.82
Complete Vortex Ring @ 3mm	2.5	22.0	2.62	+0.77
Top and Base Slot @ 3mm	2.6	20.8	2.65	+1.82

Table 5.2 Vortex Slot Configuration Results.

The single side slot positioned at 3mm from the nozzle exit produced an actual reduction in minimum flowrate of 5% this is equivalent to the reduction that is achieved through the addition of a flow conditioner to the meter inlet.

5.7.3 Vortex Ring Experimental Conclusions.

Two of the slot modifications tested demonstrate improvements in low flow performance compared to the open inlet to the standard nozzle, however, the results did not compare

with the improvements of up to 40% as reported by Yamasaki et al (1991). The modification which showed the greatest improvement in low flow performance was the single vertical slot located at 3mm from the nozzle outlet. The performance of the single slot modification was not greater than that of adding a flow conditioner to the open inlet of the standard nozzle. Using a flow conditioner as well as either a vortex ring or side slot modified nozzle made no further improvement in performance to the modified nozzle alone.

The inlet nozzle of the target meters tested by Yamasaki et al (1991) differ to the inlet of the Cranfield nozzle in that the length of the inlet nozzle of the simple target meter used is ten times the width, ie. a length to width ratio of ten, compared to 2.87 for the Cranfield nozzle. The relatively long parallel section of nozzle, used on the simple target meters, is likely to produce a parabolic flow profile at the nozzle outlet. This is due to the sustained drag effects of the walls on the flow profile as the flow travels through the parallel section of the nozzle.

5.7.4 Computational Fluid Dynamics Nozzle Investigations.

James (1994) used a finite element numerical package to simulate water flow through several nozzle configurations to determine the effects on velocity profile at the nozzle outlet after adding vortex ring modifications to the nozzle. For all simulations he used a constant Reynolds number, defined by nozzle outlet velocity, channel width and kinematic viscosity. The pipe inlet velocity was set at 0.0025m s^{-1} to give a Reynolds number of approximately 50 which is in the laminar flow regime.

A three dimensional square approximation of the Cranfield fluidic oscillator inlet nozzle was used to investigate the flow through the standard Cranfield nozzle. The inlet pipe is rectangular of dimensions 20mm × 20mm and is 20mm long to allow for some development of pipe flow. The ratio of the parallel section of the Cranfield nozzle, length to width, is 7.58 with a jet width of 2.64mm. As the system is symmetrical it was only

necessary to model half of the nozzle. The numerical mesh used to model the system is shown in figure 5.12.a.

The square approximation of the Cranfield inlet model was then enhanced to incorporate a step at the side of the parallel section to simulate a vortex slot in the nozzle. The rectangular slot dimensions are 2.64mm × 2.64mm and is 20mm high and positioned halfway along the parallel section of the nozzle.

A complete vortex ring slot was then added to the model of the square approximation of the standard Cranfield inlet model. The slot dimensions are 2.64mm × 2.64mm and is positioned halfway along the parallel section of the nozzle. Figure 5.12.b shows the numerical mesh used to model the nozzle with a vortex ring.

The target meters used by Yamasaki et al (1991) to test their vortex ring theory had a much longer parallel nozzle section with a length to width ratio of approximately 10. To investigate the flow through a nozzle with a larger length to width ratio James (1994) extended the length of the parallel section of the square approximation to the Cranfield inlet model by 20mm. The nozzle width was 2.64mm. The extended nozzle configuration was modelled without any modifications, with the addition of a single vertical slot in the sides of the parallel section, and a complete vortex ring. The dimensions of the single slot and vortex ring slot were 2.64mm × 2.64mm and were located at 2.18mm from the nozzle outlet, as in the standard Cranfield nozzle tests.

James (1994) displayed the results of the three dimensional simulations in three forms, velocity vector plots, pressure contour plots and vorticity contour plots. To aid the comparison of velocity profiles he used a flatness function to quantify the flatness of velocity profiles. Figure 5.13 shows a close-up of velocity vector plot of the standard nozzle with a vortex ring and figure 5.14 shows an extreme close-up of the slot where the length of the arrows have been multiplied by a factor of 10.

5.7.5 Vortex Ring Conclusions.

James (1994) concluded that the flow profile at the outlet of the standard Cranfield nozzle is significantly flatter than the flow profile at the outlet of the extended nozzle investigated by Yamasaki et al (1991). Using an extended nozzle allows the boundary layers of the flow to develop along the walls producing a fully parabolic profile at the nozzle exit for the low flowrate tested. The short parallel section of the Cranfield nozzle does not allow the boundary layers to develop fully.

He was able to show that the use of a vortex ring surrounding the nozzle outlet does have some effect on jet flow profile. Flatter profiles were produced for each of the three nozzle configurations modelled. The magnitude of the velocity within the slot is very small compared to the main flow. For the standard Cranfield nozzle James (1994) predicted velocity of the flow within the slot to be 6% of the velocity in the centre of the nozzle. This compared well to the flatness change of 7% due to the inclusion of the slot.

The CFD modelling and experimental work demonstrate improvements in performance with the addition of vortex rings or slots within the parallel section of the inlet nozzle of the Cranfield fluidic oscillator. The improvements are only comparable, however, to the addition of a flow conditioner upstream of the inlet contraction and no further improvements in performance are achieved by combining vortex ring nozzle modifications and a flow conditioner. The pressure drop of a conditioner is higher than the pressure drop generated by a vortex ring but the flow conditioner is capable of providing a much more linear meterfactor response, as described in Chapter 4. The results of CFD modelling and experimental work indicate that Yamasaki et al (1991) could significantly flatten the parabolic profile of their jet flow by reducing the relatively long parallel section of the nozzle of the simple target meters they investigated.

5.8. Modifications To The Feedback Channels.

The oscillation mechanism of the fluidic oscillator flowmeter is based on some of the main flow being entrained within the feedback channel, travelling through the feedback channel and impinging on the jet at an incidence normal to the jet flow. The action of the feedback flow impinging on the jet initiates the next switching action and is therefore critical to both frequency of oscillation and the minimum point of oscillation. Increasing the amount of feedback flow by reducing the resistance to feedback and encouraging the entrainment of feedback flow stimulates switching of the jet at lower flowrates and reduces the minimum point of oscillation.

The critical areas of the feedback paths which were experimentally investigated to determine their effect on minimum point of oscillation and oscillation frequency were:

.The width of the feedback channels.
.The entrance to the feedback channels, or entrainment region.
.The feedback exit, or jet contact region.

5.8.1 Width of Feedback Channels.

Flow visualisation experiments were carried out on a transparent polycarbonate moulding of a production Q_N1.0 meter to determine the effects of modification to the feedback channels. The production water meters are manufactured using acetal which is opaque, and therefore of no use for flow visualisation work. Also it does not readily bond to other materials which prevents the construction and reforming of internal components using extra material bonded to the face of the structures.

The magnet pockets within the diffuser walls of the polycarbonate meter were back-filled with methyl methacrylate. This was a gradual process, taking over three days, as the material was added in stages to ensure complete curing of the methyl methacrylate and

preventing bubbles and weak spots from forming within the material. Once the diffuser wall pockets were completely cured the solid diffuser wall section could then be machined along the rear face of the diffuser wall to reduce the width of the diffuser wall section and effectively increase the volume of the feedback channels.

The lid of the flow chamber was machined to remove the material that would normally be displaced during the lid weld process and carefully fitted to the flow chamber to give an internal height of 20mm. Also machined inserts were fitted within the lid to replace the space previously occupied by material from the rear of the diffuser wall to provide a smooth flat surface on the inside face of the flow chamber lid. The polycarbonate transducer moulding is shown in figure 5.15.

Early experimental work carried out to investigate the effect of diffuser wall width using the polycarbonate moulded meter involved four successive modifications to the feedback channels of the meter. Initially a flow visualisation experiment was carried out using the assembled polycarbonate meter without any feedback modifications. The shrinkage of the polycarbonate material is different to that of the acetal from which the production meter is moulded. This causes slight differences to the geometry of the polycarbonate transducer which alter the minimum point of oscillation. The slight differences in transducer geometry still allow comparisons of meter performance to be made however, following critical geometry modifications.

After testing the standard polycarbonate meter the rear face of the diffuser wall sections of the meter were machined with a straight cut parallel to the diffuser wall as shown in figure 5.16. Machining of the rear face is possible because the cavity is back filled with methyl methacrylate as described earlier. Modification 1 increased the width of the feedback channels by 3mm at its widest point.

Modification 2 involved a second machined cut which was made parallel to the centre line of the transducer originating from half way along the machined cut described above,

which forms the rear face of the diffuser wall. The resulting diffuser wall geometry is shown in figure 5.17.

The diffuser wall section was then reduced in width by a machined cut parallel to the diffuser wall resulting in a width of 5mm across the whole section. A second machined cut was made at the downstream edge of the diffuser wall and at right angles to the wall face to reduce the wall in length. This effectively enlarged the feedback entrainment region by 2mm. The diffuser wall modification 3 is shown in figure 5.18.

Modification 4 is a further progression of increased feedback entrainment where the diffuser wall length was reduced in length by a further 3mm. The diffuser wall entrainment region is enlarged by 5mm compared to the standard meter geometry as shown in figure 5.19.

The modified polycarbonate transducers were tested using flow visualisation techniques and three further variations of modification 3, which gave the greatest reduction in minimum flowrate for oscillation, were constructed each with a feedback entrainment region enlarged by 2mm but increasing diffuser wall widths of 4mm, 6mm, and 7mm wide.

5.8.2 Diffuser Wall Width Results.

The results of the initial feedback channel investigations are shown in table 5.3 and the results of the subsequent diffuser wall section width investigations are presented in table 5.4. Figure 5.20 shows how the minimum point of oscillation varies with the width of the diffuser wall section.

Transducer Modification	Minimum Oscillation ml s^{-1}	Temperature °C	Minimum @ 20°C ml s^{-1}	% Change in Minimum Oscillation
Standard Polycarbonate	2.3	22.6	2.45	
Modification 1	1.98	19.7	1.97	-19.6
Modification 2	2.08	19.2	2.06	-15.9
Modification 3	1.9	20.0	1.9	-22.4
Modification 4	1.98	19.8	1.98	-19.18

Table 5.3 Feedback Channel Modification Results.

Diffuser Wall Section Width	Minimum Oscillation ml s-1	Temperature °C	Minimum @ 20°C ml s-1	% Change in Minimum Oscillation
4mm Wall	1.88	19.8	1.87	-23.7
5mm Wall	1.90	20.0	1.90	-22.4
6mm Wall	2.01	20.6	1.98	-19.2
7mm Wall	2.19	21.1	2.13	-13.1

Table 5.4 Diffuser Wall Section Width Results.

The modified meter with a 4mm wide diffuser wall section and a feedback entrainment region enlarged by 2mm, gave a reduction in minimum point of oscillation of over 23% compared to the standard polycarbonate transducer.

5.8.3 Conclusions of Feedback Channel Width Investigations.

Increasing the amount of feedback flow by increasing the volume of the feedback channels reduces the resistance to feedback flow. Increasing the size of the feedback entrainment region, or the inlet to the feedback channel, also encourages flow through the feedback channels which induces switching of the jet at lower flowrates and therefore reduces the minimum point of oscillation. The minimum flowrate for oscillation produced by the modified polycarbonate transducer with a 4mm wide diffuser wall section is 1.87ml s^{-1} at room temperature. This indicates that the Q_N1.0 Class D minimum flowrate specification is achievable at temperatures above 15°C. The minimum Reynolds number for oscillation achieved for the modified transducer is 108.24.

Figure 5.20 shows that the improvements in the minimum point of oscillation with reducing diffuser wall section width becomes less significant once the section width is less than 5mm and that there would be little benefit in reducing the wall section width below 4mm. The width of the diffuser wall section is critical because it determines the volume of magnetic material that can be installed within the diffuser wall cavity. The magnetic field strength of the Class D meter needs to be as high as possible to compensate for the lower jet velocities that occur at low flowrates. A diffuser wall section of 5mm would seem to be a practical width as this would allow a 3mm wide magnet to be inserted within the wall cavity, assuming a material thickness of 1mm around the diffuser section of the transducer.

Increasing the size of the feedback entrainment region helps to encourage flow through the feedback channels but the performance diminishes if the increments made are too large. The modifications to the width of the feedback channels of the fluidic oscillator have resulted in substantial improvements in low flow performance but the Class D Q_{min} specification has not been achieved at 10°C.

5.8.4 Jet Contact Region.

During the oscillation cycle some of the main flow through the meter is entrained within the feedback channel. It travels through the channel and impinges on the jet creating a separation bubble between the jet and the diffuser wall. The separation bubble increases in size as the jet moves away from the diffuser wall until the bubble bursts as the jet switches to the opposite diffuser wall. The process is repeated through the other feedback channel and a sustained oscillation develops. At flowrates below the minimum point of oscillation the jet flow splits evenly around the target post with two recirculating loops of fluid within the feedback channels. The recirculating loops do not generate a separation bubble and are driven by the effects of viscous drag from the close proximity of the passing jet flow. Modifications to the feedback exit, or jet contact region, of the fluidic oscillator were investigated to determine if the transducer geometry could be optimised to induce the build up of a separation bubble and initiate jet switching at flowrates below the normal minimum point of oscillation.

To investigate the effects of feedback flow contact with jet flow, perspex inserts were constructed and fitted to the nozzle outlet of a modified transducer as shown in figure 5.21. The concept is to increase the velocity of the feedback flow at the exit of the feedback channel and to target the feedback flow directly at the base of the jet to cause earlier build up of the separation bubble. The inserts measured 2mm × 5mm and were 20mm in height which effectively extended the length of the rectangular nozzle section by 2mm and accelerated the feedback flow onto a jet contact region of 3mm. The jet flow contact region was previously equivalent to the full width of the feedback channel, 5mm, before the addition of the inserts. The diffuser wall section of the transducer was 5mm in width with the feedback entrainment region enlarged by 2mm.

The meter was tested for minimum point of oscillation using flow visualisation techniques and the minimum point of oscillation was 2.8ml s^{-1}. This is a significant increase compared to the meter with a 5mm diffuser wall and without inserts fitted to the feedback exit region. The increase in minimum flowrate is due to the inserts restricting the flow

through the feedback channels rather than usefully targeting the point of contact with the jet flow. This implies that an increased jet contact region is beneficial to low flow performance.

To investigate the effects of reducing the resistance to feedback flow by enlarging the feedback exit, or jet contact region, of modified polycarbonate fluidic oscillators three meters were constructed with progressively enlarged feedback channel exits. The meters each had a diffuser wall section of width 5mm and had the feedback entrainment region enlarged by 2mm. The feedback exit or jet contact region of the fluidic oscillators was increased by 1mm, 2mm and 3mm respectively as shown in figure 5.22.

The three modified polycarbonate meters were constructed with a single neodymium magnet mounted within each diffuser wall so that the electronically detectable flowrate, using the Cranfield electronics development board, could be investigated. The minimum point of oscillation was also determined using flow visualisation techniques. To visualise the flow patterns within the transducers it was necessary to project the light beam at an angle of incidence of 45° to the meter to prevent the formation of shadows or reflections from the magnets mounted within the diffuser walls.

5.8.5 Results of Jet Contact Region Investigations.

Jet Contact Region	Minimum Oscillation ml s^{-1}	Temperature °C	Minimum @ 20°C ml s^{-1}	Electronically Detectable Oscillation	% Change in Minimum Oscillation
Standard Polycarbonate	2.30	22.6	2.45		
5mm Wall Standard J.C.	1.90	20.0	1.90		-22.4
5mm Wall With Inserts	2.80	19.9	2.90		+14.3
1mm Enlarged Jet Contact	1.65	22.0	1.73	1.86	-29.4
2mm Enlarged Jet Contact	1.63	20.9	1.66	1.85	-32.2
3mm Enlarged Jet Contact	1.63	20.9	1.66	1.72	-32.2

Table 5.5 Results of Jet Contact Region Investigations.

5.8.6 Jet Contact Region Conclusions.

Enlarging the jet contact region of the feedback channel by 1mm reduces the minimum point of oscillation for a modified transducer. Further enlargements of the jet contact region do not give significant further reductions in minimum flowrate but the oscillations become stronger at equivalent flowrates with the jet flow switching more completely from side to side of the post. As the signal strength at low flowrates is proportional to jet velocity then there is a reduction in signal strength at the low flowrates required for the Class D meter specifications. When this is combined with

partial switching of the jet flow then signal detection is as great a problem as maintaining oscillation at low flowrates. Modifications which improve the strength of the oscillations at low flowrates, thereby increasing the signal strength and sensitivity of the sensor, are as important as modifications which reduce the minimum point of oscillation, however the two are inherently coupled.

5.9 Acetal Transducer Modification.

The prototype moulded polycarbonate meters differ from the production meters in that the post moulding shrinkage effects are greater for polycarbonate meters than for acetal meters. This causes slight differences in the final shape of the flow chamber which result in a worse low flow performance for the polycarbonate meter. The minimum detectable oscillation for an unmodified Q_N1.0 Class C acetal meter fitted with a flow conditioner is 2.2ml s^{-1} compared to 2.45ml s^{-1} for a polycarbonate meter. This indicates that the minimum point of oscillation for acetal versions of the meters with modified diffuser wall widths and jet contact regions would be lower than for the polycarbonate meters tested.

Acetal does not bond readily to methyl methacrylate, or any other similar material, preventing modification through back filling of the magnet pockets of the diffuser wall section and removing material through machined cuts of the remaining solid section. To investigate geometry modifications to acetal meters the diffuser wall sections were removed completely from the flow chamber leaving a precise footprint hole through the base of the meter. Diffuser wall inserts were then accurately machined from solid perspex block and fitted within the acetal flow chamber. The diffuser wall sections were fitted with neodymium magnets which were insulated from the water using methyl methacrylate which was then machine polished to give a flat finish. The base of the inserts were manufactured with very high precision because these were used to accurately position the diffuser walls when mounted within the footprint holes in the base of the flow chamber.

The lid of the meter was machined so as to seat in the same position as though following the lid weld operation and sealed and held in place with a clamping arrangement. The modified acetal chamber and machined perspex diffuser inserts are shown in figure 5.23. The cut away acetal meter allows for further investigations into transducer geometry modifications without having to mould and machine a complete meter but simply manufacture and install a new pair of diffuser inserts. Using only one flow chamber but several component inserts gives a more accurate comparison between minimum point of oscillation detectable because the same inlet contraction, nozzle and non-return valve are used in each experiment. Also because the same pair of electrodes are used in every investigation the variation in electrode passivation and surface finish is removed allowing more accurate comparisons between signal strength and minimum point of oscillation to be made.

The optimum diffuser wall configuration determined using the polycarbonate meter flow visualisation experiments was manufactured in the form of perspex inserts and inserted within the cut away acetal meter. The configuration of the diffuser wall inserts was as follows:

Diffuser wall section width:	5mm
Feedback entrainment region:	Enlarged by 2mm
Jet contact region:	Enlarged by 3mm

5.9.1 Modified Acetal Meter Results.

Table 5.6 shows the relative strength of the electronic oscillation signal and the minimum flowrate for oscillation of the acetal meter with the diffuser wall configuration described above.

Mass Water (g)	Diversion Time (s)	Temp (°C)	Rate (ml s^{-1})	Rate @ 20°C	Oscillation Strength
882.1	521.5366	18.9	1.691	1.645	Weak
1804.3	1073.9496	18.8	1.680	1.630	Weak
2829.3	1690.1773	18.7	1.674	1.620	Very Weak

Table 5.6 Minimum Oscillation of Acetal Meter With Modified Diffuser Inserts.

5.9.2 Conclusions of Feedback Channel Modifications.

Significant reductions in flowrate can be achieved by reducing the resistance to feedback flow through modification to the geometry of the diffuser wall sections within the flow chamber. An optimum diffuser wall width would be 5mm because further reductions in width do not produce significant reductions in minimum flowrate but this width allows a reasonable volume of magnetic material to be inserted within the diffuser wall. Increasing the width of the feedback entrainment region improves the minimum point of oscillation but large increases have a detrimental effect on low flow performance. Increasing the feedback exit or jet contact region reduces the minimum point of oscillation. Increasing the jet contact region from 2mm to 3mm appears to have little effect on the minimum flowrate achievable but improves the electronic signal strength at low flowrates by producing more complete switching of the jet flow rather than partial switching around the splitter post.

The electronically detectable minimum point of oscillation achieved for the modified acetal meter is 1.620ml s^{-1} at room temperature. This will provide the Q_N1.0 Class D minimum flowrate specification at temperatures above 14°C. The lowest Re_{min} value achieved was 93.8 which is a 26.4% improvement upon the production Class C fluidic oscillator water meter. Further reductions in Re_{min} were required to achieve the Class D

specifications at temperatures down to 10°C, this led to investigations into the geometry of the fluidic oscillator splitter post.

5.10 Modification To The Splitter Post.

As well as the inlet nozzle and the diffuser wall sections another critical component of the fluidic oscillator transducer design is the splitter post. The splitter post prevents the jet from simply passing through the centre line of the meter and provides a switching point for the jet to pass. Once the jet has passed to one side of the post it is drawn towards the diffuser wall on that side of the post, through the action of the coanda effect, and the feedback process maintains oscillation. At low flowrates the jet starts to become stable and oscillates around the splitter post only, without attaching to the diffuser walls. At lower flowrates the jet flow only partially switches from side to side of the post until the flowrate is so low that the jet flow splits evenly around the post and oscillation ceases.

The previous work has shown that the geometry of the feedback channels has a significant effect on minimum point of oscillation achievable but at low flowrates the oscillation is only switching from side to side of the splitter post. This indicates therefore that there is a strong dependency for minimum point of oscillation on the geometry of the splitter post itself. To reduce the minimum point of oscillation further the geometry of the splitter post was examined to determine the criteria for oscillation at lower flowrates.

As the jet flow impinges on the upstream face of the post its flow path is blocked and an unstable point of contact is created. Any slight fluctuations in upstream stability will cause the jet to pass to one side of the post and alternating flow circulation around the post causes the jet to oscillate. At low flowrates the oscillation of the jet around the splitter post is due to alternating recirculation of vortices. The alternating circulation is caused by a vortex wake formation downstream of the bluff edges of the

splitter post. The relationship between the downstream wake instabilities and the upstream instabilities caused by recirculation of vortices is highly complex, particularly when combined with the effects of feedback circulation, but it is clear that for reduced minimum point of oscillation the downstream edge of the splitter post needs to be bluff and sharp edged to produce downstream shedding and the upstream face of the splitter post should provide a point of contact that is as unstable as possible.

The dimensions of the standard splitter post are 2.4mm × 4.8mm wide. If the width of the post were reduced then the jet is more likely to split around the post. It would therefore seem that increasing the width of the splitter post would increase the levels of instability at the upstream face. This has been previously investigated by Furmidge (1991) and was found to have minimal benefits in low flow performance whilst severely reducing the linearity of the device and increasing the pressure drop at high flow rates, due to the restricted flow path between the splitter post and diffuser wall.

The worst possible shape for the splitter post would be a foil with smooth tapered upstream and downstream faces allowing the jet to split evenly around the foil and reform downstream without disturbing the stable jet flow. The opposite configuration to a convex foil is a concave semicircular recess at the front face of the splitter post. This concave front face would produce an extremely unstable point of contact for the jet flow impinging on the splitter post. The downstream edge of the standard splitter post is already suitable because it is bluff with sharp edges causing an unstable downstream wake with recirculating vortices. Figure 5.24 shows the geometry of the standard post, a worst possible geometry and the concave upstream face splitter post.

An acetal meter from the same moulding batch as the previously modified cutaway acetal meter was modified in the same way as described earlier, ie. with the diffuser wall sections removed so that they could be fitted with the diffuser wall inserts. The meter was further modified with a machine tool so that the upstream face of the meter had a semicircular cut through the length of the post. The semicircular cut was made with a 3.0mm diameter cutting tool which cut 1mm into the upstream face of the post.

A flat was left at each side of the concave section to produce a vortex region where vortices develop which help to smooth the flow path for the jet to each side of the post and help direct the jet towards the diffuser walls. Figure 5.25 shows a diagrammatic representation of the jet flow impinging on the surface of the concave face splitter post at low flowrates.

The modified acetal meter was fitted with the same diffuser wall inserts as tested previously and experimentally investigated for the minimum point of oscillation. The configuration of the acetal transducer with modified splitter post and diffuser wall inserts is shown in figure 5.26. The configuration of the diffuser wall inserts was as follows:

Diffuser wall section width:	5mm
Feedback entrainment region:	Enlarged by 2mm
Jet contact region:	Enlarged by 3mm

5.10.1 Results of Splitter Post Modification.

Table 5.7 shows the relative strength of the electronically detectable oscillation signal and the minimum flowrate for oscillation of the acetal meter with the modified splitter post diffuser wall configuration described above.

Mass Water (g)	Time (s)	Temp (°C)	Rate (ml s^{-1})	Rate @ 20°C	Oscillation Strength
1952.0	1227.4096	21.4	1.59	1.646	Strong
2432.4	1738.3932	21.0	1.399	1.433	Strong
2016.3	1446.7605	21.1	1.394	1.431	Strong
1673.1	1203.0315	21.2	1.390	1.427	Weak

Table 5.7 Minimum Oscillation of Acetal Meter With Modified Diffuser Inserts.

5.10.2 Splitter Post Modification Conclusions.

The meter with the modified splitter post will maintain oscillation at flowrates below the Q_N1.0 Class D minimum flowrate specification at temperatures below 10°C. The lowest value of Re_{min} achieved for electronic signal detection of the modified acetal transducer is 82.6. Also because the modified splitter post causes more complete switching of the jet flow at low flowrates the signal strength is much stronger because the jet is closer to the diffuser wall. The signals detected on the electrodes are used in a differential arrangement and as the switching of the jet moves away from the diffuser wall at low flowrates there is a considerable reduction in sensitivity. The overall sensitivity is reduced because as the jet moves away from the electrode near the diffuser wall the signal on that electrode is reduced, also because the jet is nearer to the electrode on the opposite diffuser wall, the signal generated on the opposite electrode is increased.

5.11 Summary.

This chapter has shown that the minimum Reynolds number for oscillation of the standard production Class C fluidic oscillator water meter is 127.3. To achieve the Q_N1.0 Class D minimum flowrate specification at temperatures down to 10°C then the meter must be capable of maintaining oscillation at a Reynolds number of 92 within the jet flow.

Several methods of reducing the minimum Reynolds number for oscillation have been investigated. Alterations to the geometry of the nozzle, other than reducing the size of the nozzle, were shown to have no benefits in low flow performance. However the results of experimental investigation did indicate the criteria required for oscillation at low Reynolds numbers. The addition of vortex ring configurations around the nozzle outlet produced a reduction in minimum flowrate for oscillation that was equivalent to the reduction achieved through the addition of a flow conditioning device to the meter inlet.

Modifications to the feedback channels of the fluidic transducer gave significant reductions in minimum flowrate for oscillation by reducing the resistance to feedback flow and inducing switching of the jet at lower flowrates. The lowest value of minimum Reynolds number achieved through modification to the feedback channels of the oscillator was 93.8.

The development of a sectioned acetal prototype transducer incorporating electrodes allowed more accurate comparisons to be made between subsequent modifications and the signal strengths generated for each modification at low flowrates. The concave face splitter post design was investigated using the acetal test meter. Combining the feedback channel and splitter post modifications resulted in a Q_N1.0 fluidic oscillator transducer capable of maintaining oscillation at a Reynolds number of 82.6. This is an overall reduction in Re_{min} of over 35% compared to the Class C design and is lower than the Reynolds number required to meet the Class D minimum flowrate

specification at temperatures above 10°C.

Also within this chapter methods of increasing the sensitivity and signal strength of the fluidic oscillator at low flowrates have been identified through transducer geometry modifications which improve the switching of the jet flow around the splitter post.

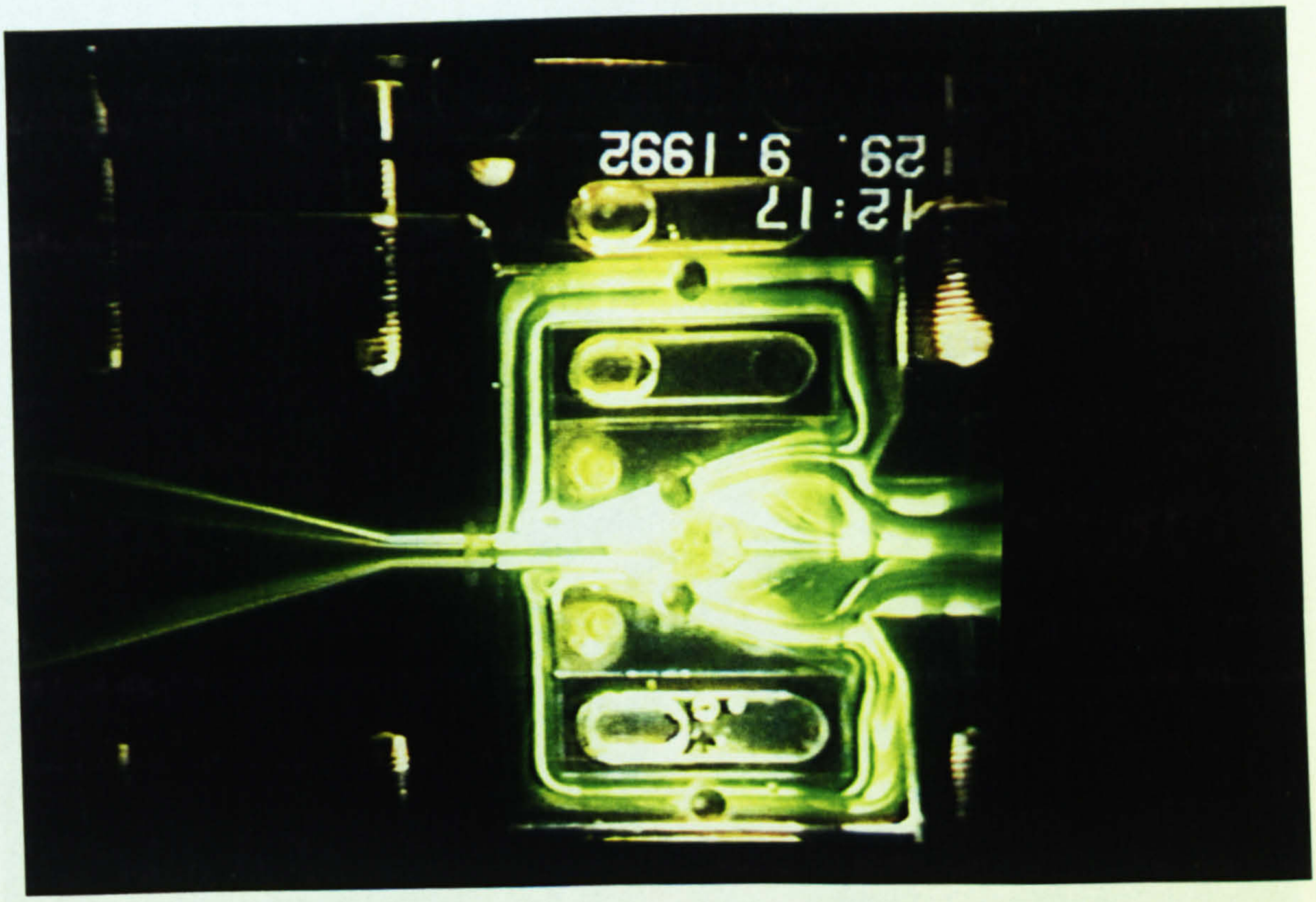

Figure 5.1: Flow Visualisation of Early Experimental Perspex Oscillator..

Figure 5.2.a: Flow Visualisations Showing Osillation Cycle of Polycarbonate Meter Moulding.

Figure 5.2.b: Flow Visualisations Showing Osillation Cycle of Polycarbonate Meter Moulding.

Figure 5.2.c: Flow Visualisations Showing Osillation Cycle of Polycarbonate Meter Moulding.

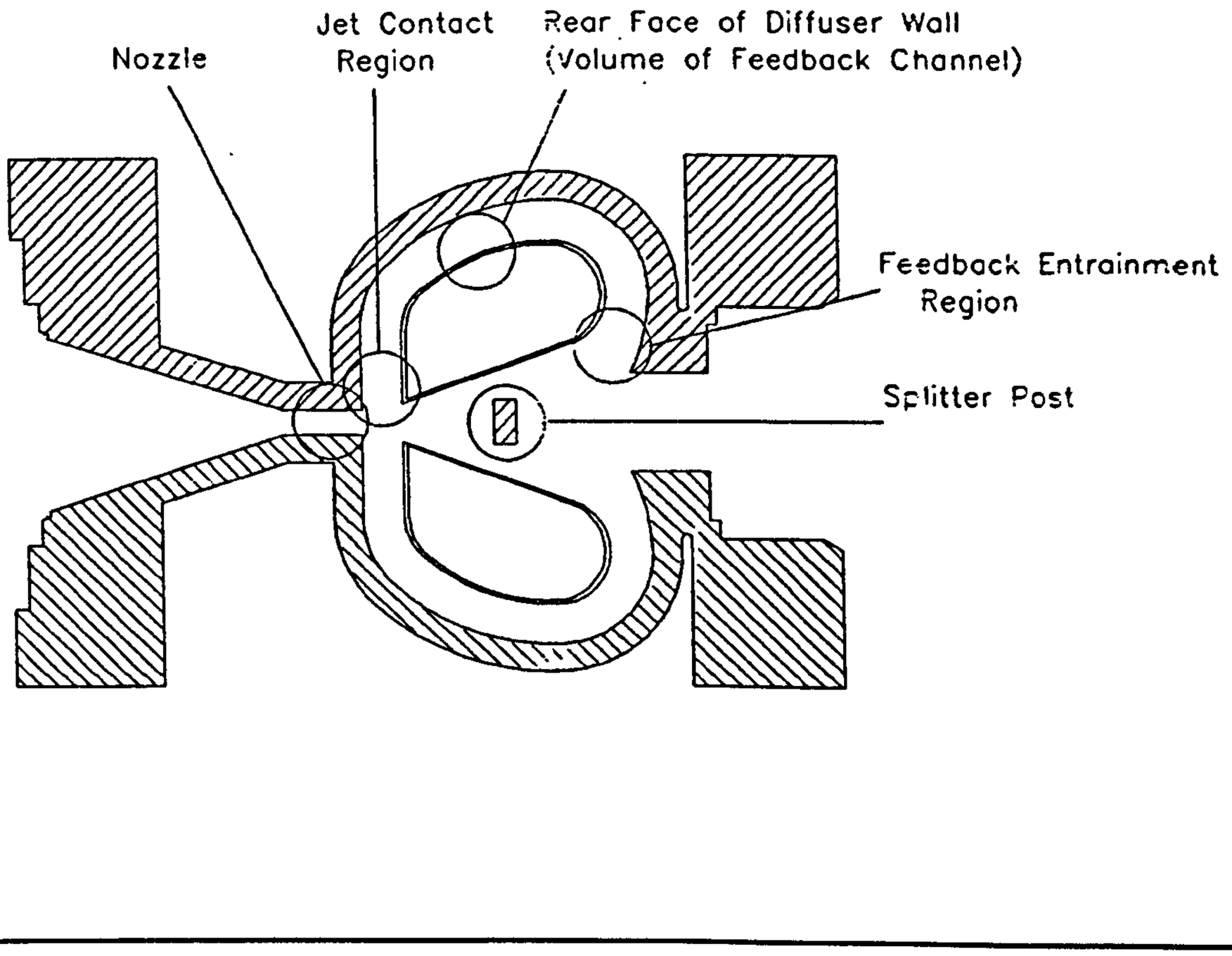

Figure 5.3: Location of Transducer Critical Design Parameters.

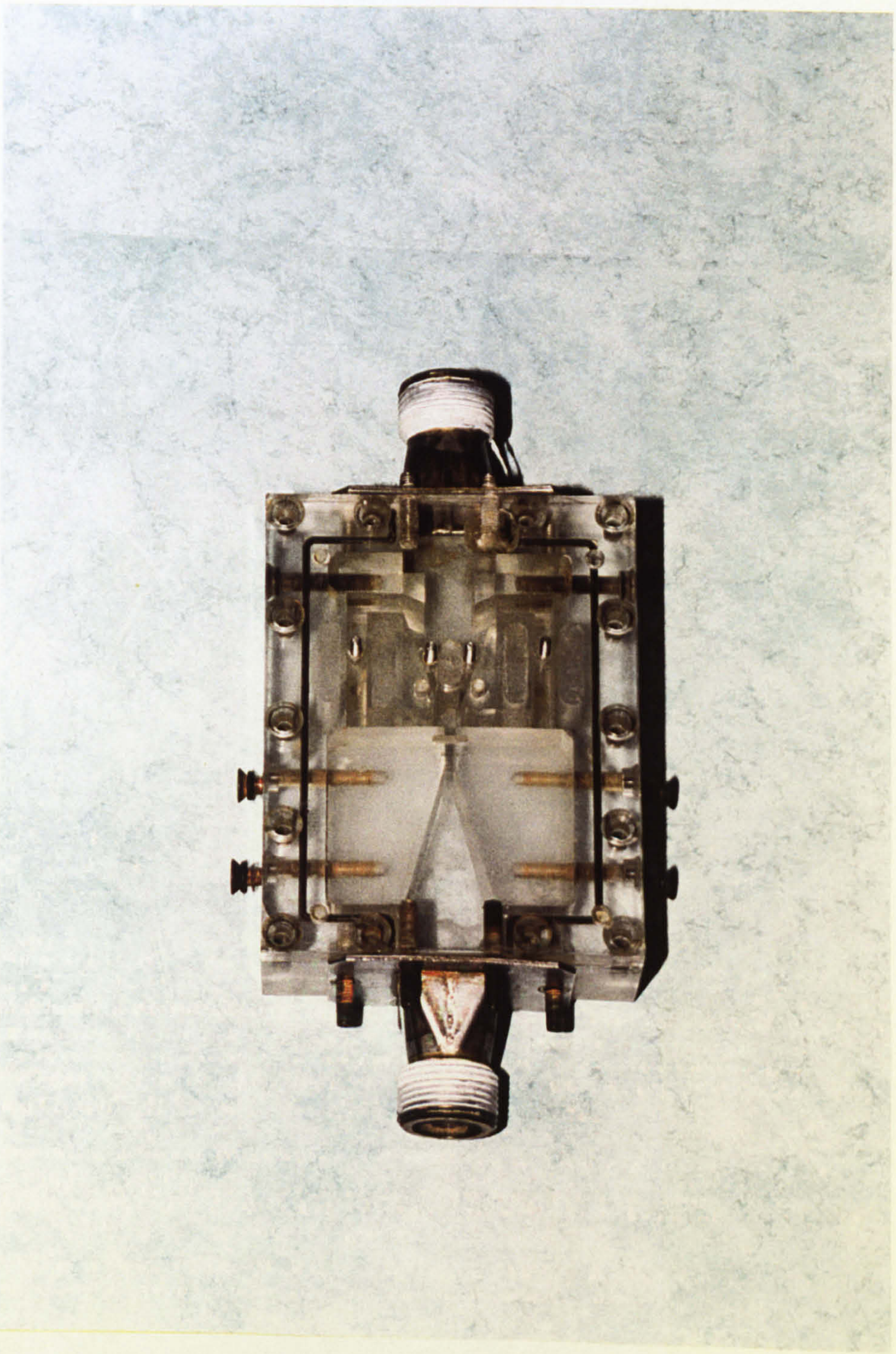

Figure 5.4: Q_N1.5 Perspex Block Component Transducer.

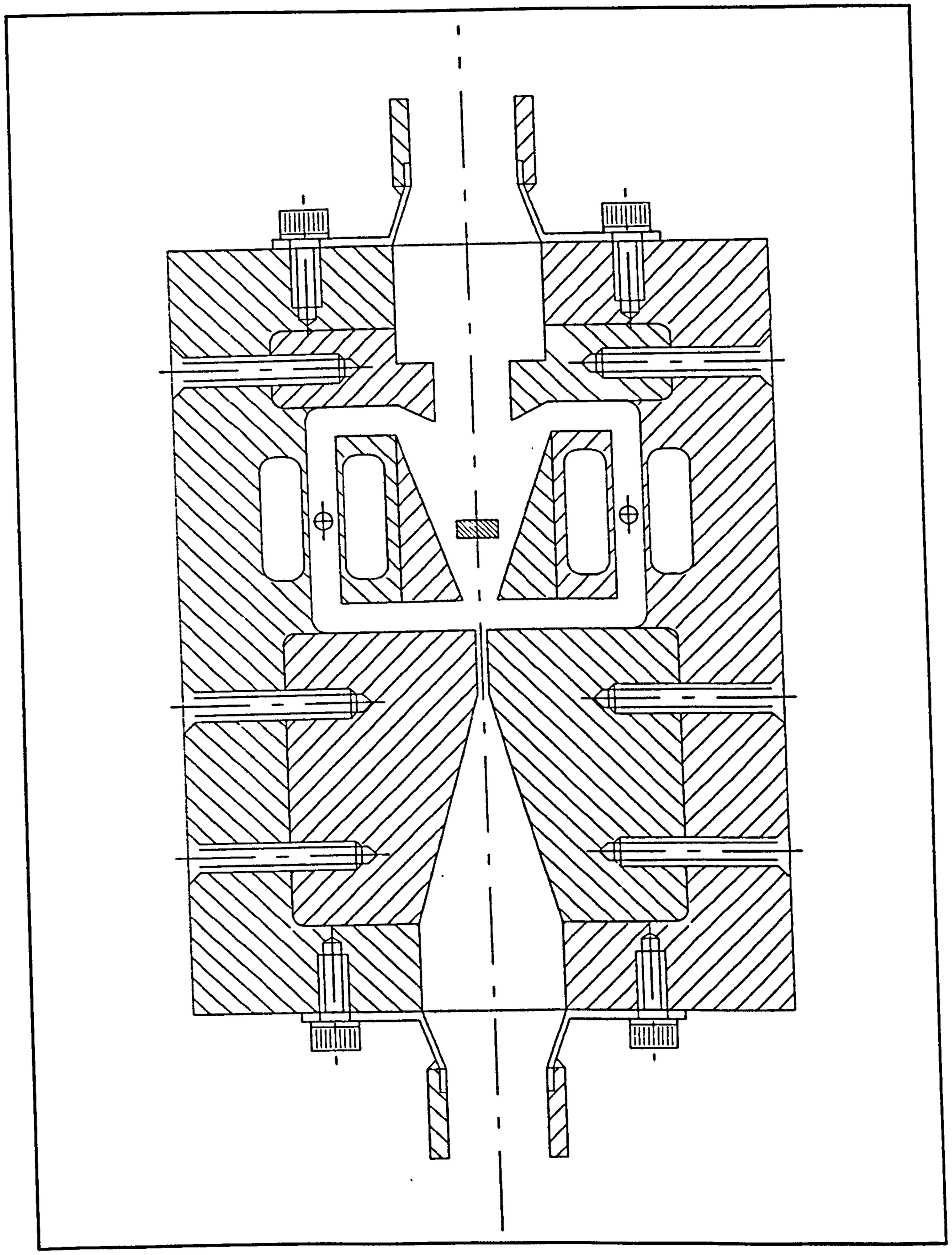

Figure 5.5: Geometry of Standard Inlet Nozzle Configuration.

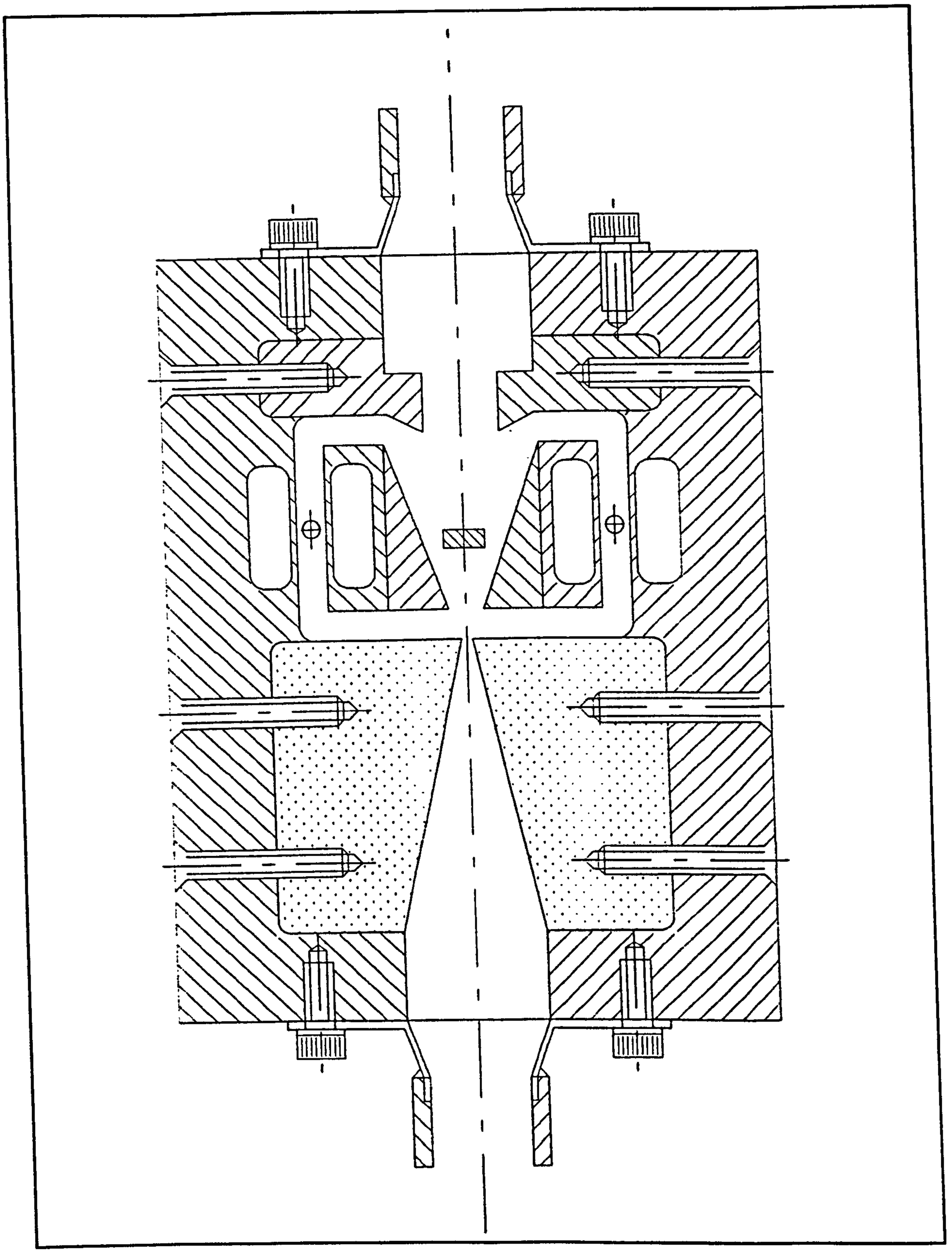

Figure 5.6: Geometry of Inlet Nozzle With Parallel Section Removed.

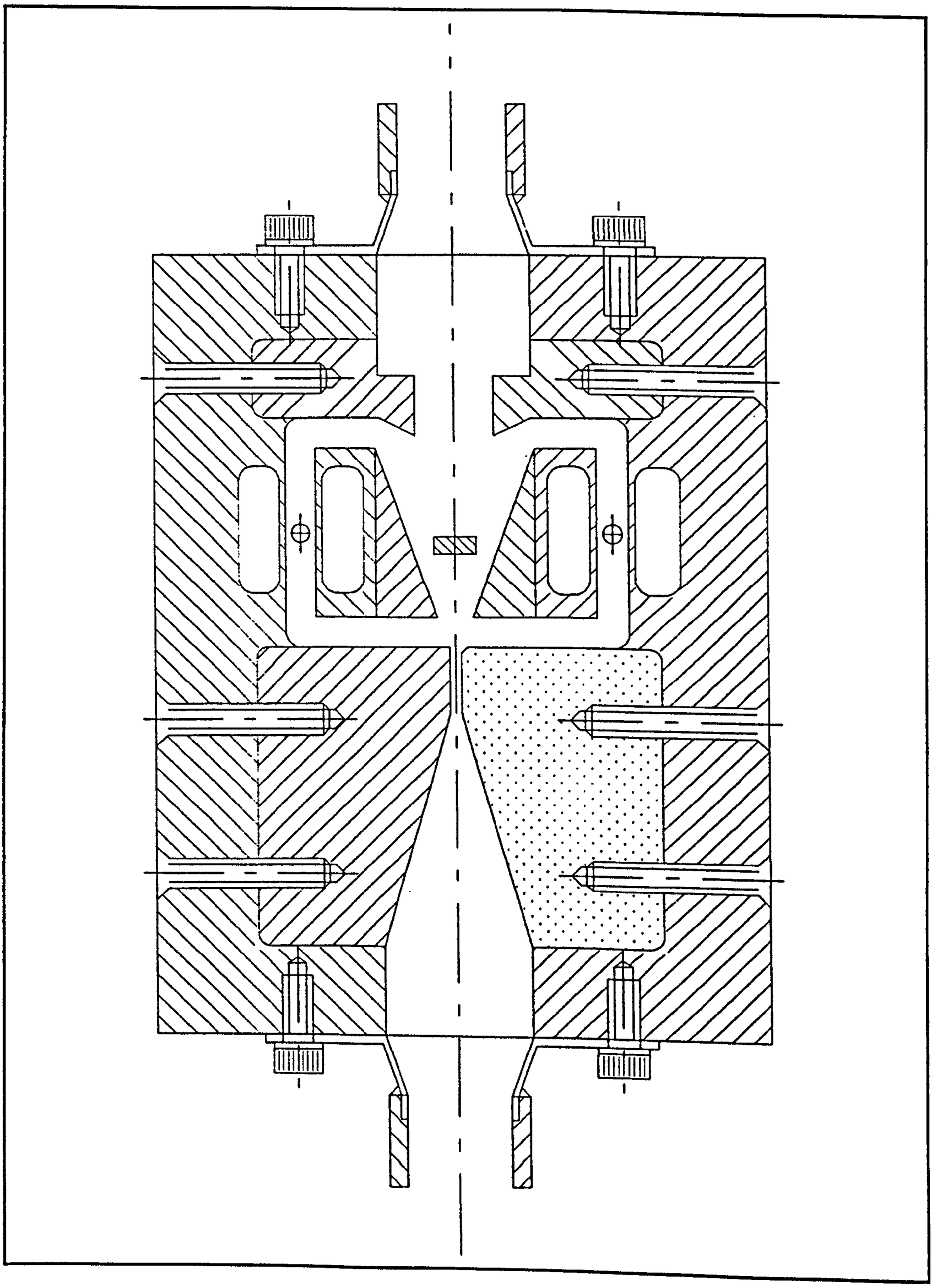

Figure 5.7: Geometry of Asymmetric Nozzle.

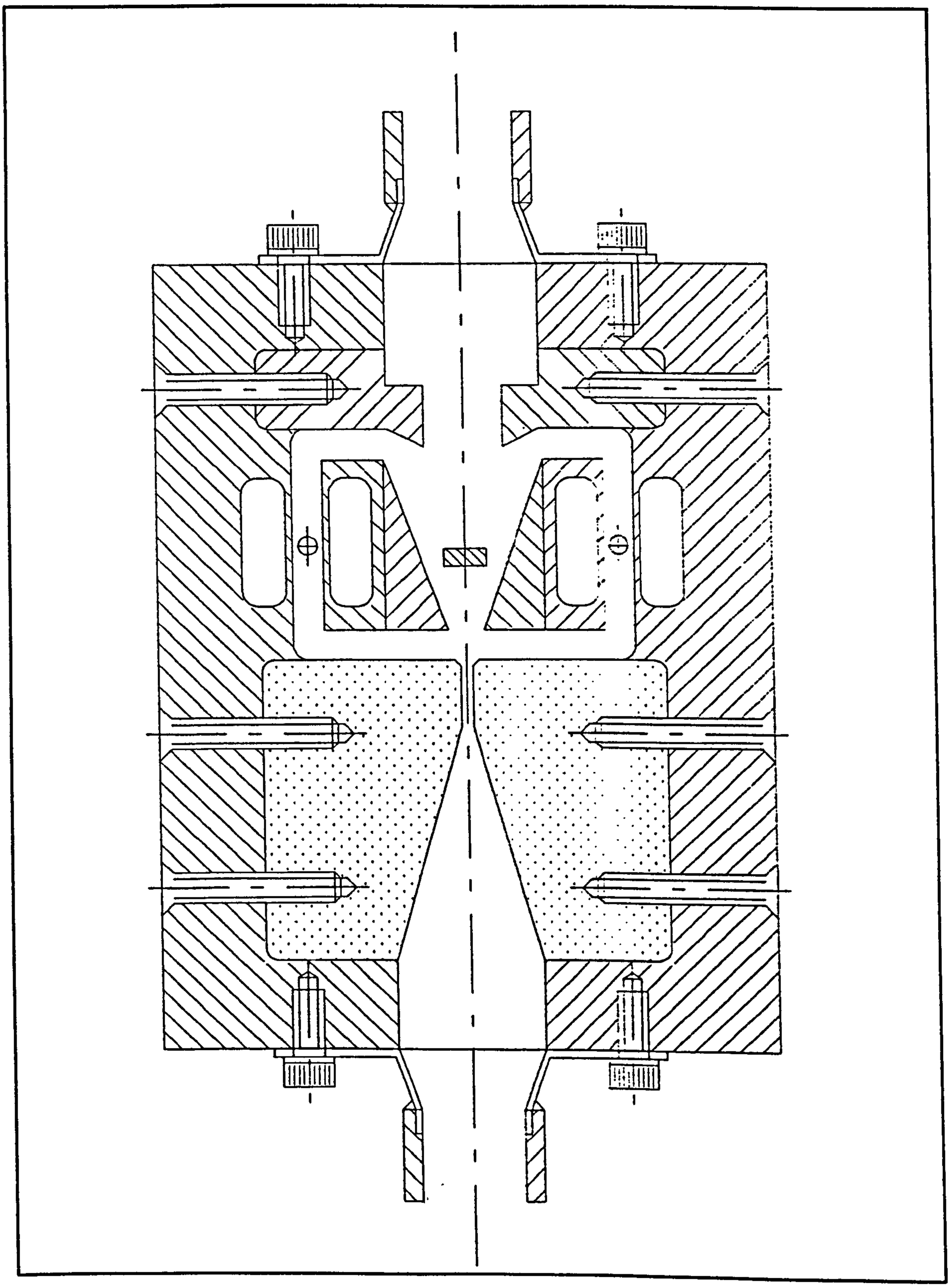

Figure 5.8: Geometry of Nozzle With Chamfered Outlet.

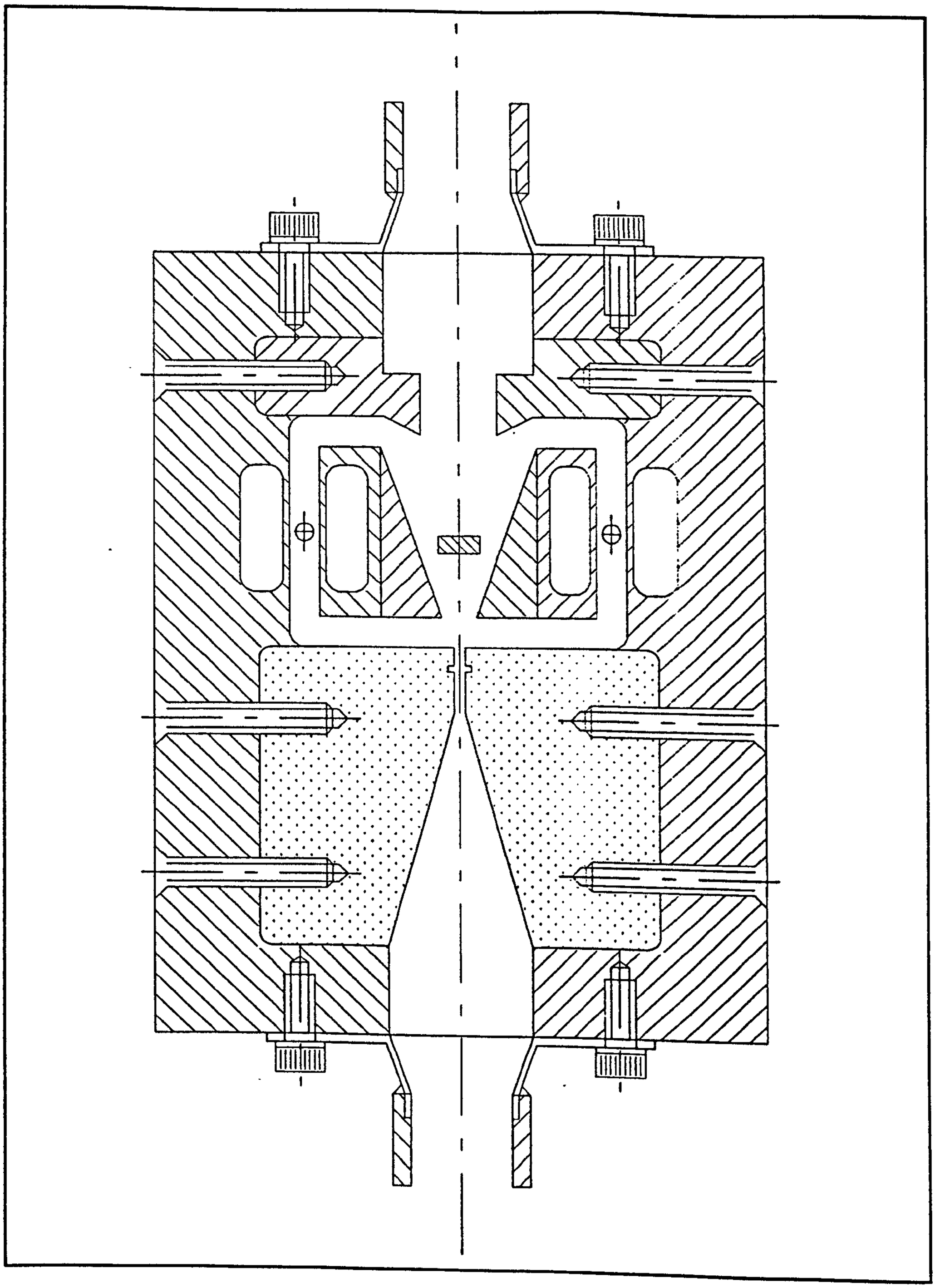

Figure 5.9: Geometry of Nozzle With 1mm × 1mm Side Slot..

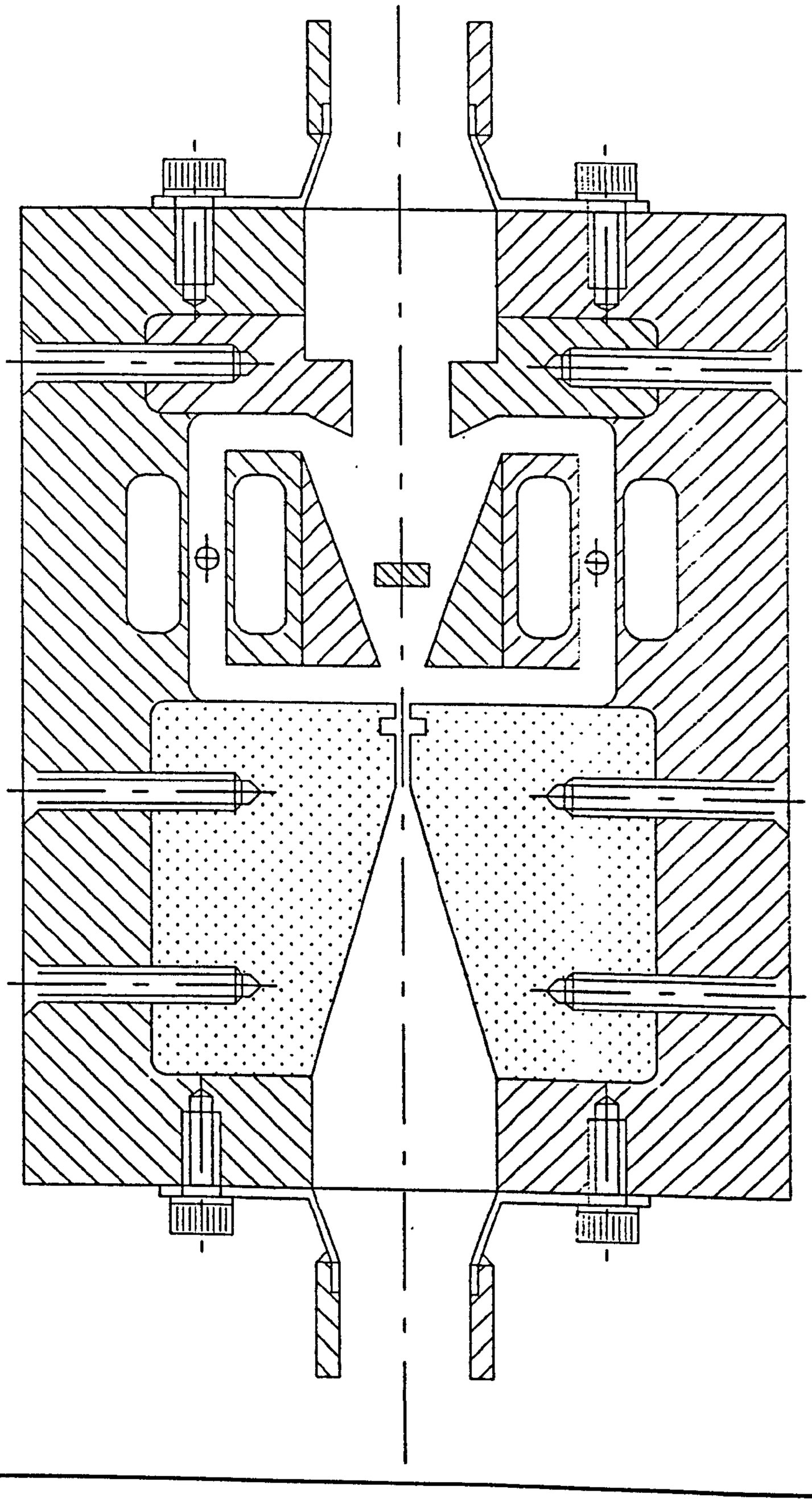

Figure 5.10: Geometry of Nozzle With 2mm × 2mm Side Slot.

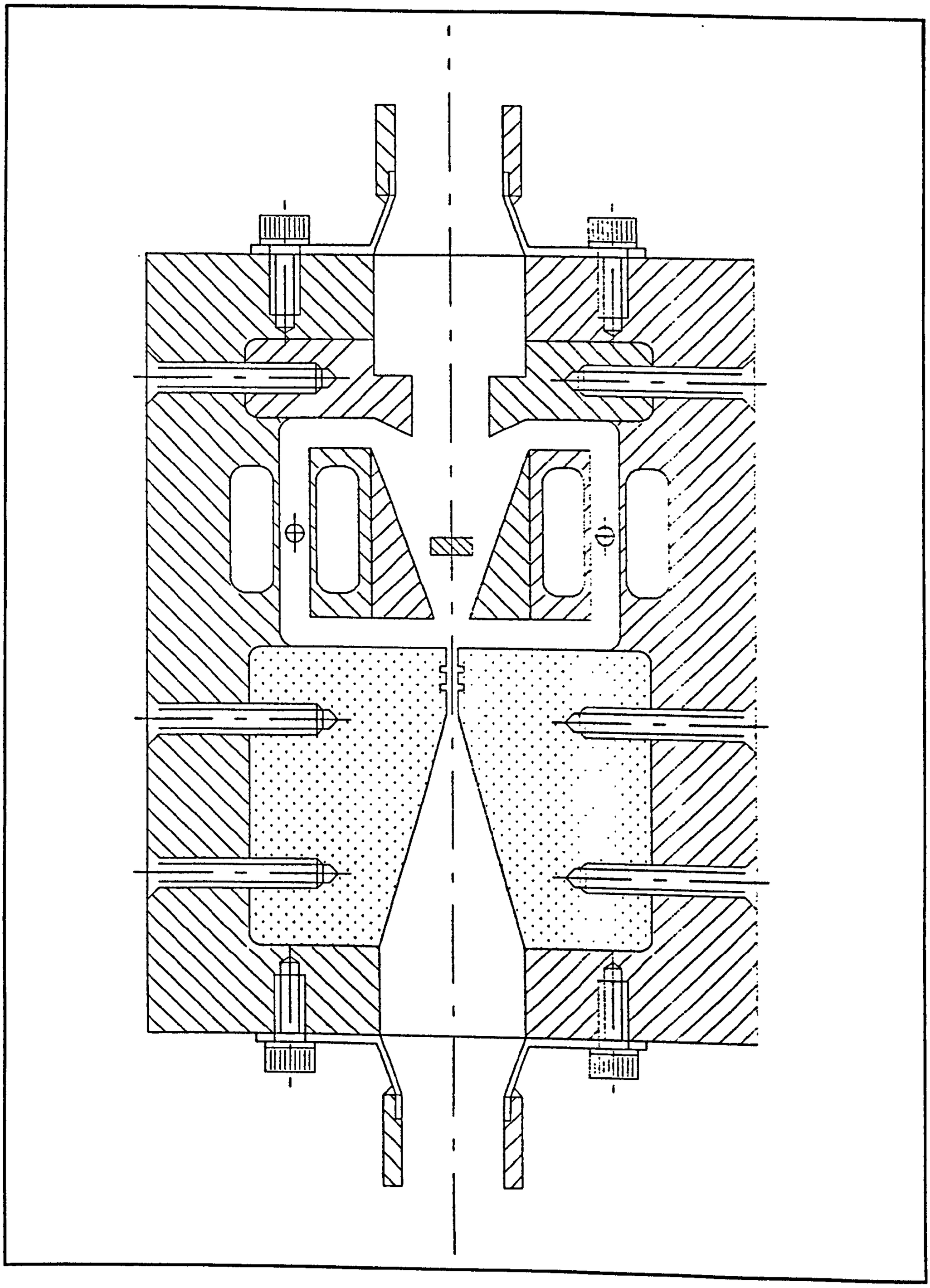

Figure 5.11: Geometry of Nozzle With Double Side Slots.

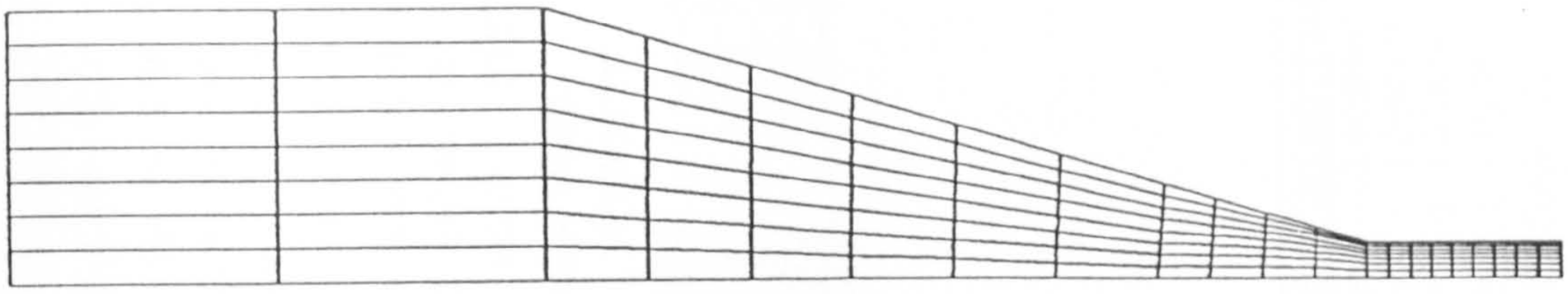

Figure 5.12.a: Numerical Mesh Used To Model Fluidic Oscillator Nozzle.

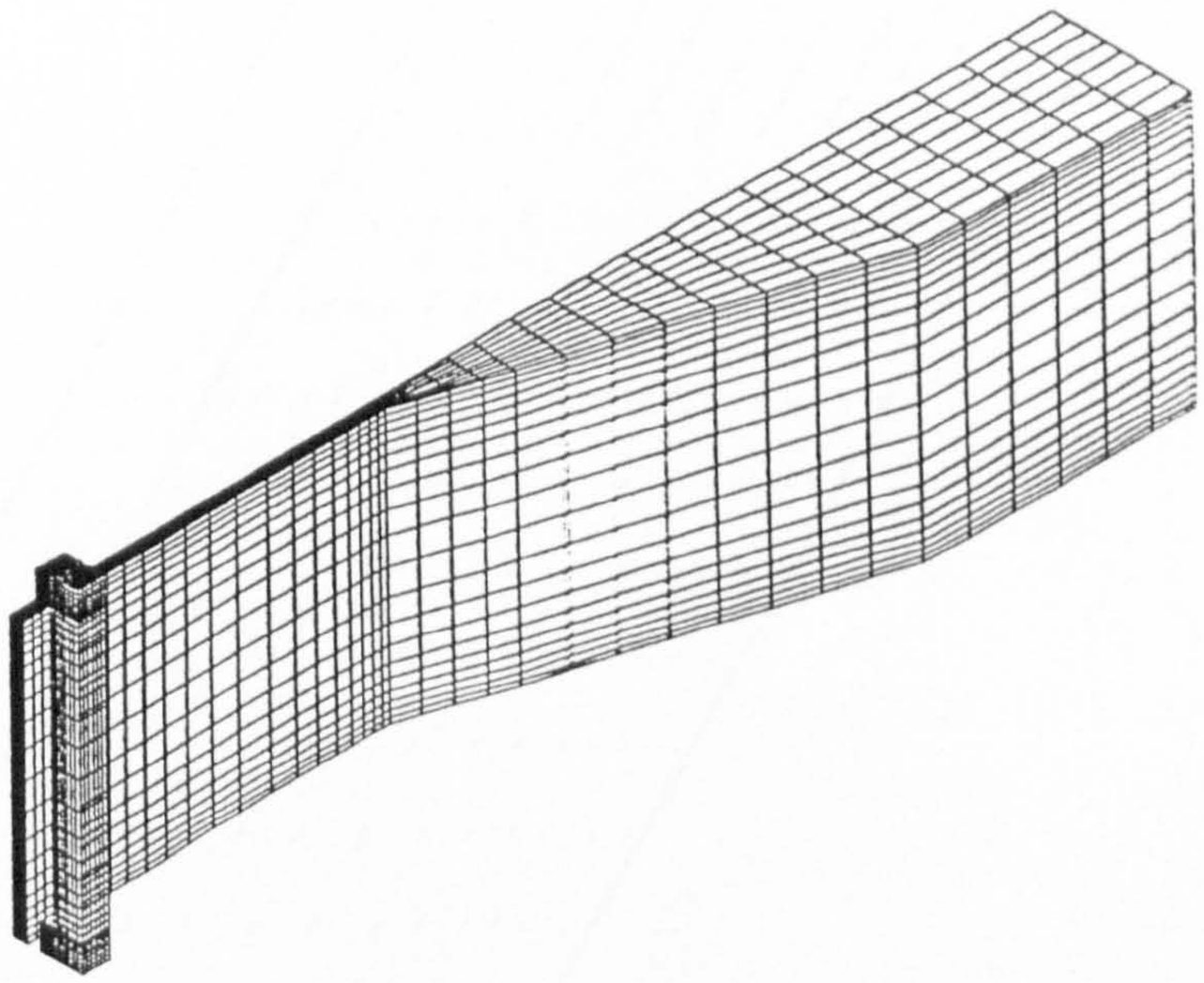

Figure 5.12.b: Numerical Mesh Used To Model Nozzle With Vortex Ring.

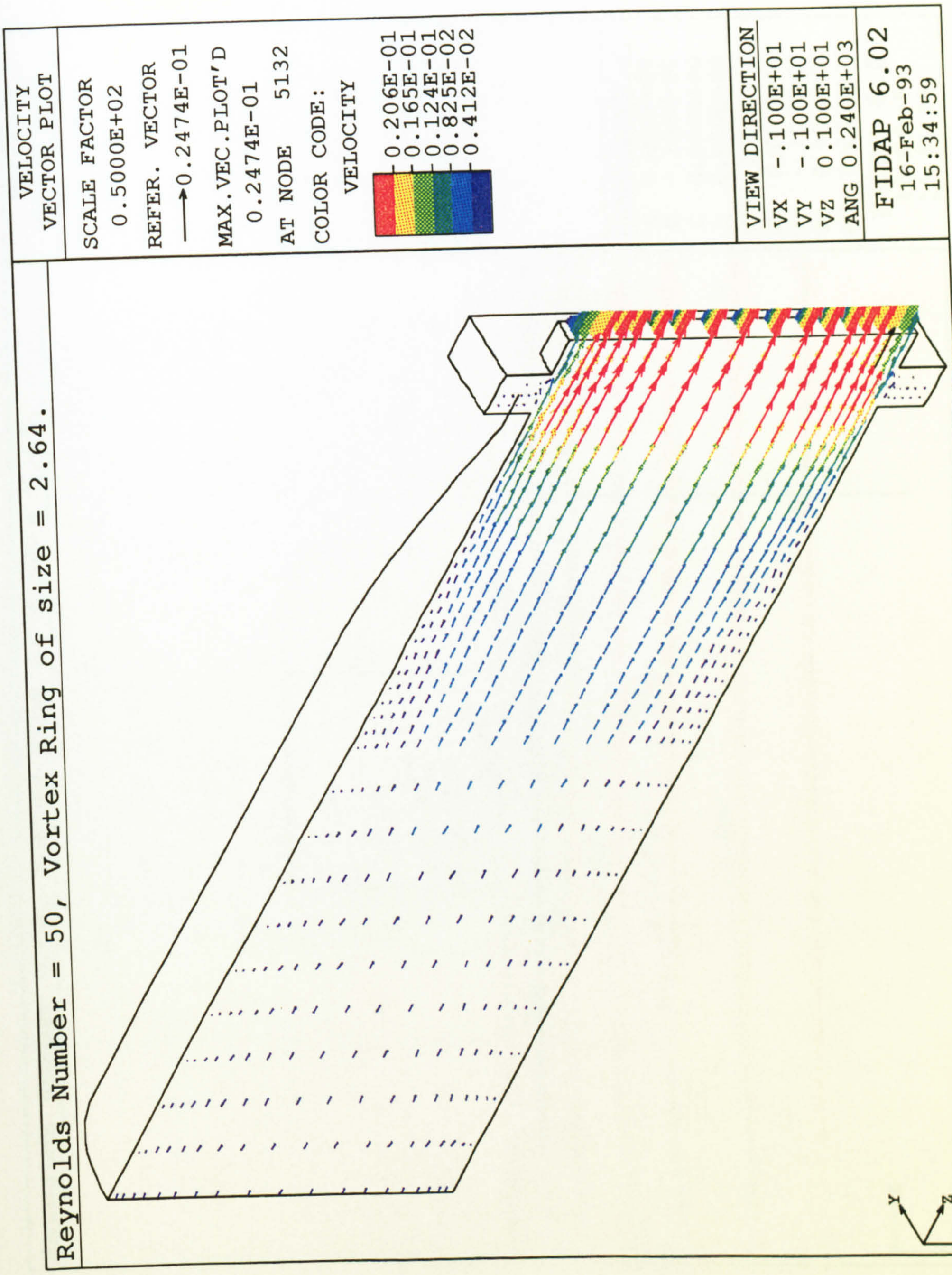

Figure 5.13: Close-Up of Velocity Vector Plot of Nozzle With Vortex Ring.

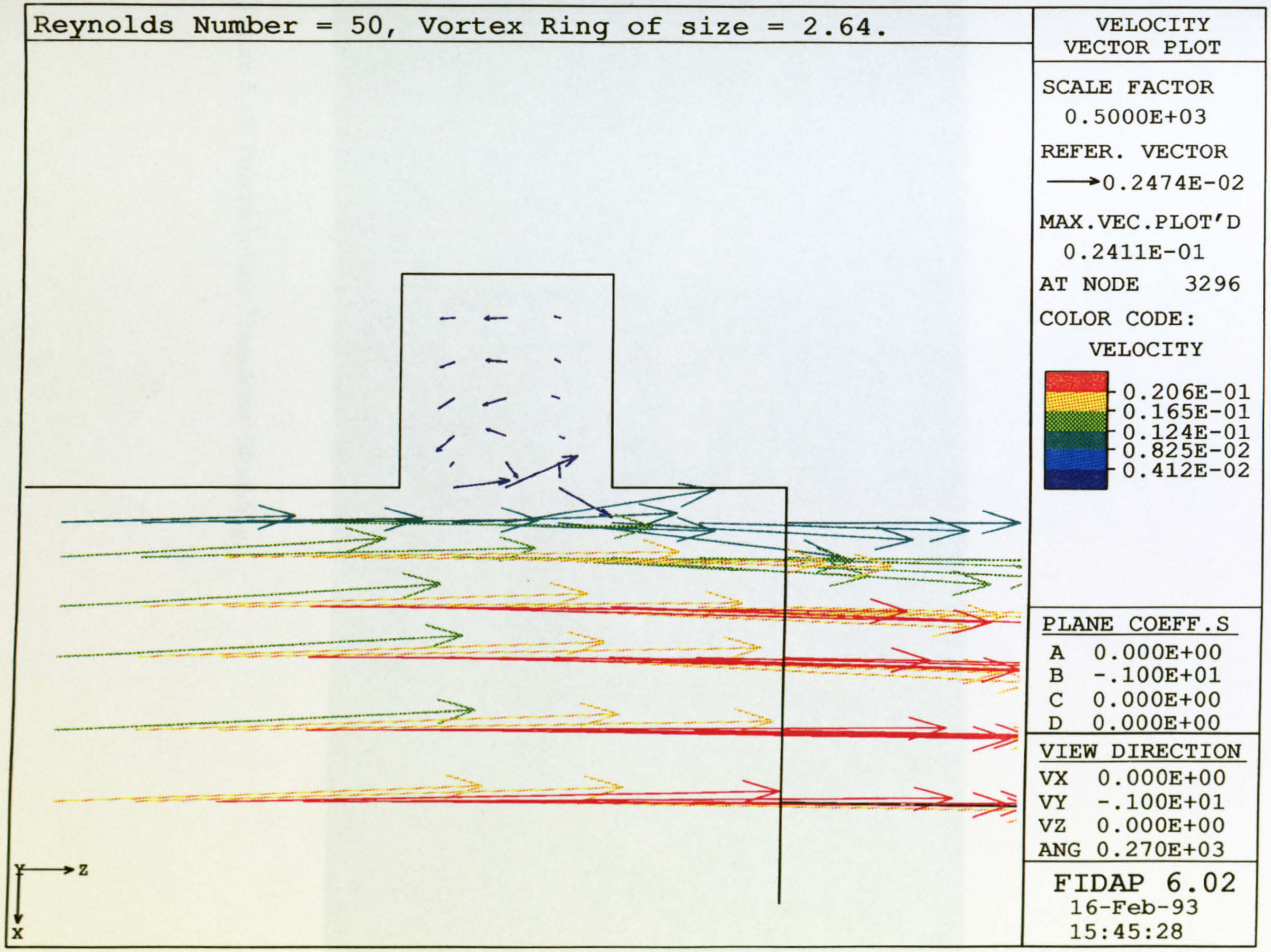

Figure 5.14: Extreme Close-Up of Slot.

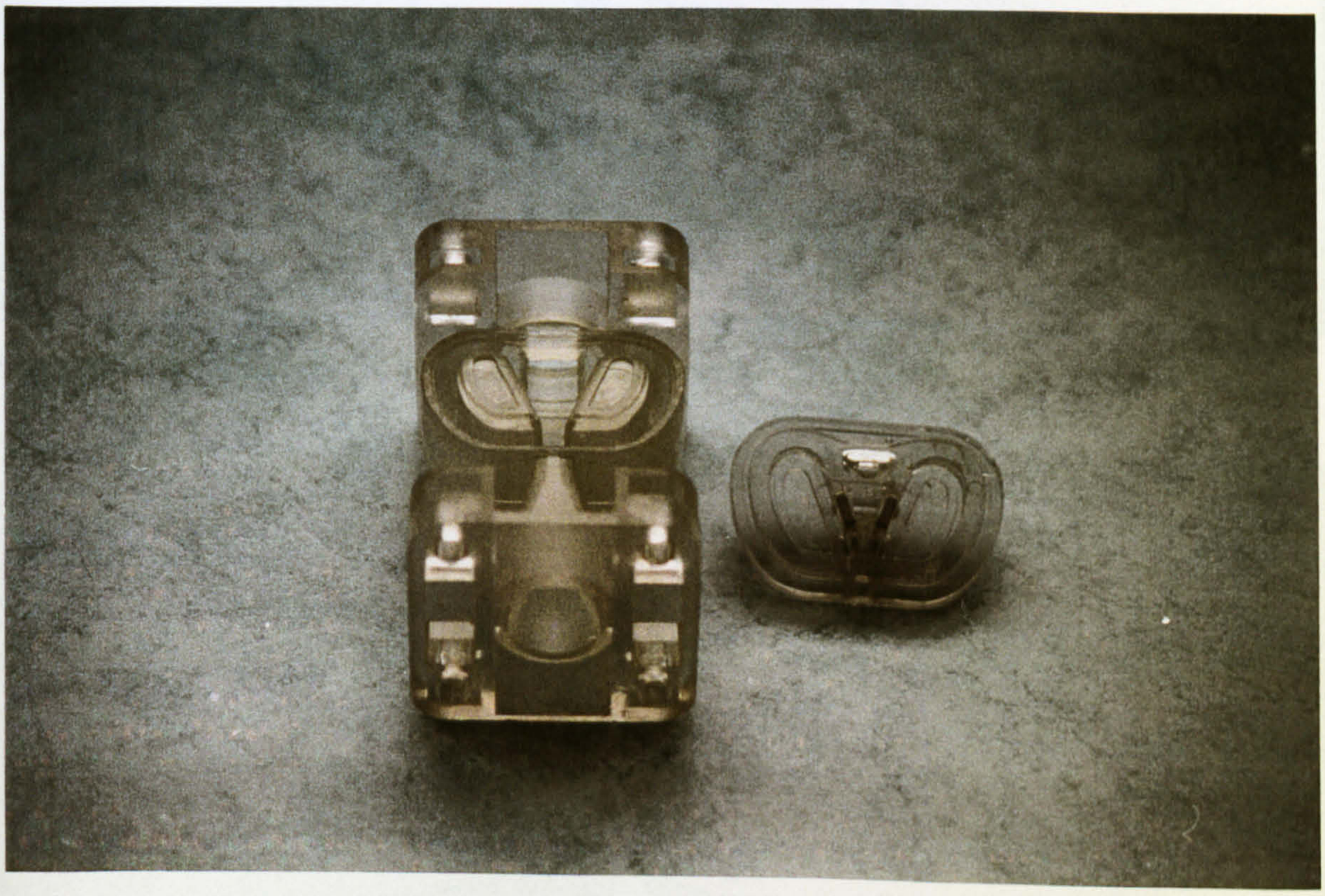

Figure 5.15: Polycarbonate Transducer Moulding.

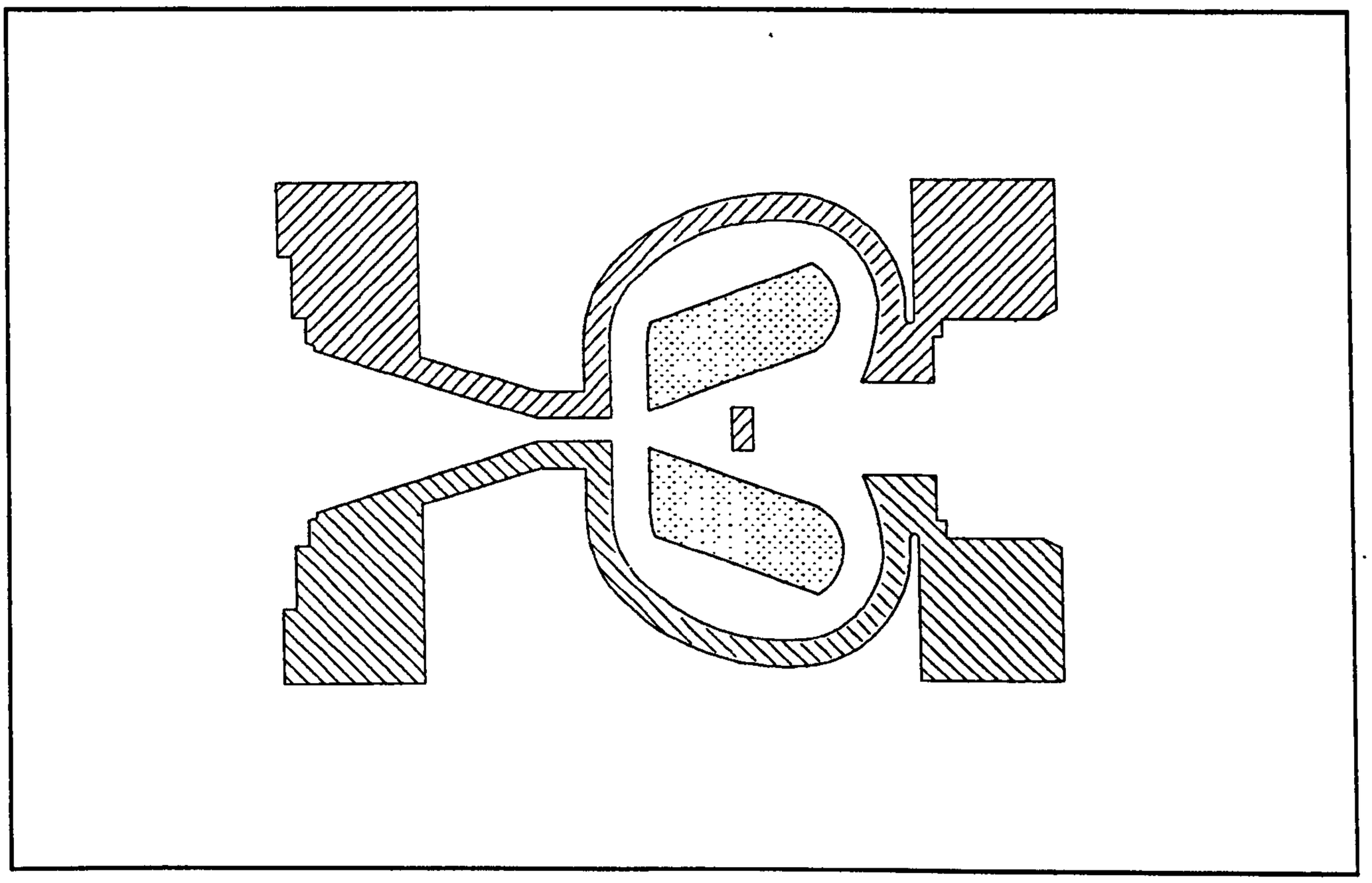

Figure 5.16: Modification 1 - Diffuser Wall Section.

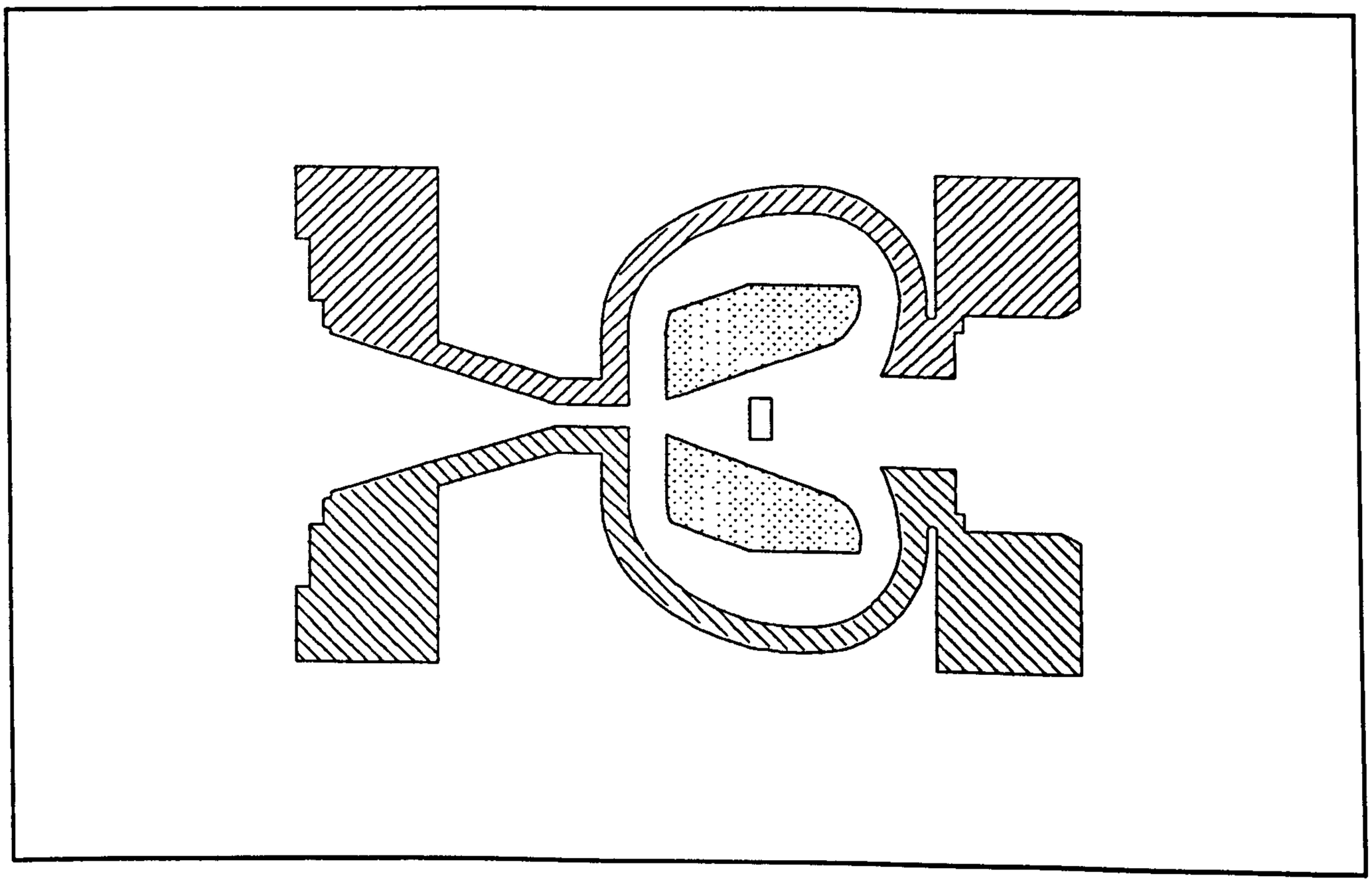

Figure 5.17: Modification 2 - Diffuser Wall Section.

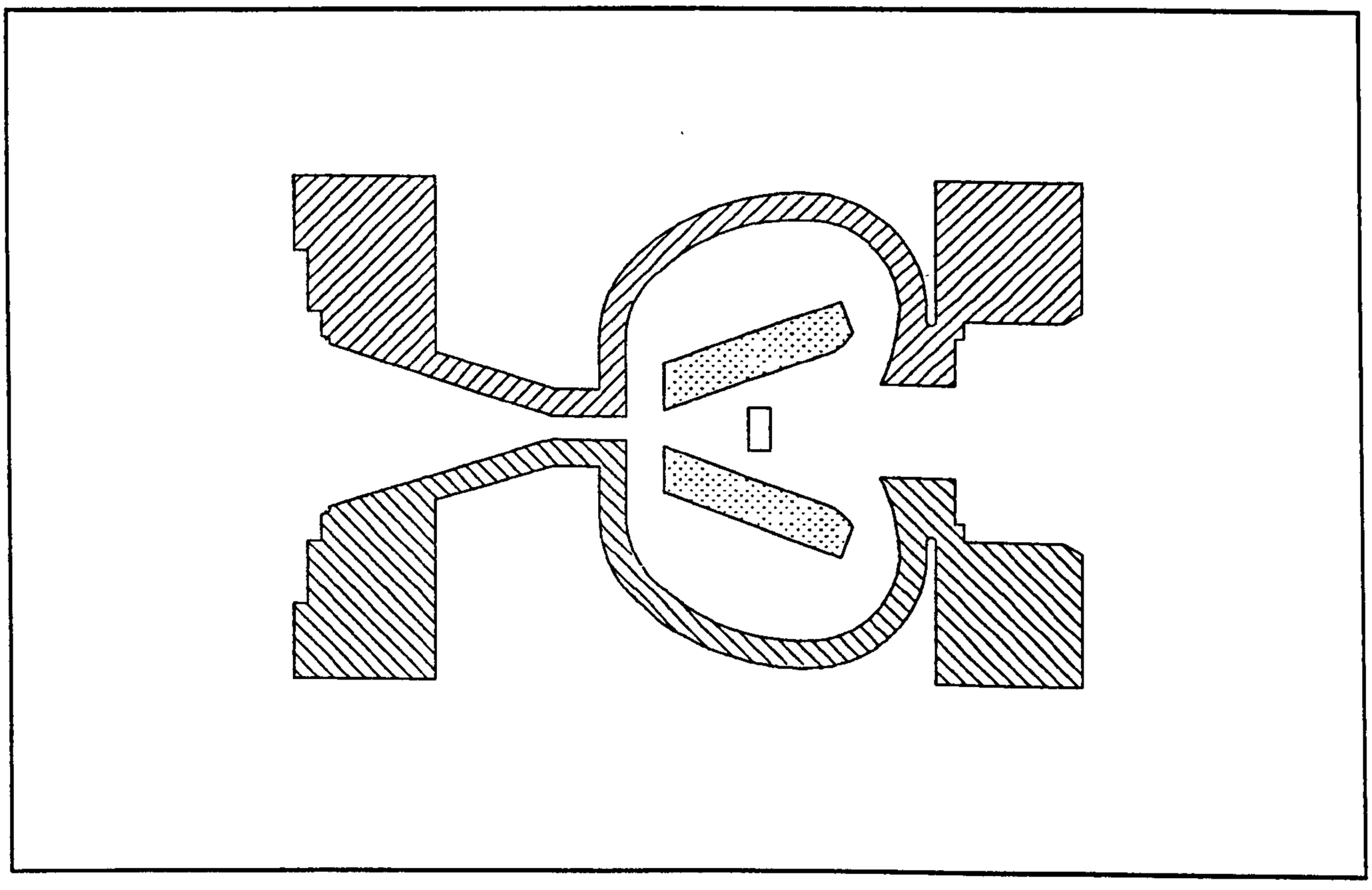

Figure 5.18: Modification 3 - Diffuser Wall Section.

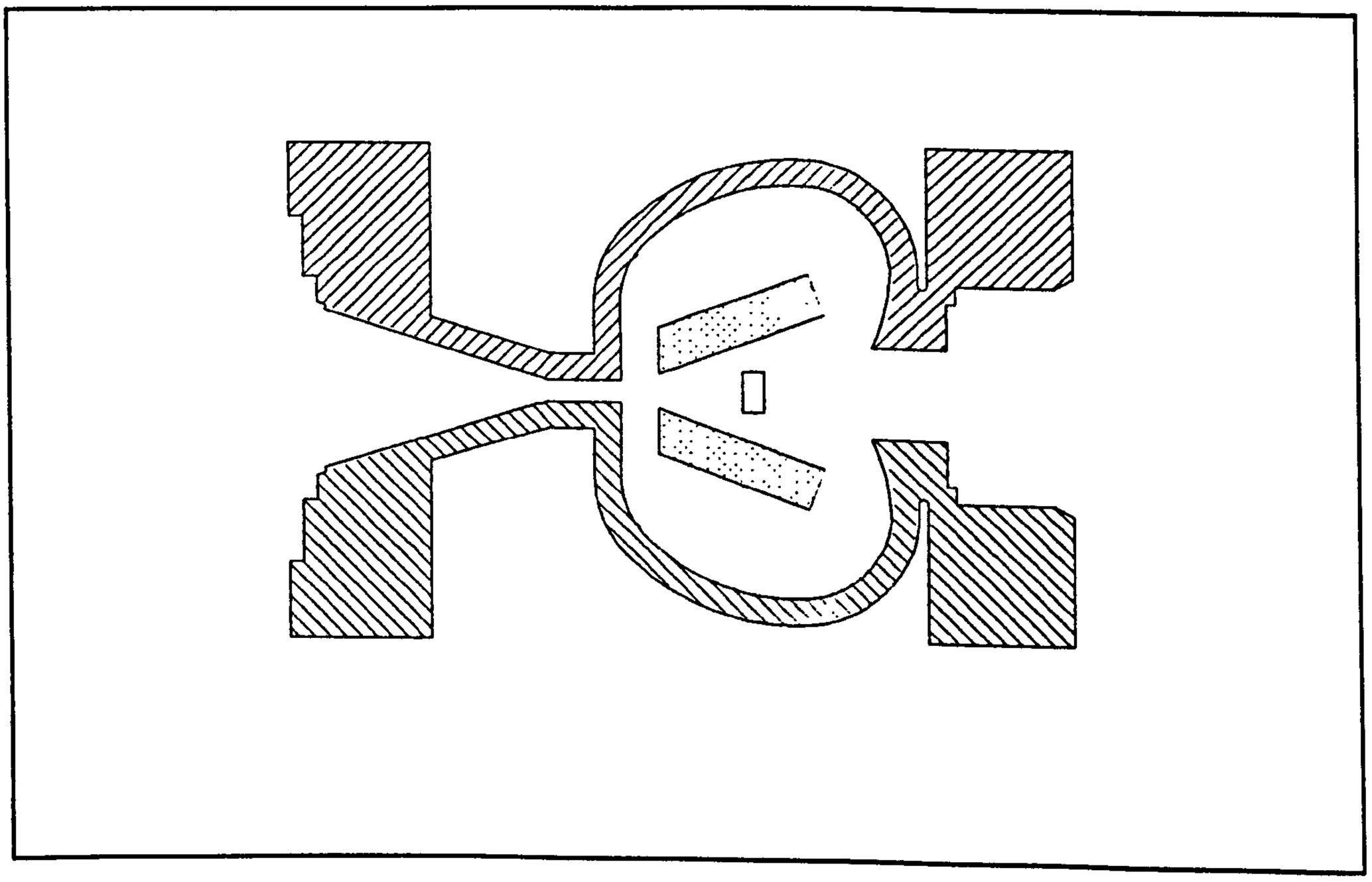

Figure 5.19: Modification 4 - Diffuser Wall Section.

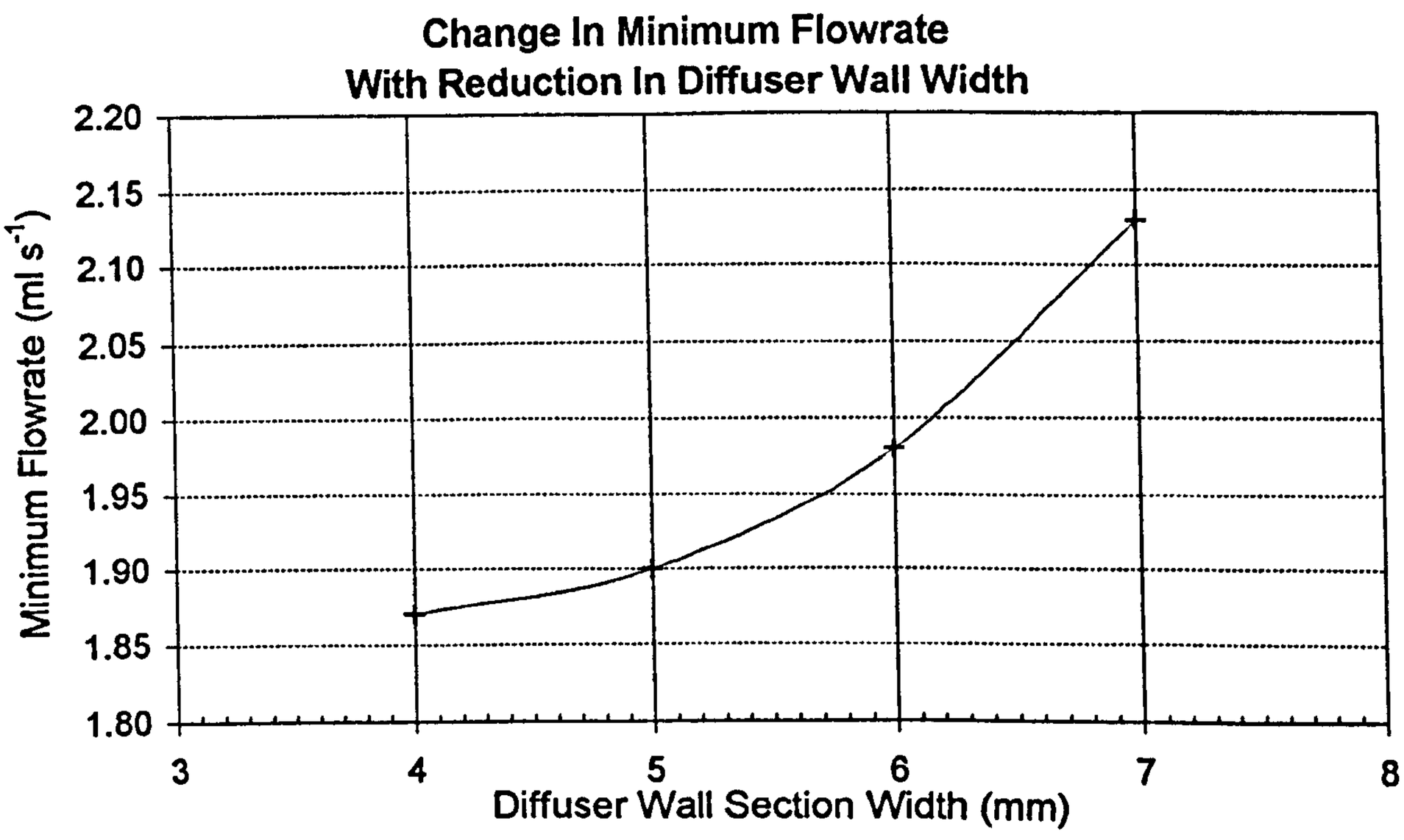

Figure 5.20: Variation of Minimum Point of Oscillation With Width of Diffuser Wall Section.

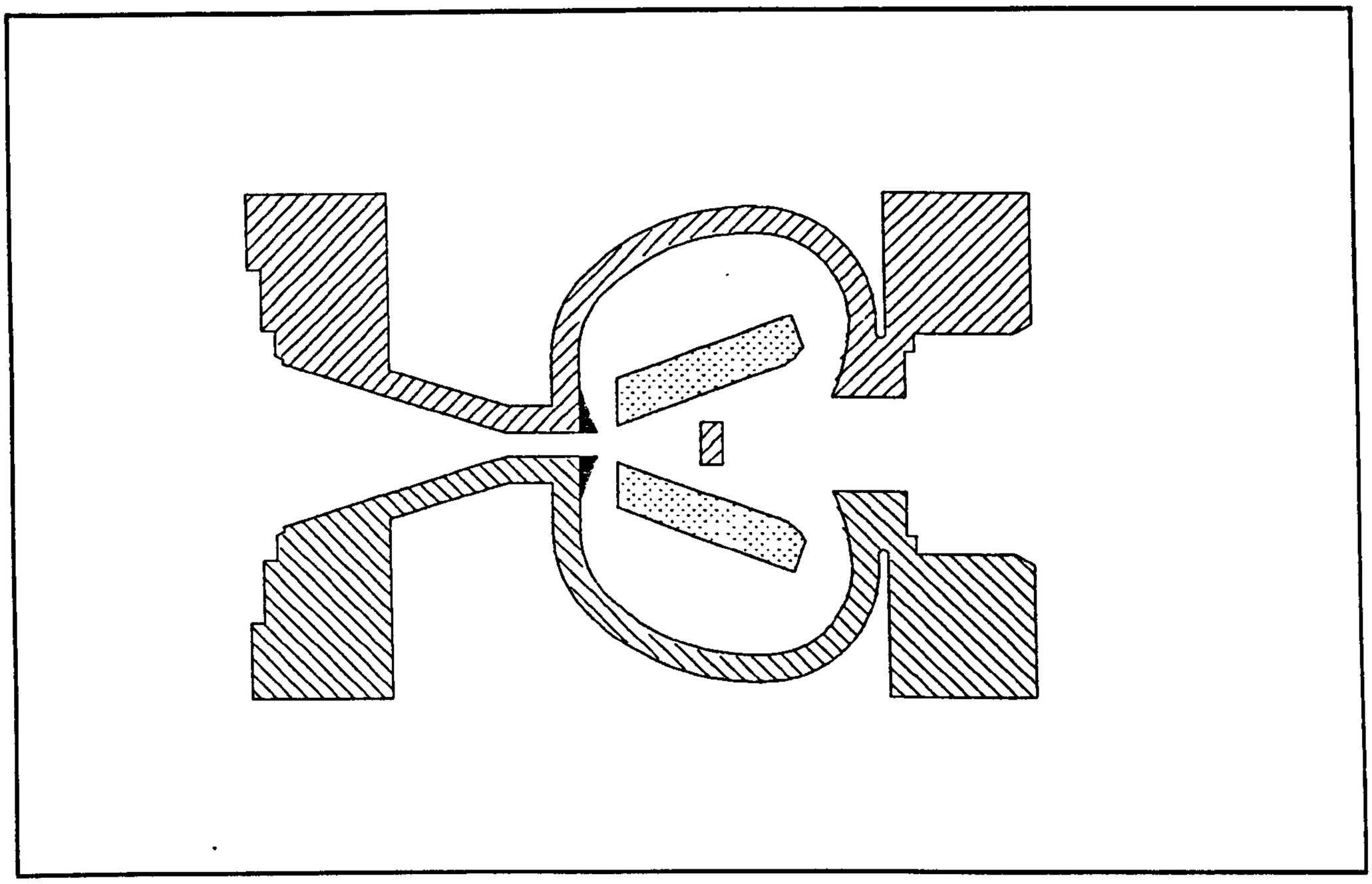

Figure 5.21: Inserts Fitted To Target Feedback Flow.

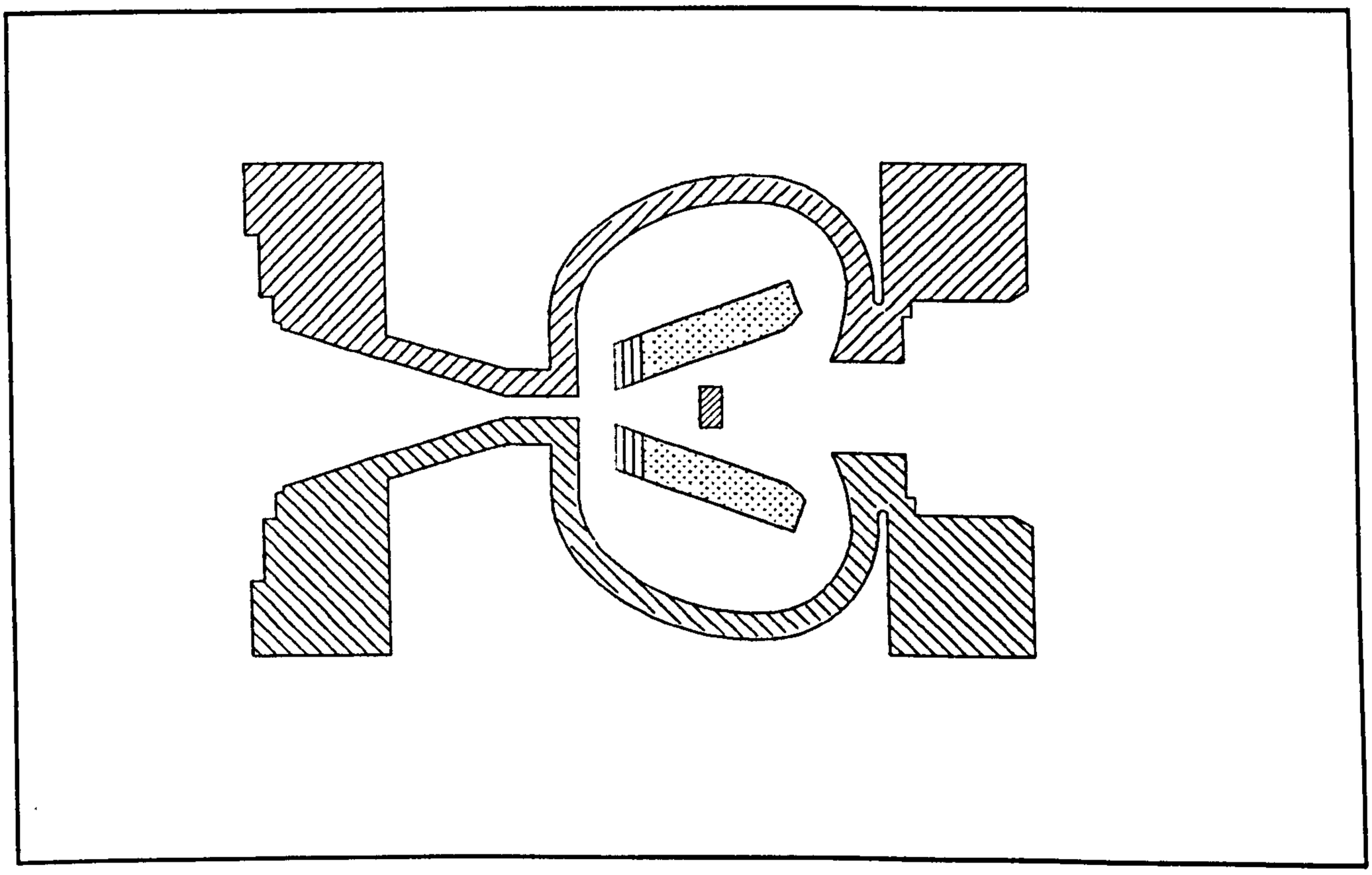

Figure 5.22: Increased Jet Contact Region.

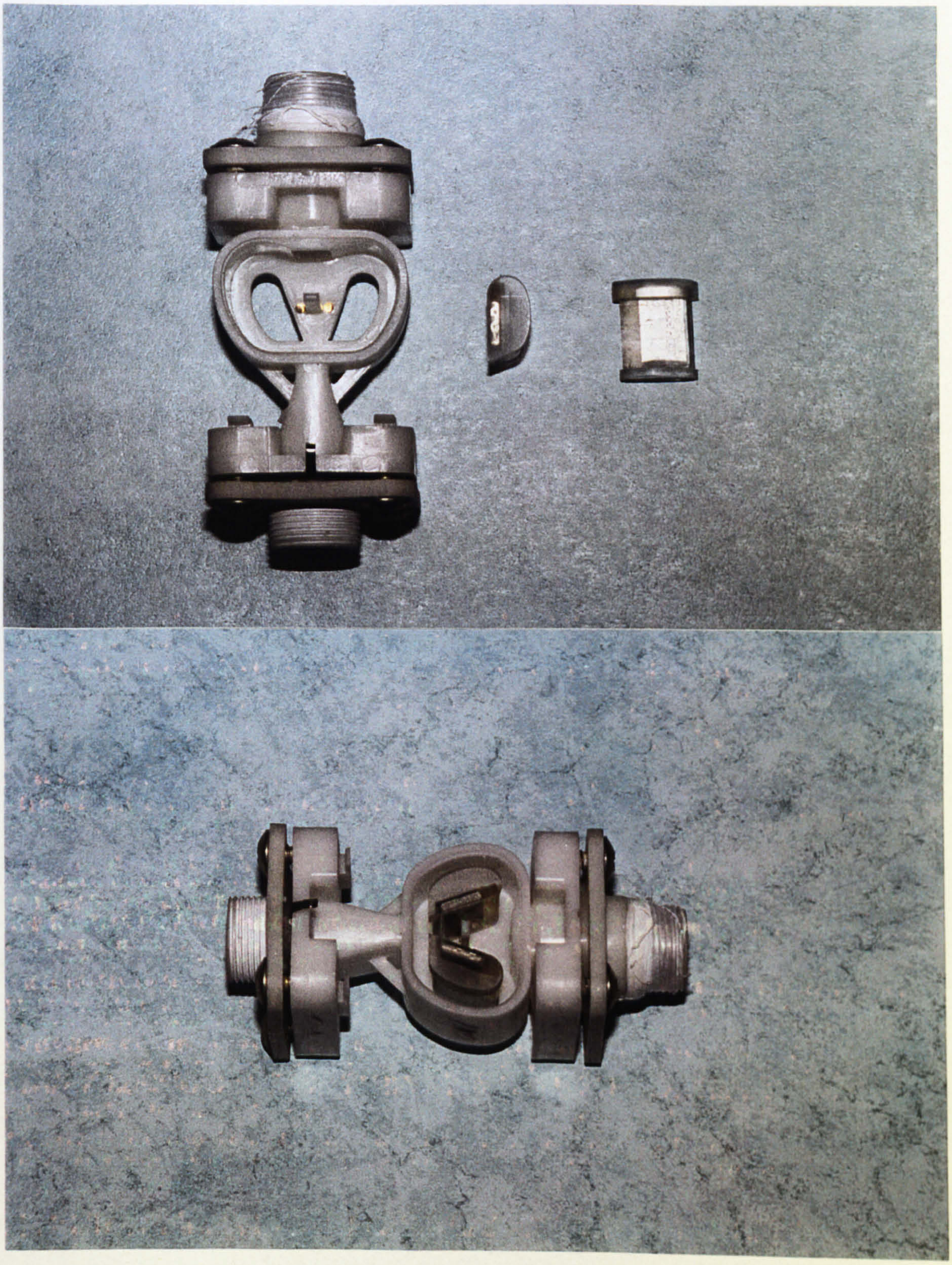

Figure 5.23: Sectioned Acetal Transducer and Diffuser Inserts.

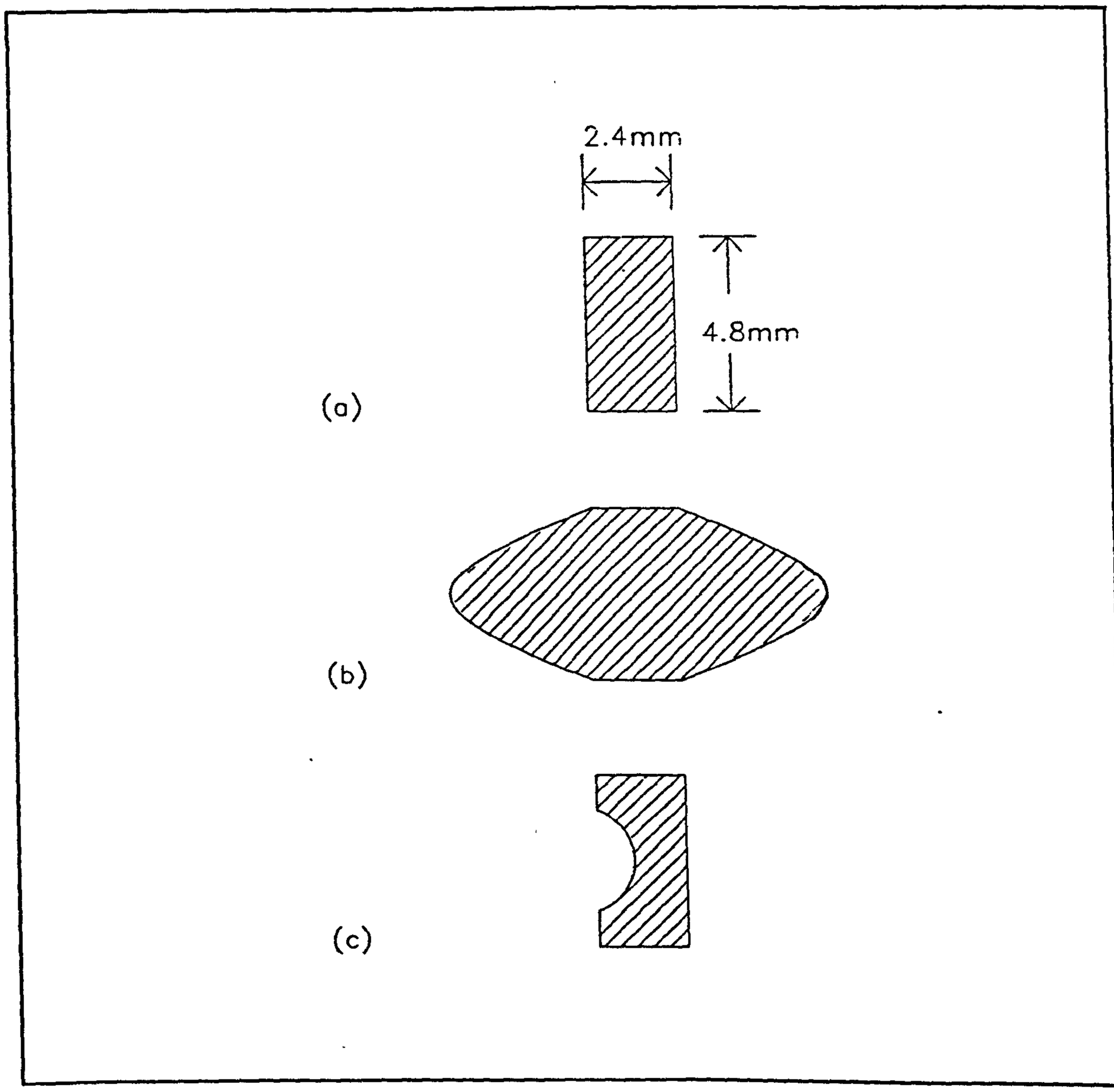

Figure 5.24: Geometry of Splitter Post (a).Standard (b).Worst Case (c).Concave Face.

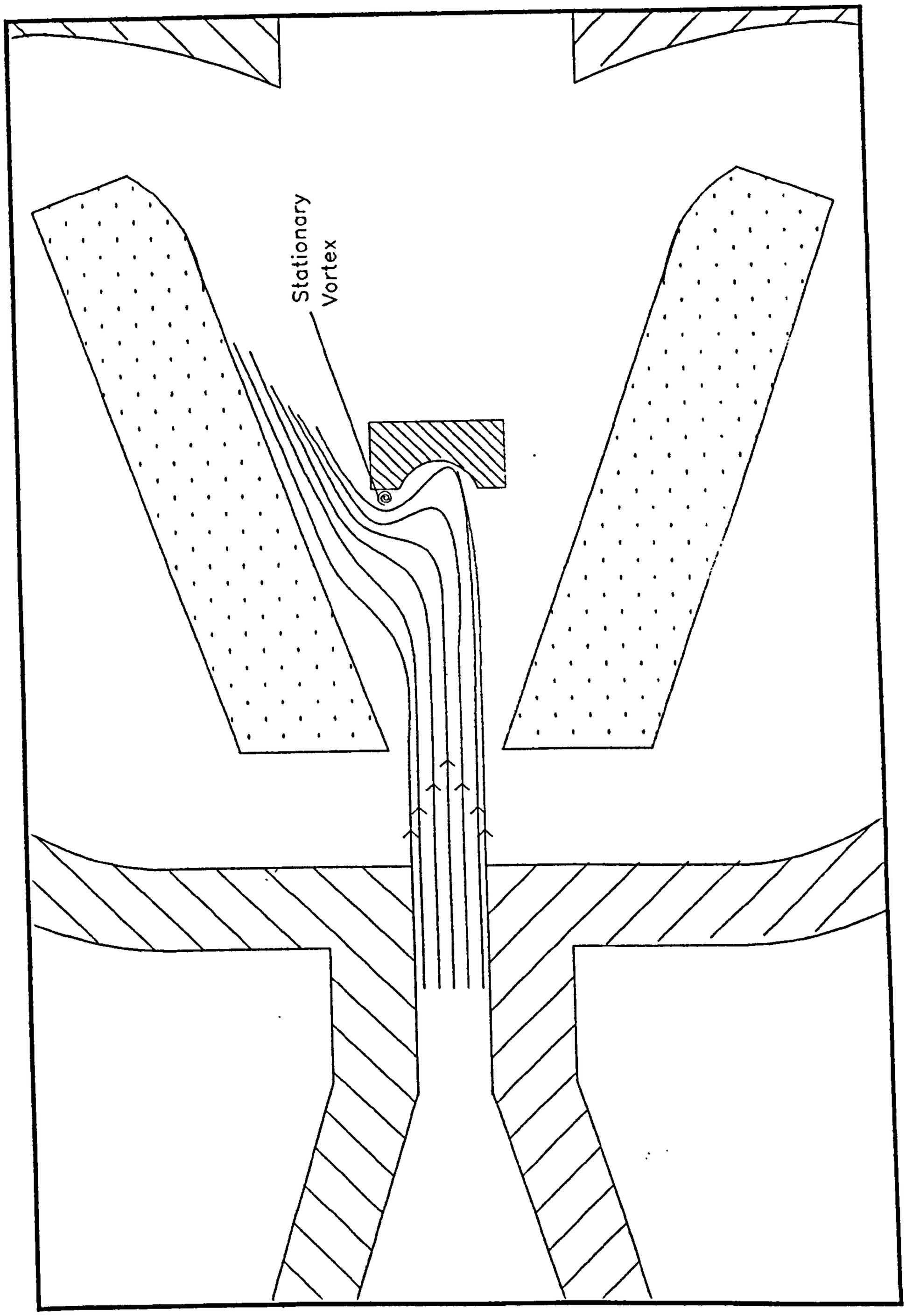

Figure 5.25: Jet Flow Impinging On Surface of Concave Splitter Post.

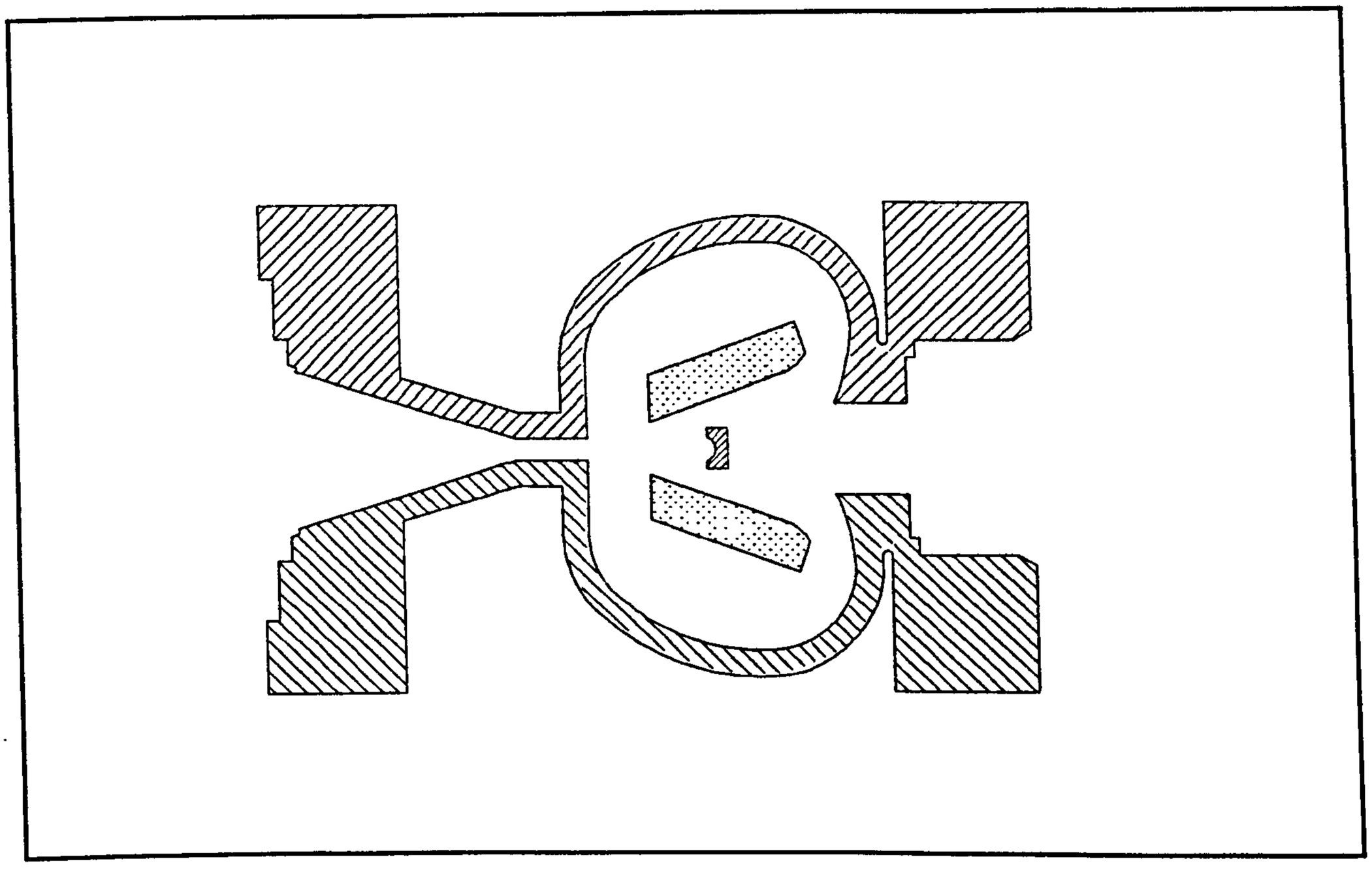

Figure 5.26: Geometry of Acetal Transducer With Modified Diffuser Inserts and Concave Splitter Post.

Chapter 6

Meterfactor Response of Modified Transducer Designs.

6.1 Introduction.

The transducer modifications developed to reduce the minimum flowrate for maintaining oscillation, described in Chapter 5, also effect the oscillation frequency and the linearity of the fluidic oscillator. The geometry modifications, which bring about reductions in minimum flowrate by reducing the resistance to feedback flow, also have a direct effect on the oscillation frequency because the transit time of the feedback flow is significantly reduced thus initiating the next switching action earlier. Also more complete switching of the jet means that the jet flow is fully attached to the diffuser wall at low flowrates and therefore flow is entrained within the feedback channels earlier than for non-complete jet switching where the jet is not fully attached to the diffuser walls. Earlier entrainment of the feedback flow also results in a reduced transit time and increased frequency of oscillation.

This chapter describes the work carried out to investigate the resulting changes in oscillation frequency and meterfactor response, created by modifications to the fluidic oscillator transducer which reduce the minimum point of oscillation for the device. The modifications were investigated individually and in successive combinations to determine if a compromise between low flow performance and acceptable transducer linearity could be achieved.

A fluidic oscillator geometry is described which achieves the $Q_N1.0$ Class D minimum flowrate specification at temperatures above 12°C whilst having a linearity and meterfactor response which is acceptable for use with a linearisation and temperature compensation scheme.

6.2 Transducer Modifications.

Chapter 5 describes the geometry modifications developed which reduce the minimum point of oscillation for the Class C fluidic oscillator water meter transducer. The successful areas of research into the transducer geometry were the:

. Width of the diffuser wall section
. Enlargement of the feedback entrainment region.
. Enlargement of the feedback exit, or jet contact region.
. Modification to the upstream face of the splitter post.

The material shrinkage rates of the early polycarbonate meters meant that the flow chamber lid was a poor fit, resulting in seals that failed when tested at high flowrates due to the internal pressure on the meter. This prevented a full meter calibration for the polycarbonate transducers from being possible. The sectional acetal transducer allows modifications to be made to individual meter components without the need to reconstruct a new complete transducer for each experiment. The meter has a high tolerance assembly allowing for reliable seals to be made to the meter components so that, if care is taken not to over pressure the device, the meter may be tested at high flowrates without damaging the seals. Therefore the acetal transducer modifications can be calibrated throughout the entire flowrange of the meter rather than being tested for the effects on minimum flowrate alone.

6.3 Linearity of the Optimum Low Flow Transducer Geometry.

Initially the modified fluidic oscillator transducer geometry with the optimum low flow performance was calibrated over the meter flowrange according to the calibration procedure described in Chapter 2 except that, as far as possible, the line pressure on the device was kept to below 2p.s.i.. At high flowrates the line pressure is higher due to the back pressure created by the flow through the nozzle of the fishtail diverter. The

geometry of the transducer is shown in figure 5.26. The transducer has a diffuser wall section of 5mm in width, the feedback entrainment region is enlarged by 2mm, the jet contact region is enlarged by 3mm and the upstream face of the splitter post is concave.

The linearity of the device is shown in the form of meterfactor against flowrate in figure 6.1. The meterfactor response of the modified transducer differs from that of the Class C meter in that the plot has a negative slope with increasing flowrate over the range from 10ml s^{-1} to 100ml s^{-1}. This corresponds to a reduction in meterfactor from 7.6ml $pulse^{-1}$ to 6.4ml $pulse^{-1}$.

The reduction in meterfactor is caused by an increased oscillation frequency due to the lower resistance to feedback flow, created by enlarging the volume of the feedback channels and the feedback entrance and exit regions. At low flowrates the oscillation is mostly dependant upon the splitter post with less dependency on the feedback flow thus resulting in a relatively low oscillation frequency per volume flowrate. At higher flowrates the oscillation frequency is mostly dependent on feedback flow therefore the modifications to the feedback channels result in an increase in the rate of change of oscillation frequency with flowrate. This produces a negative gradient in the meterfactor response until the oscillation frequency is so high that the volume flow through the feedback channel restricts the oscillation frequency and the meter again behaves in a linear manner.

It would be possible to model the meterfactor response of the modified transducer so that it may be stored within a lookup table and used within a linearisation and temperature compensation scheme because the slope is always in the same direction and the changes in gradient occur smoothly without rapid changes. The shape of the plot is not practical for mass production however, because of the steep slope of the curve which would cause meter repeatability problems. Very slight changes in meter geometry, which cause slight changes in oscillation frequency, would result in large changes in meterfactor. Similarly non steady flow conditions would cause slight variation in detected oscillation frequency which would cause large changes in

meterfactor value at that frequency. Both of these effects would result in relatively large meter inaccuracies with only slight variation in detected frequency. Ideally the meterfactor response is required to be as linear as possible without steep slopes in the response curve.

6.4 Splitter Post Modification.

Two acetal meters of the standard Class C design, taken from the same moulding batch, were welded and assembled. One of the meters had the splitter post modified with a concave recess machined into the upstream face of the post. Both flow transducers were calibrated according to the procedure described in Chapter 2 and the meter factor response plots are shown in figure 6.2.

The meterfactor response plots show that for a standard Class C meter, without any modifications to the feedback channels, the addition of the recess to the upstream face of the splitter post has no detrimental effect on meter linearity. The response curve for the meter with the modified splitter post is lower in meterfactor value because the meter has an increased oscillation frequency over the entire flow range. Both response curves are acceptable for use with the simple linearisation and temperature compensation scheme described earlier in Chapter 4.

The splitter post modification also has the benefits that it reduces the minimum point of oscillation, giving a greater margin of safety for the minimum flowrate specification for the fluidic oscillator water meter, and increases the signal strength at low flowrates by inducing more complete switching of the jet flow. The modification is also relatively simple in terms of alteration to the production moulding tool. The splitter post modification has since been incorporated within the production $Q_N1.0$ Class C meter design.

6.5 Width of the Diffuser Wall Section.

To investigate the effect of the diffuser wall section upon the linearity and meterfactor response of modified transducer designs, perspex backing plates were constructed and attached to the rear of the diffuser walls of the optimum low flow transducer. Two pairs of backing plates were constructed which increased the diffuser wall sections of the modified transducer to 7mm and 8mm wide respectively. The rear edges of the backing plates were tapered at 45°. In each case the feedback entrainment region was enlarged by 2mm and the jet contact region enlarged by 3mm.

Figure 6.3 shows a comparison of the meterfactor response plots produced by a modified transducer with a diffuser wall section width of 5mm, 7mm and 8mm respectively. The meterfactor response curves are very similar to each other and are linearly shifted in the y-axis of the plot, ie. the volume flow per pulse is increased with increasing diffuser wall width. This is because with increased diffuser wall width, and reduced feedback channel volume, there is a greater resistance to feedback flow which slows the switching time of the jet and allows more volume flow through the meter for each oscillation cycle.

This indicates that the reduction in diffuser wall width is itself not responsible for the non linear meterfactor response of the modified transducer designs. However, altering the volume of the feedback channels by increasing or reducing the width of the diffuser wall section is a useful technique for matching the range of oscillation frequency of a fluidic oscillator to the desired frequency range required by meter electronics or determined by the transient response requirements of a flowmeter. This is particularly significant for scaled fluidic oscillator designs because the oscillation frequency of a scaled meter changes according to the cube of the scaling factor. This limits the maximum size of fluidic oscillator possible because of the very low oscillation frequencies at flowrates at the lower end of the required flowrange.

6.5.1 CFD Investigation of Diffuser Wall Width.

James (1994) used CFD techniques to investigate the effect of reducing the width of the diffuser wall section of the fluidic oscillator. Numerical solution was used to predict the flow in a standard and modified oscillator over a range of Reynolds numbers. The configuration of the model used for the modified transducer is shown in figure 6.4. He presented the results in the form of velocity vector plots and pressure contour plots. The plots were taken at various stages over a period of slightly more than one oscillation cycle.

The velocity vector plots are similar for the standard and modified transducer designs however the eddies visible at the entrance to the feedback channels of the modified design are larger due to the increased size of the feedback entrainment regions. Time history plots for longitudinal and lateral velocities and pressure at various positions were produced as shown in figure 6.5 and 6.6. These show approximately sinusoidal fluctuations demonstrating the oscillation cycles. Time history plots were used to determine the oscillation frequency of the standard and modified models at a range of Reynolds numbers.

Figure 6.7 shows Strouhal against Reynolds number for both sets of simulated results and from experimental data, Furmidge (1993). The graph shows good comparison between simulated and experimental results. Reductions in the diffuser wall width cause an increase in Strouhal number, due to the increased frequency of oscillation caused by reducing the resistance to feedback flow, for both simulated and experimental results.

For a diffuser wall width of 5mm, with standard splitter post and jet contact region, the lowest flowrate found by experimental methods for strong fully switching oscillation was approximately 2.0ml s^{-1}. However a weak oscillation was maintained at 1.79ml s^{-1}. The minimum oscillating flowrate found by flow simulation is between 1.583ml s^{-1} and 2.112ml s^{-1}. It is clear that the numerical model investigated by James (1994) has been able to simulate the improvements in low flow performance following modification to

the transducer geometry and that the results compare well with experimental data.

6.6 Feedback Entrainment Region.

The effect of enlarging the feedback entrainment region of modified fluidic oscillator designs was investigated by calibrating the optimum low flow transducer configuration with a standard non-enlarged entrainment region. To save time add-on sections were constructed and fitted to the diffuser inserts, to restore the feedback entrainment region to standard size, rather than constructing a complete new set of diffuser inserts.

A comparison of meterfactor response between the modified transducer design with and without enlarged feedback entrainment is shown in figure 6.8. The shape of the meterfactor response curves are very similar to each other and the curves are linearly shifted in the y-axis of the plot, ie. the volume flow per pulse is reduced with increased feedback entrainment. This is because with increased feedback entrainment there is less resistance to feedback flow, which reduces the transit time of the feedback flow, thus increasing the oscillation frequency over the entire flowrange causing a reduction in overall meterfactor value. The increased entrainment region has no adverse effects upon the overall linearity of the modified transducer design however it reduces the minimum point of oscillation for the oscillator.

6.7 Effect of Non-Return Valve.

The fluidic oscillator can only meter flow in one direction therefore the water meter requires a non-return valve to prevent reverse flows through the meter, which may result in the customer paying for the same water twice. The non-return valve is fitted within the outlet flange of the water meter and requires a force on the valve target to open the valve. The restricted opening of the valve encourages flow into the feedback channels and therefore has an effect on oscillation frequency.

To investigate the effect of the non-return valve on the meterfactor response and linearity of enhanced performance transducers the target mechanism was removed from a valve fitted to a modified meter. The meter was tested with a 7mm wide diffuser wall section, the feedback entrainment region enlarged by 2mm and a jet contact region enlarged by 3mm.

The meterfactor factor response plots produced by the meter with and without the target fitted to the non-return valve is shown in figure 6.9. The response curves are very similar and shifted in the y-axis, ie. ie. the volume flow per pulse is increased following the removal of the non-return valve target. This indicates that the presence of the non-return valve increases the frequency of oscillation for the fluidic oscillator across the entire flowrange but does not affect overall linearity. Also the minimum point of oscillation is increased for the meter without the non-return valve target.

6.8 Jet Contact Region.

To investigate the effects on meterfactor response produced by varying the jet contact region, a set of diffuser inserts were constructed. The inserts had a standard size jet contact region, a diffuser wall section of 5mm width and the feedback entrainment region enlarged by 2mm. The modified transducer with the standard jet contact region was calibrated according to the procedure described in Chapter 2 and the meterfactor response plot is shown in figure 6.10. Also a comparison of the response produced by the same transducer configuration with the jet contact region enlarged by 3mm is shown.

The transducer with the standard jet contact region has a much more linear response than the transducer with the enlarged jet contact region. The response plot still has a negative slope in meterfactor but the gradient is lower in magnitude and the response is acceptable for use with a suitable linearisation compensation scheme. The meter has greater peak to peak deviations through the transition region of the meterfactor

response, however, it should be possible to improve the linearity of the meter through this region by tuning the flow conditioner to the design of the enhanced performance transducers.

6.9 Enhanced Performance Meter With Improved Linearity.

A set of diffuser wall inserts were developed for the acetal meter, based upon the results presented in this chapter, to produce a fluidic oscillator flowmeter capable of operation at the Class D minimum flowrate specification whilst retaining acceptable meter linearity.

The splitter post modification was incorporated within the design because this modification provides a significant improvement in low flow performance without adversely affecting the linearity of the meter. Similarly the feedback entrainment region of the feedback channels was enlarged by 2mm, compared to the Class C design, because this modification does not significantly alter meter linearity whilst providing a reduction in the minimum point of oscillation achievable.

Although increasing the jet contact region of the feedback channels significantly reduces the minimum point of oscillation and increases the signal strength at low flowrates, by inducing more complete switching of the jet flow, it has an adverse effect on the linearity of the oscillator. The new inserts therefore were constructed with a jet contact region of standard width.

A diffuser wall width of 7mm was selected as this width allows a greater volume of magnetic material to be stored within the wall section, thus boosting the signal strength at low flowrates, to compensate for the loss in signal strength caused by having a standard jet contact region. The actual minimum point of oscillation for a diffuser wall width of 7mm is greater than that for a wall width of 5mm, however, the minimum electronically detectable flowrate is similar because of the limited volume of magnetic

material that may be inserted within the diffuser wall cavity of a 5mm wide wall section.

The edges of the rear face of the diffuser wall inserts which form the feedback channels were rounded to produce an elliptical diffuser insert similar to the rear faces of the original feedback channel design but larger in volume. The geometry of the enhanced performance transducer with improved linearity is shown in figure 6.11.

The meterfactor response of the transducer is shown in figure 6.12. There are peak to peak deviations through the transition region but the transitional response would be improved by tuning the flow conditioning element to the design of the modified transducer. The linearity over the entire flowrange is not as linear as the standard Class C design but is a significant improvement compared to that of the optimum low flow transducer and is acceptable for use with a simple linearity and compensation scheme.

The low flow meter with improved linearity achieved a minimum flowrate at room temperature of 1.62ml s^{-1} which will continue to achieve the Class D minimum flowrate specification at temperatures above 12°C. This is equivalent to a minimum Reynolds number for oscillation of 80.85.

6.9.1 Effect of Flow Conditioner On Improved Response Meter.

The meterfactor response curve shown in figure 6.12 was produced by the improved linearity modified transducer fitted with the slot design flow conditioner. This conditioner design was developed for the standard Class C fluidic oscillator water meter as described in Chapter 4. The major design modifications of the enhanced performance meters are such that the meterfactor response of the transducer without flow conditioning is radically different to the Class C meter. Figure 6.13 shows the meterfactor response curve of the enhanced performance meter with improved linearity

with the slot conditioner removed from the meter inlet.

Figures 6.12 and 6.13 show the significant improvements in linearity and contour of the meterfactor response curve achieved following the addition of a flow conditioning plate upstream of the contraction. This conditioner was developed for the standard fluidic oscillator transducer design and further improvements in linearity should be possible by developing a new conditioning element specifically for use with the new transducer design.

6.10 Conclusions.

The meterfactor response of enhanced performance fluidic oscillator transducers are different to that of Class C meters because of the changes in oscillation frequency caused by altering the transit time of the feedback flow. With all modifications tested the oscillation frequency of the device is increased resulting in a lower volume flow for each oscillation cycle.

The splitter post modification has no adverse effect on the linearity of modified designs, or the standard Class C design, whilst producing a reduction in the minimum point of oscillation and improved switching, consequently giving greater strength of signal, at low flowrates. Also the design modification is simple and relatively easily tooled and has therefore been incorporated within standard production fluidic oscillator design.

The width of the diffuser wall section effects the overall meterfactor value but not the linearity of the modified designs. The minimum point of oscillation is reduced with reducing diffuser wall width but a compromise must be made between the width of the wall and signal strength at low flowrates, because of the restrictions on volume of magnetic material that it is possible to fit within the wall cavity.

The feedback entrainment region and the non-return valve both effect the frequency of

oscillation over the entire flowrange, thereby reducing the value of overall meterfactor, but do not adversely effect the linearity of modified designs.

The size of the jet contact region, at the exit of the feedback channels, is critical to overall meter linearity across the entire flow range. It causes steep gradients in the meterfactor response curve which cause repeatability problems and inaccuracies due to slight changes in detected frequency resulting in large changes in meterfactor value. The modification does increase the signal strength at low flowrates however, by generating more complete switching of the jet flow, and reduces the minimum point of oscillation but these benefits are surpassed by the adverse effects on meter linearity.

A new transducer design has been developed, based on the above information and experimental data, which has a suitable low flow performance whilst retaining an acceptable linearity. The linearity of the new fluidic oscillator design, particularly through the transitional region, may be further improved with the design of a new flow conditioner specifically for use with this meter.

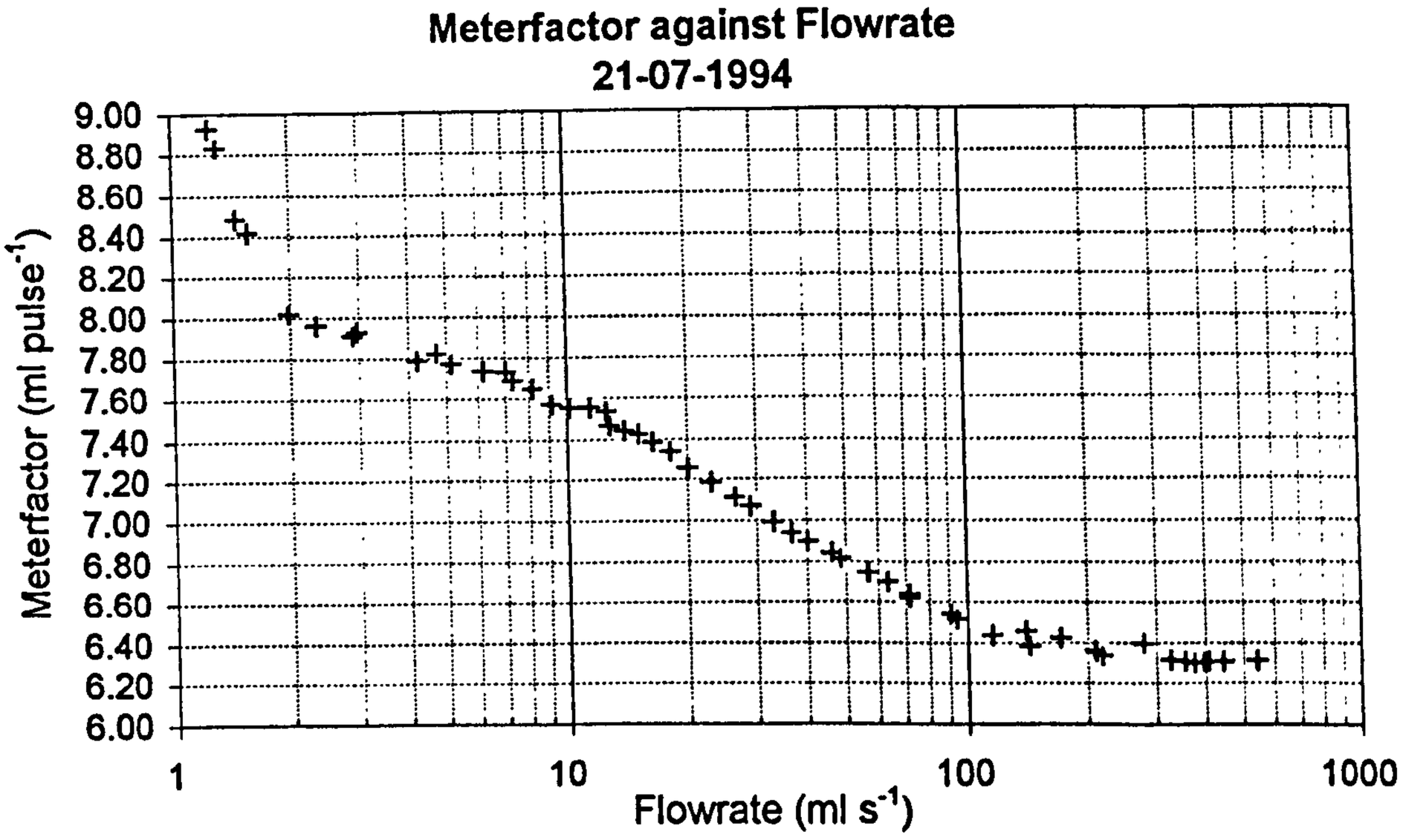

Figure 6.1: Meterfactor response of Optimum Low Flow Transducer.

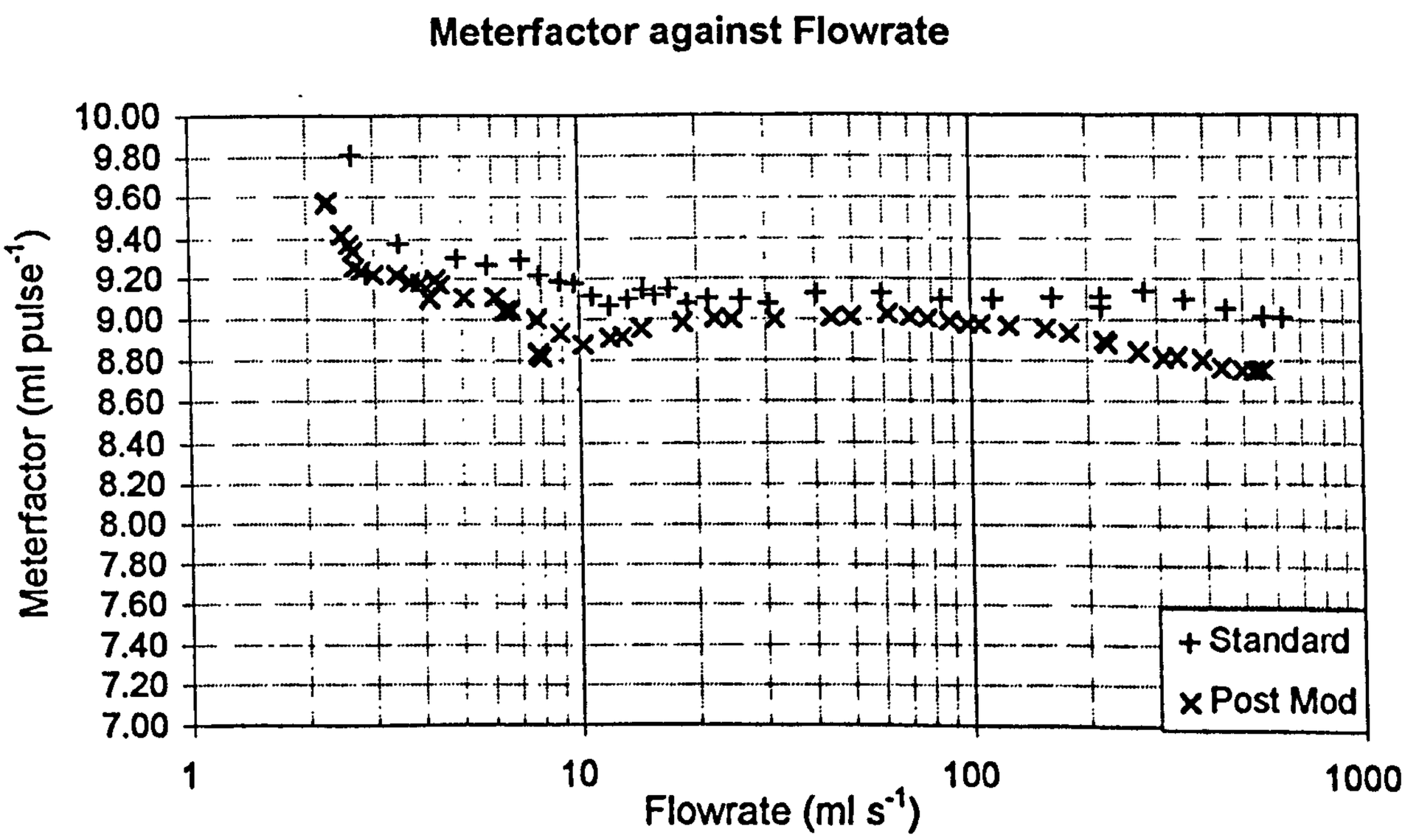

Figure 6.2: Meterfactor response of Standard Transducer With and Without Splitter Post Modification.

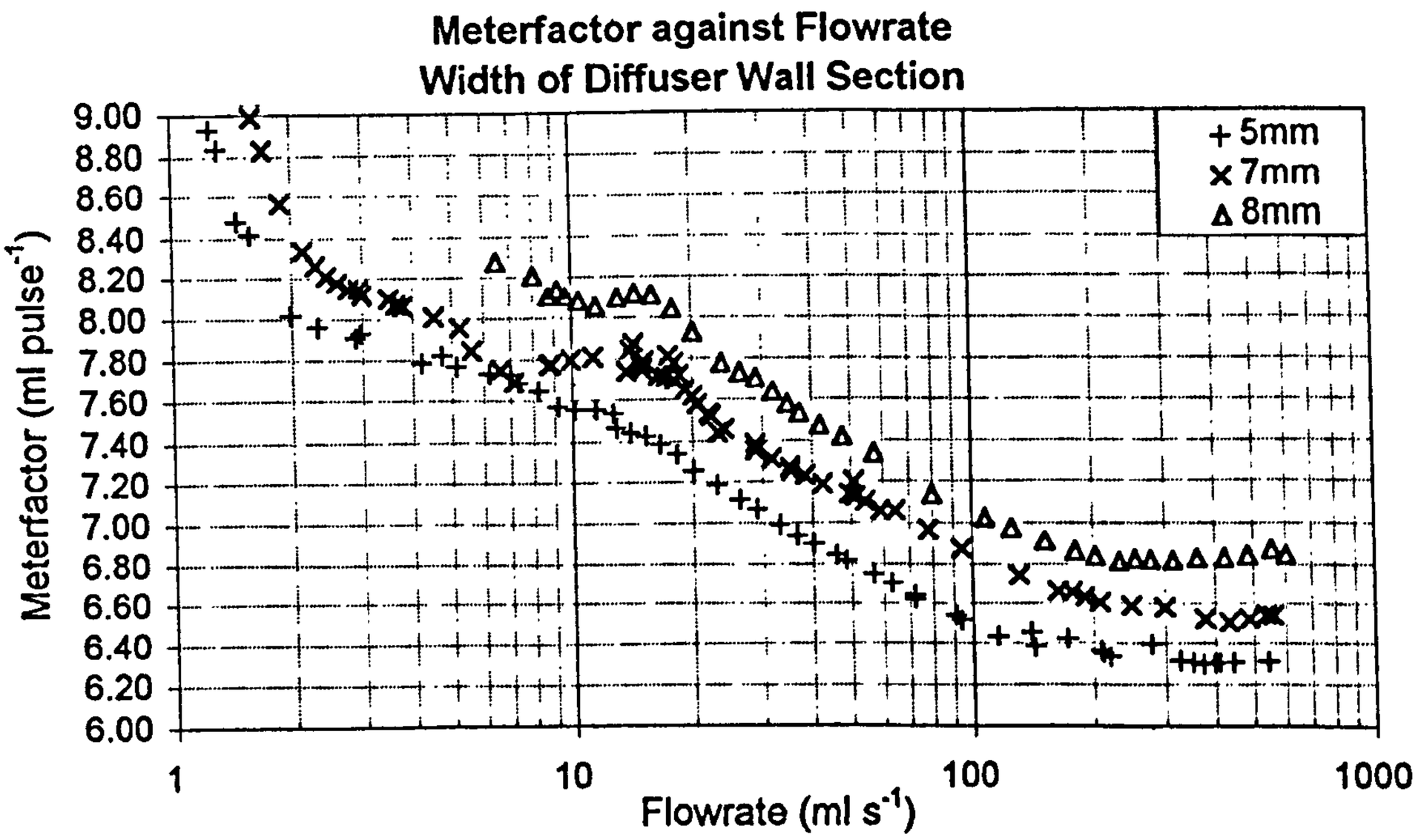

Figure 6.3: Meterfactor Response of Modified Transducer With Increasing Width of Diffuser Wall Section.

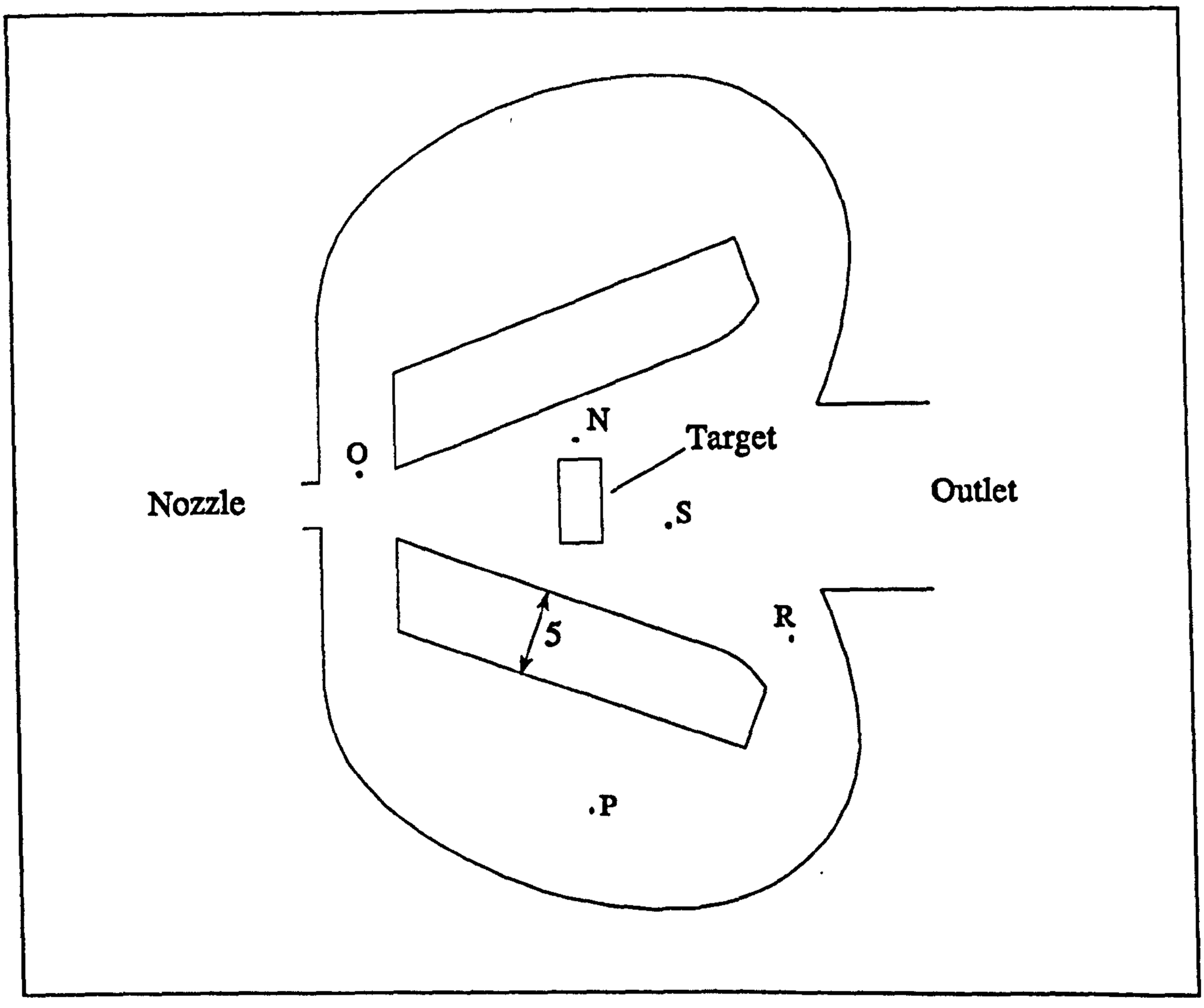

Figure 6.4: Configuration of Numerical Model For Investigation of Diffuser Wall Width.

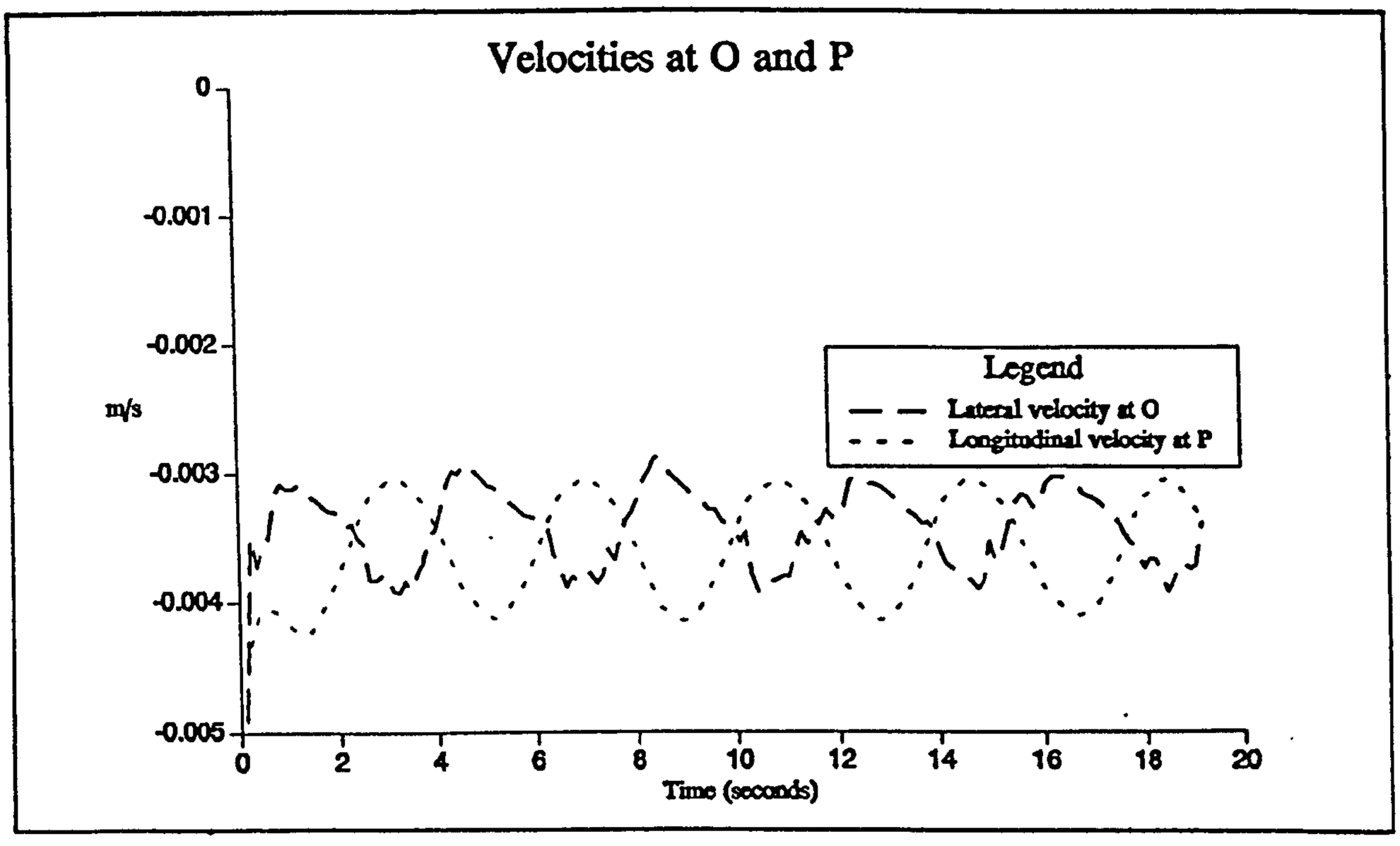

Figure 6.5: Velocity Time Histories For An Inlet Velocity of 5m s^{-1}.

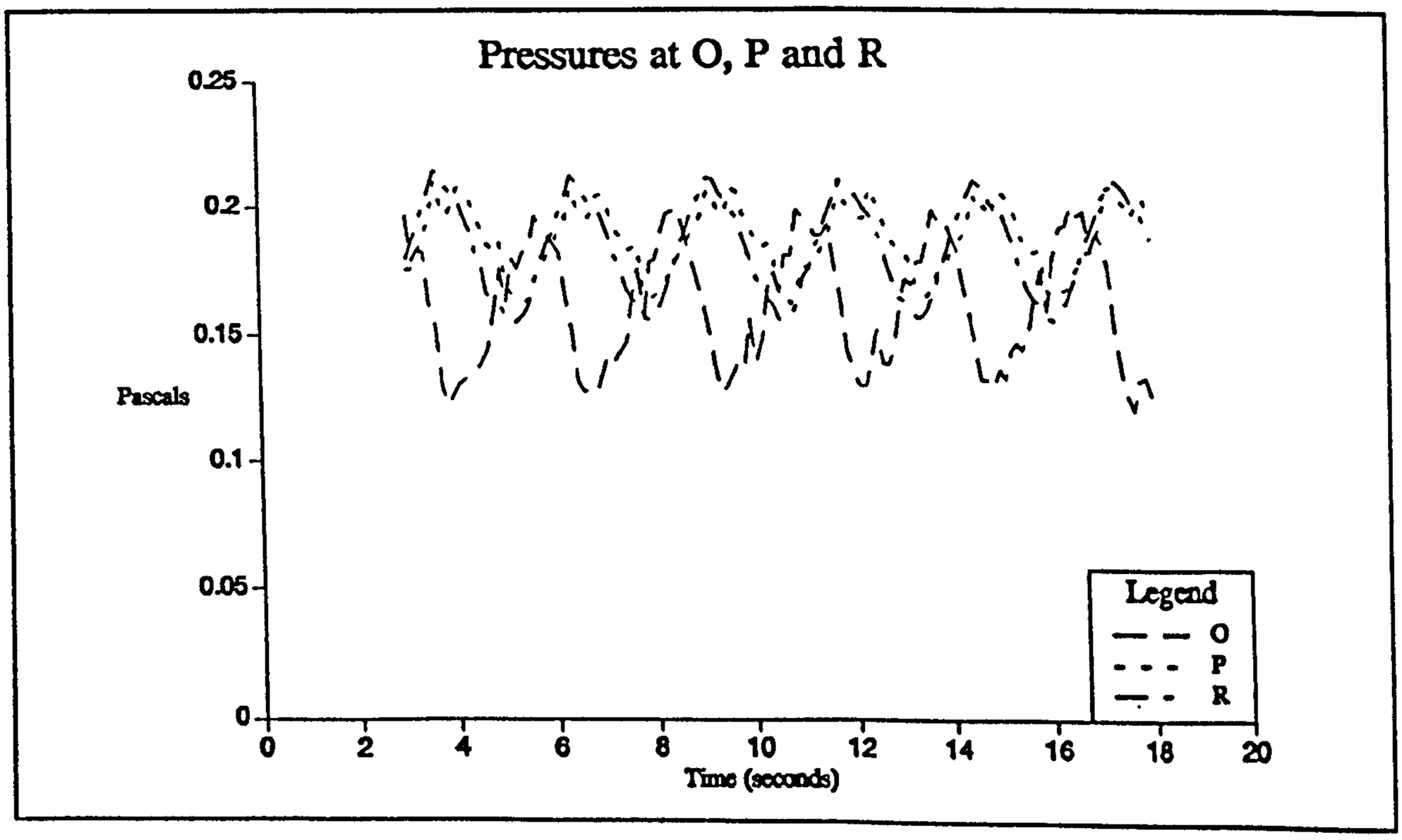

Figure 6.6: Pressure Time Histories For An Inlet Velocity of 5m s^{-1}.

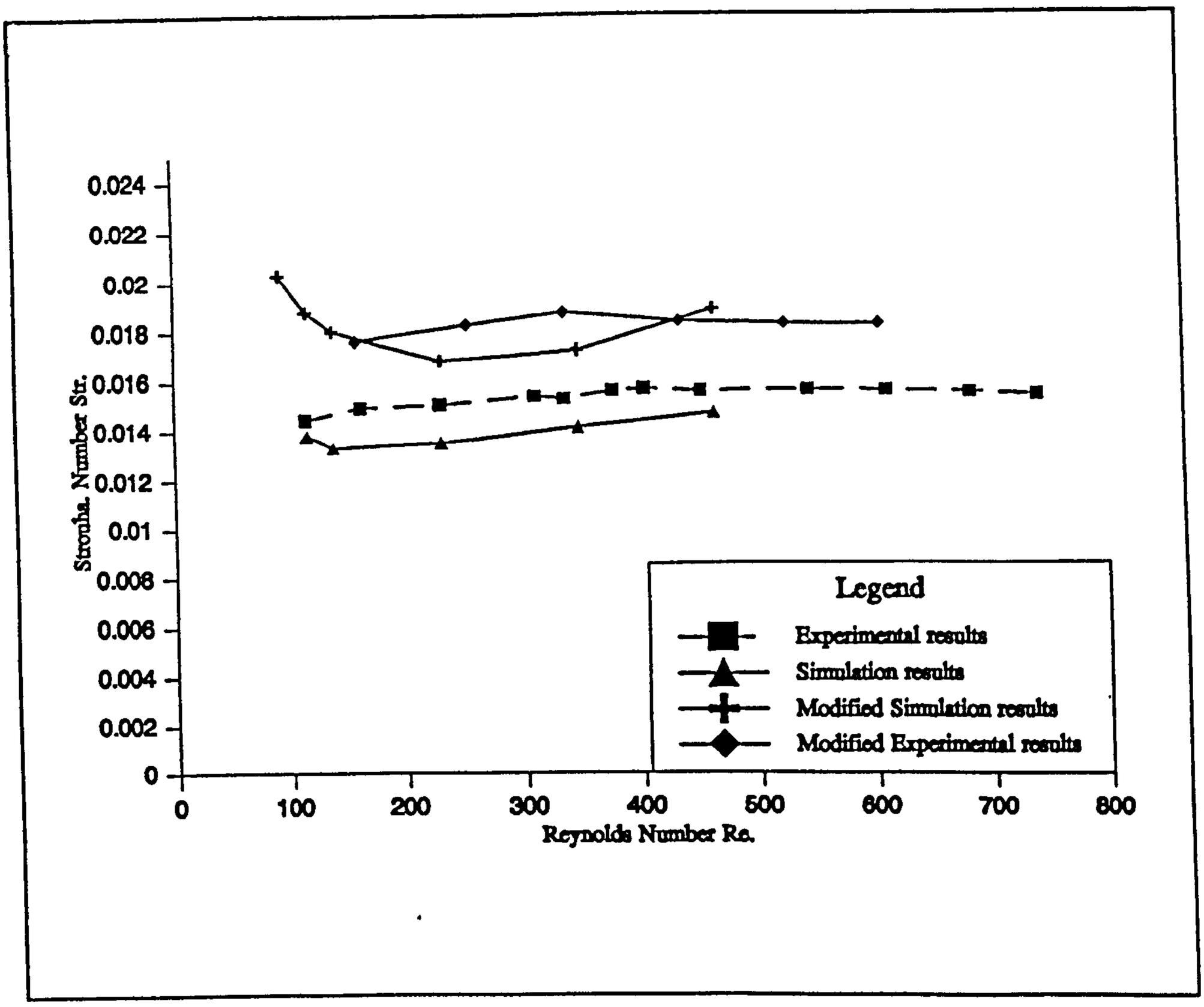

Figure 6.7: Strouhal Number Against Reynolds Number For Simulated and Experimental Results.

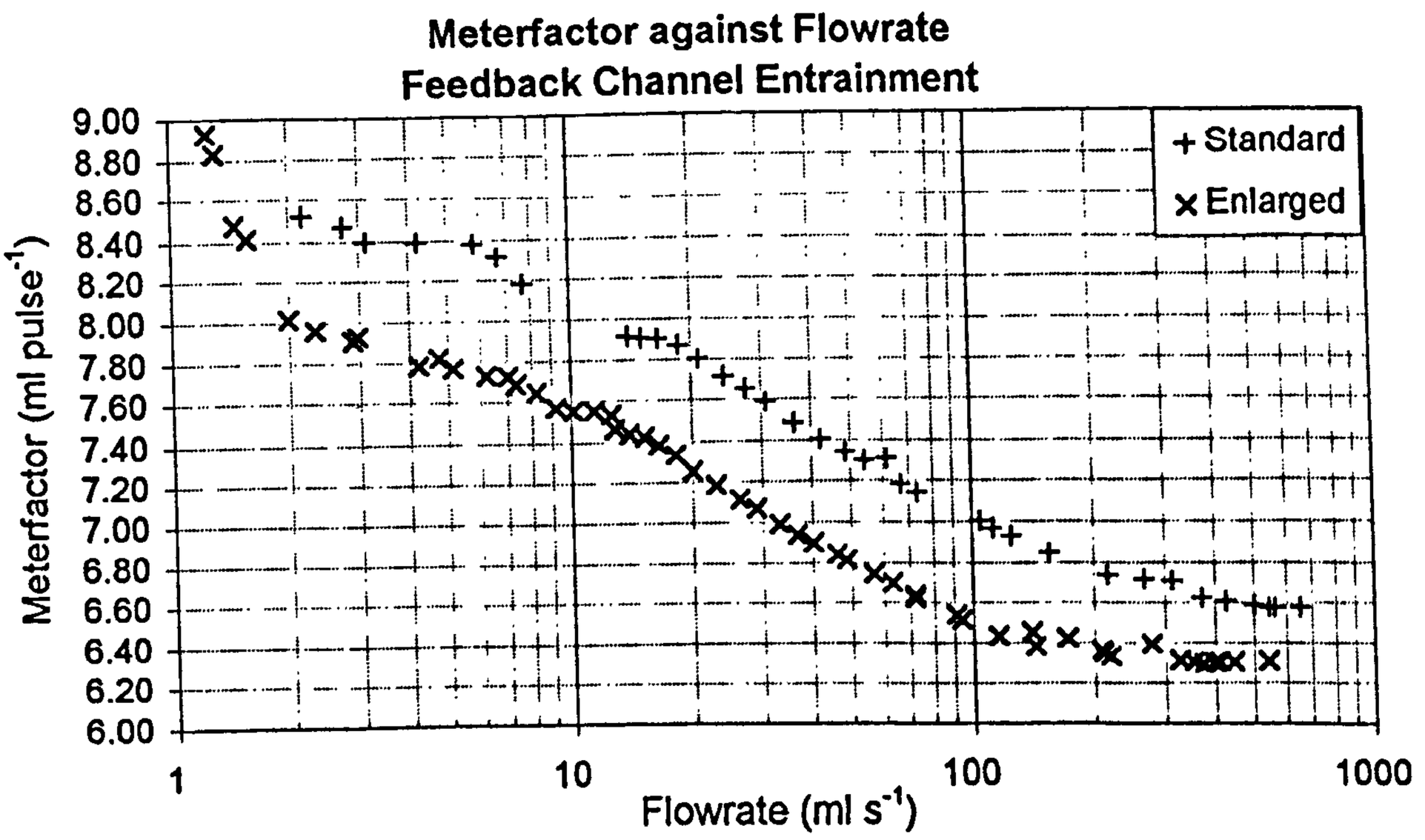

Figure 6.8: Meterfactor Response of Modified Transducer With and Without Increased Feedback Entrainment.

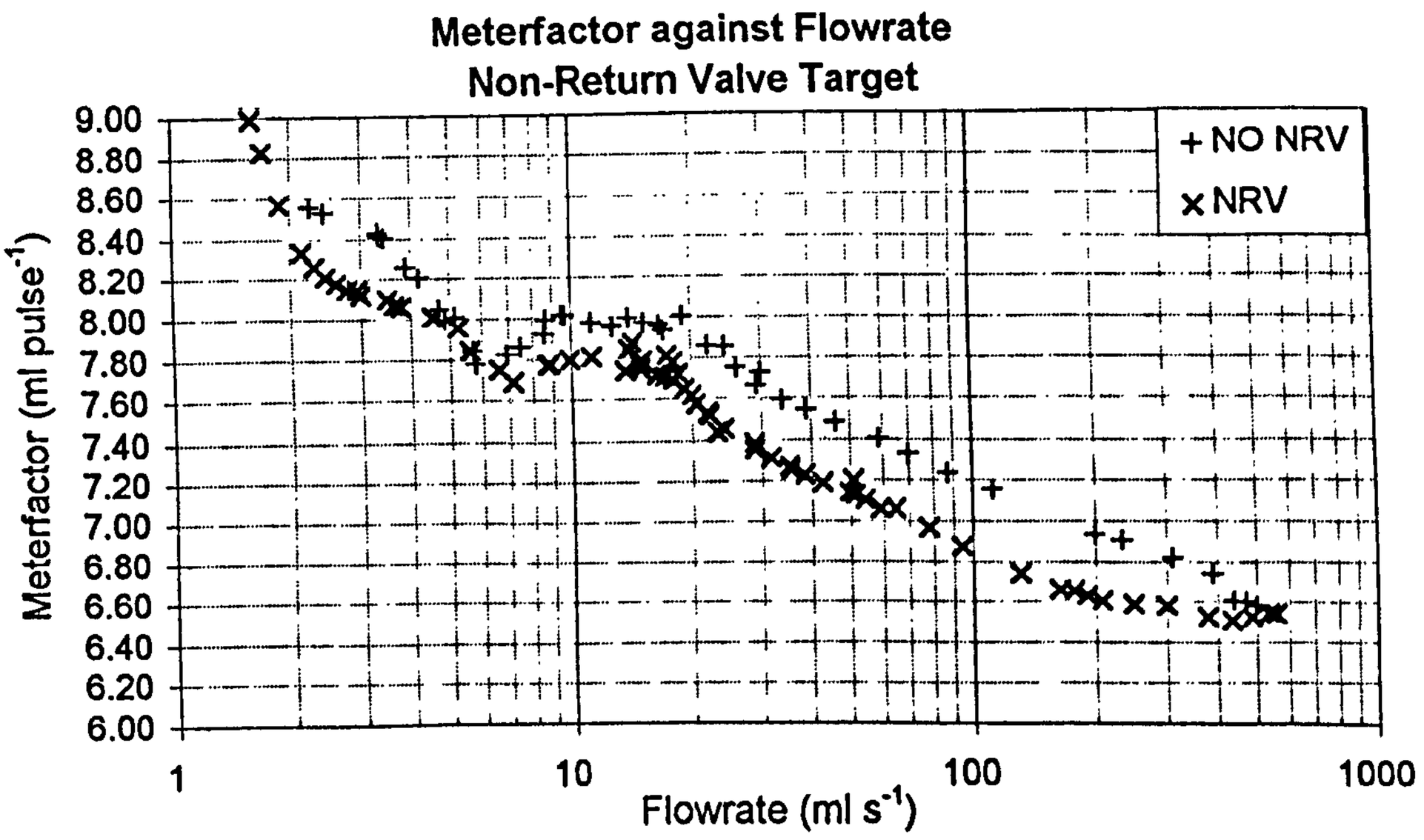

Figure 6.9: Meterfactor Response of Modified Transducer With and Without A Non-Return Valve.

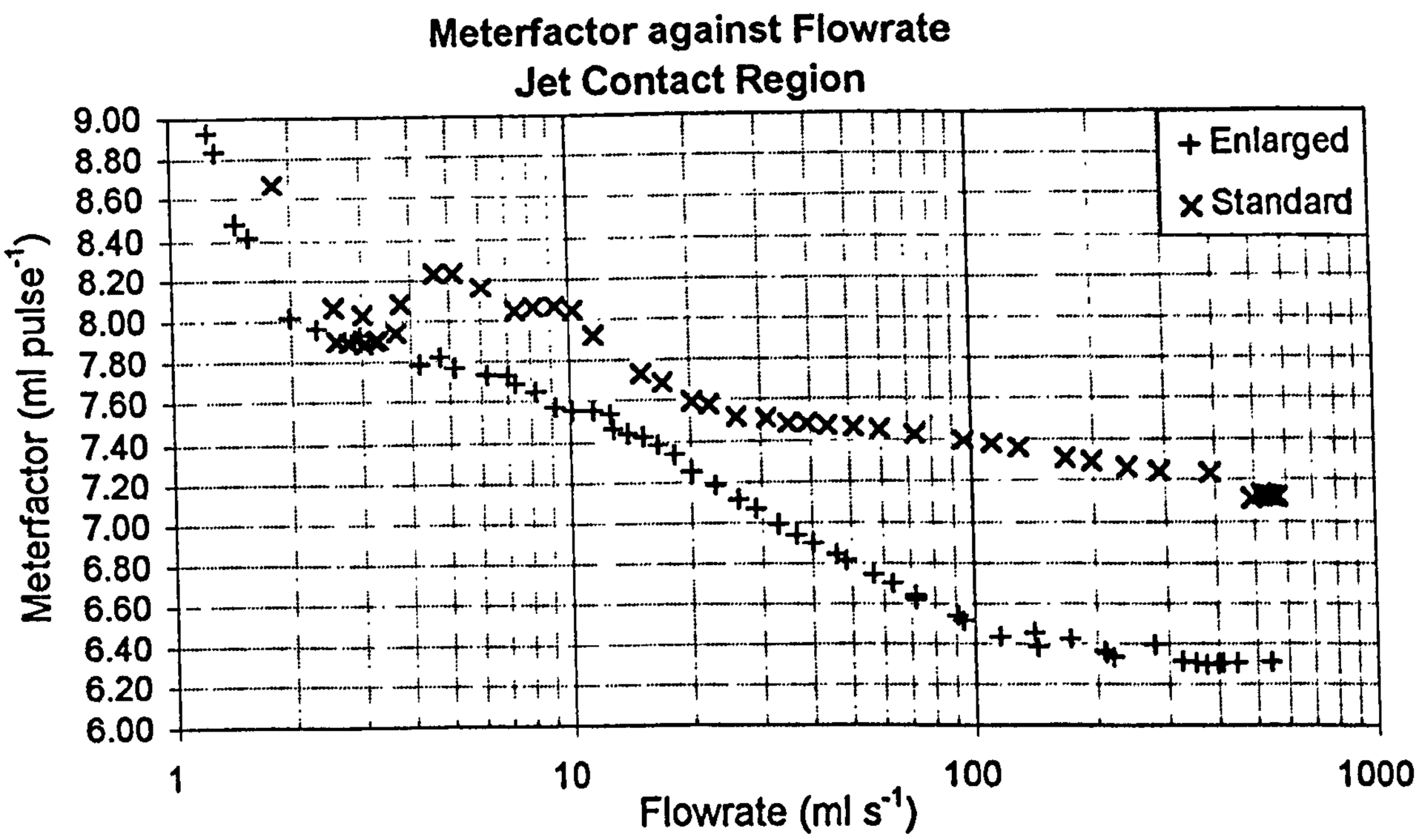

Figure 6.10: Meterfactor Response of Modified Transducer With and Without Increased Jet Contact Region.

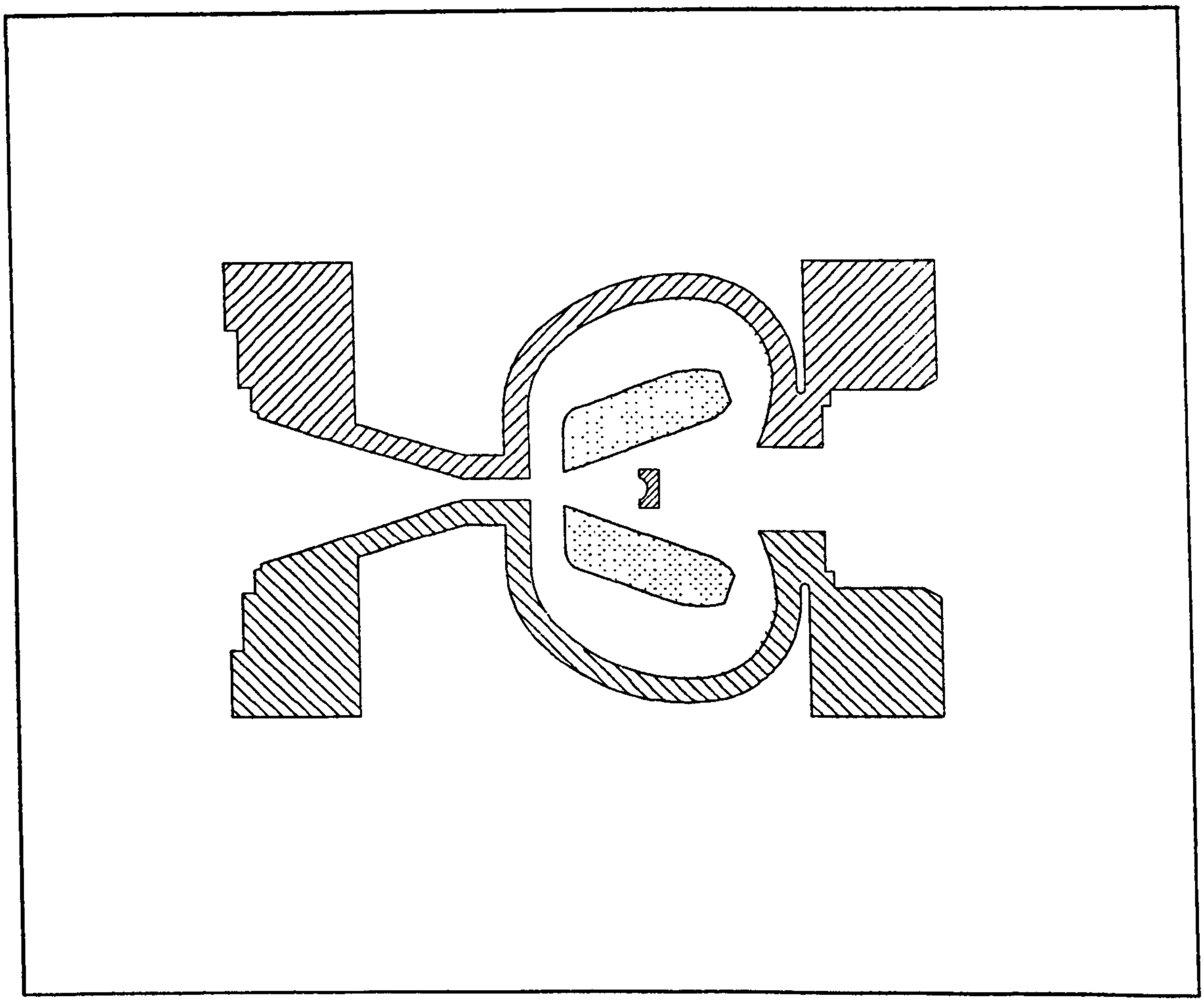

Figure 6.11: Geometry of Enhanced Performance Transducer With Improved Linearity.

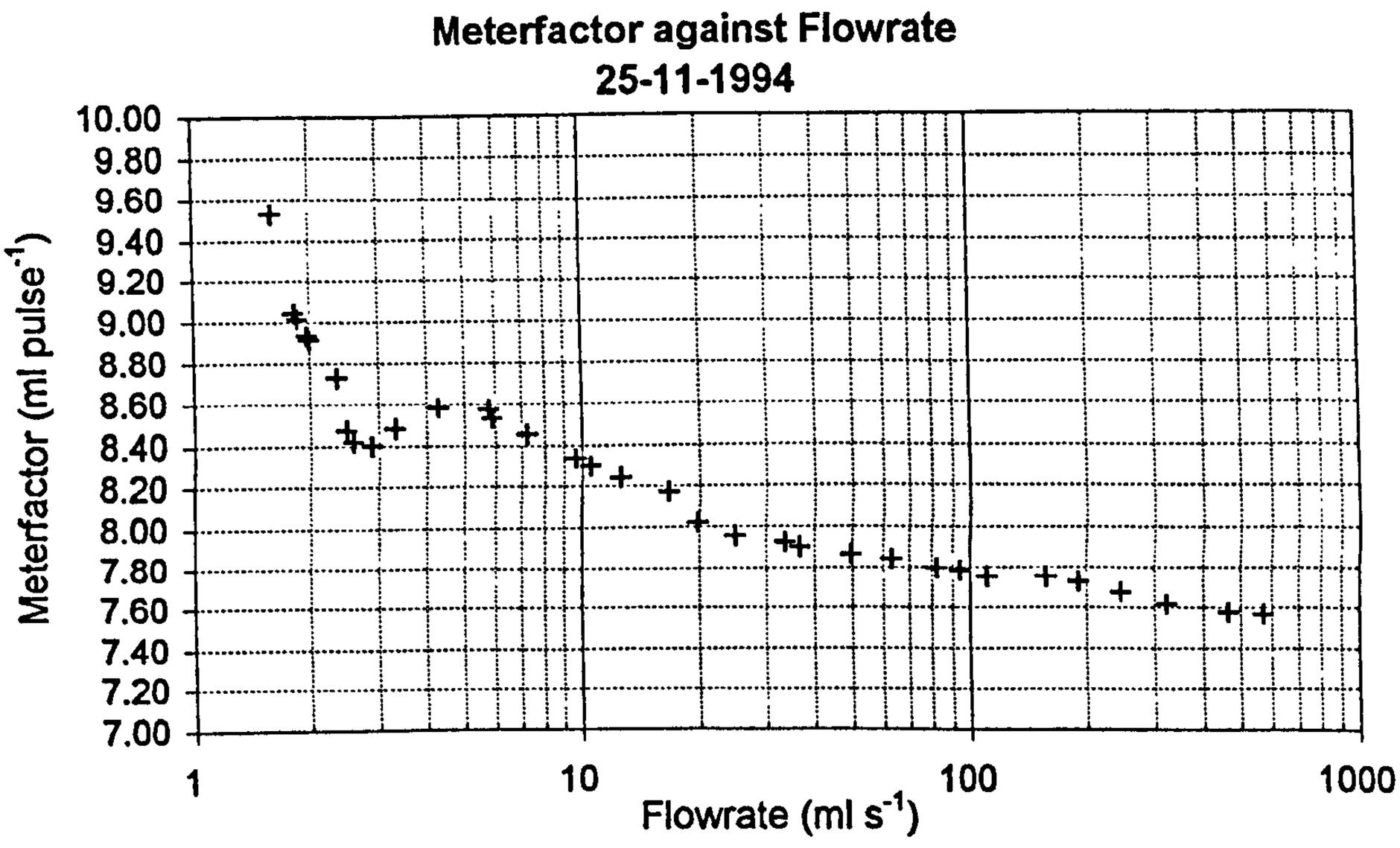

Figure 6.12: Meterfactor Response of Enhanced Performance Transducer With Improved Linearity.

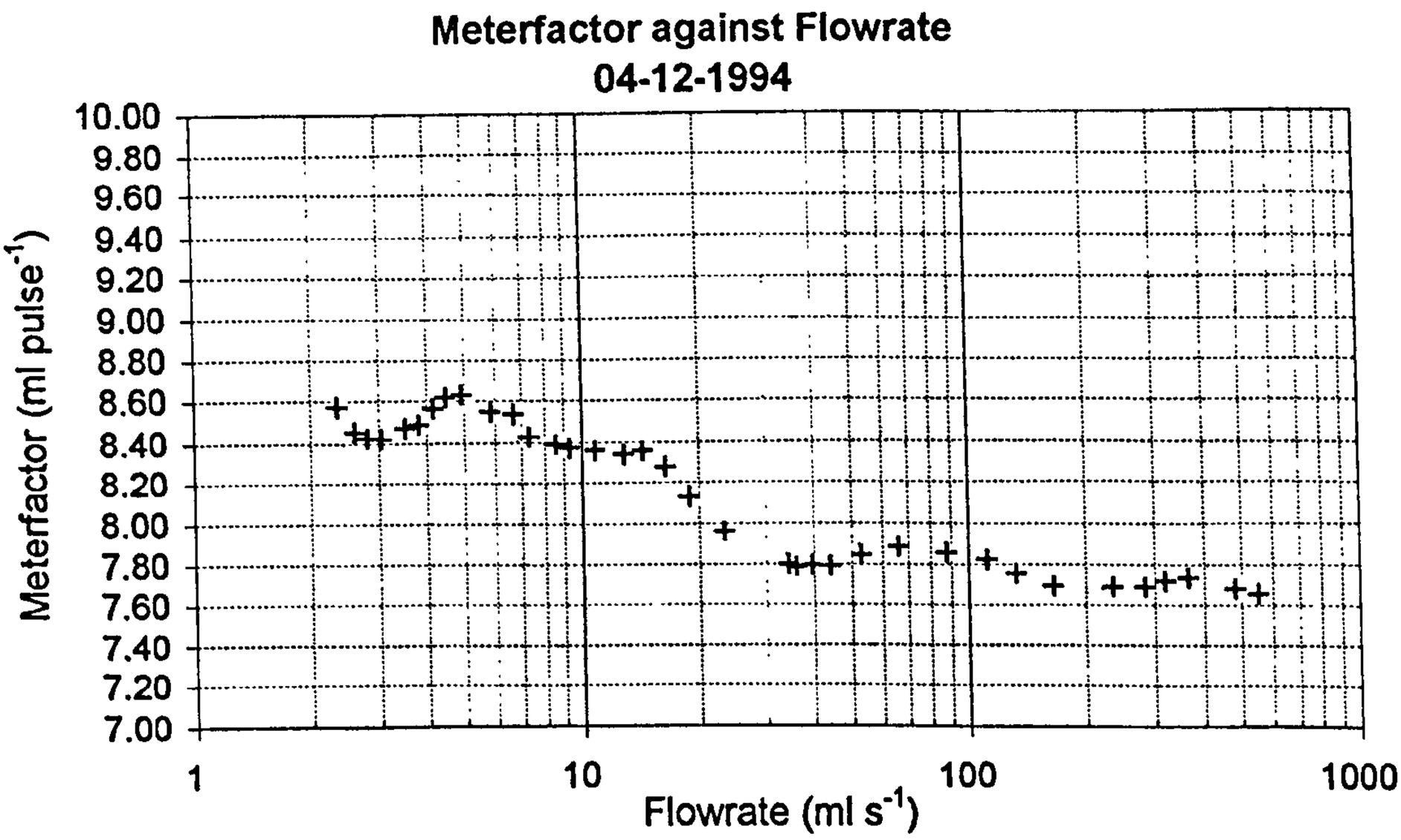

Figure 6.13: Meterfactor Response of Enhanced Performance Transducer Without Flow Conditioner.

Chapter 7

Conclusions and Recommendations For Future Work

7.1 Conclusions.

The objectives of the work described within this thesis were to enhance the performance characteristics of a feedback type fluidic oscillator transducer so that the oscillator may be developed as a domestic water meter capable of meeting the BS5728 (1979) domestic water metering specifications. The fluidic oscillator transducer must be capable of producing an output which is practical for use as a domestic water flowmeter and the fluidic water meter is required to be an advancement upon the rotating piston mechanical water meter used at present for the metering of domestic supplies.

As described in Chapter 1, the fluidic oscillator water meter has many advantages compared to the rotating piston meter, however, the main advantage is that it has no moving parts. This means that the meter is far more reliable requiring no maintenance and is not susceptible to particulate matter within the water supply.

Although using fluidic oscillators to meter domestic water supplies has advantages, in practice it is difficult to achieve the required accuracy and turndown specifications. The domestic water meter metrological performance specifications, the operating principals of fluidic oscillators and the performance criteria necessary to achieve the water meter specifications are given in Chapter 1. The problems associated with using fluidic oscillatory techniques for the metering of domestic water supplies involve achieving the large turndown range required whilst remaining within the allowed pressure drop at the maximum flowrate and ensuring that the linearity and frequency response of the device is acceptable for use with a simple temperature and linearity compensation scheme.

Early fluidic oscillator transducers, based on the now enhanced design shown in figure 1.2, were for the Q_N1.0 Class C domestic water meter. These early meters did not have sufficient signal strength to allow electronic signal detection at low flowrates below the transitional flowrate, Q_T, and they had a very non-linear meterfactor response which was too complex to be used within an electronically stored lookup table. The range of the device was insufficient for the Class C minimum flowrate specification due to lack of signal strength at low flowrates and the pressure drop across the meters was above 20p.s.i. and out of specification at the maximum flowrate. The geometry of the prototype fluidic oscillator design required enhancement to reduce the pressure drop across the device, increase the signal strength at low flowrates, significantly improve the linearity of the frequency response and increase the turndown range to meet the BS5728 (1979) specifications. Also the oscillation frequency of the transducer must be such that the meter has adequate resolution throughout the flow range.

The experimental work carried out on the fluidic oscillators was performed using the Cranfield calibration rig as per the test procedures described in Chapter 2.

Several electromagnetic induction sensing arrangements were considered for use with the fluidic oscillator as described in Chapter 3. The sensing arrangement which detects the fluctuations due to the jet moving from one diffuser wall to the other was found to provide the greatest sensitivity. The sensor consists of two Neodymium magnets, together with backing plates to boost the field strength, mounted within the diffuser walls which create a magnetic field orthogonal to the direction of flow. Flow through the magnetic field induces an e.m.f. in the flow itself which is sensed using stainless steel electrodes mounted in the surface of the flow chamber. Earthing electrodes are provided upstream and downstream of the measurement volume in the form of stainless steel rings mounted between the meter body and the inlet and outlet flanges.

The sensitivity of this arrangement is reduced by two effects. When the jet is close to the measuring electrodes the e.m.f. generated is shorted by the surrounding stagnant fluid and when the jet is on the far wall a signal is still picked up by the sensing

electrodes. These both have the effect of reducing the signal detected as the jet switches from side to side. In an oscillator employing sintered neodymium magnets the sensitivity is sufficient to allow electronic detection of the jet oscillation over the range required for a Q_N1.0 domestic water meter.

To limit the pressure drop of the fluidic oscillator meter, to within the domestic water meter specification, the dimensions of the inlet nozzle were experimentally investigated. These dimensions determine the area of the transducer which is most critical to the pressure losses across the fluidic oscillator. Increasing the width of the fluidic oscillator nozzle gap reduces the pressure drop across the meter but both the velocity of the jet flow and the distance between each jet oscillation and its opposite electrode pair are reduced. Signal strength is proportional to the velocity of the jet flow and the distance between the jet and its opposite electrode pair. Also the Reynolds number within the jet is lower at equivalent flowrates. Lowering the Reynolds number causes the jet flow to be more stable at equivalent flowrates which results in a higher minimum point of oscillation.

After increasing the width of the nozzle to 2.64mm the losses across the fluidic oscillator fitted with a flow conditioner and a non-return valve are within the maximum allowed pressure drop at the maximum flowrate. A nozzle width of 2.64mm was found to provide sufficient signal strength at low flowrates and is capable of maintaining oscillation at flowrates low enough to reach the Q_N1.0 Class C minimum flowrate specification at 10°C. Further enlargement of the nozzle width increases the minimum point of oscillation and reduces the signal strength at low flowrates whilst giving only marginal benefits in pressure drop. This is due to the distance between the splitter post and the diffuser wall becoming the limiting factor rather than the nozzle width.

To meet the water meter performance specifications, the meter is required to operate over a very wide flow range covering varying flow conditions. The changing flow patterns during these varying flow conditions cause the fluidic oscillator to behave in a non-linear way with abrupt rapid changes in meterfactor response throughout the flow

range. The linearity of the flowmeter can be significantly improved by altering the velocity profile of the inlet flow during transitional and laminar flow regimes using flow conditioning upstream of the converging nozzle. The flow conditioning device creates a disturbance at the meter inlet which is intensified as it travels through the contraction. This introduces instabilities into the jet flow where the flow would ordinarily be under fully laminar conditions. The instabilities are amplified by the coanda effect and help to simulate the conditions under which the meter would be operating during the turbulent flow regime. Maintaining turbulence during transitional and laminar flow regimes reduces the variation in Strouhal number with Reynolds number across the flow range thus improving the linearity of the device.

Investigation of conditioner plates with varying hole patterns and hole sizes led to the development of the slot conditioner design. The slot conditioner design dramatically improves the linearity of the fluidic oscillator transducer and when fitted with the flow conditioner the linearity is such that the meterfactor response may be used by a simple linearity and temperature compensation scheme. The flowmeter has an acceptable low pressure drop when fitted with the flow conditioning device and is capable of passing debris through the meter without causing blockage problems.

To increase the range of the fluidic oscillator the critical design parameters such as the nozzle geometry, diffuser wall design, feedback channels, feedback entrainment regions, feedback exit or jet contact regions and the splitter post geometry were experimentally investigated. These dimensions are the areas of the fluidic oscillator geometry which are most critical to low Reynolds number performance.

Alterations to the geometry of the nozzle, other than reducing the size of the nozzle, were shown to have no benefits in low flow performance. However the results of experimental investigation did indicate the criteria required for oscillation at low Reynolds numbers. The addition of vortex ring configurations around the nozzle outlet produced a reduction in minimum flowrate for oscillation that was equivalent to the reduction achieved through the addition of a flow conditioning device to the meter inlet.

Modifications to the feedback channels of the fluidic transducer gave significant reductions in minimum flowrate for oscillation by reducing the resistance to feedback flow and inducing switching of the jet at lower flowrates.

The development of a sectioned acetal prototype transducer incorporating electrodes allowed more accurate comparisons to be made between subsequent modifications and the signal strengths generated for each modification at low flowrates. The concave face splitter post design was investigated using the acetal test meter. Combining the feedback channel and splitter post modifications resulted in a Q_N1.0 fluidic oscillator transducer capable of maintaining oscillation at a Reynolds number of 82.6. This is an overall reduction in Re_{min} of over 35% compared to the Class C design and is lower than the Reynolds number required to meet the Class D minimum flowrate specification at temperatures down to 10°C.

The transducer modifications developed to reduce the minimum flowrate for maintaining oscillation also affect the oscillation frequency and the linearity of the fluidic oscillator. The splitter post modification had no adverse effect on the linearity of modified designs, or the standard Class C design, whilst producing a reduction in the minimum point of oscillation and improved switching of the jet, consequently giving greater signal strength at low flowrates.

The width of the diffuser wall section, the size of the feedback entrainment region and the presence of a non-return valve all affect the frequency of oscillation over the entire flowrange, thereby reducing the value of overall meterfactor, but do not adversely affect the linearity of modified designs. However the size of the jet contact region, at the exit of the feedback channels, is critical to overall meter linearity. It causes steep gradients in the meterfactor response curve which cause repeatability problems and inaccuracies due to slight changes in detected frequency resulting in large changes in meterfactor value.

A Q_N1.0 Class C transducer has been developed which, when fitted with the slot conditioner, has acceptable linearity for use with a simple linearisation and temperature compensation scheme. The meter will continue to meet the Class C Q_{min} specification at temperatures below 10°C and is within the pressure drop limits at Q_{max}. Also fluidic oscillator geometry has been developed which achieves the Q_N1.0 Class D minimum flowrate specification at temperatures above 12°C whilst having a linearity and meterfactor response which is acceptable for use with a linearisation and temperature compensation scheme. The pressure drop is within the BS5728 (1979) specification at the maximum flowrate and has a practical frequency range ensuring adequate resolution at all flowrates.

7.2 Recommendations For Future Work.

Although the flow conditioning device performs well it would be beneficial to develop a greater understanding of the complex processes taking place within the oscillator when the flow condition of the jet changes from one flow regime to another. Further work could be undertaken to investigate the relationships between the Strouhal number and shedding properties of the conditioner blocking regions and those of the splitter post. This would also involve investigation into the effect of the inlet contraction upon the vortices which are shed from the blocking regions of the conditioner. The vortices will be accelerated in the direction of flow as they travel through the contraction with increasing velocity but it is unknown what effects this will have upon the vortices and how the jet flow itself is altered as it enters the flow chamber. A large scale model of the inlet contraction and flow conditioning element manufactured from perspex would allow for flow visualisation and LDA experiments to be performed to develop a greater understanding of the role of the flow conditioner in the alteration of the jet flow through varying flow conditions.

It would also be useful to carry out further investigation into the effects on meter linearity caused by modifications to the feedback channels. This could involve

determining at what flowrate the feedback flow starts to dominate oscillation frequency rather than the recirculating vortices from the vortex wake created by the splitter post. One method would be to block off the feedback channels and calibrate the meter as an oscillating jet device similar to the simple target meter. The meter may then be calibrated with the feedback channels open but with the splitter post removed to determine the frequency response due to feedback flow only. It may then be possible to derive an expression for the relationship between the feedback flow, the recirculating vortices and oscillation frequency. This information could then be used to develop further improvements in low flow performance with improved linearity and help to determine the absolute minimum point of oscillation achievable for the fluidic oscillator.

An area of the fluidic oscillator water meter geometry that has not been altered is the aspect ratio of the transducer. Although the jet width dimension has been investigated the overall transducer height has remained the same because the chamber height is governed by the internal diameter of the inlet and outlet pipe and by the flange dimensions given in the BS5728 (1979) specifications. Equation (1.9) shows that the minimum flowrate possible is set by the lowest value of Re_{min} achievable and the product of the square root of the aspect ratio and the fourth root of the Euler number. Boucher (1995) states that the aspect ratio is an important parameter with an optimum value that changes with meter design. He found an aspect ratio of 8 to be an optimum value for the target meter and a value of 5 for the feedback design of oscillators that he investigated. The aspect ratio of the fluidic oscillator water meter is 7.58. If improvements in low flow performance are possible through changes to the aspect ratio of the transducer then it may be necessary to develop height expanding, or reducing, flanges for the water meter. In fact a lower aspect ratio would be beneficial for scaled larger size water meters.

It is clear that numerical techniques to simulate fluid flows through fluidic oscillator flowmeters will become an increasing aspect of future design work. CFD techniques have already been used to help predict the changes in oscillation frequency due to modification of the feedback channels of the fluidic water meter and to determine the

effect on the jet caused by the addition of vortex rings to the meter nozzle. It is expected that with advances in computing power and software capability the investigation of future designs of oscillators will take place numerically rather than using the costly and time consuming experimental techniques used for the work described within this thesis.

Appendix.A

A.1 Fluidic Oscillator Look-Up Table Centre Frequencies.

Frequency Bin No.	Integration Period P/s	Edges Counted N	Flow Cycles M	Maximum Frequency fmax/Hz	Minimum Frequency fmin/Hz	Centre Frequency f/Hz
1	0.0703125	12	6		78.2222	78.2222
2	0.0703125	11	5.5	78.2222	71.1111	74.6667
3	0.0703125	10	5	71.1111	64.0000	67.5556
4	0.0703125	9	4.5	64.0000	56.8889	60.4444
5	0.0703125	8	4	56.8889	49.7778	53.3333
6	0.0703125	7	3.5	49.7778	42.6667	46.2222
7	0.0703125	6	3	42.6667	35.5556	39.1111
8	0.0703125	5	2.5	35.5556	28.4444	32.0000
9	0.140625	12	6		39.1111	39.1111
10	0.140625	11	5.5	39.1111	35.5556	37.3333
11	0.140625	10	5	35.5556	32.0000	33.7778
12	0.140625	9	4.5	32.0000	28.4444	30.2222
13	0.140625	8	4	28.4444	24.8889	26.6667
14	0.140625	7	3.5	24.8889	21.3333	23.1111
15	0.140625	6	3	21.3333	17.7778	19.5556
16	0.140625	5	2.5	17.7778	14.2222	16.0000
17	0.28125	12	6		19.5556	19.5556
18	0.28125	11	5.5	19.5556	17.7778	18.6667
19	0.28125	10	5	17.7778	16.0000	16.8889
20	0.28125	9	4.5	16.0000	14.2222	15.1111
21	0.28125	8	4	14.2222	12.4444	13.3333
22	0.28125	7	3.5	12.4444	10.6667	11.5556
23	0.28125	6	3	10.6667	8.8889	9.7778
24	0.28125	5	2.5	8.8889	7.1111	8.0000
25	0.5625	12	6		9.7778	9.7778
26	0.5625	11	5.5	9.7778	8.8889	9.3333
27	0.5625	10	5	8.8889	8.0000	8.4444
28	0.5625	9	4.5	8.0000	7.1111	7.5556
29	0.5625	8	4	7.1111	6.2222	6.6667
30	0.5625	7	3.5	6.2222	5.3333	5.7778
31	0.5625	6	3	5.3333	4.4444	4.8889
32	0.5625	5	2.5	4.4444	3.5556	4.0000
33	1.125	12	6		4.8889	4.8889
34	1.125	11	5.5	4.8889	4.4444	4.6667
35	1.125	10	5	4.4444	4.0000	4.2222
36	1.125	9	4.5	4.0000	3.5556	3.7778
37	1.125	8	4	3.5556	3.1111	3.3333
38	1.125	7	3.5	3.1111	2.6667	2.8889
39	1.125	6	3	2.6667	2.2222	2.4444
40	1.125	5	2.5	2.2222	1.7778	2.0000
41	2.25	12	6		2.4444	2.4444
42	2.25	11	5.5	2.4444	2.2222	2.3333
43	2.25	10	5	2.2222	2.0000	2.1111
44	2.25	9	4.5	2.0000	1.7778	1.8889
45	2.25	8	4	1.7778	1.5556	1.6667
46	2.25	7	3.5	1.5556	1.3333	1.4444
47	2.25	6	3	1.3333	1.1111	1.2222
48	2.25	5	2.5	1.1111	0.8889	1.0000
49	4.5	12	6		1.2222	1.2222
50	4.5	11	5.5	1.2222	1.1111	1.1667
51	4.5	10	5	1.1111	1.0000	1.0556
52	4.5	9	4.5	1.0000	0.8889	0.9444
53	4.5	8	4	0.8889	0.7778	0.8333
54	4.5	7	3.5	0.7778	0.6667	0.7222
55	4.5	6	3	0.6667	0.5556	0.6111
56	4.5	5	2.5	0.5556	0.4444	0.5000
57	9	12	6		0.6111	0.6111
58	9	11	5.5	0.6111	0.5556	0.5833
59	9	10	5	0.5556	0.5000	0.5278
60	9	9	4.5	0.5000	0.4444	0.4722
61	9	8	4	0.4444	0.3889	0.4167
62	9	7	3.5	0.3889	0.3333	0.3611
63	9	6	3	0.3333	0.2778	0.3056
64	9	5	2.5	0.2778	0.2222	0.2500
65	18	12	6		0.3056	0.3056
66	18	11	5.5	0.3056	0.2778	0.2917
67	18	10	5	0.2778	0.2500	0.2639
68	18	9	4.5	0.2500	0.2222	0.2361
69	18	8	4	0.2222	0.1944	0.2083
70	18	7	3.5	0.1944	0.1667	0.1806
71	18	6	3	0.1667	0.1389	0.1528
72	18	5	2.5	0.1389	0.1111	0.1250

A.2 Contents of Fluidic Oscillator Water Meter Look-Up Table.

Bin No.	MF Multiplier	Centre Freq	BI Slope sign +0,-1	BI Slope ROM	BI Intercept ROM	BI ROM dec	BI ROM hex	BI MF @ 0°C	BI slope MF/°C
1	6	78.222	0	0	1174	1174	0496	9.554036	0.00000
2	5.5	74.666	0	0	1075	1075	0433	9.543678	0.00000
3	5	67.555	0	0	975	975	03CF	9.521484	0.00000
4	4.5	60.444	0	0	875	875	036B	9.494357	0.00000
5	4	53.333	1	0	777	33545	8309	9.484863	0.00000
6	3.5	46.222	1	0	680	33448	82A8	9.486607	0.00000
7	3	39.111	1	0	584	33352	8248	9.505208	0.00000
8	2.5	32	1	0	488	33256	81E8	9.53125	0.00000
9	6	39.111	1	1	1184	36000	8CA0	9.635416	-0.00814
10	5.5	37.333	1	1	1087	35903	8C3F	9.650213	-0.00888
11	5	33.777	1	0	976	33744	83D0	9.53125	0.00000
12	4.5	30.222	1	0	879	33647	836F	9.537760	0.00000
13	4	26.666	1	0	783	33551	830F	9.558105	0.00000
14	3.5	23.111	1	0	685	33453	82AD	9.556361	0.00000
15	3	19.555	0	0	587	587	024B	9.554036	0.00000
16	2.5	16	0	0	489	489	01E9	9.550781	0.00000
17	6	19.555	0	0	1175	1175	0497	9.562174	0.00000
18	5.5	18.666	0	0	1077	1077	0435	9.561434	0.00000
19	5	16.888	0	0	979	979	03D3	9.560546	0.00000
20	4.5	15.111	0	0	881	881	0371	9.559461	0.00000
21	4	13.333	0	0	782	782	030E	9.545898	0.00000
22	3.5	11.555	0	0	685	685	02AD	9.556361	0.00000
23	3	9.7777	0	0	587	587	024B	9.554036	0.00000
24	2.5	8	0	0	489	489	01E9	9.550781	0.00000
25	6	9.7777	0	0	1174	1174	0496	9.554036	0.00000
26	5.5	9.3333	0	0	1076	1076	0434	9.552556	0.00000
27	5	8.4444	0	0	978	978	03D2	9.550781	0.00000
28	4.5	7.5555	0	0	880	880	0370	9.548611	0.00000
29	4	6.6666	0	0	781	781	030D	9.533691	0.00000
30	3.5	5.7777	0	0	682	682	02AA	9.514508	0.00000
31	3	4.8888	0	0	582	582	0246	9.472656	0.00000
32	2.5	4	0	0	484	484	01E4	9.453125	0.00000
33	6	4.8888	0	1	1150	3198	0C7E	9.358723	0.00814
34	5.5	4.6666	0	0	1067	1067	042B	9.472656	0.00000
35	5	4.2222	0	0	969	969	03C9	9.462890	0.00000
36	4.5	3.7777	0	0	871	871	0367	9.450954	0.00000
37	4	3.3333	0	0	774	774	0306	9.448242	0.00000
38	3.5	2.8888	0	0	677	677	02A5	9.444754	0.00000
39	3	2.4444	1	0	581	33349	8245	9.456380	0.00000
40	2.5	. 2	1	0	486	33254	81E6	9.492187	0.00000
41	6	2.4444	1	0	1162	33930	848A	9.456380	0.00000
42	5.5	2.3333	1	0	1066	33834	842A	9.463778	0.00000
43	5	2.1111	1	1	986	35802	8BDA	9.628906	-0.00977
44	4.5	1.8888	1	1	891	35707	8B7B	9.667968	-0.01085
45	4	1.6666	1	1	796	35612	8B1C	9.716796	-0.01221
46	3.5	1.4444	1	1	702	35518	8ABE	9.793526	-0.01395
47	3	1.2222	1	1	607	35423	8A5F	9.879557	-0.01628
48	2.5	1	1	1	511	35327	89FF	9.980468	-0.01953
49	6	1.2222	1	1	1200	36016	8CB0	9.765625	-0.008
50	5.5	1.1666	1	1	1103	35919	8C4F	9.792258	-0.008
51	5	1.0555	1	1	1006	35822	8BEE	9.824218	-0.00977
52	4.5	0.9444	1	1	910	35726	8B8E	9.874131	-0.01085
53	4	0.8333	1	1	814	35630	8B2E	9.936523	-0.01221
54	3.5	0.7222	1	1	716	35532	8ACC	9.988839	-0.01395
55	3	0.6111	1	1	618	35434	8A6A	10.05859	-0.01628
56	2.5	0.5	1	1	521	35337	8A09	10.17578	-0.01953
57	6	0.6111	1	1	1221	36037	8CC5	9.936523	-0.00814
58	5.5	0.5833	1	1	1121	35937	8C61	9.952059	-0.00888
59	5	0.5277	1	1	1025	35841	8C01	10.00976	-0.00977
60	4.5	0.4722	1	1	928	35744	8BA0	10.06944	-0.01085
61	4	0.4166	1	1	830	35646	8B3E	10.13183	-0.01221
62	3.5	0.3611	1	1	734	35550	8ADE	10.23995	-0.01395
63	3	0.3055	1	0	626	33394	8272	10.18880	0.00000
64	2.5	0.25	1	0	525	33293	820D	10.25390	0.00000
65	6	0.3055	1	1	1268	36084	8CF4	10.31901	-0.00814
66	5.5	0.2916	1	1	1165	35981	8C8D	10.34268	-0.00888
67	5	0.2638	1	1	1063	35879	8C27	10.38085	-0.00977
68	4.5	0.2361	1	1	961	35777	8BC1	10.42751	-0.01085
69	4	0.2083	1	0	843	33611	834B	10.29052	0.00000
70	3.5	0.1805	1	0	740	33508	82E4	10.32366	0.00000
71	3	0.1527	1	0	636	33404	827C	10.35156	0.00000
72	2.5	0.125	1	0	531	33299	8213	10.37109	0.00000

References.

ADAMS, R.B. **A Fluidic Flowmeter.** *Proc. Int. Conf. Houston Texas,* Paper 73, 15-18 October 1973.

BEALE, R.B. and LAWLER, M.T. **Development of a Wall Attachment Fluidic Oscillator Applied To Volume Flow Metering.** *Flow - Its Measurement and Control in Science and Industry.* ISA Vol. 1. 1974

BOUCHER, R.F. and MAZHAROGLU, C. **Low Reynolds Number Fluidic Flowmetering.** *J.Phys. E. Sci. Instruments,* Vol.21, 977-989, 1988(a).

BOUCHER, R.F. and MAZHAROGLU, C. **Fluidic Flowmeter Scaling Equations.** *2nd Int. Sym. On Fluid - Control, Measurement, Mechanics and Flow Visualisation,* 5-9 September 1988(b).

BOUCHER, R.F. and MAZHAROGLU, C. **The Potential of Fluidic Oscillators In Domestic Gas Measurement.** *International Gas Research Conference,* 1989.

BOUCHER, R.F. **Minimum Flow Optimisation of Fluidic Flowmeters.** *Measurement Science and Technology.* Vol.6, Number7, July 1995.

BRITISH STANDARD BS5728. Measurement of Water Flow In Closed Conduits, Part1: Specification For Single Meters. 1979.

BRITISH STANDARD BS6199. Measurement of Liquid Flow In Closed Conduits Using Weighing and Volumetric Methods. Part 1: Weighing Method. 1981.

CHIWANGA, S.G. **A Study of The Effect of Particulate Matter (Within The Water Supply System) On Class D Domestic Water Meters.** *Developments In Metering Technology Seminar, Society of British Water Industries,* Leamington Spa, October 1994.

FURMIDGE, N.A. and SANDERSON, M.L. **A Novel Fluidic Flowmeter For Domestic Water Metering Applications.** *FLOMEKO, Seoul Korea,* 1993.

FURMIDGE, N.A. *Conditioner Testing and Pressure Drop Measurements For Fluidic Oscillator Flowmeter.* Cranfield Institute of Technology, Department of Fluid Engineering and Instrumentation, Report No MLS/18/420E/115, January 1992.

FURMIDGE, N.A. *Modifications To The Fluidic Oscillator Flowmeter Feedback Paths.* Cranfield Institute of Technology, Department of Fluid Engineering and Instrumentation, Report No 93/NF/FO/420/128, July 1993.

FURMIDGE, N.A. *Fluidic Oscillator Flowmeter Progress Rerport.* Cranfield University, Department of Fluid Engineering and Instrumentation, Report No 94/NF/FO/420/219, March 1994.

GLYNN, D.R. and KALSI, H.S. **Numerical Prediction of Flow in a Fluidic Oscillator.** *2nd Int. PHOENICS User Conference,* November 1987.

HONDA, S. and YAMASAKI, H. **A New Hydrodynamic Oscillator Type Flowmeter.** *FLUCOME Tokyo,* 1985.

HONDA, S. and YAMASAKI, H. **Fluidic Oscillator Type Flowmeter Without Control Ports.** *2nd Int. Sym. On Fluid - Control, Measurement, Mechanics and Flow Visualisation,* 5-9 September 1988.

JAMES, R. *Numerical Simulation of Flow Through Fluidic Flowmeters.* PhD Thesis, Cranfield University, 1994.

KADOSCH, M. **The Curved Wall Effect.** *Second Cranfield Fluidics Conference, Cambridge,* Paper A4, A4-45-56, 1967.

KALSI, H.S., MARKLAND, E., SAMUEL, N.P. and TOFIELD, G.M. **Factors Affecting Choice of Fluidic Flowmeters.** *2nd Int. Sym. On Fluid -Control, Measurement, Mechanics and Flow Visualisation,* 5-9 September 1988.

KAWANO, A., HONDA, S., HASEGAWA, T., Okabayashi, M. and Tanaka, H. **Fluidic Flowmeters With Wide Measuring Range.** *FLUCOME, Tokyo* 1985.

LUSH, P.A. **Investigation of the Switching Mechanisms In A Large Scale Turbulent Re-Attachment Amplifier.** *Second Cranfield Fluidics Conference.* Paper A1, 1967.

MEDLOCK, R.S. **Fluid Oscillatory Methods of Flow Measurement.** *Introduction To Flow Measurement,* Cranfield Institute of Technology, 22-25 January 1990.

NATIONAL METERING TRIALS WORKING GROUP. *Water Metering Trials Final Report.* Water Services Association, Water Companies' Association, Office of Water Services, WRc and Department of the Environment, 1993.

SANDERSON, M.L. and HERITAGE, J. *Fluid Flowmeters.* European Patent No. 0381334/E. US Patent No. 5063786. 1989.

SANDERSON, M.L. and SPENDEL, K.D. *An Investigation of Appropriate Technology For The Measurement of Flow In Small Diameter Pipes Carrying Cold Potable Water.* Cranfield Institute of Technology, Department of Fluid Engineering and Instrumentation, May 1987.

SHAKOUCHI, T. **Development of A New Fluidic Oscillator Flowmeter Using A Three Dimensional Nozzle.** *2nd Int. Sym. On Fluid - Control, Measurement, Mechanics and Flow Visualisation,* 5-9 September 1988.

SMITH, P. **Fluidic Water Meter Behaviour Under Adverse Service Conditions.** *Developments In Metering Technology Seminar, Society of British Water Industries, Leamington Spa,* October 1994.

TIPPETTS, J.R., ROYLE, J.K. and NG, H.K. **An Oscillating Bistable Amplifier For Use As A Flowmeter.** *2nd IFAC Symp. On Fluidics, Prague,* June 28-July2, 1971.

WILSON, M.P., COOGAN, C.H. and SOUTHALL, K. **Experimental Investigation of Fluidic Volume Flowmeter.** *J. Basic Engineering,* VOLS. 92-93 page 139, 1970-71

WRIGHT, P.H. **The Coanda Meter - A Fluidic Digital Gas Flowmeter.** *J.Phys. E. Sci. Instruments,* VOL 13, 1980.

WU, S.G., SU, H.N., WANG. **Theoretical and Experimental Investigation of a Fluidic Oscillator Flowmeter.** *20th Anniversary Fluidics Symposium,* 1980.

YAMASAKI, H. and HONDA, S. **A Unified Approach To Hydrodynamic Oscillators With Fluidic Flowmeter.** *Measurement of Flow. Soc. Instrum. and Control Eng. Japan,* 1980.

YAMASAKI, H. and HONDA, S. **A Unified Approach To Hydrodynamic Oscillator Type Flowmeters - On the Complementary Relations Between Fluidic Flowmeters and Vortex Flowmeters.** *Measurement of Flow. Soc. Instrum. and Control Eng. Japan,* 1980 (Second Report)

YAMASAKI, H., TAKAHASHI, A. and HONDA, S. **A New Fluidic Oscillator For Flow Measurement.** *2nd Int. Sym. On Fluid - Control, Measurement, Mechanics and Flow Visualisation,* 5-9 September 1988.

YAMASAKI, H., KITAZAWA, S. and ZHANG, Z.M. **Forming 2-Dimensional Jet Flow By Vortex Ring in Fluidic Devices.** *FLUCOME 91, University of Tokyo, Japan,* 1991.

ZANKER, K.J. **The Development of a Flow Straightener For Use With Orifice Flowmeters In Disturbed Flow.** *Paper D-2, Symp. On Flow Measurement, Scotland,* 1969.